Design and implementation of DNA-Directed Immobilisation (DDI) glycoarrays for probing carbohydrate-protein interactions.

Jing Zhang

▶ To cite this version:

Jing Zhang. Design and implementation of DNA-Directed Immobilisation (DDI) glycoarrays for probing carbohydrate-protein interactions.. Other. Ecole Centrale de Lyon, 2010. English. NNT : 2010ECDL0029 . tel-00605541

HAL Id: tel-00605541

https://theses.hal.science/tel-00605541

Submitted on 2 Jul 2011

ECOLE CENTRALE DE LYON

THESE

Pour obtenir le grade de

DOCTEUR DE L'ECOLE CENTRALE DE LYON

Ecole Doctorale: Electronique, Electrotechnique et Automatique

Spécialité : STIC Santé et Micro et nano technologies

Par

Jing ZHANG

Design and implementation of DNA-Directed Immobilization (DDI) glycoarrays for probing carbohydrate-protein interactions

Thèse préparée à l'INL-Ecole Centrale de lyon
Sous la direction d' Eliane Souteyrand
Co-dirigée par Yann Chevolot

Soutenance prévue le 04/11/2010 devant la commission d'examen composée de

M. François Morvan	Directeur de Recherche INSERM- UM2- Montpellier	Président
M. Jean -Claude Michalski	Directeur de Recherche INSERM- USTL- Lille	Rapporteur
M. Didier Léonard	Professeur- UCBL1- Lyon	Rapporteur
Mme. Eliane Souteyrand	Directeur de Recherche CNRS- ECL- Lyon	Directeur
M. Yann Chevolot	Chargé de Recherche CNRS- ECL- Lyon	Co-Directeur
M. Wilfrid Boireau	Chargé de Recherche CNRS- UFC- Besançon	Examinateur

Acknowledgements

TABLE OF CONTENTS

ABSTRACT

Nowadays there is a growing awareness of the significant roles of carbohydrates involving biological interactions, especially carbohydrate/lectin interactions. Technologies for rapid monitoring and evaluating such interactions are of great importance to provide deep insights relevant to carbohydrate involving biological events. However, most conventional approaches are cumbersome and material/time consuming. Thus, there is an urgent need for fast, sensitive, and high throughput technologies. Glycoarrays, which consist of numerous carbohydrates with diverse structures immobilized on solid support, have emerged as the most promising and ideal technologies for addressing this need. The DNA-directed immobilization (DDI) glycoarray takes the advantage of the specificity of DNA/DNA hybridization to immobilize glycoconjugates coupled with a single-stranded DNA moiety with its complementary nucleic acids grafted on a solid support. It has been proved to be an efficient tool to do the investigation of carbohydrate/lectin interactions. The primary aim of the thesis is to further validate and improve the capability of DDI glycoarrays for rapid, simultaneous profiling and quantitative analyzing interactions of various synthetic glycoconjugates with lectins or other targets of interest (e.g. influenza viruses).

The immobilization of carbohydrate probes is a key issue in the elaboration of the glycoarrays. DDI and direct covalent grafting were compared onto borosilicate glass slide. The DDI carbohydrate immobilization displayed more efficiency in comparison with covalent grafting methods.

The studies of carbohydrate/lectin interactions are complicated by the low affinities of carbohydrates towards lectins. However, the low affinity can be enhanced by providing multivalency and proper spatial distribution of the saccharide residues. Herein, galactose or fucose clusters with different multivalencies and spatial arrangements were tested toward the binding affinities with respect to RCA120 and PA-IL/PA-IIL lectins. Moreover, IC_{50} measurement assays were designed and carried

out on DDI glycoarray. The recognition study was performed by direct fluorescence scanning and by the determination of the IC_{50} values, with both techniques leading to similar results.

In order to amplify the capabilities of the DDI glycoarray, miniaturized analytical biosystems based on DDI glycoarray were fabricated. In this system, 40 microwells are etched on a single microscope glass slide. Each microwell displays 64 spots of covalently immobilized DNA single strands which allowed multiplex tests to be performed in one single microwell (a slide can be considered as an array of glycoarray). For proof of concept, the first miniaturized biosystem (Mb I, in abbr.) was designed to investigate two lectin/glycoconjugate specific recognition models by "in-solution" approach of DDI glycoarray. On the basis of validation of the concept of "in-solution" approach in Mb I, a developed miniaturized biosystem (Mb II, in abbr.) was set up, which potentially allowed the mixture of eight different glycoconjugates or glycoconjugate/lectin complexes to be sorted and captured by hybridization with the complementary DNA sequences printed at the bottom of each microwell of Mb II. Seven tetra-galactosyl glycoconjugates arranging in various special structures and carrying different linkers and charges as well as two glycoconjugates bearing three mannose or three galactose residues were tested with respect to RCA120 and PA-IL by two DDI strategies: "on-chip" and "in-solution" approaches. The results showed that the PA-IL lectin preferred to bind to positively charged glycoconjugates. The highest binding signal was observed for a tetra-galactosyl glycomimetic with a flexible linker towards the two lectins (RCA120 and PA-IL) in "on-chip" approach, while in "in-solution" approach, it was another tetra-galactosyl glycomimetics with a rigid linker DMCH showed the most efficient binding. Moreover, it appeared that the two lectins preferred to bind to the glycoconjugates with Comb-like structure rather than glycoconjugates arranged in antenna architecture. Moreover, a quantitative assay for the determination of IC_{50} values of five glycoconjugates was performed on Mb II (one single slide) in parallel. The results were comparable with that observed by direct fluorescence detection.

Finally, initial attempts were undertaken to implement the study of interactions of

two influenza viruses H1N1/PR8 and H3N2/Moscow with glycoconjugates on DDI glycoarray.

AIMS

The interactions of carbohydrates and lectins are involved in numerous crucial physiological and pathological processes. Thanks to the development of nanotechnologies, biochips and especially the carbohydrate chips which have become not only powerful platforms to map out the carbohydrates involving interactions but also efficient tools to decipher the glycocodes. In our laboratory, a kind of carbohydrate chip, DNA Directed Immobilization (DDI) glycoarray, has already set up and applied to investigate the carbohydrate/lectin interactions, which employed the DNA chips as anchoring platforms for immobilizing the carbohydrates (glycoconjugates). Following the initial works made in our lab, my thesis presented here address four main aims:

1) To further the validation of the DDI glycoarray efficiency.

2) To optimize and to develop DNA anchoring platforms for fabrication of new miniaturized DDI glycoarrays.

3) To study the binding efficiency of glycoconjugates with its corresponding model lectins (plant or bacteria lectins) in accordance with various parameters (numbers and charges of carbohydrates residues, nature of linkers, different spatial arrangements…).

4) Application of DDI glycoarrrays in discovery of new drugs for preventing influenza virus replication.

Chapter 1 reminds the basic notions in glycobiology, and gives a non exhaustive overview on the state of art concerning the investigations of glycoconjugates/lectins interactions. The current tools mostly used to determine the structure or elucidate the mechanisms of interactions are described. Glycoarrays, as high throughput analytical tools, are cited and their interests and limitations are mentioned. In particular, new glycoarrays based on DNA Directed Immobilization (DDI) and the two main strategies for using DDI glycoarrays are reported.

Chapter 2 describes the main materials and methods used in the study of the thesis.

Chapter 3 compares the binding affinities of glycoconjugates, which are immobilized by two different methods: DDI and direct covalent grafting, towards a plant lectin RCA120.

Chapter 4 describes the study of the affinities of different glycoclusters towards two lectins (PA-IL and RCA120) respectively and the development of a quantitative method (IC_{50} assay) performed on DDI glycoarrays.

Chapter 5 gives the last developments of high throughput miniaturized analytical systems based on DDI glycoarrays allowing multiplex analysis in one reactor and further validates the DDI strategies.

Finally, chapter 6 applies DDI glycoarray to discovery drugs of glycoconjugates blocking the hemagglutinine activities of influenza virus.

1 STATE OF ART

1.1 Carbohydrates and Glycoconjugates

1.1.1   Introduction and Classification of carbohydrates

Carbohydrates, also known as saccharides (from the Greek *sakcharon*), are the most abundant class of natural biological compounds found in organisms. Although carbohydrates can be viewed as hydrates of carbon according to their general formula of C_m (H_2O) $_n$, they are more specifically defined as polyhydroxy aldehydes or ketones and their derivatives.

There are many different classification schemes for carbohydrates. Based on the number of carbons present, carbohydrates can be divided into triose, tetrose, pentose, hexose, and so on. If considering the functional groups, four types can be classified: aldoses (contain the aldehyde group), ketoses (contain the ketone group), reducing carbohydrates (contain a hemiacetal or hemiketal group) and non-reducing carbohydrates (contain no hemiacetal groups). However, the most common scheme classified carbohydrates into four major categories according to the number of monomers (single carbohydrate units) as follows:

1)   *Monosaccharides*, formed by a single monomeric molecule, are the simplest carbohydrates. Unmodified monosaccharide usually has a general chemical formula $(C \cdot H_2O)_n$, and for example, the galactose and mannose have the same formula $C_6H_{12}O_6$. However, there are some exceptions that do not conform to the general formula, such as the fucose (a deoxy-sugar) which has a formula of $C_6H_{12}O_5$ (see Fig1-1) (*1*). Five- and six-member rings of monosaccharides are most commonly formed for chemical stability. Monosaccharides have D or L configuration which is determined by the configuration of the stereogenic center

furthest from the carbonyl group, and the configuration of a monosaccharide can be represented in Fischer or Haworth projections. However, for depicting pyranoses, the more structurally accurate chair representations are preferred (see Fig1-2) (*2*). All monosaccharides contain at least one asymmetrical (chiral) carbon and normally are optically active.
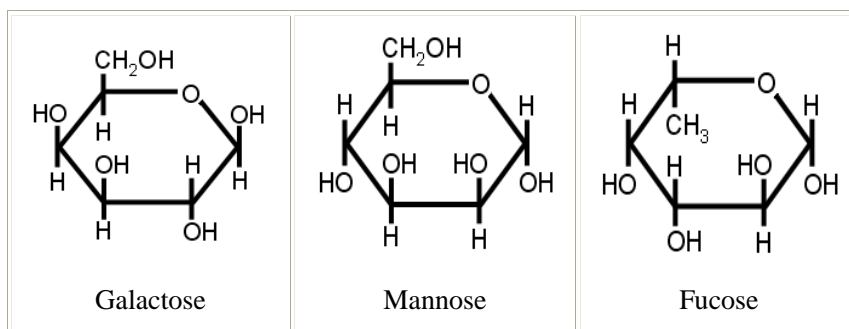
Fig1-1 Structures of galactose, mannose and fucose. Referred to http://www.ionsource.com/Card/clipart/carboclip.htm
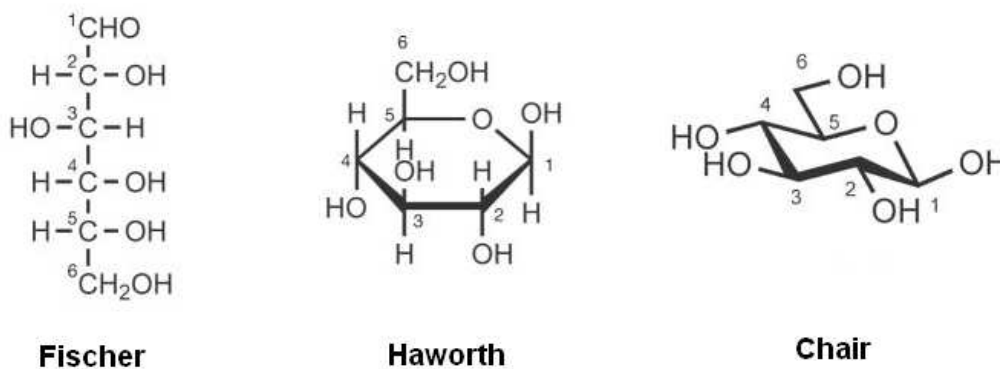
Fig1-2 Three representations of monosaccharide conformation: Fischer projection, Haworth projection and chair projection(2).

2) *Disaccharides* consist of two monosaccharide units linked together by a covalent bond. For instance, lactose, known as milk sugar, is formed by galactose and glucose.
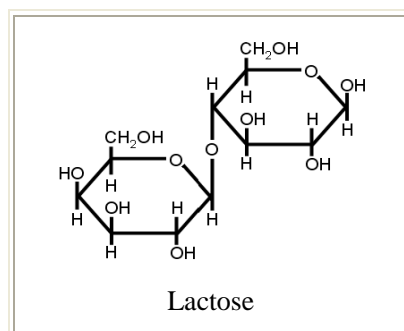
Fig1-3 Structures of lactose which is consisted of galactose and glucose residues. Adapted from http://sci-toys.com/ingredients/lactose.html

3) *Oligosaccharides* contain 3-10 monosaccharide residues that joined by glycosidic linkages and release 3-10 monosaccharides when hydrolyzed. Oligosaccharides are often found as a component of glycoproteins or glycolipids.

4) *Polysaccharides* are formed by more than 10 monosaccharides linked by glycosidic bonds. When they are composed by the same kind of monosaccharides, they are called homopolysaccharides, like starch, glycogen and cellulose (each of them are formed by hundreds of molecules of glucose linked by glycosidic linkages). If the polysaccharides molecules are formed by different kinds of monosaccharides, they are named heteropolysaccharides, e.g. hyaluronic acid.

Unlike nucleic acids and proteins, the building blocks (monosaccharides) of carbohydrates have multiple points of attachment, leading to not only linear but also highly branched structures. The structural complexity can be further increased by the possibility of α and β isomers at the anomeric centre which is a stereocentre created from the intramolecular formation of a ketal (or acetal) of a carbohydrate hydroxyl group and a ketone (or aldehyde) group. According to Lain *et al*, all possible structures of a hexasaccharide were found to be $>1.05 \times 10^{12}$ (*3*). The number of currently known natural N-linked glycans were reported more than 2000 (*4*) . Therefore the structures of carbohydrates are incredibly complex and diverse, which brings a great deal of obstacles for investigation of carbohydrates involving biological events.

1.1.2   Introduction and Classification of Glycoconjugates

Glycoconjugates are very significant compounds in biology and often found on the outside of cell membranes. They are important biomolecules, which consist of carbohydrates of varying size and complexity, attached to a non-sugar moiety as lipid or protein, so-called glycolipids, or glycoproteins (see Fig1-4).

For the glycoproteins, there are two types of glycosylation: 1) In N-glycosylation, the sugar chains can be added to the amide nitrogen on the side chain of the asparagine. 2) In O-glycosylation, the sugar chains can be added to the hydroxyl oxygen on the side chain of hydroxyproline, threonine, hydroxylysine, or serine.
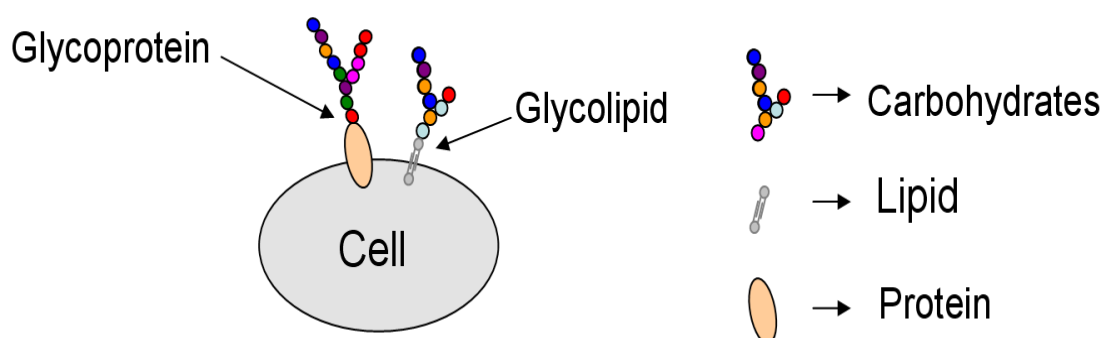
Fig1-4 Mimetic diagram of glycolipid and glycoprotein on cell surface.

1.1.3   Biological roles of carbohydrates and glycoconjugates

Carbohydrates and glycoconjugates are well known to play crucial roles during various biological processes. Besides the barrier, protective stabilizing and energy storing roles, they also participate in cell communication and adhesion, cell development and differentiation, immune responses, inflammation, tumor metastasis, bacterial adhesion and viral infections, etc... Varki has already made a comprehensive and all-embracing summary of the main roles of carbohydrates and glycoconjugates, which can be broadly classified into two groups (*2, 5*):

One group concerns the roles induced by the structural and modulatory properties. For instance,   the glycocalyx   and   the   polysaccharide   coats   can   provide

compacted   physical barrier for eukaryotic cells and prokaryotes respectively; glycans are also very important for the synthesis of polypeptides and the maintenance of protein solubility and conformation; the attachement of glycans with matrix molecules plays an important role in maintaining the structure, porosity, and integrity of the tissues; some of the glycan part of glycoproteins can protect the polypeptidic part from recognition by proteases or antibodies; glycosylation of a polypeptide can also mediate switching effect and "tuning" function. For example, the biological activity of haematopoietic growth factor will change with the degree of glycosilation (*6, 7*).

The other group concerns the role of specific recognitions (especially glycan-protein interaction) roles (*2*). It has already proved that glycans were specific ligands for cell-cell recognition and cell-matrix interaction. For example, the interaction of glycans with some selectin can mediate critical interactions between blood cells and vascular cells (*8*). Glycans are also specific ligands for cell-microbe interaction. One of the best characteristic examples is hemmagglutinin/sialic acid interaction which involve in the process of influenza virus entering into the host cell (*9-13*).

However, due to the enormous diversity of glycans in nature, the precise functions of lots of glycans are not yet uncovered.

1.2 Lectins

1.2.1   Introduction and classification of lectins

Lectins are one of the groups of glycan-binding proteins (GBPs), which can non-covalently bind to carbohydrates with high specificity. They are neither enzymes which have catalytic activity nor antibodies produced by immune response *(14, 15)*. Lectins are also referred to as hemagglutinins, or phytoagglutinins, because they were originally found in plants and can cause cell agglutination (*13, 14*).

Lectins can be obtained from almost all living organisms: microorganisms (viruses and bacteria), plants and animals *(13, 15-18)*, and they were initially studied in plants and invertebrates, then in vertebrates *(19-21)*.

The study of the molecular properties especially the structure of a biomolecule is one of the prerequisites for deep understanding of its activities at the molecular level. For the lectins, it had taken a long time, more than a century, to get the elucidation of structures since their first discovery was in 19th. The first pure lectin concanavalin A (ConA) was isolated in 1919 by Sumner (*22*). Until 1972, concanavalin A (ConA) was the first lectin whose primary sequence and 3D-structures were established by Edelman *et al*. (*23*). After that, lots of scientists were involved into this research area (*24-36*). As the processes of isolation and purification of lectins were usually time-consuming and low-yield *(37)*, the occurrence of recombinant and artificial lectins appears as an appropriate substitution. Ever since the recombinant lectin technology was first reported by Nagahora *et al*. in 1992 *(38)*, plenty of artificial lectins with new and variable carbohydrate specificities have emerged *(39-45)*. To date, about 200 lectins have established 3D structures (*13*) and almost the structure of 100 lectin/ligand complex have been elucidated (*46*). So far, the number of identified lectins is estimated to be approximately 1000 *(37)*, of which about 10 percent (~100) are commercially available (*47*).

Normally, most lectins were found to be naturally multivalent, containing two or more carbohydrate-binding sites. Some highly conserved amino acid residues which provide the framework required for binding were discovered in the carbohydrate-binding site (*15, 48, 49*). The specificity of carbohydrate-binding, however, is predicted to arise from a variability of amino acids within the other regions of carbohydrate-binding site (*15*). The carbohydrate-binding site mostly exhibits in the form of shallow depressions on the surface of the lectin. Carbohydrates interact with lectins commonly through hydrogen bonds, metal coordination, van der Waals forces and hydrophobic interactions *(50)*. Therefore, carbohydrate–lectin interactions are quite weak in comparison with other carbohydrate-protein interactions. The interaction affinity between lectin and monosaccharide is very low, usually in the

millimolar range (*51-56*). However, the weak binding of monosaccharides can be enhanced and compensated by multiple and simultaneous binding of many sugar residues (*57*). This affinity enhancement due to multivalent interactions, which is much larger than the effect of the increased concentration, is known as "cluster glycoside effect" (*54-56*).

There are several different classification schemes for the lectins:

I. Depending on the source/origin, lectins can be divided into three groups (*14, 15*): a) from animals; b) from plants; c) from microorganisms.

II. According to the monosaccharide ligand towards which they exhibit the highest affinity, lectins can be classified into five groups (*14*):

   a) mannose-specific lectins, b) galactose/N-acetylgalactosamine-specific lectins, c) Nacetylglucosamine-specific lectins, d) fucose-specific lectins and e) N-acetylneuraminic acid-specific lectins.

III. Based on structural features, lectins can be classified into three types (*14, 15*): a) simple lectins, which consist of a small number of subunits and contain an additional domain besides the carbohydrate-binding site(s); b) mosaic (or multidomain) lectins, which are composite molecules made of several kinds of protein domains, and only one of which possesses a carbohydrate-binding site; c) macromolecular assemblies lectins, which are filamentous organelles consisting of helically arranged subunits (pilins) assembled in a well-defined order, and usually exist in bacteria.

IV. According to the nature of the specific recognition of carbohydrates by cognate receptors, two general categories can be distinguished (*37, 58*): a) self recognition involving lectin as receptors within the same organism; b) non-self recognition, in which the receptors are mainly of plant, microbial or parasitic origin (hemagglutinins, adhesins, toxins, etc.).

V. According to structural and/or evolutionary sequence similarities, the lectins can be classified into several groups (*2, 56, 59, 60*): 1) β-prism lectins; 2) C-type lectins; 3) eel fucolectins; 4) ficolins-fibrinogen/collagen-domain-containing lectins; 5) garlic and snowdrop lectins and related proteins; 6)

galectins; 7) hyaluronan-binding proteins or hyaladherins; 8) I-type lectins; 9) amoeba lectins; 10) L-type lectins; 11) M-type lectins; 12) N-type lectin; 13) P-type lectins; 14) R-type lectins; 15) tachylectins from horseshoe crab Tachypleus tridentatus; 16) haevin-domain lectins; 17) Xenopus egg lectins/eglectins.

Thanks the large number of investigations, the important biological roles acted by lectins has been exhibited as reported on Table 1-1.

Microorganisms	Function of lectins
Amoeba	Infection
Bacteria (e.g. PA-IL, PA-IIL)	Infection
Influenza virus (e.g. HA)	Infection

a

Plants	Function of lectins
Various Plants (e.g. RCA120)	Defense
Legumes (e.g. Concanavalin A)	Symbiosis with nitrogen-fixing bacteria

b

Lectins from Animals	Function of lectins
P-type lectins, ERGIC-53, VIP-36	Intracellular routing of glycoconjugates
Calnexin, calreticulin	Molecular chaperones during glycoprotein synthesis
Asialoglycoprotein receptors, macrophage mannose receptor	Mediation of endocytosis
Galectins, sarcolectin, cytokines	Cellular growth regulation
Geodia cydonium galectin, other galectins,	Extracellular molecular bridging

interleukin-2	
Selectins, CD22, CD31, CD44	Cell–cell interactions for homing and trafficking
Galectins, heparin- and hyaluronic acid binding lectins	Cell–matrix interactions
Galectin-9	Scavenging of cellular debris; anti-inflammatory action
E- and P-selectins	Leukocyte trafficking to sites of inflammation
Man-6-P	Targeting of lysosomal enzymes
Siglecs	Cell-cell interactions in the immune and neural system
Spermadhesin	Sperm-egg interaction
Collectins	Innate immunity
Dectin-1	Innate immunity

c

Table1-1 Examples of the functions of lectins in accordance with the origin of microorganisms (a), Plants (b) and Animals (c) (61, 62)

1.2.2   Concanavalin A

Concanavalin A (Con A), extracted from jack bean (*Canavalia ensiformis*) by Sumner in 1919, is the first pure lectin (*22*). The structure of the protein was determined in the early 1970s (*63-65*). Native Con A exhibits dimmer-tetramer equilibrium in aqueous solution, and exists as a dimer around pH 5 (*66-68*). Each monomer of Con A consists of 237 amino acids (M_r 26500) and possesses one carbohydrate-binding site as well as a transition metal ion site (S1) (typically Mn^{2+}) and a Ca^{2+} site (S2) (*69*). They specifically bind with moderate affinity (K_d 120-500 µM) to the α anomers of D-mannose and D-glucose. Therefore, oligosaccharides

which containing these sugars will bind Con A with high affinity as a result of multivalent interactions (*70*).

The easy preparation of Con A and the large number of saccharides with which Con A can interact, have led to numerous studies on Con A (*15*). The applications of Con A include probing normal and tumor cell membrane structures and dynamics, studying glycosylation mutants of transformed cells, and yielding preparations of polysaccharides, glycopeptides and glycoproteins from Con A affinity columns etc. (*66*). Con A is also a lymphocyte mitogen which will induce proliferation of T lymphocytes. It induces mitogenicity by binding to specific receptors on T lymphocytes (*71*). Con A can also be used as neutralizing antibody to inhibit the HIV virus in in-vitro models of viral infectivity (*72*). In addition, Con A has been reported to perform as a stimulator of several matrix metalloproteinases (MMPs) (*73, 74*).

1.2.3   *PA-IL and PA-IIL*

Pseudomonas aeruginosa is a gram negative bacterium and an opportunistic pathogen (*75, 76*) responsible for the main morbidity and mortality in cystic fibrosis patients. PA-IL and PA-IIL (also referred to as LecA and LecB) are two main lectins that were extracted from *Pseudomonas aeruginosa*. In 1972 Gilboa-Garbera *et al* discovered and purified the lectin PA-IL by affinity chromatography (*77, 78*) . However, until 1982 the lectin PA-IIL was first extracted from the same bacterium cultured in a medium of different composition (*79*).

In the review (*80*) about the structures and specificity of the lectins from Pseudomonas aeruginosa, Imberty *et al*. have comprehensively summarized the properties of the two lectins. Herein some of the main characters were listed in Table1-2. PA-IL and PA-IIL are all Ca^{2+} dependent lectins consisted of four subunits (see Table1-2 and Fig1-3). PA-IL is a galactose specific lectin, however, its affinity for D-galactose is only in medium range, with K_a (association constant) of 3.4×10^4 M^{-1}obtained from an equilibrium dialysis study (*81*). PA-IIL has a high affinity for

L-fucose with K_a of 1.6×10^6 M^{-1} (*80*) .

The two lectins are primary virulence factors and cytotoxins of the *Pseudomonas aeruginosa*. They are also broad-spectrum agglutinins, which can cause bacteria to adhere to host cell leading to the respiratory epithelial damage during *Pseudomonas aeruginosa* respiratory infections (*82*) and changing the epithelial barrier function of the intestinal tract(*83*) and so on.

Main Characters	PA-IL	PA-IIL
Number of amino acids (without initiation Met)	121	114
Molecular mass (Da)	12,753	11,732
P*I(Isoelectric point)*	4.94	3.88
Oligomeric state	Tetrameric	Tetrameric
Cations observed in crystal structures	1 Ca^{2+} , Mg^{2+}	2 Ca^{2+} , Mg^{2+} and Zn^{2+}
Monosaccharide in the binding site	D-Galactose	L-Fucose D-Mannose

Table1-2 Comparison of the main properties PA-IL and PA-IIL, adapted from (80)

1.2.4 RCA120

RCA120 (Ricinus communis agglutinin 120), also called RCAI or ricin agglutinin, is an R-type lectin isolated from the seeds of the common castor bean *Ricinus communis* (*84-88*). It is a tetrameric hemagglutinin with a molecular weight of 120,000 Da composed of two types of subunit: A chains (Mr = 29,500) and B chains (Mr = 37,000), linked by a single disulfide bridge *(84, 86, 88)*. The A chain was found to be able to inhibit protein synthesis in eukaryotic cells (*89*); the B chain can specifically bind to β-D-galactosides (*86*). The structure of the RCA120 molecule is represented as B–A–A–B (*88, 90*) (see Fig1-5).Therefore, RCA120 is regarded as a bivalent lectin, which has the potential of binding two galactose residues at the same time (*91*). The pI (Isoelectric poin) of RCA120 is about 7.5-7.9 (*92*).

The lectin RCA120 has been considered to be a versatile tool for the detection of

galactose-containing oligosaccharides (*93*). Since 1980 RCA120 has already been used to study the glycoconjugates of nervous system (*94*). D'Agata and his co-workers have studied the recognition between RCA120 and a new mimic bioconjugate with Surface Plasmon Resonance imaging (*95*). RCA120 lectin can also be used as affinity adsorbent to selectively separate the glycoproteins and oligosaccharides (*96*). Recently this lectin was applied to the study of recognition with glycoconjugates on carbohydrate microarray (*97-99*).
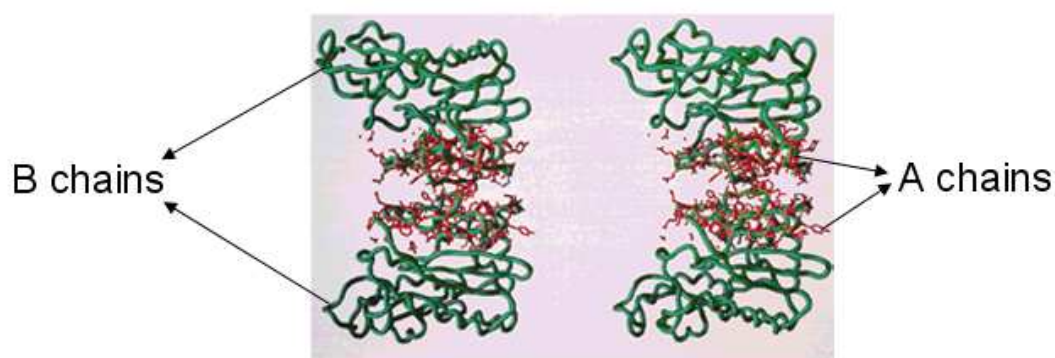
Fig1-5 Structure of the RCA120, the read chains represent A chains, the green chains represent B chains. Adapted from (90).

1.3 Traditional study methods

In this section, the main characterization techniques used for examining the glycan-protein interactions are described. They can be broadly classified into three categories: 1) biophysical methods, for example X-Ray Crystallography and NMR spectroscopy; 2) kinetic and near-equilibrium methods such as Isothermal Titration Calorimetry (ITC); 3) nonequilibrium methods such as Enzyme-Linked Immunosorbent Assay (ELISA)(*2*).

1.3.1   X-Ray Crystallography

X-Ray Crystallography is a technique that allows the elucidation of the

three-dimensional structure of biomolecules at atomic-level resolution. This is achieved by first crystallizing the purified biomolecule into ordered arrays and then using X-ray diffraction to analyze the crystals. X-rays are used because they have the same wavelength as the atomic separations so the crystal acts as a molecular diffraction grating to diffract a beam of X-rays, producing a diffraction pattern that can be captured and analyzed. A computer is then used to reconstruct the original structure. X-Ray Crystallography has been successfully employed to determine the structures of proteins (*100-102*), DNA (*103-105*), or other biomolecules. In addition, protein-ligand complexes (*106-108*) can also be determined using monochromatic X-ray diffraction techniques via kinetic trapping approaches

1.3.2   NMR Spectroscopy

Nuclear magnetic resonance is a phenomenon which occurs when the nuclei of certain atoms are immersed in a static magnetic field and exposed to a second oscillating magnetic field. Nuclear magnetic resonance spectroscopy uses the NMR phenomenon to study physical, chemical, and biological properties of matter. NMR spectroscopy was highly useful for the determination of carbohydrate and glycoconjugate sequences, conformations and dynamics (*109*). For example, in 1991 Michalski et al. analyzed the urinary fucosyl glycoasparagines in fucosidosis using 400 MHz 1H-NMR spectroscopy (*110*).

In NMR, the distances between the protons of a molecule can be obtained according to the assignment of the proton resonances by using multidimensional methods (e.g. determining the nuclear Overhauser effect). On the combination of the computational tools, the conformation of free-state glycans in solution can be imitated. There are three main methods NOESY (NOE spectroscopy), trNOESY (transferred rotating-frame Overhauser effect spectroscopy) and HSQC (heteronuclear single-quantum correlation) that can be employed to profile the conformation of bound glycans (2). Detailed insight into the binding event also can be obtained by

nuclear magnetic resonance (NMR) experiments. Angulo and his coworkers (*111*) have demonstrated the power of a combined transfer NOE/STD NMR approach for the analysis of carbohydrate–protein complexes. In spite of great informations achieved, NMR is limited by the degree to which small glycans structurally mimic the larger glycan–binding macromolecule (2).

1.3.3   *Isothermal Titration Calorimetry (ITC)*

ITC is a thermodynamic technique that directly measures the heat released or absorbed during a biomolecular binding event ITC can directly and simultaneously measure the binding constants (Ka), binding stoichiometry (n), enthalpy changes (ΔH), and entropy (ΔS) between two or more molecules in solution. Therefore, ITC can provide a complete thermodynamic profile of the interaction in one experiment.

In a typical ITC experiment (*112*), a solution of a one biomolecule ("ligand" such as a carbohydrate, protein, DNA molecule, etc) is titrated into a solution of its binding partner. The heat released upon their interaction (ΔH) is monitored over time. As successive amounts of the ligand are titrated into the ITC cell, the quantity of heat absorbed or released is in direct proportion to the amount of binding. As the system reaches saturation, the heat signal diminishes until only heats of dilution are observed. A binding curve is then obtained from a plot of the heats from each injection against the ratio of ligand and binding partner in the cell. The binding curve is analyzed with the appropriate binding model to determine Ka, n and ΔH.

ITC has a broad application, including protein-protein (*112, 113*), protein-DNA, protein-lipid target-drug, enzyme-inhibitor, antibody-antigen, and lectin-carbohydrate (*114-116*), etc. ITC is one of the strictest methods for determining the equilibrium binding constant between a glycan and a GBP (*114-116*). During the glycan-protein binding process, the glycan of interest is added with increments of concentration into a solution containing a fixed concentration of GBP. Then the heat is either generated or absorbed, so that the change of heat capacity of binding is determined. According

to the data obtained, the Kd, the enthalpy of reaction ∆H and the binding entropy ∆S can be determined. Therefore, it can provide a complete thermodynamic profile of the glycan-protein interaction in one experiment.

Nevertheless, this technology requires large quantity of materials (glycan and protein) to use a wide range of different glycans (2).

1.3.4   *Surface Plasmon Resonance (SPR)*

The SPR-based biosensors were first demonstrated by Liedberg et al. for monitoring biomolecular interaction in 1983 (*117*). SPR is an optical method that measures the change in refractive index near a sensor surface (*118*). In order to detect an interaction, firstly, one partner ligand need to be immobilised onto the sensor surface, and then its binding partner (analyte) is injected in aqueous solution through the flow cell, also under continuous flow. As the analyte binds to the ligand, the refractive index increases. This change in refractive index is measured as response in resonance units (RUs) versus time (a sensorgram) (*118*). The SPR method has been frequently used to measure carbohydrate-lectins interactions (*119-121*), for instance, it can be applied to analyze the structure of oligosaccharide (*122*), determine the lectin/carbohydrate specificity (*123, 124*) and screen lectin sources (*125*), as well as analyze mutant proteins and prognosticate cancer disease (*126, 127*).

SPR allows to follow the interaction of label-free biomolecules and to determine the kinetic and thermodynamic parameters of the reaction "in real time" (*128*). Therefore the information about the association and dissociation kinetics of the binding as well as the overall Ka and Kd can be achieved. The detection limit of SPR is from millimolar to picomolar, and the concentration range of analyte is 0.1–100 ×Kd (normal volume, 50–150 μl) (2). In addition, SPR has recently been extended to be an efficient tool to perform high-throughput analyses of biomolecular binding events (*129*).

Despite the advantages just mentioned, this technology also has some drawbacks,

such as the measure is often limited by the mass of the analytes; the detection sensibility of SPR is lower than fluorescence detection which has a detection limit of fM *(130-132)*; sometimes mass transport considerations may result in inaccurate Kd measurement.

1.3.5   Enzyme-Linked Immunosorbent Assay (ELISA)

Enzyme-Linked Immunosorbent Assay (ELISA) emerged in 1960s, and first reported by Engvall and Perlmann in 1971 *(133)*. The main procedures of a traditional ELISA are as follows: firstly, fix an unknown amount of antigen (or antibody) to the surface of a solid support; secondly, a specific antibody (or antigen) linked with an enzyme is added to bind to the fixed antigen (or antibody); finally, the enzyme is permitted to react with its substance and then the quantitative determination can be obtained according to the substance. There are a large number of categories of ELISA, while the most commonly used are three types: 1) the sandwich ELISA, 2) the indirect ELISA, and 3) the competitive ELISA *(134)*.

Currently, the traditional ELISA has been adapted to investigate glycans and glycan-binding proteins (GBPs) in various ways. Typically, GBP of interest is immobilized and the binding of glycans to the protein is measured, or the reagents are reversed *(2)*. ELISA has proven to be one of the efficient tools available to probe recognition processes of the protein/glycoconjugates (glycoprotein or glycolipid) and the glycoprotein/glycolipid interactions *(135)*. Alban and coworkers have developed an ELISA assay coating with sulfated polysaccharides to screen protein/sulfated carbohydrates recognition *(136)*. Gull *et al*. reported quantification of WGA (wheat germ) in serum in an application for lectin-mediated drug delivery by sandwich ELISA method *(137)*. Afrough and colleagues realized systematic optimization of ELISA method by the investigation of interactions of 21 biotinylated plant lectins with a glycoprotein *(138)*. In addition, ELISA methods utilizing immobilized lectins were also developed for detection of the glycoprotein of HIV and SIV *(139)*. Furthermore, the competition ELISA-type assays have been used to study the

carbohydrate-protein interaction. In this approach, competitive glycans are added and their competition for the GBP is measured by determining IC_{50} (*2*)

The advantages of this approach are the ability to perform a high-throughput assay by automated handling, to provide relative K_d and to define the relatively binding activity of a panel of glycans. The major disadvantages are that it was highly material-consuming and usually need chemical modification of glycans and proteins (*2*).

1.3.6 Enzyme-Linked Lectin Assay (ELLA)

Enzyme-Linked Lectin Assay is a method founded on modification of enzyme-linked immunosorbent (ELISA). This method was initially based on binding the lectin followed by binding an anti-lectin antibody *(140)*.

Normally, the approach of ELLA is based on binding of lectins to glycoconjugates immobilized on a microtiter plate; after the immobilization, the bound lectins are detected with labelled avidin *(141-143)*. ELLA has a huge number of applications. It can be used for quantitative determination of lectin receptors *(144-147)*; investigation of carbohydrate-lectin interactions *(148, 149)*; detection of disease-related alterations of glycoconjugates with lectins *(150-152)*, and so on.

1.4 Glycoarrays

1.4.1 Introduction

As mentioned above, the well-established traditional methods (e.g. ELISA, ITC, X-Ray Crystallography) mentioned above have been used for investigation of carbohydrate-protein interactions, most of them are highly time/material-consuming or labor intensive and not suitable for high-throughput analysis.

Glycoarrays, also referred to as carbohydrate arrays, consist of various carbohydrates immobilized on the surface of a support in a special array manner,

which mimic the natural presentation on cell surface (see Fig1-6). Glycoarrays have become a powerful platform which enable to fast and simultaneous profile interactions involving carbohydrates in a high-throughput and high-sensitivity approach using only minute materials (*153-156*).   The significant progress made in the past several years has brought glycoarrays to the study forefront of carbohydrate involving biological process.
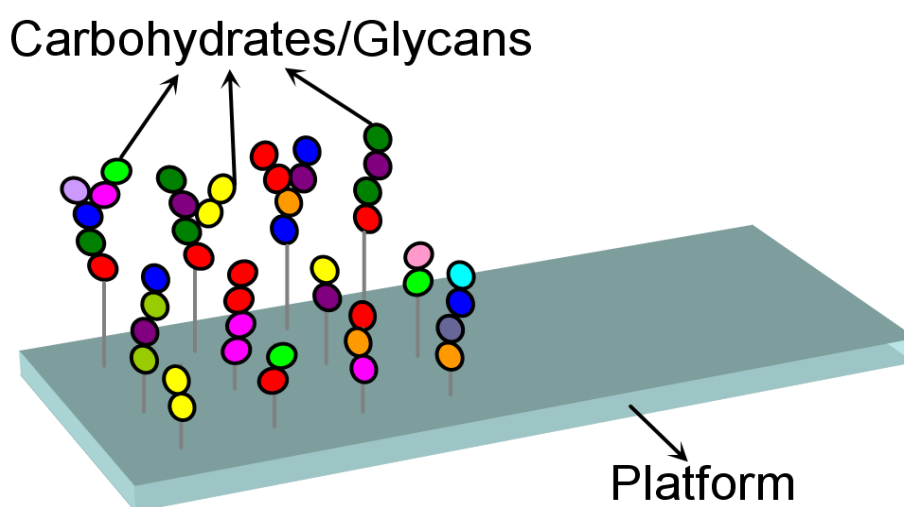
Fig1-6 Sketch map of Carbohydrates microarray.

In general, glycoarray fabrication and detection includes three main steps:

I.   ***Glycans preparation (to obtain the probe)***

The first step of glycoarray fabrication is to obtain available probes (glycans). There are two primary approaches: one is isolation from nature sources; the other is chemical or enzymatic synthesis (*157, 158*). The glycans acquired from isolation approach is usually limited, low-yield and not easy to purify (*159*). The synthetic approach obviously has potential to complement limited availability of glycans isolated from natural sources (*157, 158*). However, current carbohydrate synthesis methods are always time-consuming, labor intensive and mostly carried out in specialized laboratories (*157*). The development of a fully automated oligosaccharide synthesis is still a great challenge due to the inherent complexity of carbohydrates (*157*). In addition, the glycans obtained either from nature sources or synthesis

approach, sometimes, may required further modifications for the subsequent glycan immobilization and for detection (e.g. fluorescence labeling).

II.   *Glycan immobilization on the support*

Glycan efficiently immobilized on the surface of the support is a prerequisite for the successful preparation of glycoarrays (*160*). Therefore, the surface immobilization of oligosaccharides is a one of crucial steps of glycoarray fabrication. In order to set up an efficient glycoarray, many important factors should be taken into account (*99, 161*): the space between saccharides; the distance from the saccharide to the surface of the substrate; the orientation and spatial structure of the saccharide towards its target, etc. Plenty of immobilization strategies have been performed on diverse supports (see 1.4.2).

III.   *Binding detection*

For the binding detection on glycoarrays, three methods are most commonly used. They are 1) Fluorescence detection, 2) Surface plasmon resonance (SPR) detection and 3) Coupling of glycoarrays with mass spectrometry (MS).

Fluorescence detection is much more popular compared with other two methods. It has a high sensitivity and can perform semi quantitative measurement. Fluorophore-labelled proteins and glycans have been widely used. However, protein labeling often results in protein denaturation and maybe interference with carbohydrate ligand binding. Kawahashi *et al*. have developed a method to prevent denaturation of proteins by incorporating a fluorophore-puromycin conjugate into proteins at the C-terminus (*162*).

Surface Plasmon Resonance (SPR) can also be applied to glycoarrays detection (*163-165*). SPR enables reading an array format in real time, providing both kinetic and affinity constants of interactions (*166-168*). Its high sensitivity allows the detection of low-affinity binding. For instance, SPR detection was successfully used for the recognition study of glycans by multiple plant lectins (*167*). SPR imaging (SPRi) studies have been applied to the determination of carbohydrate-lectin interactions (*169, 170*). However, as mentioned before, SPR has less sensitivity than the fluorescence detection method. Although glycan-based biosensors have been

reported (*171, 172*), to our knowledge no electrochemical methods were applied to the detection of glycoarray.

Mass spectrometry (MS) not only can be used for characterization and sequencing of carbohydrate and glycoconjugates (*173-176*) but also for detecting the modification of carbohydrates on glycan microarrays (*177*). Coupling of glycan arrays with mass spectrometry (*178*), tremendously enhances abilities in the discovery of new glycan-binding ligands. In addition, MALDI-TOF-MS technology is also considered to be one of promising ways for glycoarray detection (*179*).

1.4.2 *Classification of glycoarray*

I. Based on the structural characteristics of the carbohydrates displayed on chips, carbohydrate microarrays can be classified into three types (*158, 180*): 1) monosaccharide chips (*154*), 2) oligosaccharide chips (*155, 181*), and 3) microarrays of carbohydrate-containing macromolecules (*153*), which include polysaccharides and various glycoconjugates .

II. Various types of supports substrate can be used for carbohydrate microarrays depending among others on the type of transducers (detection) (*157, 158*): Nitrocellulose membrane chips (*155*), microtiter plate (*177*), modified black polystyrene slide, glass slide (*99*), plastic chips (*182*) and gold surface slide (*154, 183*), or chips based on beads in fibre-optic wells (*184*), etc.

III. Considering the immobilization strategies for carbohydrates on a solid surface, general categories of carbohydrate microarrays can be distinguished (*160*):

1) Noncovalent adsorption (Physisorption).

Noncovalent adsorption is a relatively simple immobilization method because of no need of modified surface and chemical-link techniques, however it usually requires materials large enough to provide tight adsorption (*160*). There are two subtypes, one is nonspecific and noncovalent adsorptions on the solid

surface, e.g. Wang *et al* fabricated a microbial polysaccharides chip on glass slide by nonspecific physical adsorption (*153*). The other is site-specific but noncovalent immobilization of chemically conjugated carbohydrates, e.g. Fukui and his co-workers immobilized neoglycolipids on a nitrocellulose and obtained efficient immobilization via this approach (*155*).

2) Covalent grafting.

The covalent immobilization is broad-spectrum method and more suitable than the noncovalent approach (*185*). This approach also can be divided into two subgroups: One is covalent immobilization of chemically unmodified carbohydrates or glycoconjugates on the modified surface (*168, 186-188*), the most common method consists in using the reducing end of the saccharides as anchoring point, which often results in the opening of the reducing end ring and influence the whole structure of the glycoconjugate (*186*). The other is covalent immobilization of chemically conjugated carbohydrates or glycoconjugates on the modified surface (*185*). This strategy has been far more documented in the literature. Lots of reactions were employed for carbohydrate immobilization, such as through photochemistry (*189-193*), reaction of amines with activated esters (*194*), aldehydes (*195*) or epoxy-modified substrates (*196*), reaction between a cyanuric chloride and an aminophenyl group (*197*), reaction of thiols with double bonds (*198-200*), or thiol-derivatised surfaces (*201*), cycloaddition reaction (*154, 202*), Staudinger ligation (*203*).

3) Specific biological based interactions

In this approach, carbohydrate can be immobilized through biotin/streptavidin interaction (*204, 205*), or by DNA-directed immobilization (DDI) through DNA/DNA hybridization (*97-99, 206*) has been reported. That implies that specific biological tag (biotin or single strand DNA) was previously coupling with carbohydrate whereas the surface of array was (bio) functionalized with streptavidin or complementary single strand DNA respectively.

1.4.3   Application and limitation of glycoarray

As the most promising and advanced technology, glycoarrays have become powerful tools not only for basic biological research, but also for medical diagnosis. Glycoarrays have very broad applications:

- Carbohydrate microarrays can be utilized to determine the binding profile of glycan-binding proteins and identify novel carbohydrate-binding proteins (*12, 200, 207*);

- They can be used to characterize carbohydrate-cell interactions, such as detection the bacteria in blood(*208*), typing of the influenza strains (*12*), and study of the interactions between carbohydrates and eukaryotic cells (*209*);

- They may provide high-throughput screening of inhibitors that will disrupt the carbohydrates-protein interactions for drug discovery (*202*);

- They can be applied to assay the activity of the enzymes (*161*);

- And they also can be exploited to profile of carbohydrate–antibody interactions and to detect of specific carbohydrate-binding antibodies for the diagnosis of diseases (*153, 210*).

Currently, although glycoarray technologies have large-scale applications and have attracted more and more scientists involving into the glycoarray research fields, this technology is still in its development and validation phase. Assortments of sophisticated platforms of glycoarray have been reported, no one yet dominates (*179*). Many limitations and challenges still remain. Firstly, the available sources of carbohydrates for fabrication of glycoarray have been far from exploited (*160, 211*). The development of new isolation and purification method (isolate carbohydrates or glycoconjugates from nature sources) and the establishment of new synthetic strategies are two crucial approaches to circumvent the obstacle. Moreover libraries of carbohydrates, antigens, antibodies, enzymes and lectins should be established to make these materials available to carbohydrate researchers (*180*). Secondly, glycoarray should be improved for detecting proteins with weak binding affinities (e.g.

lectins) *(160),* the presenting methods of carbohydrates (carbohydrate printing) on the support, thereby, need to be developed and optimized. Thirdly, a useful glycoarray also requires an efficient detection method, therefore the improvement of detection technologies is also very important *(160).* Finally, concerning the determination of glycoarray information, different labs usually use different formats and standards. As a consequence, direct comparisons between platforms are largely lacking and therefore glycan arrays still serve primarily as a qualitative tool. That is why standardized informations and results are strongly desired to facilitate meta-analyses *(179, 211).*

1.5 Glycomimetics

Despite the increased awareness of the crucial function of carbohydrates, the investigation of biological events involving carbohydrates is extremely difficult and formidable. This is mainly ascribed to the unique structural complexity and diversity of carbohydrates mentioned before. The intrinsic character of carbohydrate structures render the isolation of pure, structurally defined glycan compounds from natural sources hard and cumbersome. In addition, the glycans cannot be cloned, and they are production of the intricate biosynthetic action of multiple glycosyltransferases and many other modifying enzymes. Synthetic methods, thereby, provide a great alternative allowing for the preparation of synthetic oligosaccharides or glycoconjugates. As mentioned before the frequent branching and linkage diversity of carbohydrates result in greater structural complexity in comparing with nucleic acids and proteins. Due to the incredible complex structures of oligosaccharides, it is very hard to synthesize compound with structure and functions identical to glycans obtained form nature. For detailed biological investigation the natural glycans may not have enough chemical stability and bioavailability *(212).* Therefore, there is an urgent need to develop new method to address the problem. A combinatorial approach to synthesize diverse artificial compounds with simple building blocks and possessing

similar or even better functions in a rapid manner seems to be an appropriate choice (*213*). For instance, a fast and flexible glycomimetics synthetic strategy using microwaves and "click chemistry" was established by Vasseur's team (*214*), which permit introducing different number of various carbohydrate residues and enable to adjust the physico-chemical and structural parameters such as the spaces between every two residues, the hydrophilic/lipophilic balance, charge... Moreover, they can also synthesize single strand DNA coupled with glycoconjugates and added a fluorescent tag (see Fig1-7).
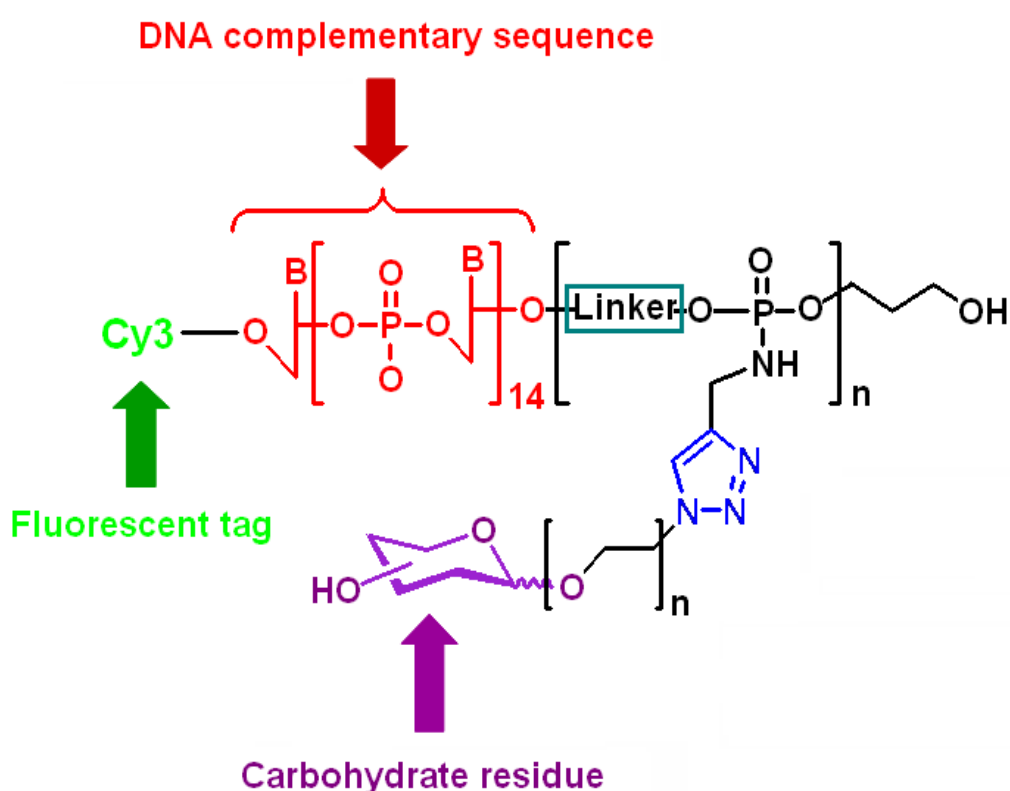
Fig1-7 Schematic structures of a kind of glycomimetics (carbohydrate/DNA conjugates), adapted form (206, 214)

Glycomimetics, as structurally modified simple analogs (mimics) of carbohydrates, then appeared to meet the requirement. Those glycomimetics can also mimic the bioactive function of carbohydrates (see Fig1-8). Over the years, tremendous progress has been made toward the synthesis of glycomimetics (*215-224*). Plenty of

glycocomimetics have applied to drug design or discovery (*225-229*), study the interactions with carbohydrate-binding proteins (*215, 230-235*), and establish neoglycopeptide libraries or carbohydrate-oligonucleotide conjugates (*55, 214, 236-239*), etc.
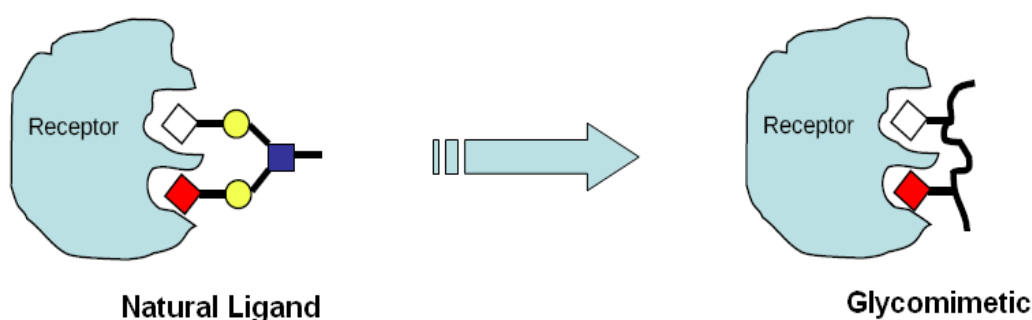
Fig1-8 Sketch map of natural glycoconjugate replaced by glycomimetic.

1.6 DDI glycoarray

1.6.1 Introduction

As noted before, the immobilization of glycans is one of the important steps for fabricating a useful glycoarray. An efficient immobilization should provide ideal orientation and density of the glycans fixed at the surface of the support and take full benefit of the "cluster effect" (*206*). The "cluster effect" also referred as the "cluster glycoside effect" is a phenomenon where the multivalent glycoside ligands show enhanced activity compared to the corresponding monovalent ligand on a per mole of saccharide, or valence-corrected basis (in other words which is substantially higher than the effect of increased concentration) (*240*). In addition to the two common immobilization methods, physisorption and chemical covalent immobilization, DDI, as a new immobilization strategy, was applied to the glycoarray.

DNA-directed immobilization (DDI) method takes the advantage of specific Waston-Crick base pairing to immobilize biomolecules coupled with a single-stranded DNA moiety by providing a specific recognition site for complementary nucleic acids

on a solid support *(241, 242)*. The rigid structure of the DNA double helix might guarantee proper orientation of the probe (*241*). In addition, using the DNA chips as immobilization matrices, DDI method can offer parallel immobilization of various probes under chemically mild conditions. The DDI was first introduced into the fabrication of protein microarray in order to study biological events involving proteins and peptides (*243, 244*). In 2004, Wacker and coworkers made a comparison of three antibody immobilization methods on microarray: direct covalent immobilization, biotin/streptavidin interaction mediate immobilization and DDI. The results showed that the DDI led to the most efficient antibody immobilization. Moreover, DDI was also successfully applied to immobilize cell-surface ligands for building a live-cell microarray *(245)*.

DDI was first introduced to glycoarray fabrication by Chevolot *et al.* in 2007 *(246)*. In their studies, using DNA chips as universal anchoring platforms, the glycoconjugates coupled with a complementary DNA tag were addressed onto the surface of the microarray (see Fig1-9).

(a)   *(b)*
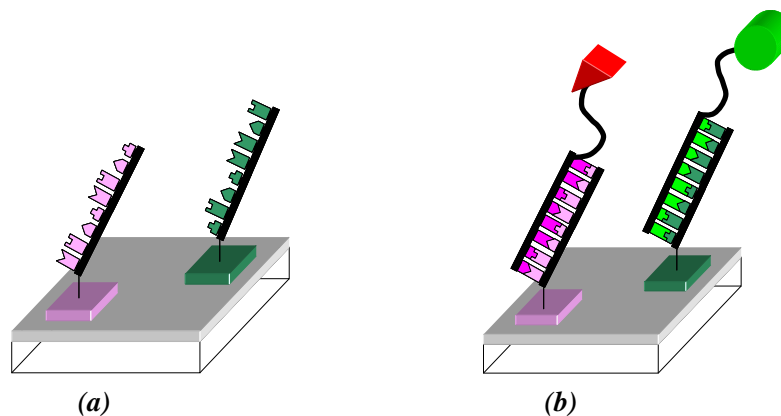
Fig1-9 Principle of DDI Glycoarrays: (a) a classical DNA chip is used as an anchoring platform. Each spot contains one type of single strand DNA sequence; (b) Glycoconjugates bearing a complementary single strand DNA sequence are immobilized through the DNA hybridization. Adapted from (206)

In addition, a Cy3 tag was introduced into the glycommimetics fabrication in order to visualize the relative surface density of the glycomimetics and control the quality of the immobilization. Glycomimetics bearing one or three galactose residues

with two different linkers (L1: Cyclohexanedimethanol and L2: Tetraethyleneglycol) were efficiently immobilized onto the surface of the chip and tested with respect to the Cy5-labelled RCA 120 lectin (see Fig1-7). The DNA-directed immobilization (DDI) of glycoconjugates (*97-99, 206*) has been proved to be very efficient, site-selective and reversible immobilization methods.

1.6.2 Two test strategies of DDI glycoarray

1.6.2.1 "On-chip" approach

The first strategy of DDI glycoarray is the "on-chip" approach. In this strategy, a DNA chip would be fabricated by printing ssDNA (single-stranded DNA) onto the surface of the substrate. Then the Cy3 labelled glycoconjugates bearing the complementary ssDNA would be immobilized on the desired spot of the surface by hybridization with the ssDNA printed on the substrate. Finally, the Cy5 labelled lectins would interact with the corresponding glycoconjugates on the chip and be prepared for detection (see Fig1-10).
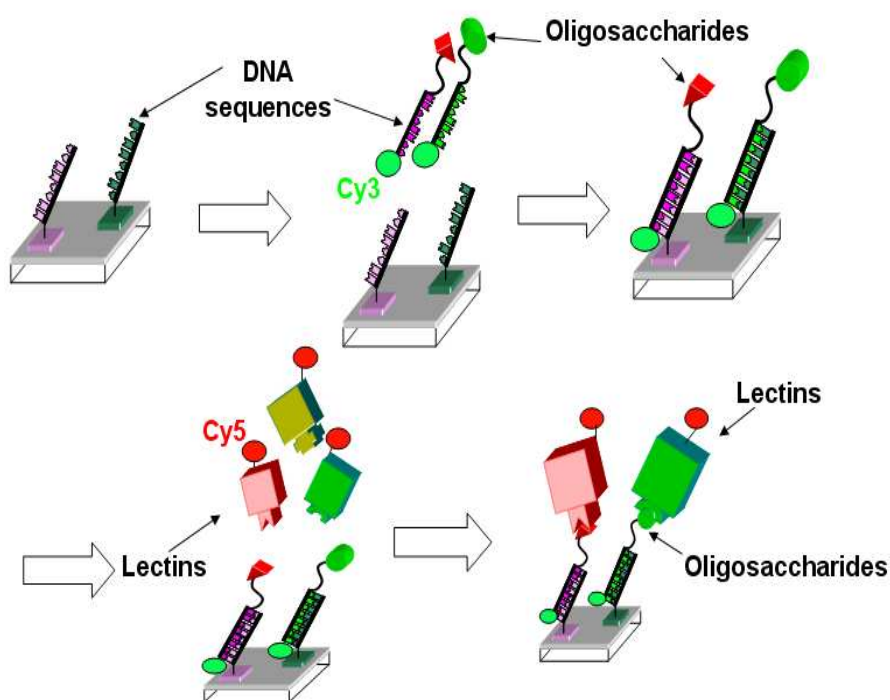
Fig1-10 Sketch map of "on-chip" approach of DDI glycoarray fabrication. Adapted from(206)

1.6.2.2 "In-solution" approach

The "in-solution" approach is the second strategy for DDI glycoarray fabrication. In this approach, the first step is also to fabricate a DNA chip. The second step however, unlike the "on-chip" approach, the interaction of Cy5-labled lectin with Cy3-labelled glycoconjugates would performed in the solution and the resulting lectin/glycoconjugate complex would be addressed to the corresponding spots on the substrate by DNA hybridization (see Fig1-11).
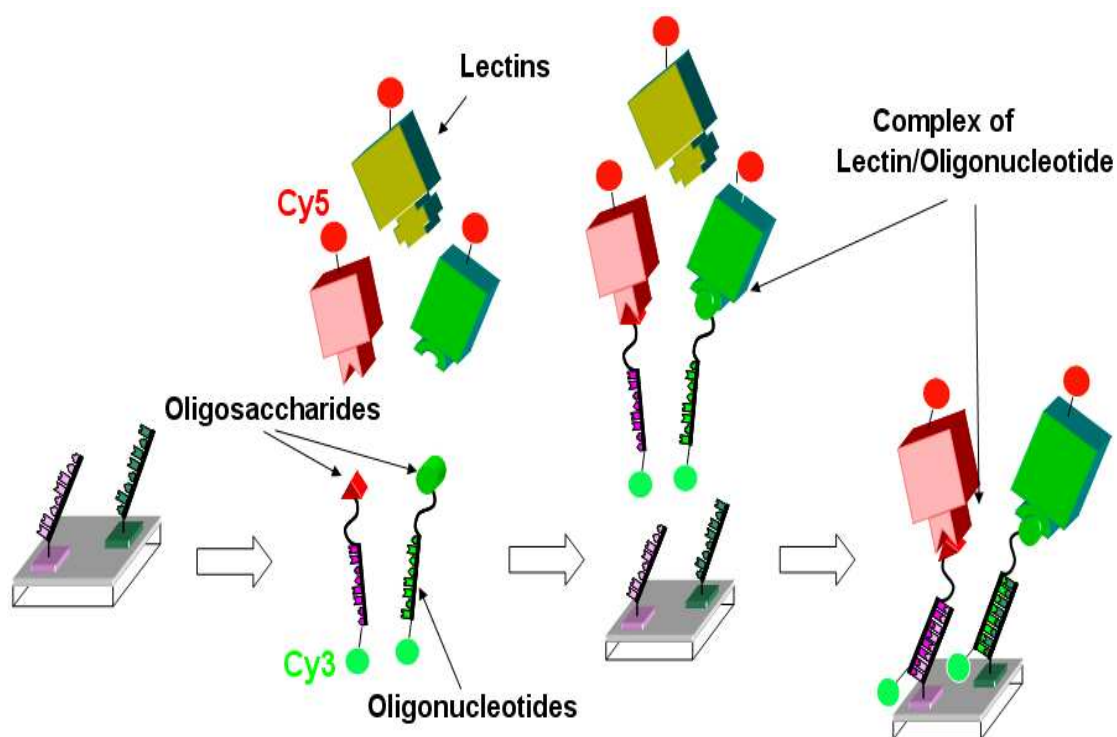
Fig1-11 Sketch map of "in-solution" approach of DDI glycoarray fabrication. Adapted from (206)

1.6.2.3 Advantages and limitations of DDI glycoarray

A first proof of this concept has been made with "glycoconjugate/ RCA 120 lectin" as model system. The advantages of DDI have been demonstrated as follows: very minute concentration of material (glycoconjugates) is necessary for the detection, as low as 0.5µM (*99*) and the detection limit is in the range of 2-20nM (*206*).

Moreover, because the single DNA strands were covalently grafting on the surface chip, the subsequent DDI glycochip can be reusable due both to the reversibility of DNA hybridization (*206*) and the robustness of chip towards the stringency washings. As quality control of glycocomimetics immobilization and recognition with the lectin can be realized by introducing the fluorescence labelling Cy3, Cy5 and Alexa647 (*97-99, 206*), DDI glycoarray can take full advantage of the detection tools available for DNA-chip.

Although DDI glycoarray has many advantages mentioned above, some drawbacks still remain. For example, like other glycoarrays DDI glycoarray can be also limited by the available glycan materials (however thanks to the glycomimetic synthetic strategy developed by IBMM, this can be circumvented); the fluorescence detection is only a semi quantitative measurement. Therefore, more efforts still should be taken to improve the power of DDI glycoarray. Indeed in Chevolot et al (*206*), the device was developed with only one DNA tag and validate with a model plant lectin.

1.7 Objectives of the study

The main goal of the thesis is to develop a device for the screening of carbohydrates/lectins interactions. This implies to improve and optimize the DDI glycoarray study method. For this, we will compare two methods of glycomimetics immobilization: the DDI immobilization and the covalent immobilization. Next in order to get semi-quantitative insight on the affinity of studied interaction an IC_{50} assay was developped. IC_{50} assay is a commonly used method for the measurement of the effectiveness of a substance (inhibitor) in inhibiting biological interactions, the IC_{50} value is the concentration of an inhibitor where the interaction is reduced by half. In order to improve the high throuput capacity of DDI glycoarrays and reducing the required materials and experiments, several glycomimetic/lectin interactions are expected to be performed in parallel in one reactor of DDI glycoarray. Therefore the ability to multiplex the analysis and to miniaturize the glycochips will be the main

challenges of this work.

In order to validate the progress in glycoarray technology, we will investigate the interactions of different glycoclusters with various properties (structure, residue, charge…) towards two lectins (PA-IL and RCA120) respectively. RCA120 was a model lectin widdly reported in literature. PA-IL is suspected to be in volved in the adhesion of *Pseudomonas aeruginosa* to the host cells. The affinity studies will be performed either by "on chip" or "in solution" approach.

At last, DDI glycoarray was applied to investigate carbohydrate/hemagglutinin with whole viruses interactions in order to i) discover new glycomimetic ligands of Hemagglutinins (HA) blocking their activity, ii) rapidly diagnose the infection by influenza viruses in the population at risk and iii) distinguish the human and avian influenza viruses.

2 MATERIALS AND METHODS

In this chapter, the main experimental materials and methods used throughout this dissertation (Chapter 3, 4, 5) are listed and described. This includes the materials and methods employed in the construction of DNA anchoring platform, in the fabrication of DDI glycoarrays and in the detection procedures of the glycoconjugate/lectin biological interactions. It would provide a more detailed framework and overview of the study.

2.1 Glycomimetics

All glycoconjugates (glycomimetics) mentioned in this thesis were drawn in Annexe1. Most of the glycoconjugates were synthesized by our co-workers(*97-99, 206*) in the IBMM of Université de Montpellier 2 and ICBMS of Université lyon 1, except the two kinds of calix[4]arene-based glycoclusters of Glycoconjugate 6 and 7 (see Annexe1), which were provided by the IBMM and the University of Ferrara (*98*). The experimental procedure for the synthesis of Glycoconjugate 1-9 are showed in Annexe 2. The synthesis of Glycoconjugate 10-24 have not been published yet. In consequence the experimental procedure for their synthesis is not given.

Herein, we recall the general structure of glycoconjugates.

Tables 2.1 and 2.2 summarize the main characters of the glycoconjugates used (name, geometrical structure, linker, charge, potential target lectin…). Thanks the high flexibility in the glycoconjugate building methodology, various geometrical structures (comb like, antenna, and crown glycocluster using calixarene core) of glycoconjugates were provided by our partners. Table 2.3 relates to the properties of their DNA tag (name, sequence, GC%, and melting temperature Tm).
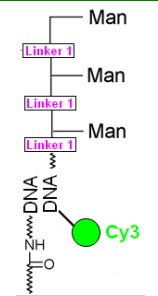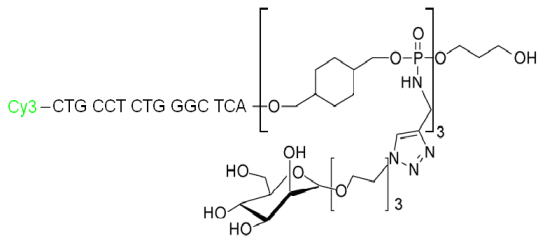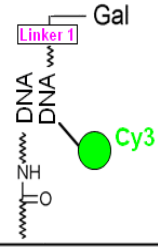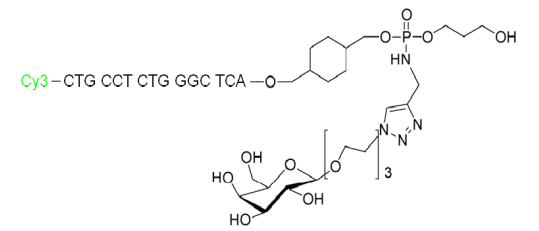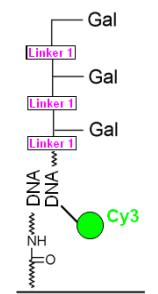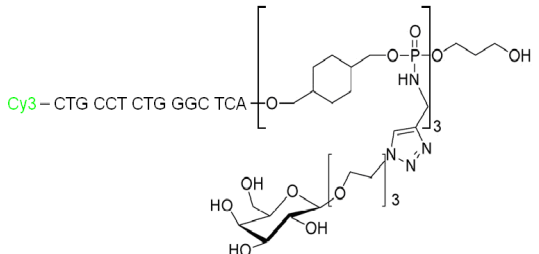
Name	Internal Reference	Molecular Schema	Structure	Linker [a]	Charge (number)
G 1 **Molecule 1 (in chapter 5)**	3ManDMCH			Cyclohexanedimethanol （DMCH）	0
G 2	1GalDMCH			Cyclohexanedimethanol （DMCH）	0
G 3	3GalDMCH			Cyclohexanedimethanol （DMCH）	0

Table2-1 Main characters of glycoconjugates—(I) Linker [a] refers to the Linkage between every two phosphodiesters of the structure of the glycoconjugates not
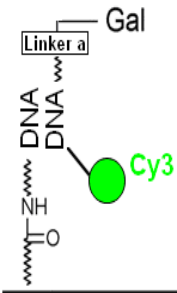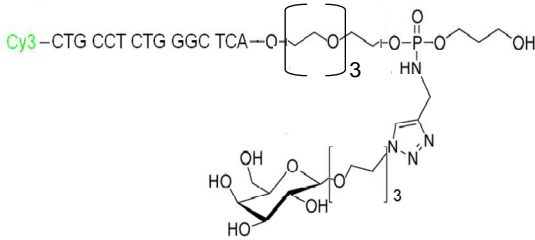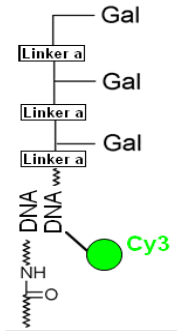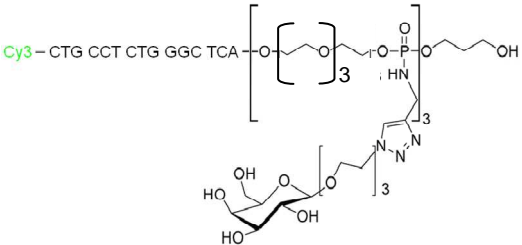
Name	Internal Reference	Molecular Schema	Structure	Linker	Charge (number)
G 2a	1Gal TEG			Tetraethyleneglycol (TEG)	0
G 3a	3Gal TEG			Tetraethyleneglycol (TEG)	0

Table2-1 (Continued).
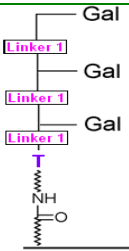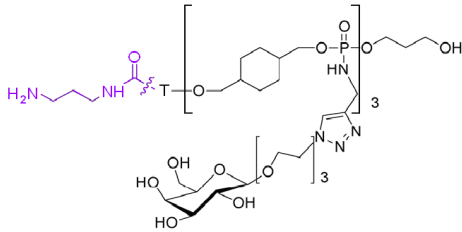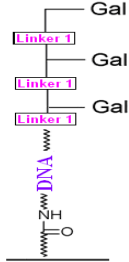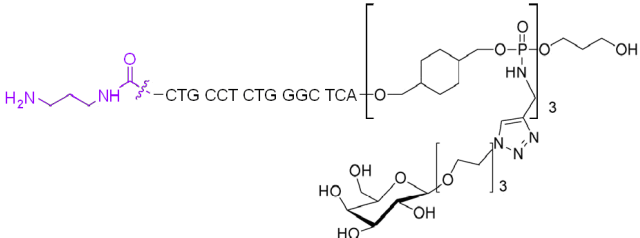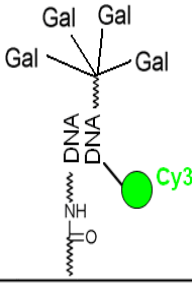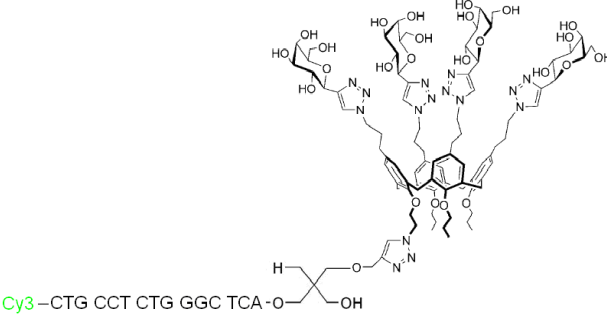
Name	Internal Reference	Molecular Schema	Structure	Linker	Charge (number)
G 4	Molecule 1			Cyclohexanedimethanol（DMCH）	0
G 5	Molecule 2			Cyclohexanedimethanol（DMCH）	0
G 6	LM1 (4Gal 1calixarene)			Trishydroxymethylethane	0
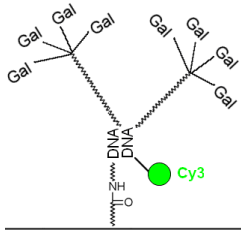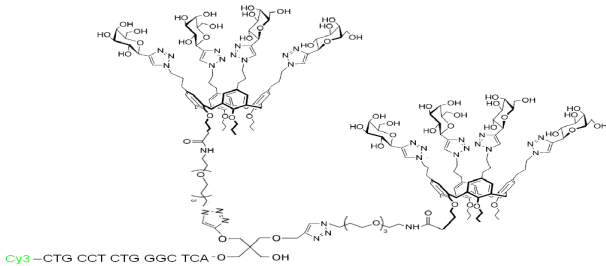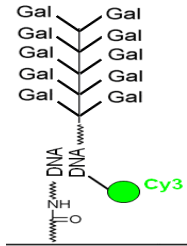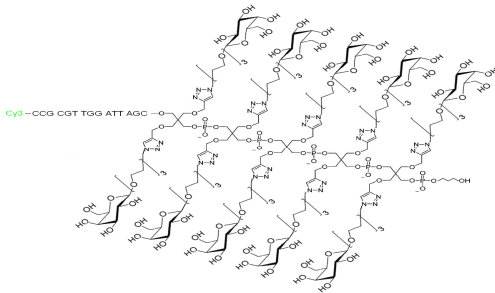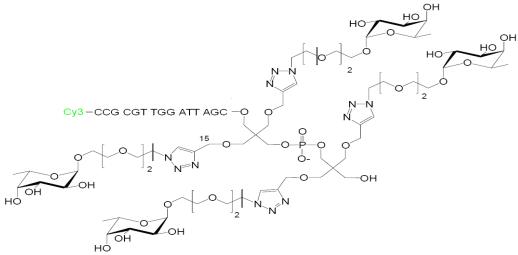
Table2-1 (Continued).

Name	Internal Reference	Molecular Schema	Structure	Linker	Charge (number)
G 7	LM2 (8Gal 2calixarene)			Trishydroxymethylethane	0
G 8	10Gal penta			Pentaérythritol	-(5)
G 9	4Fucose	————————		Pentaérythritol	-(1)

Table2-1 (Continued).

Name	Internal Reference	Molecular Schema	Structure	Linker	Charge (number)
G 10 **Molecule 5 (in chapter 5)**	FM1DMCH			Cyclohexanedimethanol （DMCH）	0
G 11 **Molecule 2 (in chapter 5)**	GWP40			Trishydroxymethylethane	-(3)
G 12 **Molecule 3 (in chapter 5)**	FM2TMOE			Trishydroxymethylethane	0

Table2-1 (Continued).
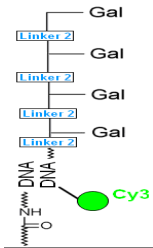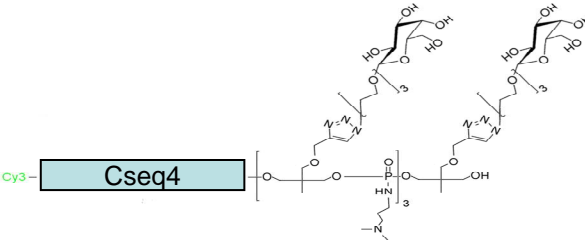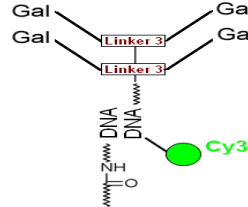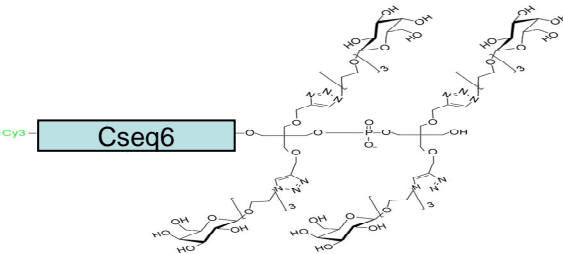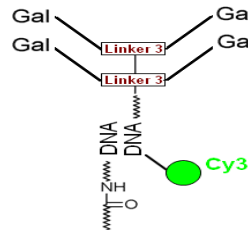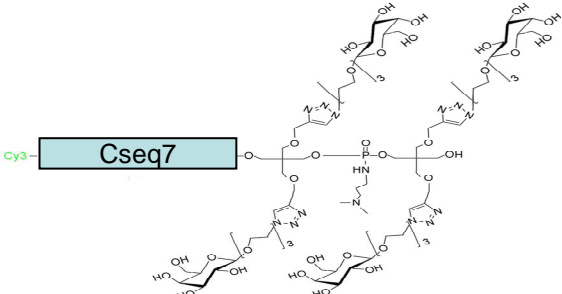
Name	Internal Reference	Molecular Schema	Structure	Linker	Charge (number)
G 13 **Molecule 4 (in chapter 5)**	FM3TDMAP			Trishydroxymethylethane	+(3)
G 14 **Molecule 6 (in chapter 5)**	FM1PEPO			Pentaerythritol	-(1)
G 15 **Molecule 7 (in chapter 5)**	FM3PEDMAP			Pentaerythritol	+(1)
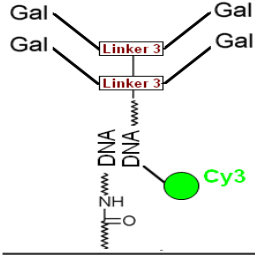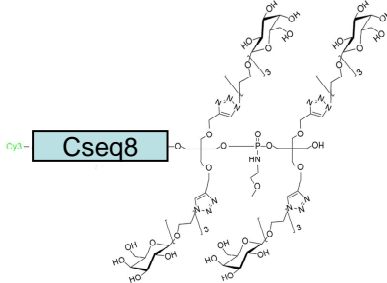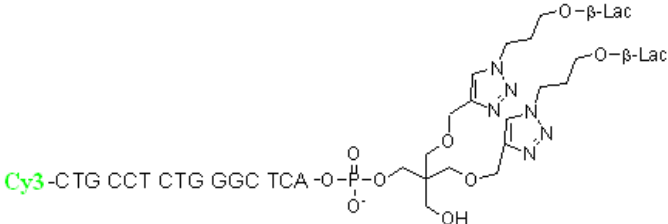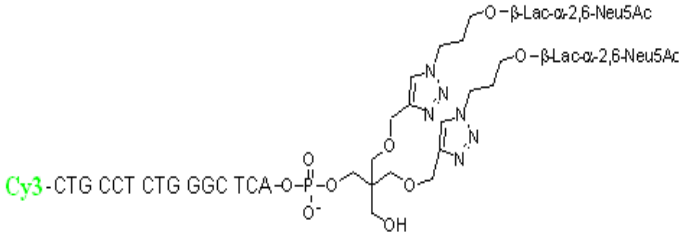
Table2-1 (Continued).

Name	Internal Reference	Molecular Schema	Structure	Linker	Charge (number)
G 16	FM2PEMOE			Pentaerythritol	0
G 17	**GWP50L**			Pentaerythritol	0
G 18	GWP50S			Pentaerythritol	0

Table2-1 (Continued).

Name	Internal Reference	Molecular Schema	Structure	Linker	Charge (number)
G 19	GWP45	——————		Tetraethyleneglycol	-(4)
G 20	GWP48	——————		Tetraethyleneglycol	0
G 21	GWP60	——————		Cyclohexanedimethanol（DMCH）	-(7)

Table2-1 (Continued).
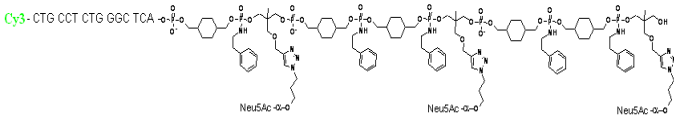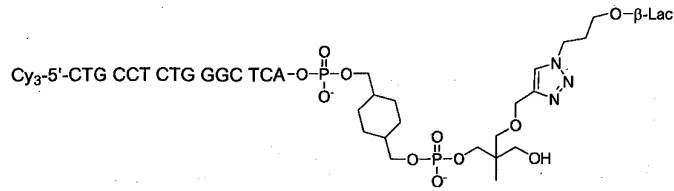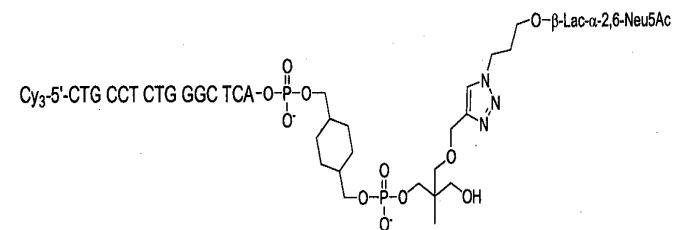
Name	Internal Reference	Molecular Schema	Structure	Linker	Charge (number)
G 22	GWP63	——————		Cyclohexanedimethanol （ DMCH ）	0
G23	73A	——————		Cyclohexanedimethanol （ DMCH ） and Trishydroxymethylethane	-(1)
G24	73B	——————		Cyclohexanedimethanol （ DMCH ） and Trishydroxymethylethane	-(1)

Table2-1 (Continued).

51

Name	DNA Tag [a] (Complementary sequences)	Sequence [b]	Carbohydrate residue (number)	Potential lectin affinity [c]
G 1	DNA Tag 1 (Cseq 1)	Sequence 1	Mannose (3)	————
G 2 (G 2a)	DNA Tag 1 (Cseq 1)	Sequence 1	Galactose (1)	RCA 120 & PA-IL
G 3 (G 3a)	DNA Tag 1 (Cseq 1)	Sequence 1	Galactose (3)	RCA 120 & PA-IL
G 4	————	————	Galactose (3)	RCA 120 & PA-IL
G 5	DNA Tag 1 (Cseq 1)	————	Galactose (3)	RCA 120 & PA-IL
G 6	DNA Tag 1 (Cseq 1)	Sequence 1	Galactose (4)	RCA 120 & PA-IL
G 7	DNA Tag 1 (Cseq 1)	Sequence 1	Galactose (8)	RCA 120 & PA-IL
G 8	DNA Tag 9 (Cseq 9)	Sequence 9	Galactose (10)	RCA 120 & PA-IL
G 9	DNA Tag 9 (Cseq 9)	Sequence 9	Fucose (4)	PA-IIL
G 10	DNA Tag 5 (Cseq 5)	Sequence 5	Galactose (4)	RCA 120 & PA-IL
G 11	DNA Tag 2 (Cseq 2)	Sequence 2	Galactose (4)	RCA 120 & PA-IL
G 12	DNA Tag 3 (Cseq 3)	Sequence 3	Galactose (4)	RCA 120 & PA-IL
G 13	DNA Tag 4 (Cseq 4)	Sequence 4	Galactose (4)	RCA 120 & PA-IL
G 14	DNA Tag 6 (Cseq 6)	Sequence 6	Galactose (4)	RCA 120 & PA-IL
G 15	DNA Tag 7 (Cseq 7)	Sequence 7	Galactose (4)	RCA 120 & PA-IL
G 16	DNA Tag 8 (Cseq 8)	Sequence 8	Galactose (4)	RCA 120 & PA-IL
G 17	DNA Tag 1 (Cseq 1)	Sequence 1	Lactose (2)	————
G 18	DNA Tag 1 (Cseq 1)	Sequence 1	Lac-α-2,6-Neu5Ac (2)	Hemagglutinin
G 19	DNA Tag 1 (Cseq 1)	Sequence 1	Lac-α-2,6-Neu5Ac (3)	Hemagglutinin
G 20	DNA Tag 1 (Cseq 1)	Sequence 1	Lac-α-2,6-Neu5Ac (3)	Hemagglutinin
G 21	DNA Tag 1 (Cseq 1)	Sequence 1	Lac-α-2,6-Neu5Ac (3)	Hemagglutinin
G 22	DNA Tag 1 (Cseq 1)	Sequence 1	Lac-α-2,6-Neu5Ac (3)	Hemagglutinin
G 23	DNA Tag 1 (Cseq 1)	Sequence 1	Lactose (1)	————
G 24	DNA Tag 1 (Cseq 1)	Sequence 1	Lac-α-2,6-Neu5Ac (1)	Hemagglutinin

Table2-2 Main characters of glycoconjugates—(II). DNA Tag [a] is the ssDNA sequences in the glycoconjugate, which are also complementary sequences corresponding to Sequence [b], the main characters of DNA tags are listed in Table2-3; Sequence [b] is the ssDNA sequence printed on the surface of the chips (see Table 2-4); Potential lectin affinity [c] is the lectin with which the glycoconjugate has potential to interact, according to the carbohydrate residues of the glycoconjugate.

Name of DNA tag	Internal reference	GC%[a]	Tm[b]
DNA Tag 1 (Cseq1)	Czip 1.1.1	66.7	54.7
DNA Tag 2 (Cseq2)	Czip 1.7.1	36.8	49.6
DNA Tag 3 (Cseq3)	Czip 1.8.1	52.6	59.4
DNA Tag 4 (Cseq4)	Czip 1.9.1	57.9	59.6
DNA Tag 5 (Cseq5)	Czip 1.10.1	46.7	44.0
DNA Tag 6 (Cseq6)	Czip 1.11.1	31.6	44.7
DNA Tag 7 (Cseq7)	Czip 1.14.1	26.3	46.7
DNA Tag 8 (Cseq8)	Czip 1.13.1	52.6	61.7
DNA Tag 9 (Cseq9)	Czip 1.2.1	52.6	59.4

Table2-3 Main characters of DNA tags of glycoconjugates

GC%[a] and Tm[b] were calculated by on-line software Primer3 (http://biotools.umassmed.edu/bioapps/primer3_www.cgi)

2.2 Set up a DNA anchoring platform

The glass slides (Borosilicate, Nexterion D, Schott GMBH, Germany) were used as substrate supports (*97-99, 206*). The setting up of the anchoring platform comprises three steps:

1. Fabrication of microreactors onto glass slides by photolithography and wet etching.

2. Surface chemical functionalisation of the supports leading to NHS ester activated glass slides.

3. Covalent immobilisation of amino-modified oligonucleotides acting as anchoring points for the subsequent immobilisation of the glycoconjugates.
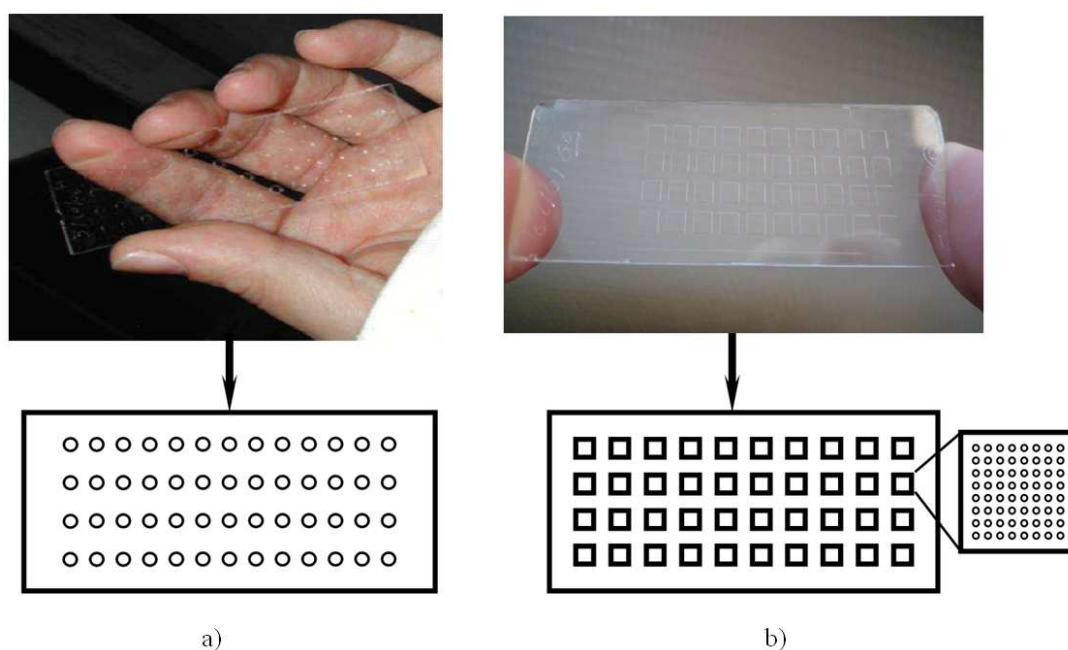
Fig2-1 Photo and sketch map of the substrates. Glass slide featured 52 round microreactors a) or featured 40 square microreactors b).

2.2.2   Fabrication of microreactors (Substrate preparation)

Microreactors are designed onto flat glass slides by means of photolithography and wet etching. Two kinds of microreactors bearing glass slides have been used:

➢ One featured 52 round microreactors (*98, 99, 206*) of 2 mm diameter, 65-100 μm deep with less than 1% variation in depth for one etching lot, with a volume near

1μL (See Fig2-1 a).

➢ The other featured 40 square microreactors (*97*) *of* (3 mm by side, 60 ± 1μm depth, with a 4.5 mm spacing between each microreactor in order to be compatible with the spotting robot and multi-canal micropipettes (See Fig2-1 b).

Technology process of the microreactor fabrication was adapted from the protocol developped by Mazurczyk et al (*247*). The process flow is shown in Fig2-2.
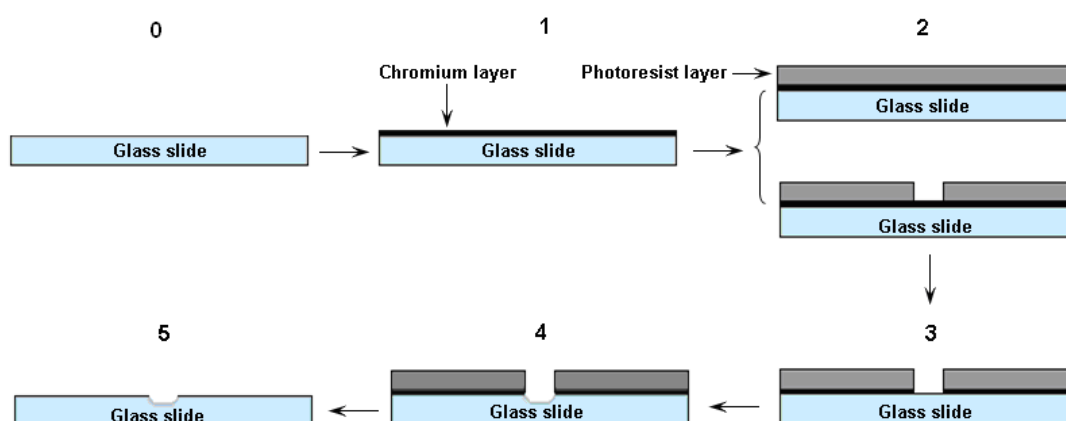
Fig2-2 Technology processes of microreactors fabrication. 0. The original glass slide. 1. The deposition of a chromium layer. 2. A photolithographic step. 3. Opening of the chromium. 4. Glass etching. 5. Removing of the protective layers .Adapted from(247).

2.2.2.1 *Deposition of the Chromium layer*

Before photolithography, a chromium layer was deposited on the surface of the slide, in order to promote the adhesion of photoresist film with the slide and offer an additional protection against harsh etching solutions (*247*). Firstly, the glass slides were washed successively with TDF4 detergent (Franklab SA, Billancourt, France) solution, a fresh Piranha mixture (96 % Sulphuric acid (Riedel de Haen, Puriss, Seelze, Germany): 35 % hydrogen peroxide (Fluka, Puriss, Steinheim, Germany), 7:3 volume) for 10 min, then rinsed with DI water (18.2 MΩ) and dried by centrifugation. A 150 nm chromium layer was deposited using magnetron sputtering (MRC822 system). The system was operated at a RF power of 5 kW, reflected power was 2 W, and turret voltages 2.6 kV. The argon flux was set to 50 sccm and the working pressure was 2.6 10^{-3} Torr.

2.2.2.2 Photolithography

SPR 220 4.5 photoresist (Rohm Haas electronic materials, Lucerne, CH) was spin-casted at 4 000 rpm for 30s resulting in a 4μm thick layer. A first bake at 115 °C on a hot plate for 1 min 30 seconds was performed. Photolithography was carried out with a Karl Suss MJB3 Mask Aligner, and a 22 second illumination was performed. The slides were immersed in MF26 A developer for 1 minutes, rinsed in running DI water for 5 min, dried under a dry nitrogen flux and post-baked at 115°C for 2 minutes(*247*).

2.2.2.3 Etching

The chromium windows on the glass slides were opened using chromium etchant (Merck, Darmstadt, Germany). The slides were then rinsed in running DI water for 15 minutes and immersed in a freshly prepared wet etching solution (Buffered Oxide Etchant - abbreviated BOE, 7/1, Hydro fluoridric acid: ammonium fluoride, Honeywell): 37%hydrochloric acid (HCl, Riedel de Haen, Seelze, Germany): DI water (H_2O, 18.2 MΩ), 1/2/2, v/v/v) at room temperature for 1h and 15 minutes. The slides were rinsed in running DI water for 15 minutes. Complete removal of the photoresist was achieved by rinsing with acetone (Riedel de Haen), ethanol and water. Finally, the chromium layer was removed with chromium etchant (Merck, Darmstadt, Germany). Depth of the microwells was monitored with a mechanical profiler (Alfa-step 500 from KLA Tencor)(*247*).

2.2.3 Silanization and activation of the glass slides

The microfabricated slides were washed with fresh Piranha solution for 20 min, and rinsed in deionized water for 10 minutes/4 times and dried by centrifugation. After heating the slides under dry nitrogen for 2 h at 150 °C in a sealed reactor, 250ml dry pentane was added at room temperature, followed by 300μL of tert-butyl-11-(dimethylamino)silylundecanoate. After incubation at room temperature under dry nitrogen for 2 hours, pentane was evaporated under reduced pressure and the slides were heated at 150 °C overnight and then washed in Tetrahydrofuran (THF, Riedel de Haen, Seelze, Germany) 10 minutes under sonication and rinsed with DI water.

The tert-butyl ester was converted into the corresponding carboxyl group by immersing the slides in glacial formic acid (Riedel de Haen, Seelze, Germany) for 7 h at room temperature, washed successively 10 min in THF (Sonication) and 10 minutes in water sonication.

NHS activation of the carboxylic functions for the covalent immobilization of the amino-modified oligonucleotides was performed as follow: The glass slides were immersed in N-hydroxysuccinimide (Riedel de Haen, Seelze, Germany) 0.1 M and di(isopropyl)carbodiimide (Riedel de Haen, Seelze, Germany) 0.1 M in dry THF solution and allowed to react overnight at room temperature. Finally, the slides were rinsed successively in THF 10 minutes and dichloromethane 10 minutes under sonication leading to the NHS activated glass slides.

2.2.4 Immobilization of single-strand DNA

All amino modified DNA sequences (see Table2-4) were purchased from Eurogentec and prepared for fabrication of DNA anchoring platforms.

➤ For the slide featured 52 round microreactors, each microreactor has been used as a spot. So each microreactor has been full filled with 1µl of desired amino oligonucleotides in PBS10× (pH 8.5) at 25 µM for single strand DNA probes immobilization.

➤ For the slide contained 40 square microreactors, each microreactor has been used as a microchip. So amino modified nucleotides were deposited by a Biorobotics MicroGrid microarrayer (Digilab), resulting 64 spots per well.

In both cases, after deposition, the oligonucleotides were allowed to react with the carboxylic activated glass slides overnight at room temperature in a water vapor saturated chamber, and then the solutions were slowly evaporated overnight at room temperature. Finally, the slides were washed with 0.1% (w/v) sodium dodecyl sulfate (SDS, Sigma Steinheim, Germany) at 70°C for 30 min, and rinsed with DI water.

Name	Internal reference	GC%[a]	Tm[b]
Sequence N (Seq N)	Zip 1.12.1	44.4	53.5
Sequence 1 (Seq 1)	Zip 1.1.1	72.2	64.4
Sequence 2 (Seq 2)	Zip 1.7.1	31.8	55.0
Sequence 3 (Seq 3)	Zip 1.8.1	47.6	61.1
Sequence 4 (Seq 4)	Zip 1.9.1	52.4	61.7
Sequence 5 (Seq 5)	Zip 1.10.1	38.9	51.1
Sequence 6 (Seq 6)	Zip 1.11.1	27.3	50.2
Sequence 7 (Seq 7)	Zip 1.14.1	22.7	52.4
Sequence 8 (Seq 8)	Zip 1.13.1	45.5	65.1
Sequence 9 (Seq 9)	Zip 1.2.1	56.0	73.6

Table2-4 Main characters of DNA sequences used for DNA anchoring platform fabrication. GC%[a] and Tm[b] were calculated by on-line software Primer3 (http://biotools.umassmed.edu/bioapps/primer3_www.cgi)

2.3 Blocking

In order to limit further non specific adsorption phenomena, a blocking step was performed by immersing the slide bearing DNA in 4% Bovine Serum Albumin (BSA, Sigma, Steinheim) solution for 2 h at 37°C. The slide was then washed in PBS 1× (pH 7.4)-Tween 20 at 0.05% for 3×3min followed by PBS 1× (pH 7.4) 3 times, and finally rinsed with DI water and dried by centrifugation.

Glass slides were ready to be used either for the "on chip approach" or "in solution approach" as described below. They also can be stored in refrigerator at 4°C.

2.4 Immobilization of glycoconjugates

2.4.1 Covalent immobilization of glycoconjugates

In the studies of chapter 3, two glycoconjugates (glycoconjugate 4 and glycoconjugate 5, see Table2-1) were immobilized on the glass slide by covalent grafting. 0.5µM and 25µM of glycoconjugates in PBS 1× (pH 7.4) were placed at the bottom of the corresponding microreactor on the slide with a micropipette. After incubated at room temperature in a water vapour saturated chamber for 24h, the slides were washed with 0.1% (w/v) SDS (Sigma Steinheim, Germany) at 70°C for 30 min, and rinsed with DI water.

2.4.2 Immobilization of glycoconjugates by hybridization

For the "on-chip approach" (see Chapter1, Fig1-10), before recognition with lectins, glycoconjugates were first immobilized through the hybridization with the complementary sequences present on the glass slide. At desired concentration, the solutions of glycoconjugates (PBS 1× pH 7.4) were placed at the bottom of the corresponding microreactor on the slide with a micropipette at the appropriate volume (about 0.8µl for the slide featured 52 round microreactors, 1-2.5µl for the slide

contained 40 square microreactors), and allowed to hybridize for 3h at room temperature in a water vapour saturated chamber. The slide was then washed successively in Sodium Saline Citrate (SSC 2×) 0.1% Sodium Dodecyl Sulphate (SDS, Sigma Steinheim, Germany) at 51°C for 1min followed by SSC 2× at room temperature for 5 min and dried by centrifugation.

2.5 Biological recognition

2.5.1 *Lectin labeling*

Ricinus communis agglutinin 120 (RCA120, Sigma, Steiheim, Germany) lectin was labeled by following the manufacturer protocol of Cy5 Ab Labelling Kit (Amersham Biosciences, GE Healthcare, Buckinghamshire, UK). Protein concentration and the dye to protein ratio were estimated by reading the absorbance at 280 and 650 nm (Nanodrop). Lectin concentration was estimated to be 4 μM bearing an average of 4 dyes per protein.

Pseudomonas aeruginosa lectin I (*98*) and *Pseudomonas aeruginosa* lectin II (*97*) (noticed PA-IL and PA-IIL, provided by Dr. Anne Imberty, CERMAV) were labeled with Alexa647 by using a kit from Invitrogen. Protein concentration was estimated according to the manufacturer protocol by reading the absorbance at 280 and 650 nm. The final concentration of monomeric lectin was estimated at 28 μM with a degree of labeling of 0.4 for PA-IL, at 24.5 μM with a degree of labeling of 0.04 for PA-IIL.

2.5.2 *"On-chip" recognition*

The labeled lectin was diluted to the desired concentration in PBS 1× (pH 7.4), CaCl$_2$ (Sigma, Steinheim, Germany; final concentration 1μg/ml) and 20% BSA (Sigma, Steiheim, final concentration 2%) to prepare the "on-chip" recognition solution. After that, the lectin solution was deposited with a micropipette in each microreactor of the slide bearing glycoconjugates and allowed to incubate at 37°C in a water vapor saturated chamber for 2 h. The slide was then washed in PBS 1× (pH

7.4)-Tween 20 (0.02%) (Roth, Karlsruhe, Germany) for 5min and dried by centrifugation.

2.5.3 *"In-solution" recognition (Hybridization of complexes glycoconjugate and lectin)*

Glycoconjugates and lectins (at desired final concentration) were diluted in PBS-Tween 20 (0.02%) solution, BSA (2% final concentration) and $CaCl_2$ (1μg/ml final concentration) to prepare the "in-solution" recognition solutions. Each solution was pipetted down in its corresponding microwell of the slide and incubated 2h at 37°C in water saturated chamber. Finally the slide was washed with PBS 1× (pH 7.4)-Tween 20 (0.02%) for 5min and dried by centrifugation.

2.5.4 *Quantitative Analysis (IC_{50} determination) of binding affinities of glycoconjugates/lectins*

IC_{50} of binding affinities of glycoconjugates/lectins was determined by introducing the inhibitor (lactose). A series of solutions containing increasing concentrations of the inhibitor (lactose) were prepared by adding different volumes the lactose (at desired concentration in PBS 1×) to the "on-chip" recognition solution (see 2.5.2.) or the "in-solution" recognition solutions (see 2.5.3.). The solutions were then deposited into corresponding microreactors on the slide respectively with a micropipette and incubated 2h at 37 °C in water saturated chamber. Finally the slide was washed with PBS1× (pH 7.4)-Tween20 (0.02%) for 5min and dried by centrifugation.

2.6 Fluorescence scanning

As mentioned before, three fluorochromes (see Table 2-5) were employed in this study. Cy3 was used to label glycoconjugates, whereas Cy5 and Alexa647 were used to label lectins.

Thus the slides can be scanned with the Microarray scanner GenePix 4100A

software package (Axon Instruments, Sunnyvale, USA) at excitation wavelengths of 532 and 635 nm. The fluorescence signal of each conjugate was determined as the average of the mean fluorescence signal of corresponding spots. In order to study the binding affinities of different glycomimetics towards the target, the immobilization yield of glycomimetics should be comparable, which means the Cy3 fluorescence intensities should be similar. Otherwise, the binding signals (the Cy5 or Alexa647 fluorescence intensities) need to be corrected according to the Cy3 fluorescence intensities of glycomimetics (see Table2-6). However, such correction can not be applied to the "in-solution" approach, due to the Fluorescent Resonance Energy Transfer (see chapter 3)

Dye	Color	Color of Fluorescence	MW(g/mol)	λ Abs (nm)	λ Em (nm)	QY(%)
Cy3	Pink	Green	767	550	570	0.15
Cy5	Blue	Red	792	649	670	0.28
Alexa647	Blue	Red	1300	650	665	0.33

Table2-5 Main characters of fluorescence dye. Referred to (248) and http://flowcyt.salk.edu/fluo.html

MW: Molecular weight; **Abs**: Peak absorption wavelength λ_{max} (nm); **Em**: Peak emission wavelength λ_{max} (nm); **QY**: Quantum yield (%)

	Fluorescence intensity		
	Cy3	**Cy5 or Alexa647**	**Cy5 or Alexa647 (after correction)**
Glycomimetics 1	A_1 [a]	B_1	$C_1 = B_1 \times \dfrac{A_1}{A_1} = B_1$
Glycomimetics 2	A_2	B_2	$C_2 = B_2 \times \dfrac{A_1}{A_2}$

Table2-6 Correction of Cy5 or Alexa647 fluorescence intensity according to ratio of the Cy3 fluorescence intensity of glycomimetics

A_1 [a] (the Cy3 fluorescence intensity of Gycomimetics 1) is regarded as a reference date (standard).

3 COMPARISON OF DIRECT COVALENT IMMOBILIZATION AND DDI OF GLYCOMIMETICS

3.1 Introduction and context

The main objective of this part of work was to compare the performances of DDI with direct covalent immobilization of glycomimetics onto the solid surface. For this, the recognition by RCA 120 of the same glycomimetic structure exhibiting three galactose residues (Glycoconjugate 3, 4 and 5; see chapter 2, Fig2-1) immobilized either by a covalent bond with a short linker (see Fig3-1, G 4) or a long linker (see Fig3-1, G 5), or by DDI (see Fig3-1, G 3) was compared.   G 4 and G 5 have a 5'-end amine function to insure their covalent immobilization by reaction with ester activated modified glass slides. The immobilization of G 4 and G 5 led to the amide derivative of these molecules after coupling. They are still referred to as G 4 and G 5 after immobilization for the concision and clarity of the text. G 4 has a deoxythymidine linker. In order to ensure that the observed differences are related to the immobilization mode (Covalent vs. DDI), G 5 has an oligonucleotide based spacer with exactly the same sequence as G 3. G 3 was immobilized by DDI.

G 1 (Glycoconjugate 1) (see chapter 2, Fig2-1) exhibited the same glycomimetic structure but the galactosyl residues were replaced by mannosyl residues. So, G 1 is a negative control against RCA 120.

The glycomimetics were immobilized at two different concentrations (0.5 µM and 25 µM) in order to study the effect of glycomimetics concentration in the immobilization solution on the subsequent interaction with RCA 120.

After the incubation of Cy5 labelled RCA 120 with the immobilized

glycomimetics, washing and drying, the chips were analyzed with Axon scanner. The fluorescence intensity signal and lower detection limit were compared.
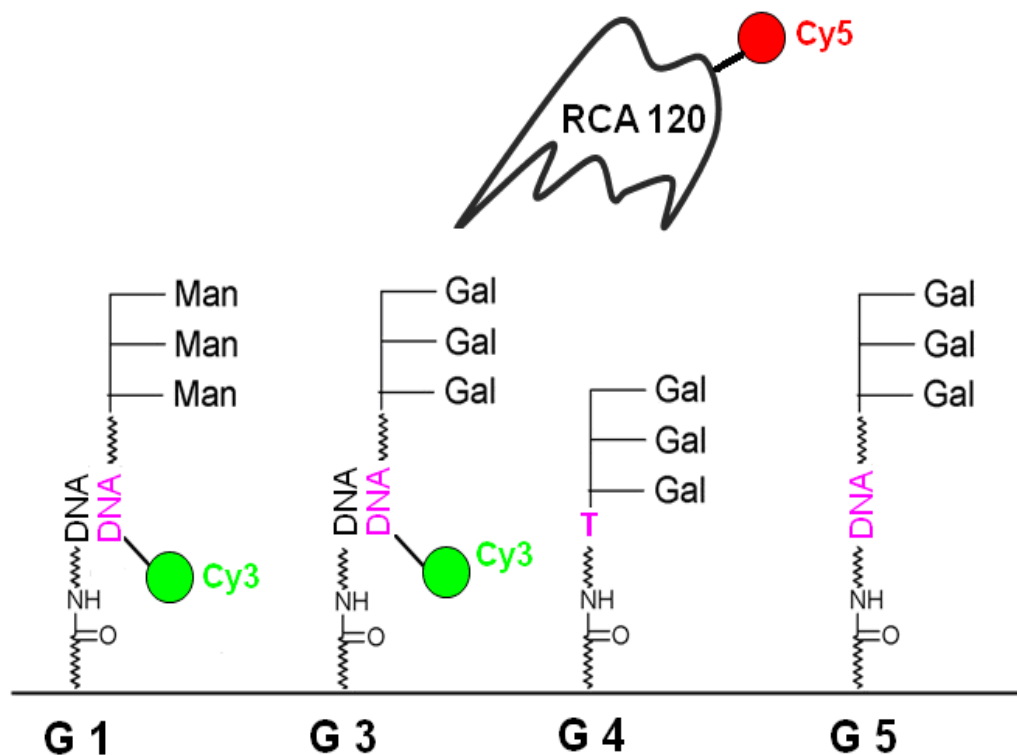
Fig3-1 Sketch map of the structures of four immobilized glycoconjugates. G 4 and G 5 were directly immobilized on activated ester modified glass slides, while G 1 and G 3 were immobilized by DDI. Cy3 allows the quality control of the DDI immobilized molecules. The interaction with the Cy5 labelled lectin Ricin Communis Agglutinin was probed by fluorescence scanning. G 1 is a negative control with regard to RCA 120 (galactose specific lectin). The DNA sequence of G 1, 3 and 5 is the same.

3.2 Results and discussion

Most of the following results were adapted from (*99*).

3.2.1 Comparison of direct covalent immobilization and DNA-directed immobilization (DDI)

G 4 and G 5 were covalently and directly grafted onto activated ester functionalized borosilicate glass slides whereas G 3 and G 1 were immobilized by DDI through the specific hydridization between the 3'-amine modified oligonucleotide tag borne by the glycoconjugate and the complementary DNA sequence previously grafted onto the surface. The Cy3 labelling allowed to control if hydridization was well occurred. At the same concentration (0.5µM), the Cy3 fluorescence signals in wells containing G 3 and G 1 were similar (See Fig3-2), demonstrating an efficiently immobilization of glycomimetics with similar surface density. After incubation with the lectin RCA120, a 4-fold decrease of the Cy3 signal corresponding to G 3 was observed (See Fig3-2 a; Fig3-3, a). This was attributed to Fluorescent Resonance Energy Transfer (FRET) between the Cy3 as a donor and Cy5 as an acceptor (*249, 250*). When the glycoconjugate Cy3-G 3 were recognized by the lectin Cy5-RCA120, the two fluorophore Cy3 and Cy5 were in very close proximity, so that the FRET would occur: the acceptor (Cy5) would take the energy from the donor (Cy3) and emit photons of different color which would not be detected at 532nm. Therefore, the fluorescence intensity observed at 523nm for Cy3-G 3 was reduced, however the decrease of Cy3-G 3 signals did not indicated the loss of glycoconjugate G 3. By contrast, when the same experiment was performed with G 1, we measured a fluorescence intensity of 38962 a.u. and 47316 a.u. respectively before and after lectin incubation (See Fig3-2 a; Fig3-3, a). In this case, as no interaction between lectin and G 1 occurred, the intensity of the Cy5 signal was in the background (61 a.u; see Fig3-3, b) and no FRET was observed. These results demonstrated that the DNA duplexes were stable under the lectin incubation conditions, and the non-specific adsorption was very limited.
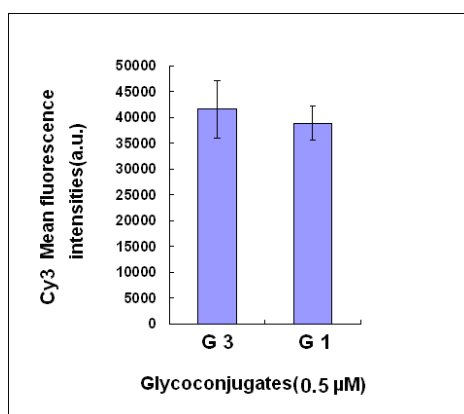
Fig3-2 Mean fluorescence intensities obtained at 532nm (a.u.) for glycoconjugates (G 3 and G 1) at 0.5µM before interact with RCA120.

a)   b)
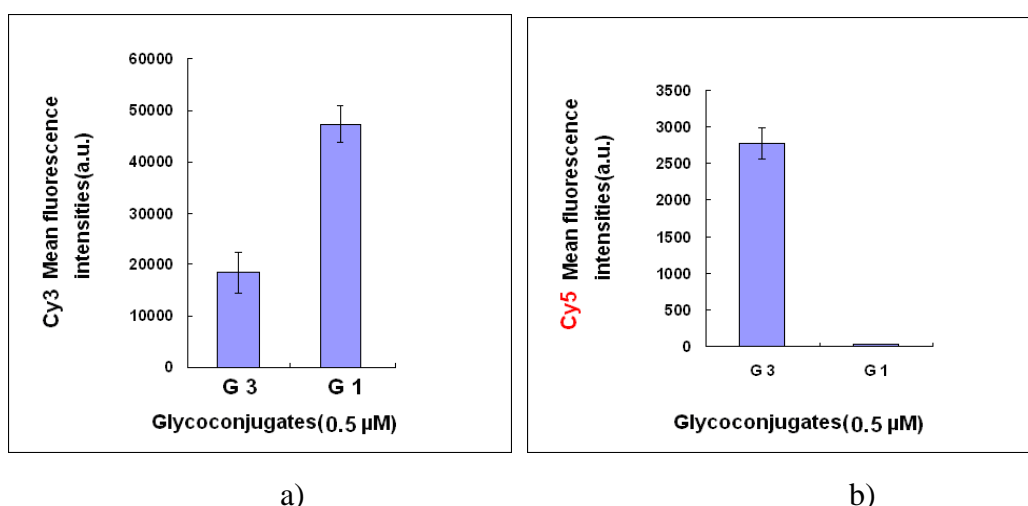
Fig3-3 Mean fluorescence intensities obtained at 532nm (a.u.) and 635nm (a.u.) for glycoconjugates (G 3 and G 1) at 0.5µM after interact with RCA120.

In the following test, two concentrations (0.5µM and 25 µM) of glycoconjugates have been used. Next, glass slides were incubated with Cy5 labelled RCA120 solution of different concentrations. After incubation, the slides were washed and scanned.

Fig3-4(a) and (b) respectively gives the Cy5 fluorescence intensities as a function of the concentration of Cy5-RCA 120 lectins obtained after recognition with different glycomimetics.

In the two cases, signal resulting from G 1/RCA 120 interaction was not reported in Fig3-4 because the fluorescence signal was at background level (30 a.u.), confirming that no recognition of RCA 120 towards mannose based structure occurs as expected.
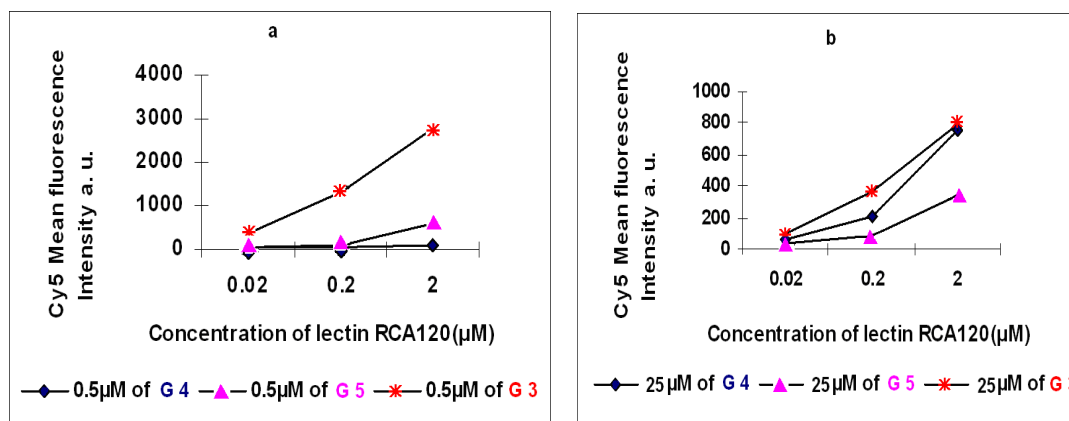
Fig3-4 Fluorescence intensities (a.u.) for Cy5 at 635 nm obtained after recognition by Cy5-RCA 120 lectin. Concentration of glycoconjugates (G 3, G 4 and G5) used for their immobilization: (a) 0.5 and (b) 25µM. Adapted from (99)

When glycoconjugates were immobilized at a 0.5µM concentration, we found that DDI led to a higher Cy5-RCA 120 fluorescence signal than that observed with direct covalent immobilization (G 4 and G 5) (see Fig3-4 a) and especially when the lectin was used at concentrations of 0.2 and 2µM. Furthermore, at a 0.02µM concentration of lectins, the signal-to-noise ratio was below 3 for G 4 and G 5 (1.03), while it remained higher for G 3 (7.4). When glycoconjugates were immobilized at a 25µM concentration, the differences in the fluorescent Cy5-RCA 120 signal between DDI and covalent immobilization are lower than those observed with a 0.5µM solution (see Fig3-4 b).

Finally, we observed that glycomimetics G 4 and G 5 anchored respectively by a short and a long linker to the surface led to a similar recognition by lectin when immobilized at 0.5µM. By contrast, when they were immobilized at 25µM concentration, glycomimetic G 4 was more prone to bind the lectin than G 5. This result suggested that the distance between the glycomimetic and the surface is not the only factor to consider but the rigidity of the linker should also be taken into account. Another explanation may relate to additional forces between the substrate and the molecules leading to a different orientation of the glycomimetics moiety between G 4 and G 5.

Glycomimetics G 5 and G 3 displayed a similar distance to the surface but bind lectin with different affinities. Single-stranded DNA is rather flexible and can bend, while double stranded DNA is more organized in space as a double helix, leading to a much more rigid linker.

In the field of protein microarrays, Wacker *et al (241)* compared DDI, biotin/streptavidin based immobilization and direct covalent immobilization of antibodies. They found that DDI and covalent attachment led to higher fluorescence signal intensities than streptavidin/biotin based immobilization. They also found that DDI required 100 times less antibody for preparing the antibody than we have observed on DDI-based glycoarrays in this report. This observation has been attributed to the rigidity of the DNA duplex holding the probe straight on the surface, and to the dynamics of hybridization that allow improved packing compared to covalent attachment.

3.2.2 Influence of glycomimetic concentration on the hybridization yield and subsequently on its interaction with RCA 120

Taking into account the efficiency of DNA Directed Immobilization of G 3, the effect on its subsequent interaction with Cy5-RCA 120 was studied as a function of the concentration of G 3 used during DDI. The results are displayed in Fig3-5.

Fig3-5a corresponds to the Cy3 fluorescence signal measured before incubation with the lectin and it relates to the amount of G 3 hybridized with its complementary immobilized DNA sequence (its relative surface densities). Fig3-5b corresponds to the Cy5 fluorescence signal measured after incubation with Cy5-RCA 120.

The Cy3 signal increases very slowly from 0.025 to 0.25µM, followed by a rapid increase of the relative surface density between 0.25 and 0.5µM leading to a plateau. Using exactly the same chemistry and ^{32}P labelled oligonucleotides, Dugas *et al (251)*

have demonstrated that the surface density of covalently immobilized amino-modified oligonucleotides was in the range 10^{11}- 10^{12} molecules.cm^{-2}. These findings were confirmed by AFM observations (*252*). The measured surface density of the ^{32}P hybridized target was around $1–4\times10^{10}$ molecules.cm^{-2}. It means that the hydridization yield is 10-20 % of immobilized probes. On oxide based substrate, a similar average hybridization yield in the 10-20% range has been reported by Herne(*253*). It may well be that the saturation plateau obtained in Fig3-5a corresponds to this 10-20% hybridization yield observed by these authors.

Nevertheless, this result suggested that a concentration of only 0.5µM of oligonculeotide -glycomimetic is necessary to obtain optimal immobilization by DDI. Thus, the amount of G 3 used for its immobilization was only 0.5 picomoles per spot. After incubation with Cy5-RCA, the same fluorescent signal trend was observed at 635 nm due to the increase in the labelled lectin surface density (see Fig3-5b).
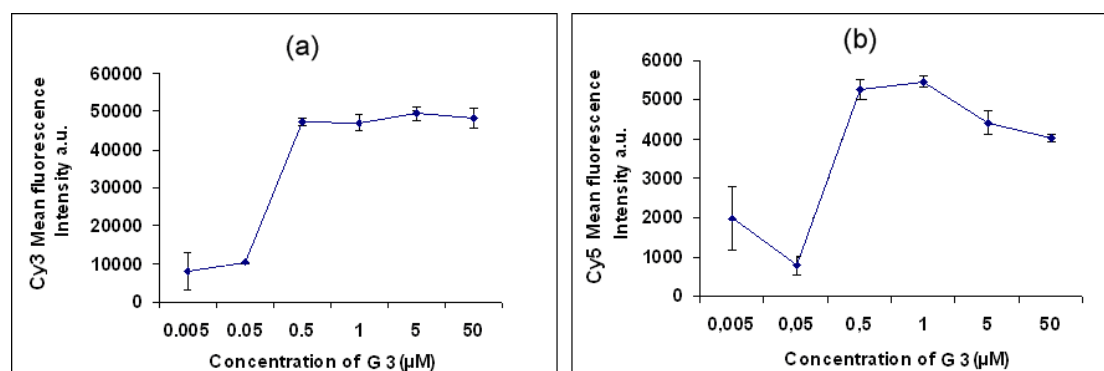
Fig3-5 (a) Fluorescence intensity for Cy3 at 532nm obtained after hybridization of G 3 with concentrations of 0.005, 0.05, 0.5, 1, 5, and 50µM; (b) fluorescence intensity for Cy5 at 635 nm obtained after recognition with Cy5-RCA 120 used at 2µM concentration. Adapted from (99)

3.3 Conclusions

In this chapter, it was demonstrated that DNA-directed immobilization is an efficient strategy for anchoring glycomimetics on surface using minute amounts of material as low as 0.5 picomole per spot. The subsequent interaction of the DDI

immobilized glycomimetics with Cy5 labelled lectin RCA 120 led to a stronger fluorescence signal than covalently immobilized systems. It may well be that the rigidity of the DNA duplex stands the glycomimetic straight out of the surface or a denser packing of the probes due to DNA hybridization is responsible for this difference, as observed for antibodies (*241, 254*).

4 COMPARATIVE STUDY OF THE AFFINITIES OF GLYCOCONJUGATES TOWARDS PA-IL AND RCA 120 LECTINS

4.1 Introduction and context

Carbohydrate/lectin interactions are generally weak (in the µM to mM range) due to the swallow binding site of lectins with half time of the carbohydrate/lectin complex in the seconds range (*228*). Decreasing of the Gibbs free energy (improvement of the binding affinity) requires to decrease the enthalpy of reaction or/and to increase the entropy contribution. This can be achieved by three means:

- by stabilizing the complex through additional interactions (decreasing the enthalpy). This approach is particularly efficient if the binding pocket is well-structured(*228*). For example, hydrophobic amino-acid residues are often present within or near the binding domain of lectins. This is the reason why great effort have been devoted for the synthesis of glycosides bearing hydrophobic aglycons (*255*). Successful examples are the neuramidase inhibitor zanamivir and oseltanamivir (*235*).

- by pre-arranging the ligand in its active conformation prior to its interaction with the lectin in order to decrease the entropic cost (*228*).

- by taking advantage of multivalent ligands (entropic contribution and the so-called cluster effect) (*256*). In nature, monovalent interactions between lectin and carbohydrate are generally weak as written above. However this

affinity can be increased exponentially as a function of multivalency providing that the spatial distribution of the residues matches the receptor binding sites. Entropy seems to play a key role in the design of multivalent ligand (*257, 258*). Unfortunately, the design of multivalent ligands is often an empiric approach.

Herein we have tested glycoclusters with three different geometric characters (Comb-like, crown geometry and antenna). Comb-like and antenna glycoclusters were synthesized according to the methodology reported in (*55, 206, 214*). This strategy is based on a combination of oligonucleotide phosphoramidite or H phosphonate chemistry on solid support and microwave assisted click chemistry. Diols building blocks eventually bearing pending alkyne functions are assembled through a series of a standard process of detritylation, coupling, oxidation and capping used for the synthesis of oligonucleotides to give the glycocluster scaffold. In the case of antenna shaped cluster, a dialkyne phosphoramidite building block was used. In the case of Comb-like cluster, alkyne functions were introduced by oxidative amination of H phosphonate.

Crown glycoclusters were based on a Calix[4]arenes core (*98*). Calix[4]arenes can be synthesized in various blocked conformations, thus providing a series of well-defined geometries for the display of sugar ligands. A recent study demonstrated that N-glycosylated calix[n]arenes of variable valencies and geometries are capable of distinguishing among lectins of a family (*259*).

The affinities of all these glycoclusters bearing ssDNA-tags were evaluated towards the lectins PA-IL (*260*) and RCA 120, galactose-specific lectins from Pseudomonas aeruginosa and Ricinus communis, respectively.

Quantitative or semi-quantitative data are usually measured by SPR (*167, 170, 261*) or through inhibition experiments such as IC_{50} measurements (*199, 201, 262*). In this work, two methods have been used in order to investigate the effect of multivalency on affinity. Qualitative data were obtained on the affinity of the different ligands for PA-IL and RCA 120 by direct fluorescence read out on DDI glycoarrays. Moreover, we have developed an IC_{50} measurement assay of glycomimetics immobilized by DDI. The IC_{50} value of glycomimetics was measured with respect to

their interaction with RCA 120, and using lactose as inhibitor.

4.2   Results and discussion

Most of the following results were adapted from (*98, 99*).

4.2.1   Characters of glycoconjugates

Eight glycoconjugates (Glycoconjugate 1, 2, 3, 2a, 3a, 6, 7 and 8. see Chapter 2, Fig2-1) were tested (see Fig 4-1). G 1, a trimannosyl conjugate, was expected to be a negative control, which can not be recognized by the two lectins PA-IL and RCA120. Other seven glycoconjugates were all galactosyl glycomimetics. G 2 and G 3 were glycoconjugates bearing one or three galactose residues with linker 1: (Cyclohexanedimethanol) and in Comb-like structure; G 2a and G 3a are very similar to G 2 and G 3 respectively, except possessing different Linker a (Tetraethyleneglycol); G 6 and G 7 contained four and eight galactose residues respectively and supported by calix[n]arene backbone (*98*). G 8 was consisted of ten galactose residues arranging in antenna structure.
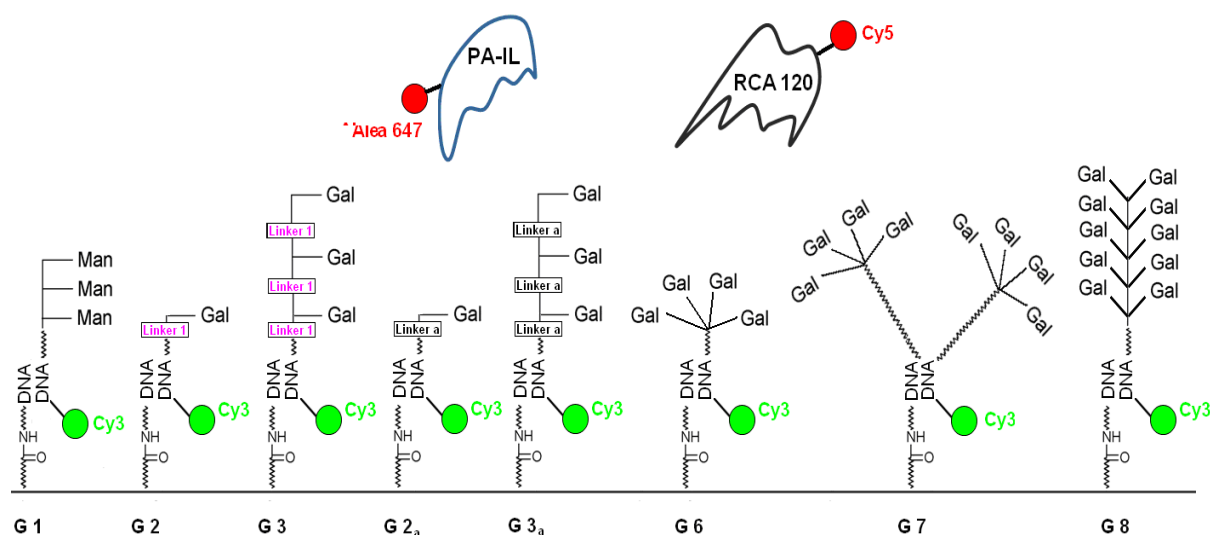
Fig4-1 Sketch map of the structures of eight immobilized glycoconjugates G 1, G 2, G 3, G2a, G3a, G 6, G 7 and G 8. Cy3 allows the quality control of the DDI immobilized molecules. The interaction with the Cy5 labelled RCA 120 lectin and Alexa647 labelled PA-IL were probed by fluorescence scanning. G 1 is a negative control with regard to the two galactose specific lectins.

4.2.2 Preparation of DNA-based glycoarrays to probe lectin–carbohydrate interactions

Our methodology (*206*) included the elaboration steps as fellows:

1) Construction of DNA chips with 52 wells on glass slide.

2) Immobilization of the prepared glycocluster-oligonucleotide conjugates bearing the complementary DNA sequence and the fluorescent dye Cy3 by hybridization.

3) Incubation in each well with either the Cy5-RCA 120 or Alexa 647-PA-IL lectins (See Chapter 1 Fig1-10).

Therefore, the 3'-amino-oligonucleotides, the sequence of which was complementary to that of the glycoconjugates prepared, were first covalently immobilized on functionalized (*251*) 52-well glass slides (*247*). Then, the glycocluster oligonucleotide derivatives G 1(with 3Man), G 2 and G 2a (with 1Gal), G 3 and G 3a (with 3Gal), G 8 (with 10Gal), G 6 (with 4 Gal) and G 7 (with 8 Gal) were hybridized onto the chip in order to compare their lectin-binding properties. In this part of work, notice that all glycoconjugates have the same DNA tag (Sequence 1) except G8 (Sequence 9) (see Chapter 2, Table2-2). All glycoconjugates bear a Cy3 label. The Cy3 fluorescent signal relates to the relative surface density of the glycoconjugates.

Two DDI glycoarrays a) and b) were prepared for the following study of the binding affinities with two lectins PA-IL and RCA120 respectively (see Fig4-2).
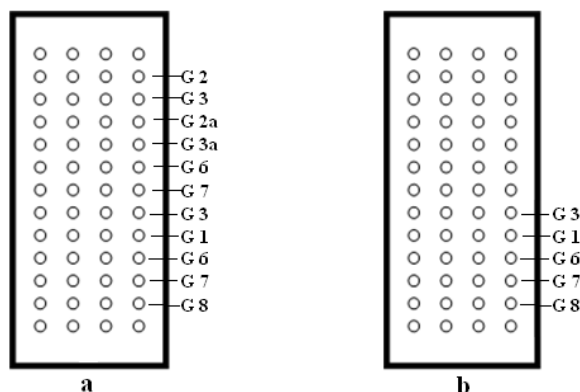
Fig4-2 Sketch map of DDI glycoarray: a) prepared for study the affinity of all eight glycoconjugates (G 1, G 2, G 3, G2a, G3a, G 6, G 7 and G 8) with PA-IL. b) prepared for study the affinity of five glycoconjugates (G 1, G 3, G 6, G 7 and G8) with RCA120.

After immobilization of glycoconjugates by hybridization (4 spots on the same line per glycoconjugates), scanning of the Cy3 fluorescence signal was performed at 532 nm. Fig 4-3 gives the Cy3 mean fluorescence intensities for each glycoconjugate. Each column corresponds to the average of the recorded values on four spots.

The figure (see Fig4-3 a, b) displays a homogeneous hybridization of all conjugates on each of the two DDI glycoarrays, except for G8 (10Gal), which included an oligonucleotide sequence that was different from that in the other glycoconjugates. The smallest value of fluorescent signal can provide from either a bad hybridization yield of the DNA tag with its complementary sequence or dimensions of glycoconjugates G 8 hindering their immobilization.
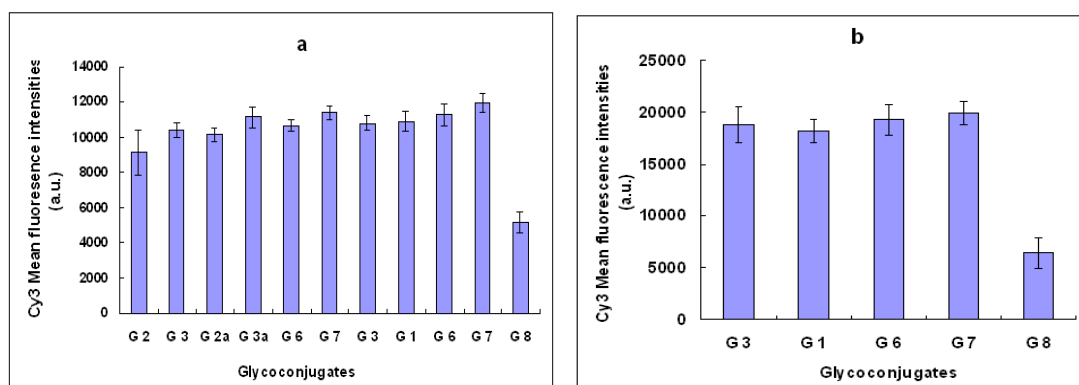
Fig4-3 Mean fluorescence intensities at 532 nm (a.u.) obtained for the Cy3-labeled glycoconjugates on two DDI glycoarrays: a) prepared for study the affinity of all eight glycoconjugates with PA-IL; b) prepared for study the affinity of five glycoconjugates with RCA120.

4.2.3   Study of the affinities of glycoconjugates with PA-IL and RCA120

We next studied the interactions of the different glycoconjugates mentioned above with two different galactose-binding lectins: PA-IL (*260*) (*Pseudomonas aeruginosa* lectin) and RCA 120 (*Ricinus communis agglutinin*). PA-IL and RCA 120 properties and structures are described in Chapter 1 *1.2.2* and *1.2.3*. PA-IL was labeled with Alexa 647 whereas RCA 120 was labeled with Cy5.

Incubation with PA-IL:

After immobilization of glycoconjugates by hybridization, the Alexa 647-labeled PA-IL was deposited in each well at 2.8 µM concentration (monomer), and after incubation for 2h and washing of the glass slide with Tween 20 in PBS solution (0.02 %), the chip a) was scanned at 532 and 635 nm. The fluorescence signal of each conjugate was determined as the average mean fluorescence signal of four spots (see Fig4-4). The fluorescence image of Cy3 (see Fig4-4, left) showed that the glycoconjugates were still present after lectin incubation, whereas the fluorescence image of Alexa647 (see Fig4-4, right) was observed as a result of the binding of PA-IL with glycoconjugates.

The relative affinities of PA-IL towards the glycoconjugates can be directly monitored through the intensity of the Alexa 647 fluorescence signal (see Fig4-5). This signal was at background level for the mannose-bearing glycoconjugate G 1(3Man) whereas a significant fluorescence was observed for the corresponding galactose derivatives G 2, G 3, G 2a, G3a and G 8 and demonstrating a selective affinity of PA-IL.

a
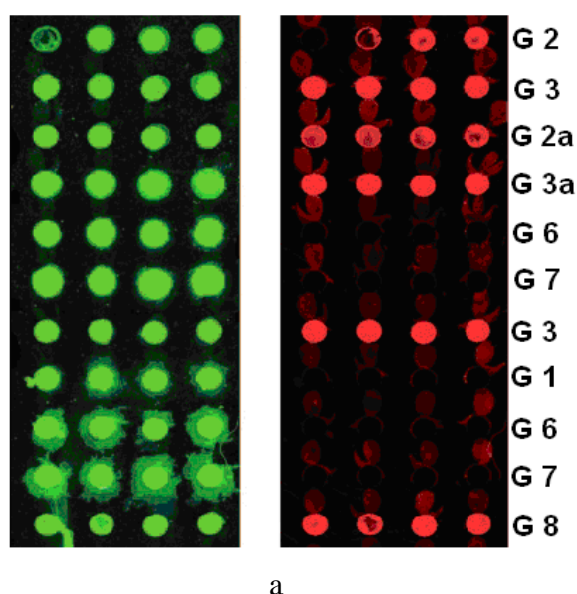
Fig4-4 Fluorescence images recorded at 532 nm (left) and at 635 nm (right) after incubation of immobilized all eight glycoconjugates (G 1, G 2, G 3, G2a, G3a, G 6, G 7 and G 8) glycoconjugates with Alexa 647-labeled PA-IL on DDI glycoarray a).
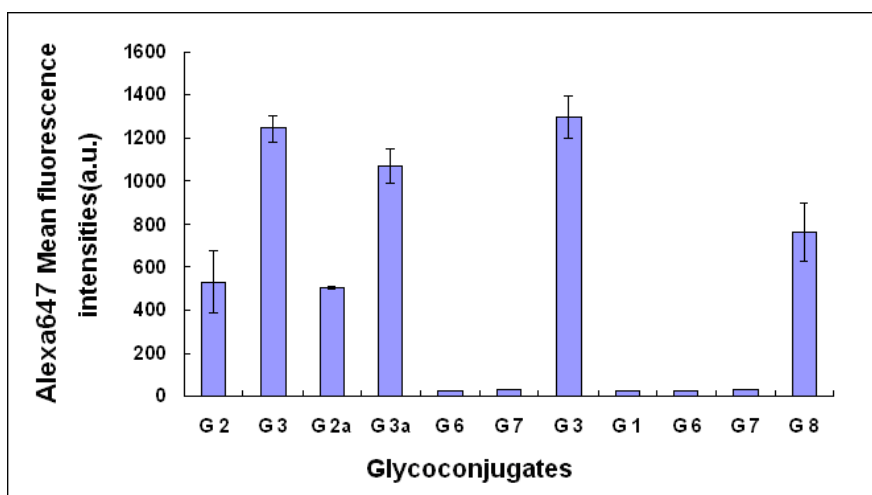
Fig4-5 Mean fluorescence intensities (after correction) at 635 nm (a.u.) of Alexa 647-labeled PA-IL after incubation with immobilized glycoconjugates G 1, G 2, G 3, G 2a, G 3a, G 6, G 7 and G 8.

As previously observed with RCA 120 (*206*), glycoconjuguates possessing three galactose residues (G 3 and G3a) had better affinities towards PA-IL than those with only one residue (G 2 and G2a), due to the expected cluster effect(*240, 257*). Surprisingly, lower affinities were observed when the number of galactose moieties was increased. Thus, the deca-galactosyl conjugate G 8 displayed a fluorescence signal weakened by a factor of two, whereas for both glycoconjugates G 6 and G 7, as well as for the negative control G 1, they were at background level, thus indicating that G 6 and G 7 did not have affinities towards PA-IL lectin (see Fig4-4 and Fig4-5). Actually, it was expected that PA-IL should recognize G 6 and G 7 highly effectively, because they each featured a triazole ring β-D-linked to the galactose moiety, a molecular motif closely related to phenyl β-D-galactoside, the most potent known ligand for PA-IL. Two possible explanations for this finding can be advanced by considering either: 1) that steric hindrance might arise, or 2) that glycosylated calixarenes can sequester calcium ions, thus removing them from the binding site of the lectin. ^{1}H NMR experiments were therefore carried out to evaluate the complexation abilities of calix[4]arene-based glycoclusters toward calcium (II) ions by addition of anhydrous Ca (ClO$_4$)$_2$ (*98*). Controlled experiments were performed

with Na ClO$_4$. It was found that addition of anhydrous Ca (ClO$_4$)$_2$ to the solution of calix[4]arene-based glycoclusters in CD$_3$OD, lead to upfield shift of aromatic protons and from the triazole ring while protons from the center of the spectrum (4.5-37 ppm) shifted downfield. The cation selectivity of the recognition process was confirmed as no significant shift was observed with NaClO$_4$ in the CD$_3$OD solutions. It suggested that both glycoclusters can complex Ca^{2+} ions when installed on the oligonucleotide chains and exposed to the lectin. This conclusion contrasted with the finding that no molecular recognition was detectable even on increasing the amounts of calcium ions in the tris/HCl buffer used instead of phosphate buffer. Therefore, we conclude that calcium sequestration cannot be taken as a causative effect for the lack of binding of G 6 and G 7 to PA-IL lectin. At this stage a convincing explanation for that observation is open to conjecture and may rather be related to steric hindrance. Indeed, other groups have observed strong affinity between PA-IL and calix[4]arene-based glycoclusters. In this case, longer linker between calix[4]arene and carbohydrate residues were used (*263*).

These data showed that PA-IL recognizes glycoclusters with Comb-like spatial structures more efficiently than it does those with antenna (G 8) and calixarene (G 6 and G 7) structures. This result suggests that too close proximity between the galactose moieties has a negative effect on the recognition by PA-IL. In addition, G 8 carried 5 negative charges. Under our experimental conditions (pH 7.4), PA-IL (pI 4.94) was negatively charged, and therefore electric repulsion between G 8 and PA-IL can not be excluded.

Incubation with RCA 120:

A literature overview about RCA 120 can be found in chapter 1 *1.2.3*. Cy5-labeled RCA 120 was deposited in each well at 2μM concentration. After incubation and washing of the glass slide with Tween 20 in PBS solution (0.02 %), it was scanned at 532 and 635 nm. The fluorescence image of Cy3 (see Fig4-6, left) confirmed that the glycoconjugates were still present after lectin incubation, whereas the fluorescence image of Cy5 (see Fig4-6, right) was observed as a result of the

binding of RCA 120 with galactose residues.
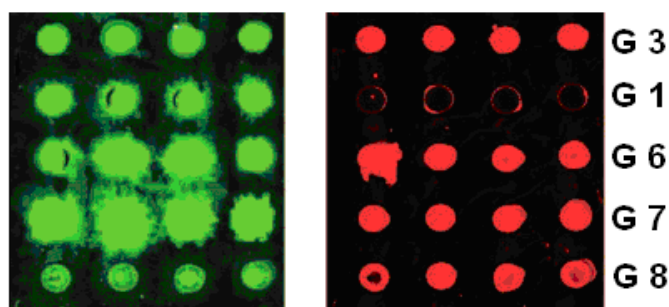
b

Fig4-6 Fluorescence images recorded at 532 nm (left) and 635 nm (right) after incubation of immobilized glycoconjugates G 1, G 3, G 6, G 7 and G 8 with Cy5-labeled RCA 120 on DDI glycoarray b).

In previous studies, Chevolot *et al (206)* had investigated the binding affinities of G 2, G 3, G 2a and G 3a with RCA120 and observed that G 3 bearing three galactose residues with linker DMCH showed the most significant fluorescence signal. Therefore, herein we chose G 3 as a positive control of the study. In Fig4-7, the fluorescence signal of each conjugate was determined as the average of the fluorescence signals of four spots. The Cy5 signal was at background level for the mannose-bearing glycoconjugate G 1. On the contrary to the data obtained with PA-IL, we found that all galactosylated glycoconjugates were able to bind RCA 120 including calix[4]arene based glycoclusters. The molecular recognition of the sugar ligand by the lectin was not prevented by calixarene scaffold nor triazole linker. The glycoconjugate G 7, bearing eight galactose residues, displayed an affinity similar to that observed for G 3, featuring only three galactose moieties. The ratio of the intensities of the Cy5 signals for G 7 and G 6 was in the 1.2–2 range (from independent experiments), whereas the ratio of the galactose residues linked to these glycoconjugates was 2. Surprisingly, RCA 120 bound with a lower affinity to the compound G 8 bearing ten residues in an antenna-based spatial arrangement. These results indicate that the three-dimensional orientation of the sugar units is more important than their number. In fact G 3, bearing three galactose residues in a

Comb-like arrangement, was the most potent ligand out of the five glycoconjugates tested in this study. In the case of RCA120, the charge effect (e.g. electric repulsion) can not be evoked. RCA120 (pI 7.5-7.9) is almost neutral at pH 7.4.
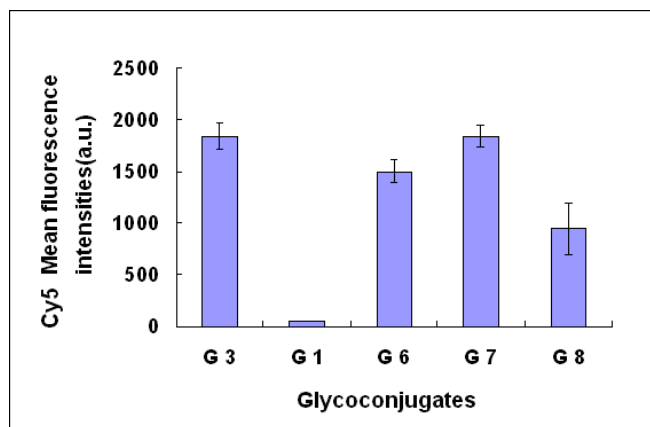
Fig4-7 Mean fluorescence intensities (after correction) at 635 nm (a.u.) obtained for Cy5-labeled RCA 120 after incubation with immobilized glycoconjugates G 1, G 3, G 6, G 7 and G 8.

4.2.4 Determination of IC_{50} values for glycoconjugates G 6, G 7, G 2 and G 3 interaction with RCA 120

In order to provide a semi-quantitative analysis of the binding affinities between lectin RCA 120 and glycoconjugates G 2 (monogalactose) , G 3 (trigalactose), G 6 (tetragalactose) and G 7 (octagalactose) the corresponding IC_{50} values were measured as reported in (*199*). After the immobilization of the glycoconjugates (G 2, G 3, G 6 and G 7) on the slides by hybridization, each spot was individually incubated with Cy5-labeled RCA120 (final concentration 2µM) and increasing concentration of inhibitor (lactose, final concentration 0.05µM to 9mM). After incubation and washing with Tween 20 in PBS solution (0.02 %), the chips were scanned at 532 and 635 nm (see Fig4-8).
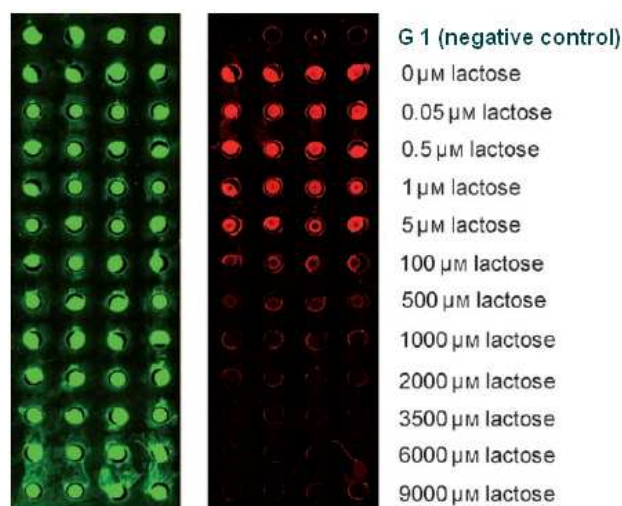
Fig4-8 Typical fluorescence images obtained at 532 nm (left) and 635 nm (right) after incubation of glycoconjugates with Cy5-labeled RCA 120 and increasing concentrations of lactose. Adapted from (98) (This chip corresponds to the G7 glycoconjugate).

The interaction of RCA 120 with glycomimetics G 2, G 3, G 6 and G 7 was inhibited by lactose, thereby confirming the specificity of the interaction. IC_{50} values is defined as the concentration of lactose required to decrease by 50% Cy5 fluorescent signal related to Cy5- RCA 120 conjugate bound to the immobilized glycoconjugates on the slide. Fluorescence images at 635 nm were obtained after washing of the glass slides to remove the unbound lectins. Each experimental point is an average value of four spots. The Cy5 fluorescence intensities were tabulated against logarithmic lactose concentrations (see Fig4-9). The IC_{50} values for glycoconjugates G 2, G 3, G 6 and G 7 are displayed in Table 1. The IC_{50} value measured for molecules G 2 and G 3 was the same whatever concentration was used for their immobilization (0.5 or 1μM). The IC_{50} values found here are comparable with those observed by Kuno *et al* (*264*) when they used a lectin microarray (IC_{50} =94μM) for asialofetuin (2 nM) using lactose as an inhibitor.
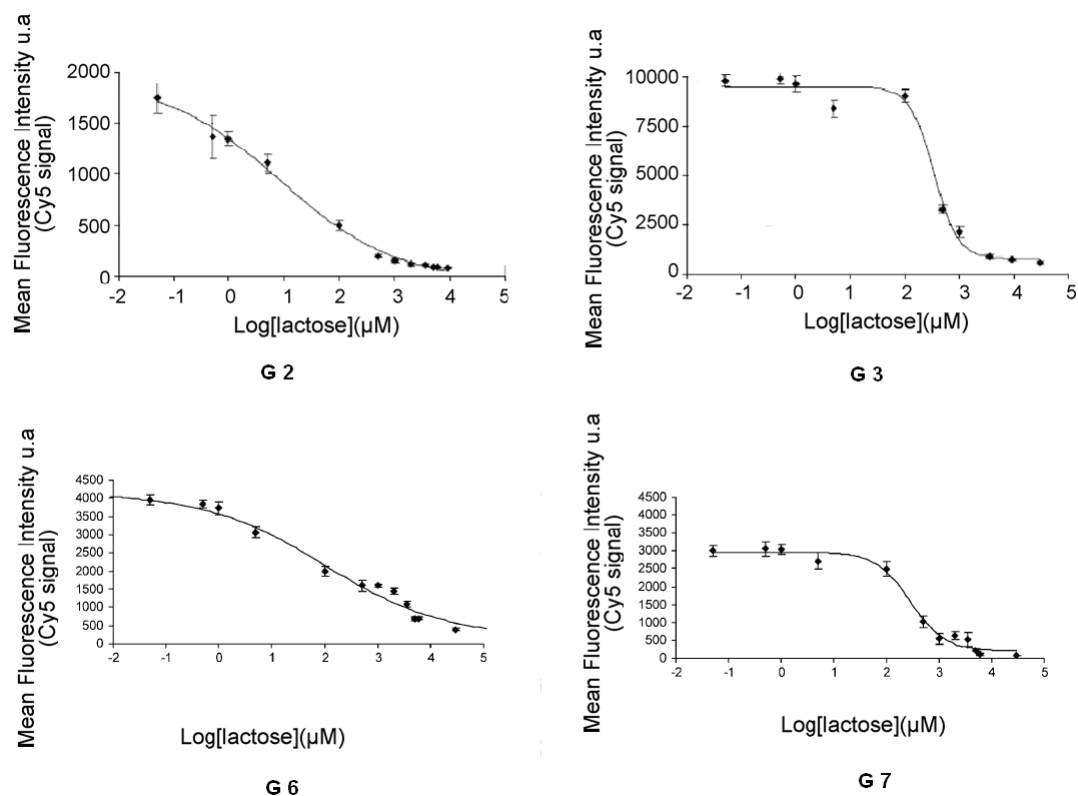
Fig4-9 Determination of IC$_{50}$ values using carbohydrate microarrays. Concentrations of lactose required to inhibit 50% of RCA 120 binding to glycoconjugates G 2, G 3, G 6 and G 7. Fluorescence intensity for Cy5 at 635 nm obtained after recognition between glycoconjugates and RCA 120 with concentrations of inhibitor (lactose) of 0.05, 0.5, 1, 5, 100, 500, 1000, 2000, 3500, 6000, 9000μM.

Glycoconjugate	Valency	IC$_{50}$ (μM)	Relative potency[a]	Potency per galactose residue[b]
G 2	1	5.6 ± 2.8	1	1
G 3	3	385 ± 45	69	23
G 6	4	114 ± 14	20	5
G 7	8	305 ± 22	54	7

Table4-1 IC$_{50}$ of glycoconjugates-RCA120 binding

➤ **[a] Calculated as the ratio of monomer glycoconjugate to other glycoconjugates IC$_{50}$ values.**

➤ **[b] Calculated as the ratio of relative potency to the number of galactose residues.**

According to the measured IC_{50} values, a nearly 23-fold increase in potency toward RCA120 per galactose residue was observed from G 3 to G 2 (see Table 4-1). In the absence of lactose, the ratio of the Cy5 fluorescence signal between molecule G 3 and molecule G 2 is below three, as observed previously(*206*). Hence, the resulting potency per galactose residue determined by direct fluorescent scanning is similar for G 3 and G 2. IC_{50} measurements also confirmed that RCA 120 had affinities for compounds G 3 and G 7 in the same range. Moreover, the IC_{50} value for G 7 was 2.7 times higher than that for G 6, leading to an affinity per residue increased by a factor of 1.3, whereas values in the 1.2–2 range were obtained when analyzed by fluorescence of Cy5 (see Fig5-6). These dependencies on the magnitude of the cluster effect with the assay have already been reported in the literature (*257*).

Our strategy is based on a qualitative assay using the fluorescence signal to select good candidates for targeting a desired lectin. The affinity of the selected candidates will then be further studied more closely using this IC_{50} measurement assay.

4.3   Conclusions

Each class of galactose cluster (Comb-like, calixarene, and antenna) was recognized with different affinities by PA-IL and RCA 120 lectins. Our results showed that the spatial arrangement was more important than the number of galactose residues, because the Comb-like trivalent clusters (G 3) were better able to bind lectins than antenna (G 8) and calixarene (G 6 and G 7) ones with ten, four, and eight galactose moieties, respectively. Furthermore, we showed that PA-IL is more selective than RCA 120, because galactosyl-calixarene derivatives G 6 and G 7 were not recognized by PA-IL. The difference in affinity of PA-IL towards comb-like (G 3) and antenna (G 8) structure may also relate to charge effect (e.g. electric repulsion). To determine impact of different parameters, e.g. spatial arrangement and charge effect, specific studies will be described in chapter 5.

The importance of the spatial arrangement of the glycoside residues in the lectin

recognition process has been assessed for the asialoglycoprotein receptor (*206, 265, 266*). We found that the trigalactose cluster with the largest distance between the sugar residues presents the optimal recognition (*265*). The recognition study was performed by direct fluorescence scanning and by the determination of the IC_{50} values, with both techniques leading to similar results. This IC_{50} assay performed on glycoarray, using tiny amounts of glycomimetic and lectin, can be miniaturized, unlike conventional methods (ELLA or ELISA), which require a large amount of glycomimetics. The synthesis of the glycoconjugates could therefore be performed on a fairly small scale, but the miniaturization through the microarray technology provided the biological data for a complete study.

5 DEVELOPMENT OF MINIATURISED ANALYTICAL BIOSYSTEMS BASED ON DDI GLYCOARRAY

5.1 Introduction and context

Miniaturized analytical systems and microarrays are key technologies for major breakthroughs in the fields of biology and biotechnology, including diagnosis and drug discovery. Such systems offer the perspective of high throughput analysis, improved lower detection limits, lower sample and reagent consumption, and increased signal to noise ratios. Due to the large diversity and the limited amount of available carbohydrates and glycoconjugates, there is an urgent need for developing high throughput glycoarrays and miniaturized biosystems.

As described in the previous Chapters, based on the DDI glycoarrays which were fabricated on the glass slide featured with 52 round microwells (see Chapter 2, Fig2-2), it was demonstrated that:

1) DDI glycoarrays are efficient tools to study the interaction of glycomimetics bearing different number of galactoses in various spatial arrangements with *Ricinus communis agglutinin* 120 (RCA120) and *Pseudomonas aeruginosa* lectin (PA-IL) (*98, 99, 206*).

2) Although the inherently weak, carbohydrate-lectin interactions can be compensated and enhanced by multivalency and "cluster effect" (*56, 262*). The comparison studies on DDI glycoarray had proved that the polyvalency, the spatial presentation and arrangement of the glycomimetics are important factors for the lectin binding capacity (*98*).

3) The IC_{50} values of different glycomimetics with RCA120 were also successfully determined on the DDI glycoarray (*98, 99*).

4) The DDI method can be performed following two different approaches as

described in (*206*). The "on-chip approach" uses glycomimetics immobilized on the chip and subsequently allowed to specifically interact with a lectin, and the second one, called the "in-solution approach", where the glycomimetics and the lectin are allowed to interact in solution prior to DDI of the whole complex. Surface chemistry can affect the overall results (ligand to protein affinity)(*267, 268*), as well as surface density and the organization of the probes. The "in-solution approach" was expected to reduce some of these limitations.

However, in those previous studies, only one DNA sequence was immobilized at the bottom of each microwell of DDI glycoarray and thus one single glycomimetic was incubated with the lectin for interaction studies in each microwell. In order to improve the high throughput ability and capacity of DDI glycoarrays, to reduce the required materials/experiments and to perform several glycomimetic/lectin interactions in parallel in one reactor (microwell), new DDI glycoarrays or miniaturized analytical systems needed to be designed and fabricated. These devices should allow multiplex analysis in one single microwell under the same experimental conditions and with the same surface chemistry.

In this chapter, further developments of DDI glycoarrays are reported taking advantage of the specificity of DNA hybridization for multiplexed assays. Thus in principle, the two DDI strategies "on-chip approach" and "in-solution approach" can be performed with multiple glyconjugates per microwell. In Fig5-1 ("on-chip"), different glycomimetics bearing different ssDNA tags were immobilized onto the bottom of one microwell of the glycoarray by hybridization with the corresponding complementary ssDNA sequences printed on the surface of the microwell. Then the lectin can be added to the microwell for binding to the glycoconjugates. In Fig5-2 ("in-solution"), different glycomimetics bearing different DNA tags were mixed in solution with lectins, each glycomimetic interacting with its specific lectin and the resulting complexes would be sorted, according to their DNA tags, at the surface of microreactor bearing immobilized complementary DNA sequences.
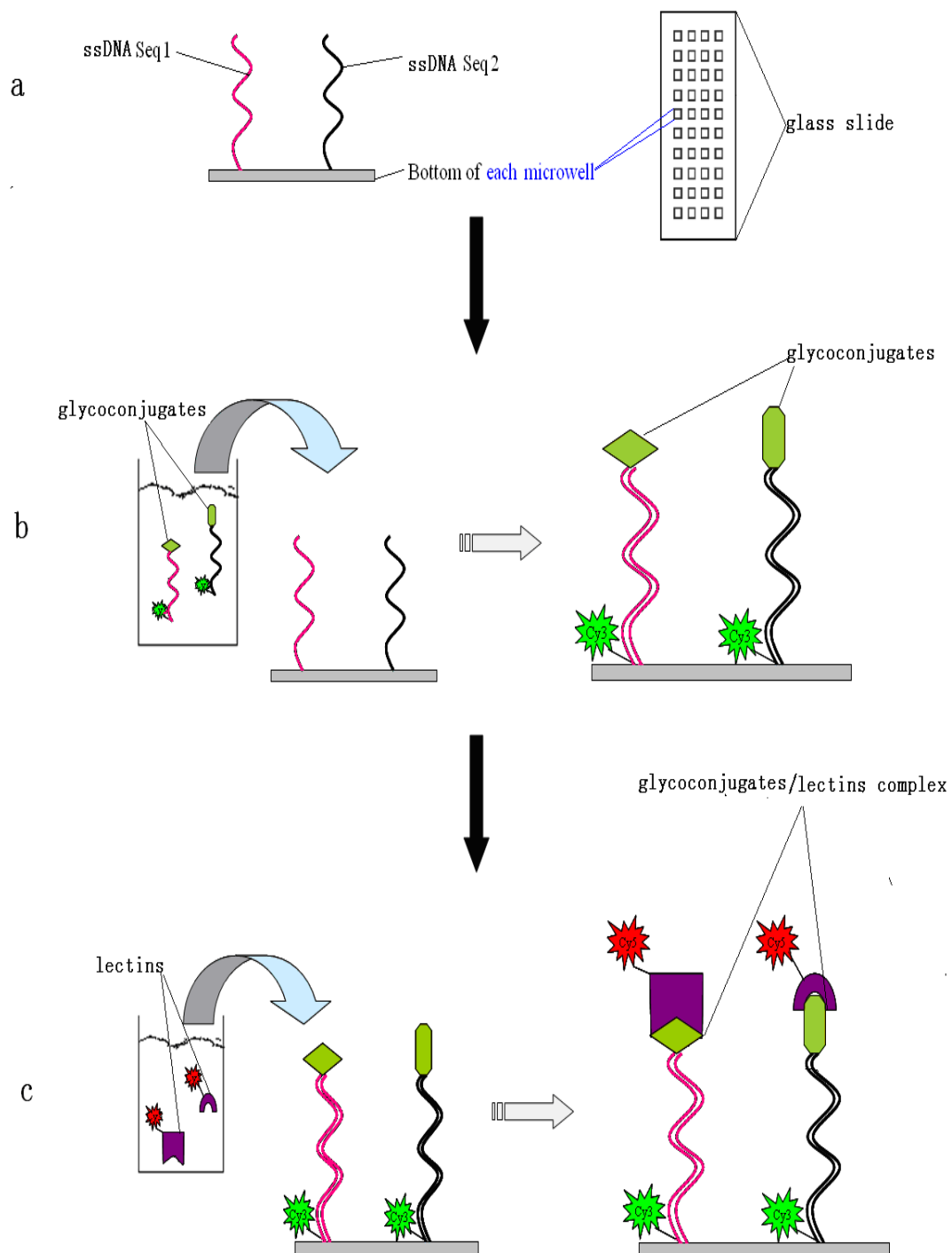
Fig5-1 Sketch map of "On –chip approach" of miniaturized biosystem: a) Immobilization of different single-strand DNAs (fabrication of DNA chip). b) Immobilization of glycoconjugates bearing different DNA tags by hybridization. c) Biological recognition of glycoconjugates towards lectins.
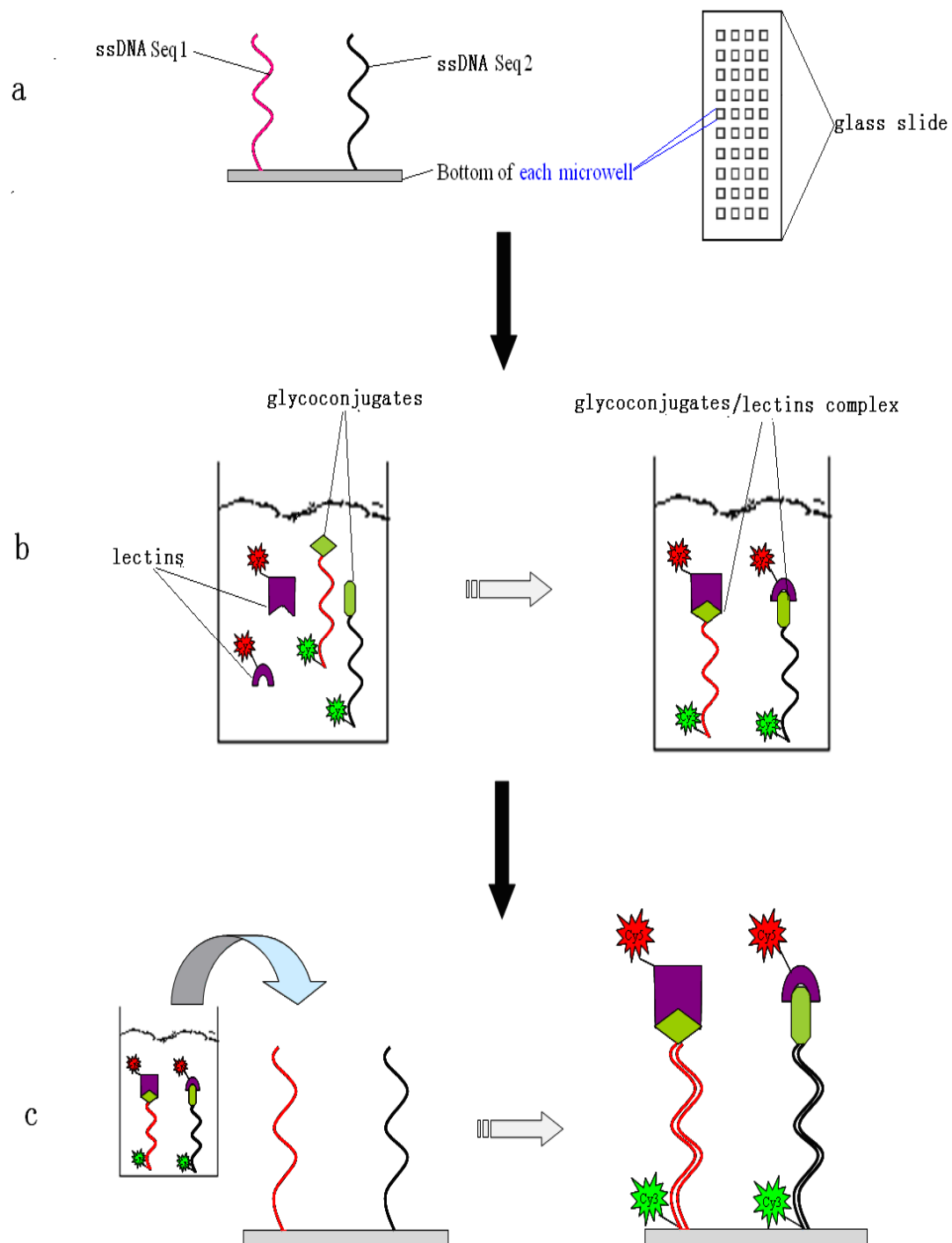
Fig5-2 Sketch map of "In –solution approach". a) Immobilization of different single-strand DNAs (fabrication of DNA chip). b) In-solution biological recognition of glycoconjugates bearing different DNA tags towards lectins. c) Immobilization of glycoconjugate/lectin complex by hybridization.

Firstly, as a proof of concept, a miniaturized biosystem (Mb I, in abbr.) was fabricated. Two ssDNA sequences were printed in alternative lines of eight spots on the bottom of each microwell. In order to validate the "in-solution approach" concept in this miniaturized biosystem (Mb I), two lectin/carbohydrate recognition models: RCA120/Galactose and PA-IIL/Fucose were tested.

Secondly, 7 new glycoconjugate affinities (see Chapter 2, Glycoconjugate 10-16) were screened against RCA 120 and PA-IL in parallel, each molecule beared 4 galactose residues arranged in various special structures, with different hydrophilic or lipophilic character and different charge. The developed miniaturized biosystem (Mb II, in abbr.) permitted to immobilize 8 different glycomimetics (or complexes of glycomimetics/lectins) bearing different ssDNA tag in one single microwell by hybridization with 8 different complementary ssDNA sequences printed on the surface of each microwell. First, cross-hybridization tests of each glycomimetics with all the covalently immobilized ssDNA sequences were performed in order to access the specificity of the hybridization. Then, binding affinities of these glycomimectics towards RCA120 and PA-IL adopting the two DDI methods ("on-chip approach" and "in-solution approach") were studied.

Finally, based on the developed miniaturized biosystem (Mb II), quantitative analyses (IC$_{50}$ values determination assay) of binding affinities of 5 glycomimetics toward PA-IL lectin were simultaneously performed on one single chip.

5.2 Development of miniaturized biosystem based on DDI glycoarray

In this section the aim is to establish the feasibility of a multiplexed test of the "in-solution" DDI with two different glyconjugates. A model microsystem Mb I was fabricated.

The results of this section were mainly adapted from (*97*).

5.2.1 Fabrication of DNA anchoring platform

Two different glycomimetics (see Chapter 2, Glycoconjugate 3 and 9) bearing a specific DNA tag were synthesised: a tri-galactosyl glycomimetic (3Gal, in abbr.)(*206*) and a tetra-fucosyl glycomimetic (4 Fuc, in abbr.).

Microwells were fabricated on borosilicate glass slides using photolithography and wet etching (*247, 269*) leading to 40 square microreactors (3.2 × 3.2 mm) per slide with a 65 mm depth (see Chapter 2, Fig 2-2 b). Next, the glass slides were functionalized into ester activated surfaces (*251*). Two 3'-Amino-linker oligonucleotides Sequence 1(Seq1) and Sequence 9 (Seq9) (see Chapter2, Table2-4), complementary to ssDNA tag of the two glycomimetics 3Gal and 4Fuc respectively, were printed at the bottom of each microwell from 25μM solutions, leading to their covalent immobilization. The final microwells displayed alternate lines of sequence Seq1 and Seq9 of 8 spots per line with 64 spots per microwell (see Fig5-3). The resulting analytical miniaturized biosysteme (Mb I) potentially allows 40 independent experiments to be performed on one slide with sample volumes between 0.5 to 2μL per experiment (e.g. different lectins/viruses/cells or inhibitor concentrations in an IC_{50} determination assay). Furthermore, thanks to the specificity of DNA hybridization, the analytical system can be envisioned as a molecule sorting tool enabling biomolecular interactions to be performed in solution with very minute volumes and the resulting complexes to be sorted according to their tags (see Fig5-2).

5.2.2 Validation of the analytical tool

In order to first validate the biosystem and then to implement the microsystem for large multiplexing analysis, we studied the interaction of two different lectins: RCA120, a galactose specific lectin, and PA-IIL(*260*), a fucose specific lectin, with glycoconjugates 3Gal and 4Fuc bearing galactose and fucose residues, respectively (see Fig5-3 and Fig5-4). We expected that 3 Gal interact with RCA 120 whereas 4 Fuc specifically bind with PA-IIL. Six conditions (Condition1-Condition6) were tested

(see Fig5-3). 3Gal was incubated in solution with Cy5 labeled lectin RCA120 (see Fig5-3, Condition 1) or with Alexa647 labeled lectin PA-IIL, (see Fig5-3, Condition 2), respectively, and then the interaction mixtures 1 and 2 were deposited in the corresponding microwell. Under Conditions 3 and 4, 3Gal was replaced by 4Fuc. Finally, under Conditions 5 and 6, both 3Gal and 4Fuc were incubated with either RCA120 or PA-IIL, respectively.
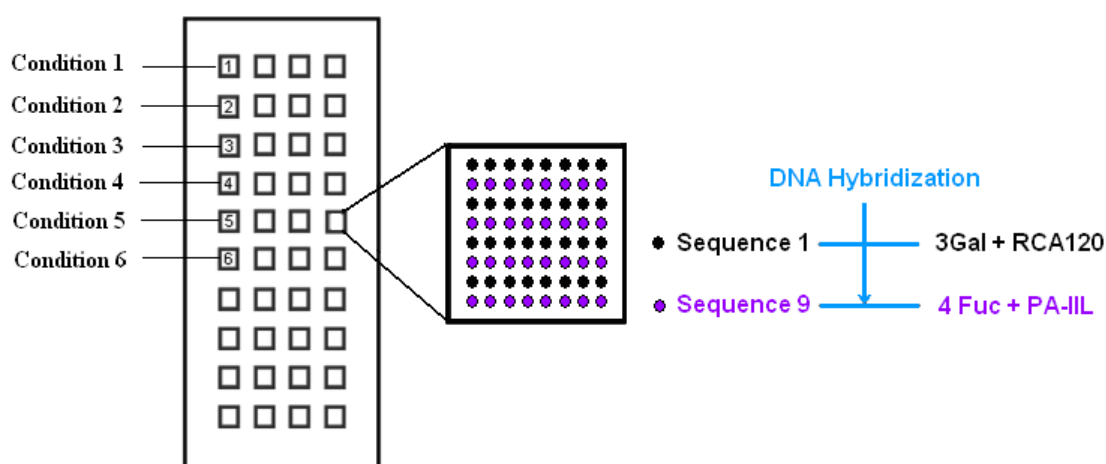
Fig5-3 Sketch map of miniaturized biosysteme (Mb I): In theory, the Complex of "3Gal + RCA120" and "4Fuc + PA-IIL" can be addressed to the bottom of the microwell by hybridization with Sequence 1 and Sequence 9 respectively（modified from (97)）.

➢ **Condition 1: incubation of 3Gal with RCA 120**

➢ **Condition 2: incubation of 3Gal with PA-IIL**

➢ **Condition 3: incubation of 4Fuc with RCA120**

➢ **Condition 4: incubation of 4Fuc with PA-IIL**

➢ **Condition 5: incubation of 3Gal and 4Fuc with RCA120**

➢ **Condition 6: incubation of 3Gal and 4Fuc with PA-IIL**

As already noted, our system uses a dual readout, so that Cy3 and Cy5 (or Alexa 647) fluorescence signals are related to the surface density of the glycomimetics and to the lectin surface density, respectively. As illustrated in Fig5-4 and quantified in Fig5-5 (top), the surface densities of immobilized molecules related to the Cy3

fluorescence signal are comparable independently of the DNA sequence or the structure of the glycomimetics and are only observed for complementary sequence spots. Thus, 3Gal and 4Fuc were selectively addressed by hybridization to immobilized Seq1 and Seq9, respectively. Incubation of 3Gal with Cy5-RCA120 or with Alexa 647-PA-IIL gave a significant fluorescence signal (860 a.u.) at 635 nm only when RCA120 was present under condition 1 (Fig. 5-5, top). Likewise, in conditions 3 and 4, 4Fuc was only recognized by PA-IIL with a very strong fluorescence (3500 a.u.) under condition 4 (Fig5-4).

These results demonstrated the specific recognition of 3Gal and 4Fuc by RCA120 and PA-IIL, respectively. Furthermore, there is no non-specific adsorption of both lectins on the chip since a fluorescence signal of 50 a.u. comparable to the background signal (40 a.u.) measured when 3Gal or 4Fuc were not present (with their target lectin).

Finally, when 3Gal and 4Fuc were incubated together with Cy5-RCA120 (Fig5-4, Condition 5), the Cy3 fluorescence signal was similar on lines Seq1 and Seq9 illustrating that both molecules were correctly addressed, but fluorescence at 635 nm (Cy5 or Alexa 647) was only observed for line Seq1 while it remained comparable to background level on line Seq9. This result demonstrates that the RCA120 lectin specifically recognized 3Gal from the mixture of 3Gal and 4Fuc and that the lectin–glycoconjugate complex was efficiently addressed to the desired spot in the microwell due to the specificity of DNA/DNA hybridization. A similar result was obtained with PA-IIL (Fig5-4, condition 6), where the Alexa 647 fluorescence signal was only observed on Seq9 lines where 4Fuc was hybridized.

These results showed that the two specific recognitions (RCA120/3Gal and PA-IIL/4Fuc) were successfully performed and well addressed onto the miniaturized biosystem, which demonstrated the proof of concept. In the following studies, more complex and larger multiplexing test would be performed.
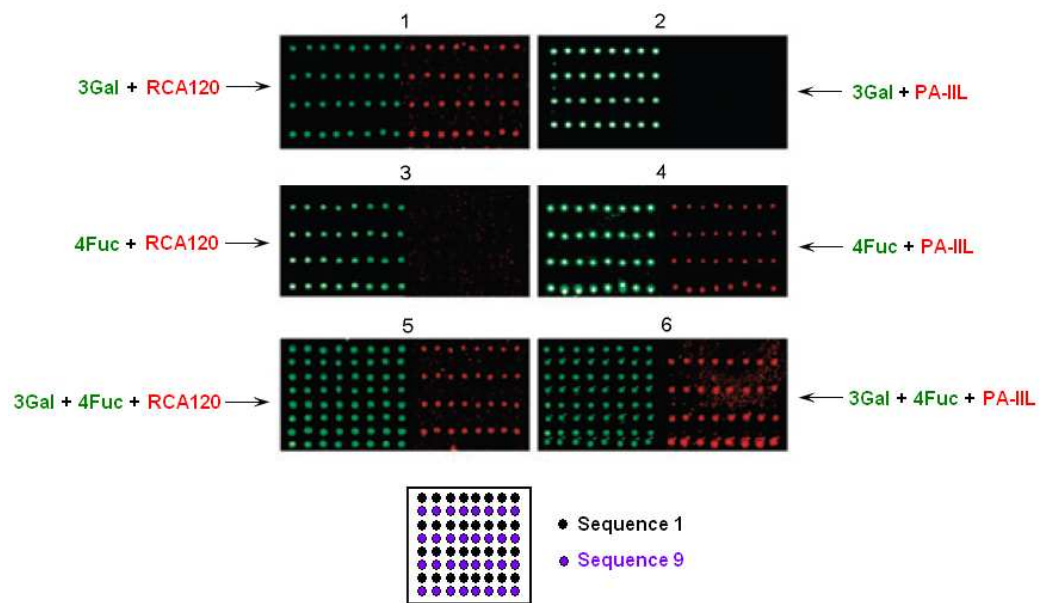
Fig5-4 Fluorescence images recorded at 532nm (a.u.) of the glycoconjugates (green color): Cy3-labeled 3Gal or 4Fuc, and at 635 nm (a.u.) of the lectins (red color): Cy5-labeled RCA120 or Alexa-labeled 4Fuc. (Modified from (97))
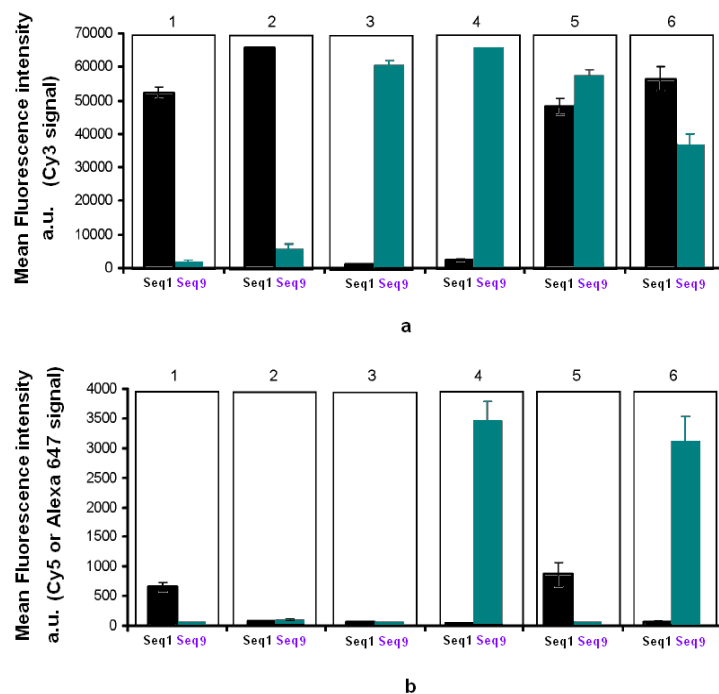
Fig5-5 Mean fluorescence intensities of Cy3-labeled 3Gal or 4Fuc (at 532nm) and Cy5-labeled RCA120 or Alexa-labeled 4Fuc (at 635 nm) abstained from condition 1-6. (Modified from (97))

5.3 The use of developed miniaturized biosystem for studying the lectins/glycomimetics affinities

Our aim in section 5.3 was to study the affinity of seven glycoconjugates towards the lectins RCA120 and PA-IL in a multiplexed test, in other words to probe in one single microwell the all seven glycoconjugates for one lectin. To achieve this goal we needed to:

1) define seven DNA tags for each glycoconjugate;

2) immobilize all the seven sequences which are complementary sequences of the DNA tag of the glycoconjugates at the bottom of each microwell;

3) insure that each glycoconjugate would be specifically addresses by hybridization with its complementary sequence under "on-chip" and "in-solution" approach experimental condition;

4) insure that hybrization would perform with similar yield under "in-solution" and "on-chip" approach experimental condition.

Next the binding affinities of each lectin for the seven glycoconjugates was probed in one single experiment in one microwell and finally the IC_{50} of five glycoconjugates was determined in a multiplexed test (in other words, in one microwell, five glycoconjugates were incubated with one lectin and one concentration of inhibitor). The IC_{50} test was based on the "in-solution" approach allowing determining the IC_{50} of the five conjugate on one single slide with picomoles of lectins and glycoconjugates.

5.3.1 Fabrication of DNA anchoring platform

Six new Cy3 labeled tetra-galactosyl glycomimetic bearing different ssDNA tag were synthesized (Glycoconjugate 10 – 15, see Chapter 2, Fig2-1 and Table2-1). The six new glycoconjugates as well as 3Man and 3Gal (see Chapter 2, Fig2-1, Glycoconjugate 1 and 3) were prepared for the following study.

In order to perform multiplexed test of the affinities of seven glycoconjugates towards the lectins in one single microreactor (microwell) of the DDI glycoarray, the key issue is to make sure that all the seven glycoconjugates could be well addressed to the desired positions and display homogeneous surface densities on the DDI glycoarray. Therefore each glycoconjugate should bear a specific ssDNA tag. Each specific tag (noted Cseq) would be complementary to corresponding ssDNA sequence printed at the bottom of the microreactor for anchoring the glycoconjugate by hybridization. That is to say, in one single microreactor at least seven different ssDNA should be printed for anchoring the seven glycoconjugates. The main challenge is to find out a set of DNA sequences that are able to stably anchoring those glycoconjugates under the same experimental conditions with equivalent yields of hybridization and without cross-hybridization. From the DNA database of our lab, cross-hybridization tests were performed for fourteen ssDNA sequences and their complementary sequences, of which 8 sequences (Sequence1-8, see Chapter 2, Table2-4) were chosen for the fabrication of these DNA anchoring platforms. As shown in Table2-4 (see Chapter 2), the eight sequences almost have the same length and have   melting temperatures ranking from 50°C -65°C. This implies that under our experimental temperature (RT or 37°C), the DNA duplexes of those sequences should be stable. The other influencing factor for the stability of the hybridization is the GC-ratio. Due to the lower stability of AT than GC pairs, usually the higher the GC-ratio is, the more stable the hybridization is. Therefore in theory, Sequence 1 with GC-ratio of 72.2% and Sequence 7 with GC-ratio of 22.7% should be the most stable and unstable sequence respectively, while other sequence almost share the same moderate level. It should be noticed that the shift often observed between the theoretical calculations and experimental results. This is the reason for which experimental validation was first required.
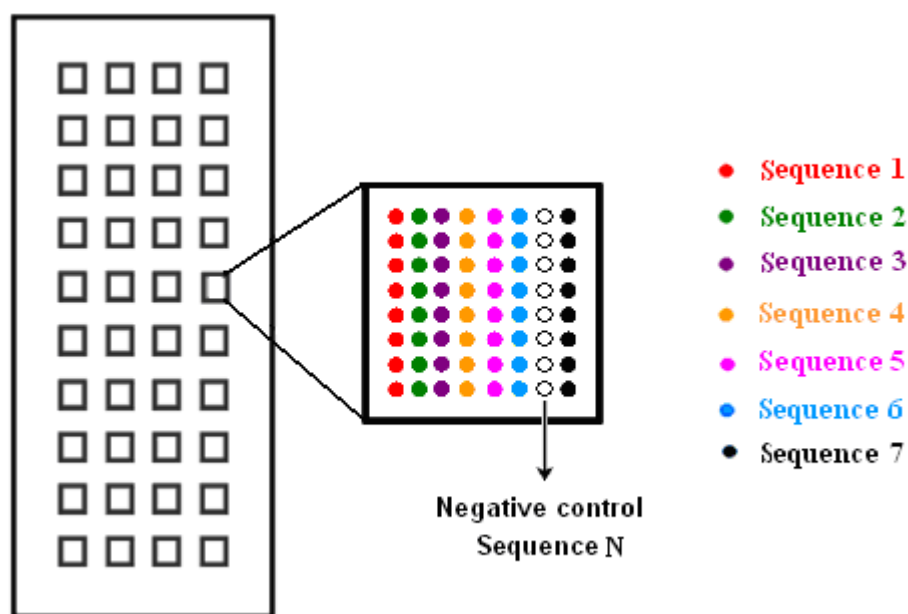
Fig5-6 Sketch map of DNA anchoring platforms of Mb II: Sequence N (negative control) and Sequence 1-7 were printed on the bottom of each microwell resulting in one column and eight spots for each sequence, 64 spots in all.

Based on the miniaturized biosystem (Mb I), a new miniaturized biosystem (Mb II) was set up. The DNA anchoring platform Mb II also had 40 square microwells and was fabricated on borosilicate glass slides using the same method as described before (see Chapter 2 Fig2-2 b). Eight 3'-Amino-modified DNA sequences (Sequence N, Sequences 1 to 7, see Chapter2 Table 2-4) were spotted at the bottom of each microwell with a Biorobotics MicroGrid microarrayer. Sequence N was considered as a negative control for estimating the non-specific adsorption because any tag complementary to sequence N was not used during experiments. The resulting microwell featured with 8 spots (one column) per sequence, 64 spots per well. Therefore, each microwell on the glass slide can be regarded as a mini DNA chip.

Name of ssDNA Complementary sequences	Internal reference	GC%[a]	Tm[b]
Cseq1	Czip 1.1.1	66.7	54.7
Cseq2	Czip 1.7.1	36.8	49.6
Cseq3	Czip 1.8.1	52.6	59.4
Cseq4	Czip 1.9.1	57.9	59.6
Cseq5	Czip 1.10.1	46.7	44.0
Cseq6	Czip 1.11.1	31.6	44.7
Cseq7	Czip 1.14.1	26.3	46.7

Table5-1 Main characters of ssDNA complementary sequences carried by the glycoconjugates and noted Cseq1 to Cseq7.

Cseq1 to Cseq7 are complementary sequences of Seq1 to Seq7 listed in table2-4(see Chapter 2) respectively.

GC%[a] and Tm[b] were calculated by on-line software Primer3 (http://biotools.umassmed.edu/bioapps/primer3_www.cgi)

5.3.2 Cross-hybridization tests of glycoconjugates

As mentioned before, each microwell of Mb II can be used as a tiny DNA anchoring platform (mini DNA chip). Therefore, Mb II has the potential to perform a parallel study of the interactions of 7 different glycoconjugates bearing different 7 DNA tag (see Table 5-1) with its targeted lectin in one single microwell. To achieve such a goal, the prerequisite is to make sure that each glycoconjugate can be addressed to its corresponding spots by correct hybridization with its complementary ssDNA sequences printed on the surface of the microwell. However, when the mixed solution of different glycoconjugates with various DNA tags are deposited into the microwell, cross-hybridization may take place between DNA tag of the probe (glycoconjugate) and non-complementary sequences presented on the surface of the microwell. The cross-hybridization can be an especially severe problem and a significant contributor to false-positive noise. Cross-hybridization assays are, thereby, very important and essential works prior to the investigation of interactions between the probe (glycoconjugates) and the target (e.g. lectin). In addition, nonspecific adsorption of the glycoconjugate (or lectins) may also result in serious measurement error, so that a negative control sequence is necessary to be printed onto the surface of microwell for monitoring the nonspecific adsorptions. Moreover, for a cross-hybridization assay, each glycoconjugate solution should be added into each microwell of Mb II respectively, which means that the presence of one glycoconjugate per microwell should be guaranteed. However, after incubation of glycoconjugate, the slide needs to be washed. During the washing steps, the glycoconjugates from different microwells may contaminate adjacent microwell leading to false cross-hybridization results. In order to tackle this problem, during the glycoconjugate incubation processes, complementary sequences without any fluorescent label (see Table5-1) were employed to block the sequences with which the glycoconjugate are not supposed to hybridize.

In this context, two cross-hybridization tests were designed and performed on the DNA anchoring platform (see Fig5-6) under the two DDI glycoconjugates hybridization conditions ("on-chip" and "in-solution" methods). Indeed under the "on-chip" condition, hybridization is conducted at room temperature in Saline Sodium Citrate 5x Sodium Dodecyl Sulphate 0.1 % buffer while it performed in phosphate

buffer saline (pH 7.4, 37 °C) in the "in-solution" approach (due to the presence of lectin).

5.3.2.1   *Cross-hybridization tests under "on-chip" condition*

Under "on-chip" glycoconjugate hybridization condition, firstly the cross-hybridization tests were carried out on DNA anchoring platform at three concentrations of glycoconjugates: 1µM, 0.5µM and 0.1µM. Fig5-7 gives the sketch map of cross hydridization assay. The glycoconjugates used in these experiments were nommed molecules: from molecule 1 to molecule 7, which correspond to Glycoconjugate 1, Glycoconjugate 11, Glycoconjugate 12, Glycoconjugate 13, Glycoconjugate 10, Glycoconjugate 14, and Glycoconjugate 15 respectively. These seven molecules with their respective DNA tag (Cseq1 to Cseq7) can hybridize with their corresponding sequences (sequence1 to sequence7) covalently immobilized at the surface of the microwell.

From condition 1 to condition 7 (see Fig5-7), at 1µM each of the seven molecules was added into the relevant microwell accompanied by six oligonucleotides corresponding to the other complementary sequences (Cseqs). In other words these six oligonucleotides consisted of DNA sequences different from the one of the added glycoconjugate. For example, in condition2 molecule2 was added into microwell 2 with six Cseqs: Cseq1, and Cseq3 to Cseq7.We recall that these Cseqs did not carried fluorescent groupement.

Likewise, for condition a-g and condition A-G, the molecules and complementary sequences were added into the corresponding microwells using the same method as condition 1-7, but at different concentrations: 0.5µM and 0.1µM.

For condition I, however, all seven molecules were mixed together and deposited into each microwell.

After about 3h of incubation at room temperature, the slide was scanned at 532 nm with the GenePix 4100 microarray scanner. Fluorescence image (see Fig5-8) and mean fluorescence intensities (see Fig5-9) were recorded. The Fluorescence intensity of each glycoconjugate was determined as the average mean fluorescence signal of eight spots in one column. As shown in Fig5-8, for each microwell of Condition I, Cy3 signal was observed for the seven columns of spots which printed from

Sequence1 to Sequence7 respectively, no signals were detected from the negative control Sequence N, which demonstrated no non-specific adsorption of glyconconjugates. In the case of conditions 1-6, conditions a-f and conditions A-F, for which only one single molecule (molecule1 to molecule 6) was added into each microwell, Cy3 signals was detected for only one column for each microwell, whatever concentration was used (1µM, 0.5µM and 0.1µM). Moreover, the positions at which the Cy3 signals for every molecule (molecule1 to molecule 6) appeared in each microwell of conditions 1-6, conditions a-f and conditions A-F perfectly matched the positions of the complementary sequences in each microwell (see Fig5-6) It indicated that under conditions 1-6, conditions a-f and conditions A-F, each of the six molecule (molecule 1 to molecule 6) were correctly addressed to the desired spots by hybridization. For example, under Condition 2 under which only molecule 2 was added, Cy3 signals of 8 spots (one column) were detected in microwell 2, the positions of the 8 spots was just where the Sequence 2 was illustrating that molecule 2 was well addressed. Furthermore, the mean fluorescence intensities of each of the six molecules which hybridized with its corresponding complementary sequences were very strong comparing to those hybridized with other non-complementary sequences, about 8000 a.u.-25000 a.u. for the former, and some 30 a.u.-200 a.u for the latter which is comparable with the fluorescence intensities for the negative control sequence N (30 a.u.-80 a.u.) (see Fig5-9). The ratio of fluorescence intensities of specific versus non-specific hybridization (herein specific hybridization means the glycoconjugate was specifically immobilized to the desired spots by hybridizing with its corresponding complementary sequence) for Molecule 1- Molecule 6 have been calculated to be about $10-10^2$ (see Table5-2), so that the cross-hybridization for the six molecules (molecule 1 to molecule 6) were almost negligible. However for Molecule 7, under Condition 7, Condition g and Condition G, Cy3 signals were detected not only from Sequence 7, but also from Sequence 6(see Fig5-8). The fluorescence intensities obtained for Molecule 7 which hybridized with Sequence 7 were higher than those obtained for the same molecule cross-hybridized with Sequence 6 (see Fig5-9). Interestingly, with decreasing concentration of molecule 7 from 1 µM to 0.1 µM, the ratio of specific/non-specific hybridization increased from 2.4 to 12 (see Table5-2). Another interesting observation is that although the concentration of Molecule 7 was reduced to 0.1µM, the mean fluorescence intensities are quite similar to those obtained at 1µM and 0.5µM (see Fig5-9, Fig5-10). However,

for most of other six molecules, as the concentration decreased the mean fluorescence intensities were not stable, especially for Molecule 1 and Molecule 5 (bearing 3 mannoses and 4 galactoses in comb-like structure respectively), a sharp drop-off were observed (see Fig5-10). At 1µM, the mean fluorescence intensities displayed a homogeneous value (20000-25000 a.u.) for all the seven molecules (see Fig5-9, Fig5-10), indicating that the relative surface density of the seven glycoconjugates were comparable.
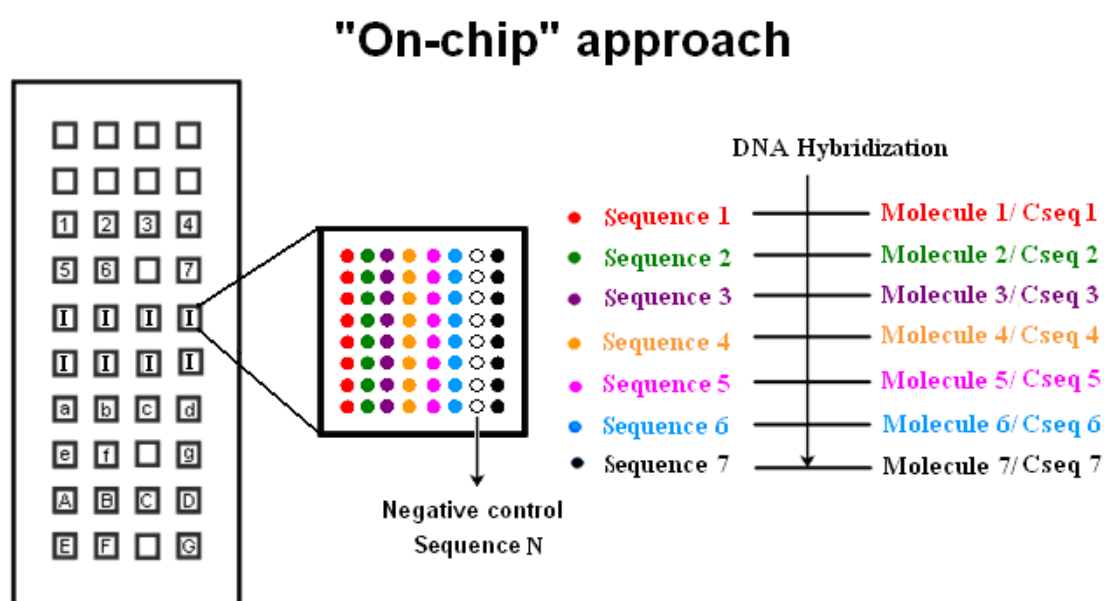
Fig5-7 Sketch map of cross-hybridization assay of seven molecules (molecule 1-7) under "on-chip" glycoconjugate hybridization condition on the DNA anchoring platform a).Negative control sequence N is used to monitor the non-specific adsorption of glycoconjugates. Each of the seven sequences (sequence1-7) was expected to only hybridize with its corresponding molecule (molecule1-7) or complementary sequences (Cseq1-Cseq7).

➢ **Condition 1-7: At 1µM, in each microwell, incubation of one of the seven molecules (molecule 1-7) with other six Cseq (complementary sequences) except its corresponding complementary sequences. e.g.: for condition 1, incubation molecule 1 with Cseq2-Cseq7 except Cseq1; for condition2, incubation molecule 2 with Cseq1, and Cseq3-Cseq7 except Cseq2.**

➢ **Condition I: At 1µM, in each microwell, incubation of all seven molecules (molecule 1-7).**

➢ **Condition a-g: At 0.5µM, in each microwell, incubation of one of the seven molecules (molecule 1-7) with other six Cseq (complementary sequences) except its corresponding complementary sequences.**

➢ **Condition A-G: At 0.1µM, in each microwell, incubation of one of the seven molecules (molecule 1-7) with other six Cseq (complementary sequences) except its corresponding complementary sequences.**
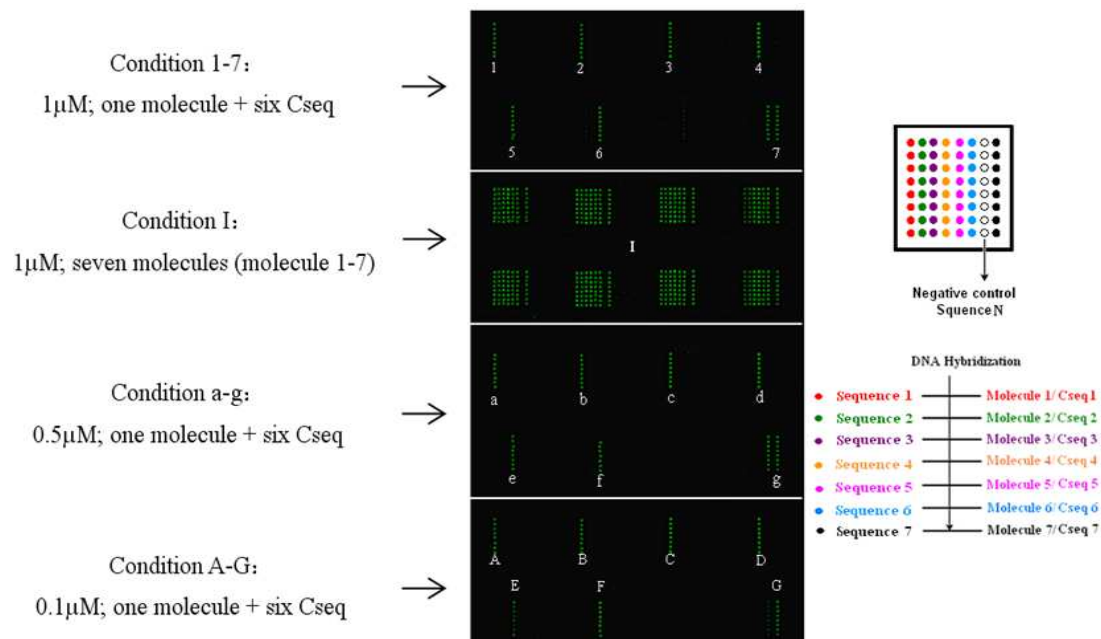
Fig5-8 Fluorescence image recorded at 532nm (a.u.) of the glycoconjugates, after cross-hybridization test under "on-chip" glycoconjugate hybridization condition on the DNA anchoring platform a).
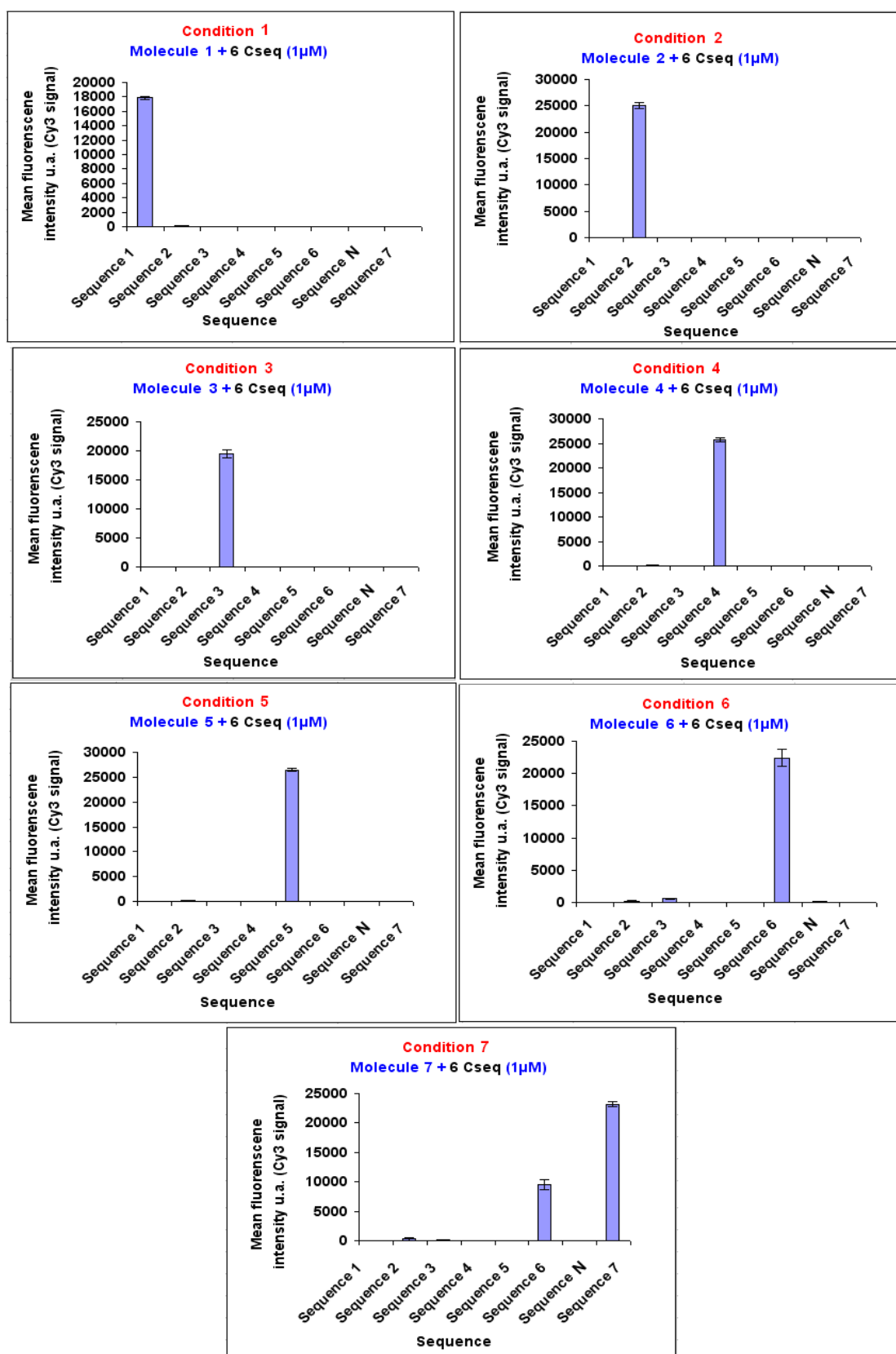
Fig5-9 Mean fluorescence intensities obtained at 532nm (a.u.) for the glycoconjugates of condition1-7, condition a-g and condition A-G, after cross-hybridization test under "on-chip" glycoconjugate hybridization condition on the DNA anchoring platform a).
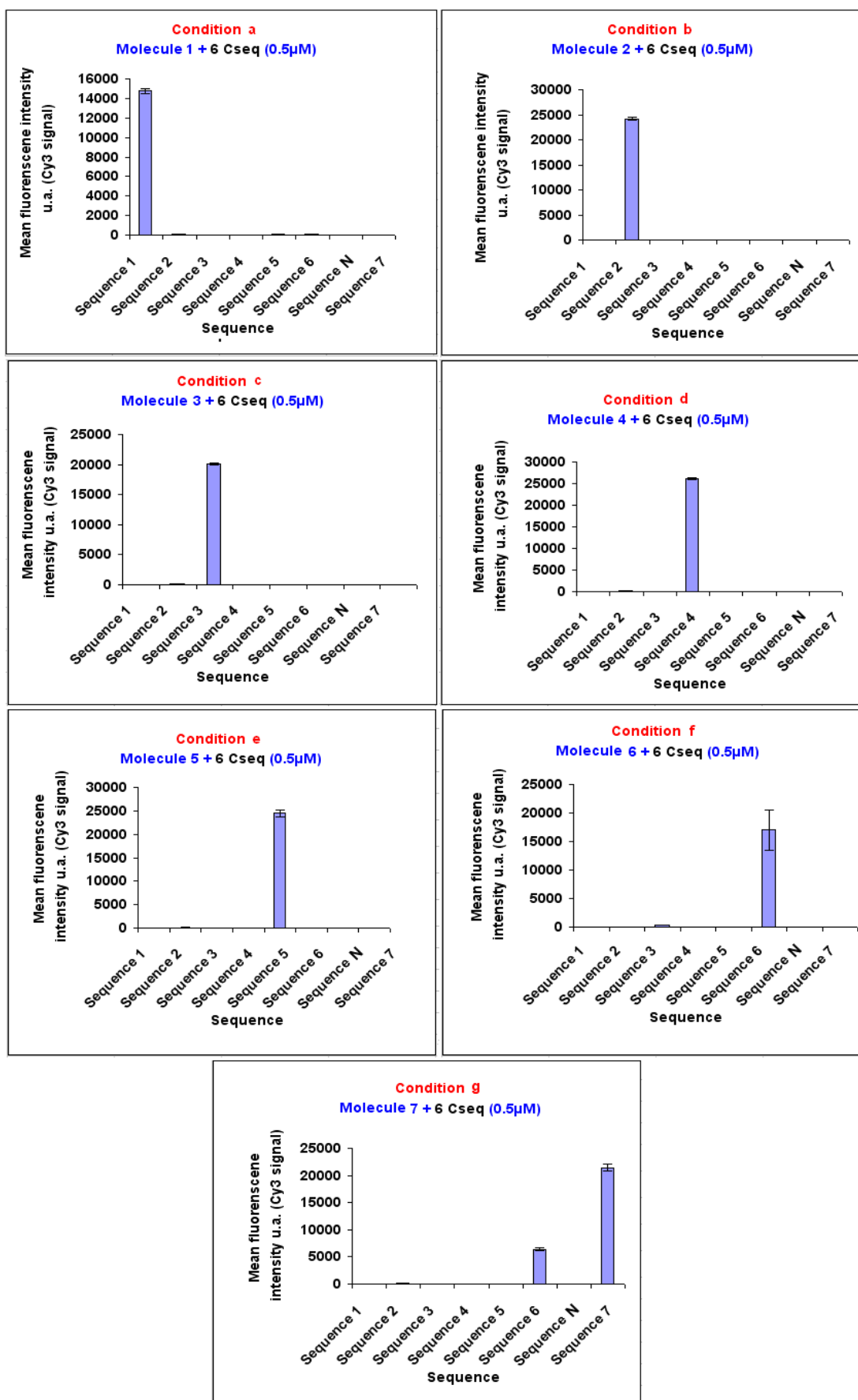
Fig5-9 (Continued)
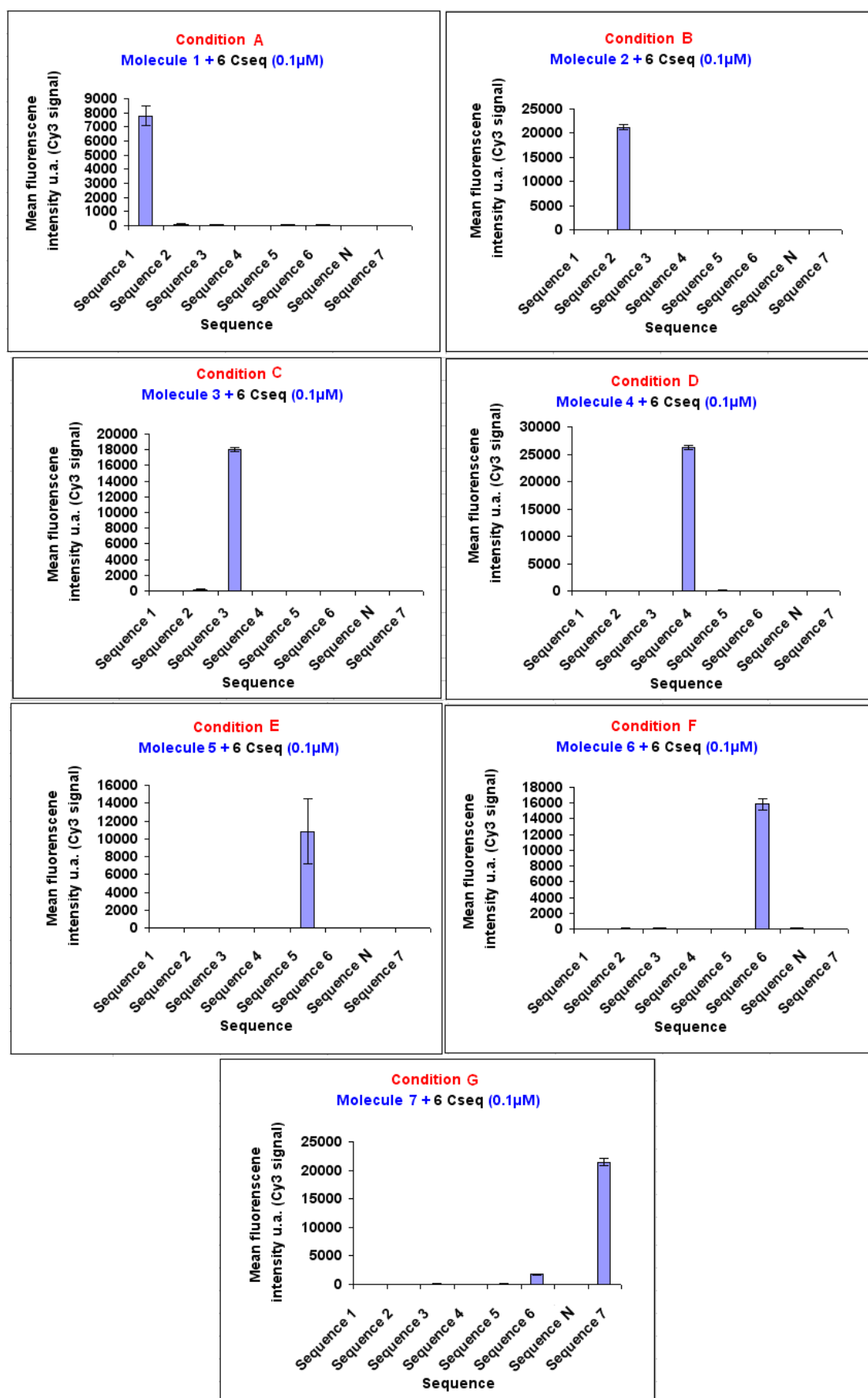
Fig5-9 (Continued)

	Ratio of fluorescence intensity (specific vs. non-specific hybridization)		
	Condition 1-7 1µM	Condition a-g 0.5 µM	Condition A-G 0.1µM
Molecule 1	190	150	70
Molecule 2	300	330	320
Molecule 3	270	190	110
Molecule 4	110	160	280
Molecule 5	130	290	260
Molecule 6	40	49	84
Molecule 7	2.4	3.3	12

Table5-2 Ratio of fluorescence intensity of specific vs. non-specific hybridization of seven molecules for Condition1-7, Condition a-g and Condition A-G, after cross-hybridization test under "on-chip" glycoconjugate hybridization condition on the DNA anchoring platform a).
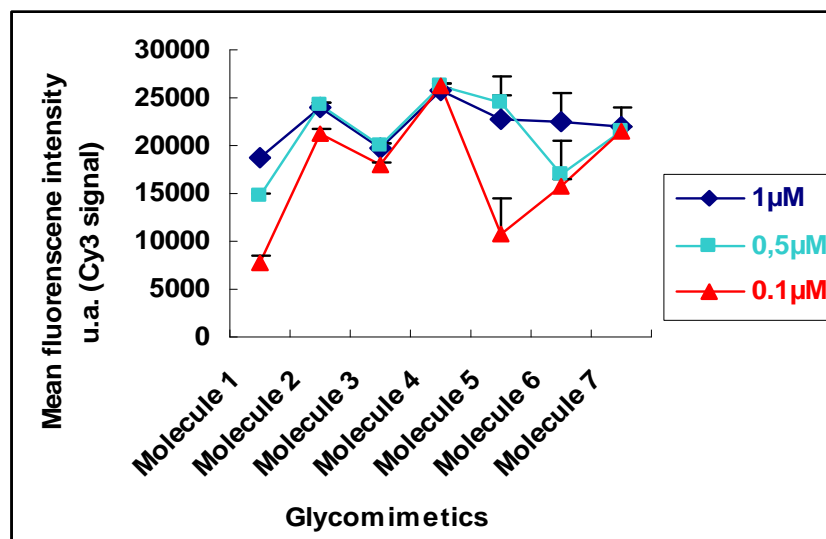
Fig5-10 Variation of mean fluorescence intensities at 532nm (a.u.) of the seven molecules when the concentration changed from 1µM (condition1-7), 0.5µM (condition a-g) to 0.1µM (condition A-G).

All the above results demonstrated that no matter which concentration of glycoconjugates (1μM, 0.5μM or 0.1μM) were used, under "on-chip" approach conditions most of the tested glycoconjugates Molecule 1-6 (Glycoconjugate 1 and Glycoconjugate 10-14) except Molecule 7 (Glycoconjugate 15) could be specifically addressed by hybridization with its complementary sequences immobilized in each microwell of MbII. However, only at 1μM, the glycoconjugates displayed almost homogeneous fluorescence intensity yields.

5.3.2.2   Cross-hybridization tests   under "in-solution" condition

,Cross-hybridization tests of molecule 1-molecule 7 were carried out with Mb II under "in-solution" condition (See Fig5-11). Using the same cross-hybridization determination method described before, each molecule was mixed together with the other six oligonucleotides corresponding to the other complementary sequences. The mixture was deposited into its corresponding microwell at two concentrations 1μM and 0.1μM (see, Fig5-11, Condition 1-7 and Condition A-G). The mixture of seven molecules was deposited into each microwell of Condition I.

After incubated at 37° C for 3h, the slide was washed and scanned. The results shown in the Fluorescence image (see Fig5-12) and the mean fluorescence intensities for each condition (see Fig5-13) were analogous to results obtained under "on-chip" conditions (see Fig 5-8, Fig5-9).
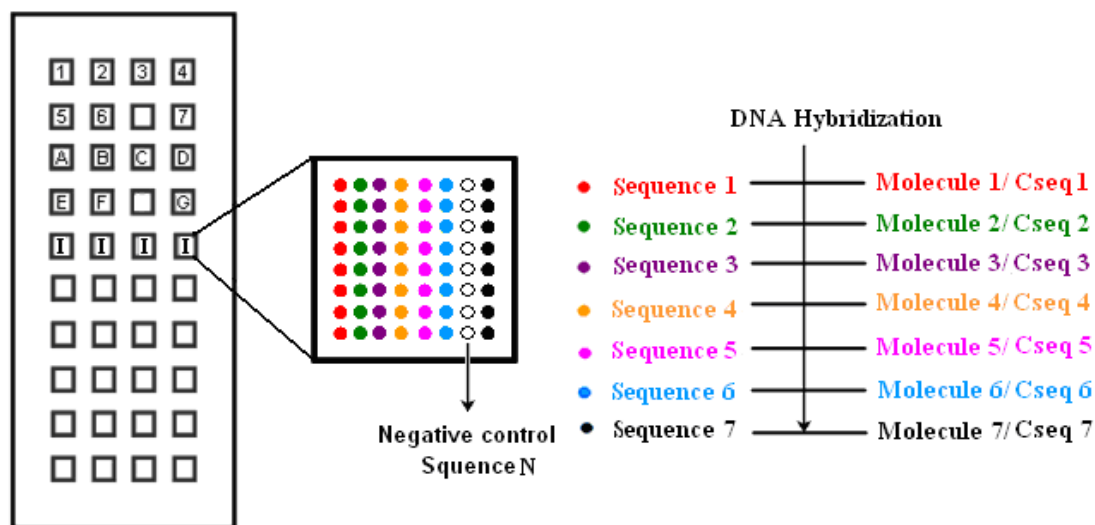
Fig5-11 Sketch map of cross-hybridization assay of seven molecules (molecule 1-7) under "in-solution" recognition condition on DNA anchoring platform of MbII.

➢ **Negative control sequence x is for monitor the non-specific adsorption of glycoconjugates.**

➢ **Condition 1-7: At 1μM, in each microwell, incubation of one of the seven molecules (molecule 1-7) with other six Cseq (complementary sequences) except its corresponding complementary sequences. e.g.: for condition 1, incubation molecule 1 with Cseq2-Cseq7 except Cseq1; for condition2, incubation molecule 2 with Cseq1, and Cseq3-Cseq7 except Cseq2.**

➢ **Condition A-G: At 0.1μM, in each microwell, incubation of one of the seven molecules (molecule 1-7) with other six Cseq (complementary sequences) except its corresponding complementary sequences.**

➢ **Condition I: At 1μM, in each microwell, incubation of all seven molecules (molecule 1-7).**
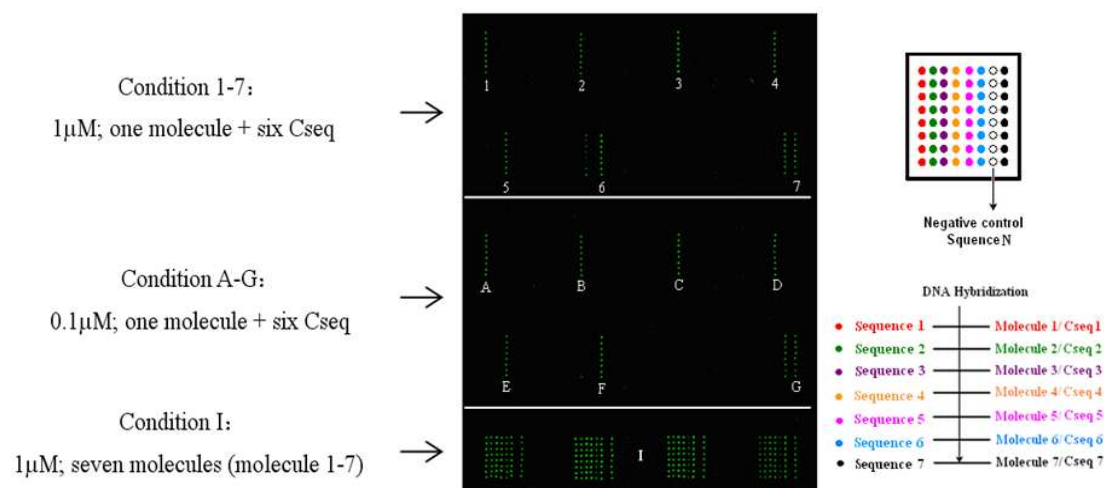
Fig5-12 Fluorescence image recorded at 532nm (a.u.) of the glycoconjugates (molecule 1-7), after cross-hybridization test under "in-solution" glycoconjugate hybridization condition on the DNA anchoring platform a).
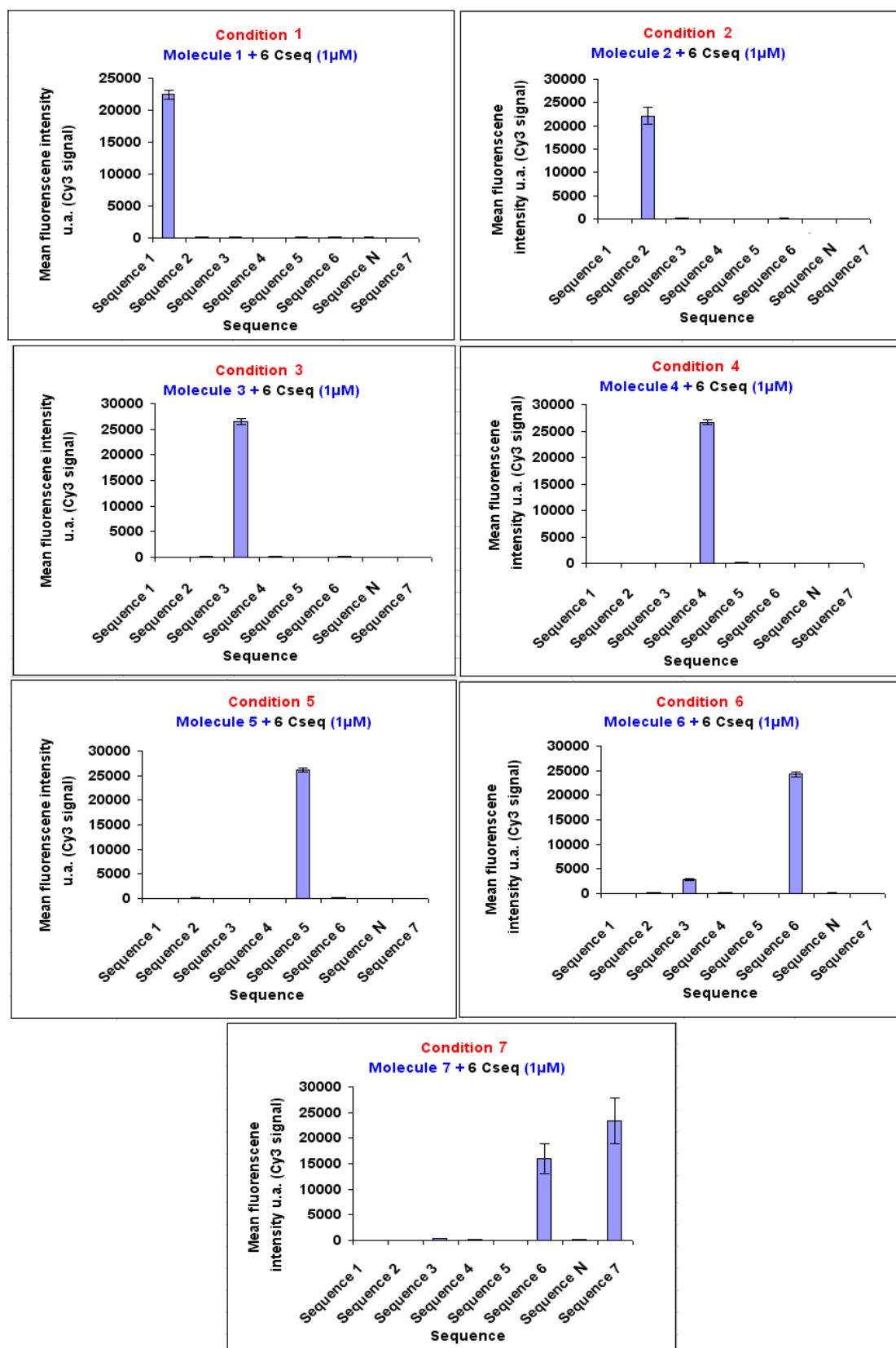
Fig5-13 Mean fluorescence intensities obtained at 532nm (a.u.) for the glycoconjugates of condition 1-7 and condition A-G, after cross-hybridization test under "in-solution" glycoconjugate hybridization condition on the DNA anchoring platform a).
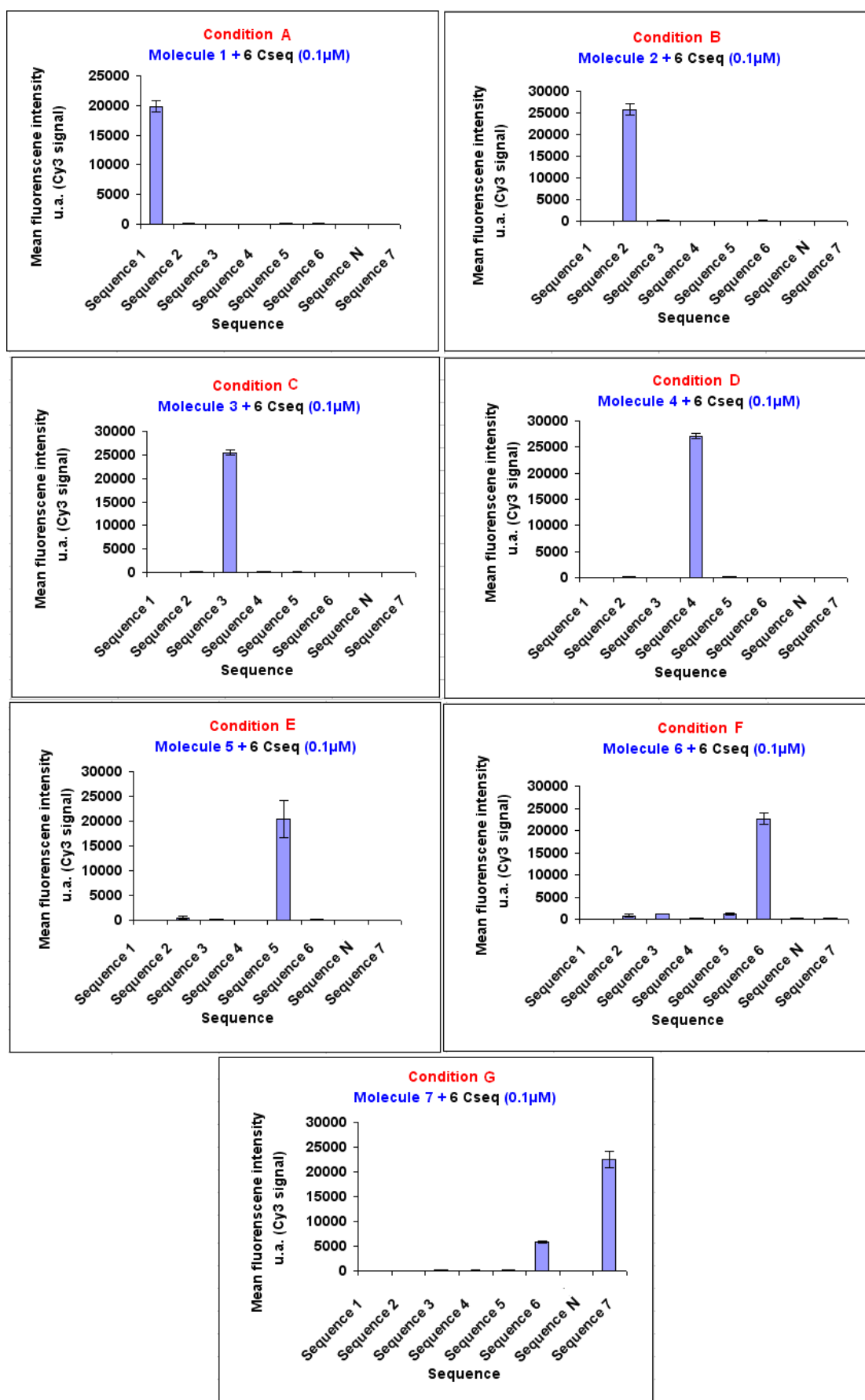
Fig5-13 (Continued)

	Ratio of fluorescence intensity (specific vs. non-specific hybridization)	
	Condition 1-7 1µM	Condition A-G 0.1µM
Molecule 1	130	160
Molecule 2	160	150
Molecule 3	210	190
Molecule 4	250	210
Molecule 5	130	180
Molecule 6	8.4	18
Molecule 7	1.5	3.8

Table5-3 Ratio of fluorescence intensity of specific vs. non-specific hybridization of seven molecules for Condition1-7 and Condition A-G, after cross-hybridization test under "in-solution" condition on the DNA anchoring platform of MbII.
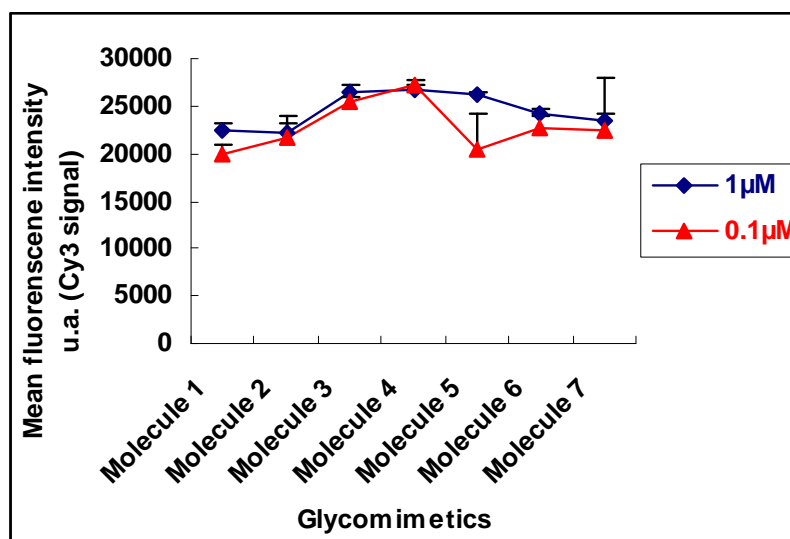
Fig5-14 Variation of mean fluorescence intensities at 532nm (a.u.) of the seven molecules when the concentration changed from 1µM (condition1-7) to 0.1µM (condition A-G).

Although for Molecule 6, at 1μM (Condition 6), Cy3 signals were observed for two columns corresponding to the Sequence 6 and Sequence 3 were printed. The Cy3 intensities ratio of specific vs. non-specific hybridization was 8.4 (see Table 5-3). There were no cross-hybridizations for Molecule 1 to Molecule 5, as the ratios for the five molecules were greater than 10^2. Molecule 7 was still the only one that cross-hybridization was significant. The Cy3 intensities ratio of specific vs. non-specific hybridization was 1.5 at 1μM, 3.8 at 0.1μM (see Table 5-3). Similarly to the "on-chip" conditions, the reducing of the concentration from 1μM to 0.1μM resulted in the improvement of the ratio of specific hybridization vs. non-specific (increased from 8.4 to 18 for Molecule 6, from 1.5 to 3.8 for Molecule 7) (see Table 5-3) in the decrease of the mean fluorescence intensities of Molecule 1 and Molecule 5. Moreover, at 1μM, the mean fluorescence intensities were also at the same level (23000-28000 a.u.) for all the seven molecules (see Fig5-13, Fig5-14), suggesting that the seven glycoconjugates were homogeneously immobilized in each microwell.

In summary, under "in-solution" condition six glycoconjugates (Molecule 1- 6) were well immobilized to the desired spots without cross-hybridization and displayed similar fluorescence intensities at 1μM. Like observed under "on-chip" condition, cross-hybridization was also detected from Molecule 7 (Glycoconjugate 15)

5.3.3 Study of binding affinities of glycoconjugates toward RCA120 and PA-IL in MbII

Following the cross-hybridization tests, we tried to use MbII to study the binding affinities of the six new glycoconjugates (Molecule 2-Molecule 7) as well as 3Man (Molecule 1) and 3Gal (Glycoconjugate 3, see Chapter 2 Fig2-1) with two galactose specific lectins: RCA120 and PA-IL.
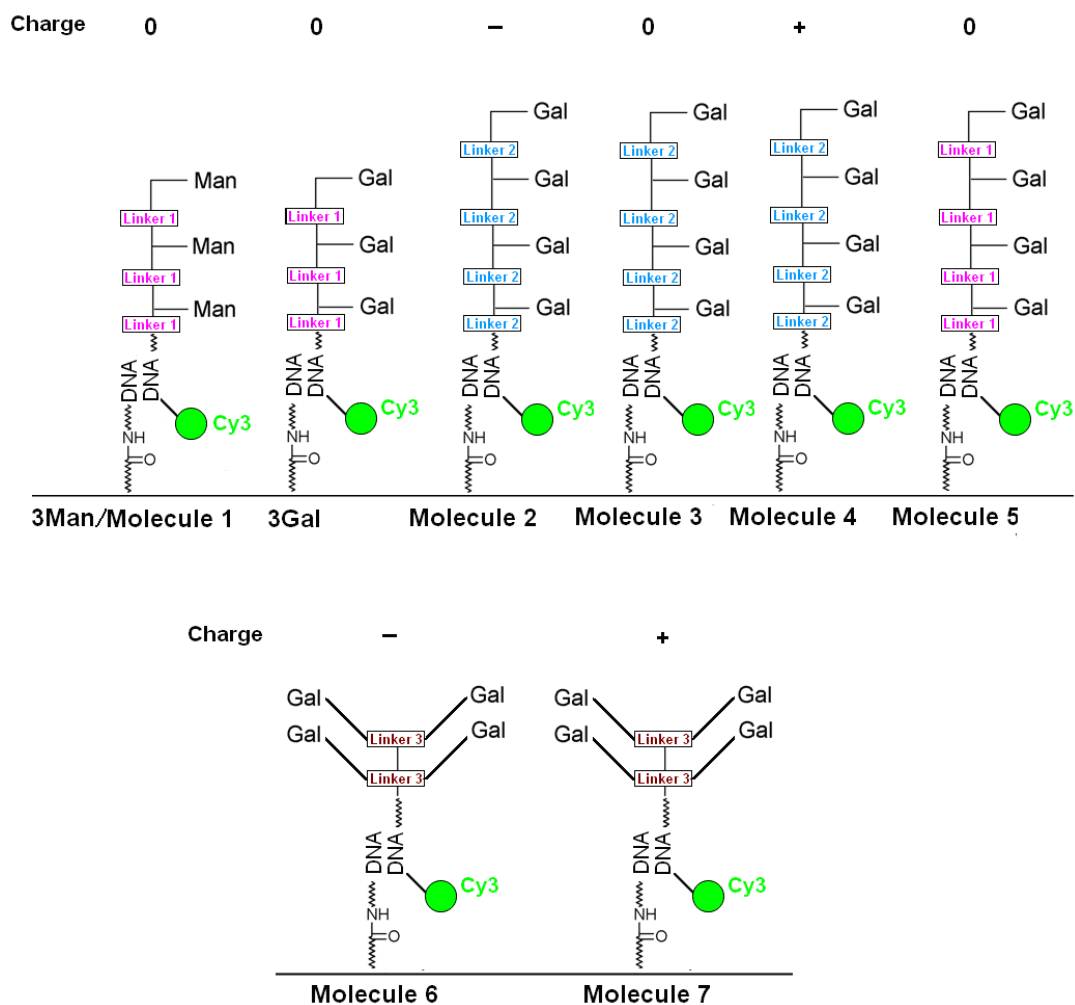
Fig5-15 Sketch map of the structures of eight immobilised glycoconjugates, 3Man is a negative control for the two galactose-specific lectins.

In chapter 4, some differences in the behaior of binding affinity of PA-IL between comblike and antenna structures have been observed. This difference may be related to the spatial arrangement or due to the charge of the glycomimetics. Herein, 6 new glycomimetics with various spatial arrangements and different charges have been tested.

The main characters of the glycomimetics were displayed in Table5-4 and Fig5-15. Molecule 1 (3Man) bearing three mannose residues was expected to be a negative control for monitoring the non-specific adsorption of lectins. 3Gal was used as a positive control, which contains three galactose residues supported by a Comb-like scaffold with a linkage Linker 1(1, 4-cyclohexanedimethanol, DMCH) between every two phosphodiesters and could be efficiently recognized by RCA120

or PA-IL on a DDI glycoarray (*98, 99*). 3Man and 3Gal having the same DNA tag (Sequence 1), they can not be immobilized simultaneously in the same microwell. Molecule 5 consists of four galactose residues arranged on a Comb-like backbone similarly to 3Gal. Regarding Molecule 2, Molecule 3 and Molecule 4 (see Table5-4, Fig5-15 and Chapter 2, Fig2-1 or Table2-1), the three glycoconjugates have almost the same structures: they all bear four galactose residues coupled with Linker 2 (Trishydroxymethylethane) arranging in a Comb-like structure. They only differ by the electrostatic charge of the glycomimetic structure (-, 0 and +) respectively. The last two glycoconjugates (Molecule 6 and Molecule 7) are also tetra-galactosyl glycomimetics with two different charges, exhibiting an antenna structure including the linkage Linker 3 (Pentaerythritol).

Name[a] of glycoconjugate	Alias[b]	Saccharide residue (Number)	Charge (Number)	Linker[c]	Spatial arrangement
G 1	3Man /Molecule 1	Mannose (3)	0	Linker 1	Comb-like
G 3	3Gal	Galactose (3)	0	Linker 1	Comb-like
G 11	Molecule 2	Galactose (4)	- (3)	Linker 2	Comb-like
G 12	Molecule 3	Galactose (4)	0	Linker 2	Comb-like
G 13	Molecule4	Galactose (4)	+ (3)	Linker 2	Comb-like
G 10	Molecule 5	Galactose (4)	0	Linker 1	Comb-like
G 14	Molecule 6	Galactose (4)	- (1)	Linker 3	Antenna
G 15	Molecule 7	Galactose (4)	+ (1)	Linker 3	Antenna

Table5-4 Main characters of glycoconjugates (3Gal and Molecule 1-7)

[a] Name of glycoconjugate designated in Chapter 2 (see Fig2-1 and Table2-1)

[b] Name of glycoconjugate designated in this Chapter

[c] Linkage between every two phosphodiesters of the structure of the glycoconjugates(*206*). Linker 1, Linker 2 and Linker 3 correspond to 1, 4-cyclohexanedimethanol (DMCH); Trishydroxymethylethane and Pentaerythritol.

First of all, we investigated the binding affinities of seven glycoconjugates (Molecule 1-Molecule 7) towards RCA120 and PA-IL on MbII by the two approaches of DDI (see Fig5-16). Two slides were prepared, one for "on-chip" approach, the other for "in-solution" approach.
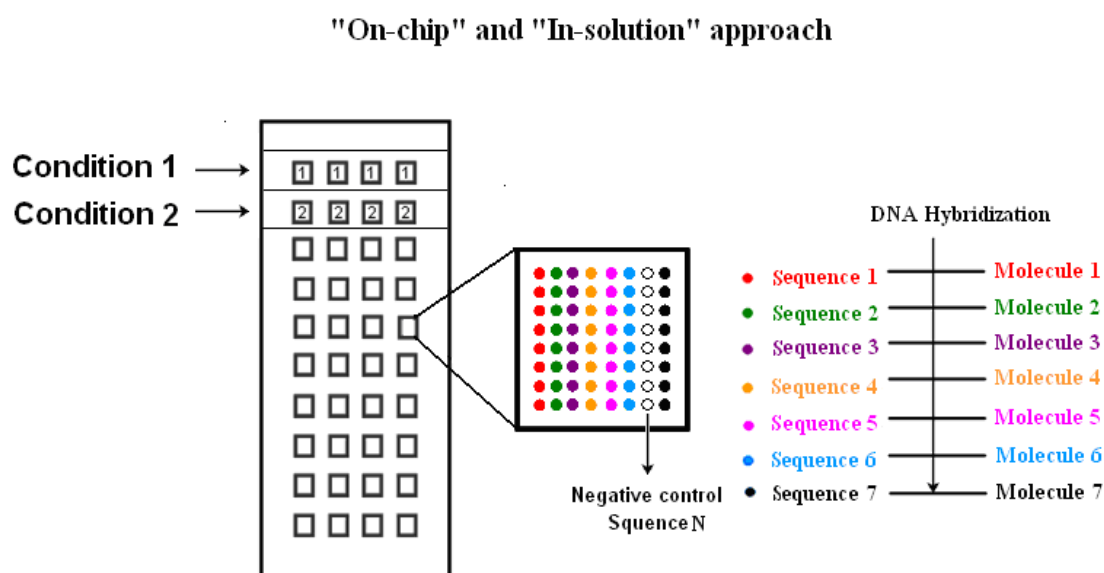
Fig5-16 Sketch map for the determination of binding affinities of molecule 1 to molecule 7 towards RCA120 and PA-IL on DNA anchoring platform a) adopting two DDI methods: "on-chip" and "in-solution" approach.

➢ **Condition 1: seven molecules were incubated with RCA120**

➢ **Condition 2: seven molecules were incubated with PA-IL**

5.3.3.1 "On Chip" approach:

In the case of "on-chip" approach, mixed solution of seven molecules (final concentration 1µM for each) was deposited into each of the 8 microwells of Condition 1 and Condition 2 (see Fig5-16). After hybridization of the glycoconjugates, the Cy5-labeled RCA120 (final concentration 1.5µM) and Alexa 647 labeled PA-IL (final concentration 2.8µM, monomer) were added into the microwells of Condition 1 and Condition 2 respectively for recognition.

The results are displayed in Fig5-17 and Fig5-18. As shown in the fluorescence images (see Fig5-17), the green signals corresponded to the Cy3-labeled

glycoconjugates, whereas the red signals were observed for the binding Cy5-labeled RCA120 or Alexa647 labeled PA-IL. Green signals were detected from seven columns except the column where the negative control Sequence N printed, indicating that there were no non-specific adsorption of glycoconjugates. As expected, there were almost no red signals and extremely low fluorescence intensity (50-200 a.u.) obtained for 3Man (Molecule 1) which could not be recognized by the two lectins. The fluorescence intensity of each molecule was determined as the average of the fluorescence intensities of 32 spots from 4 microwells of each Condition (8 spots per microwell). Molecule 4, which bear 4 galactose residues in Comb-like structure with three positive charges, displayed the strongest binding towards the two lectins with fluorescence intensity about 20000 a.u. for RCA120 and 7000 a.u. for PA-IL (Fig5-18). However, although Molecule 2 and Molecule 3 almost have the same structures as Molecule 4 except carrying different charges, the fluorescence intensities of these molecules were relatively low, especially towards PA-IL with a ratio about 1:3 and 1:5 compared to Molecule 4. Moreover, considering Molecule 6 and Molecule 7 which share the same antenna structure but carry different charge (negative and positive charge respectively), as shown in Fig5-18, the fluorescence intensity of Molecule 7 was a little bit higher than Molecule 6 with a ratio about 1.04:1 for RCA120 and 1.35:1 for PA-IL. As a matter of fact, that was not the real ratio of Molecule 7 vs. Molecule 6, according to the cross-hybridization test (see Fig5-7), it has been demonstrated that Molecule 7 cross-hybridized with the Sequence 6 with which Molecule 6 should be hybridized (see Fig5-8 and Table5-2). Thus, the real ratios of Molecule 7 vs. Molecule 6 should be higher than what has been obtained, which means the two lectins, especially the PA-IL bind Molecule 7 better than Molecule 6. Nevertheless, in the case of PA-IL, positively charged glycomimetic structure enhanced the binding to a greater extent than RCA 120.

One possible explanation relates to electrostatic interaction between the lectin and the glycomimetic. At a pH equal to the pI (isoelectric point) of a protein, a protein has no electric charge. At a pH above its pI, a protein will carry a net negative charge. In this part of work, the recognition processes was carried out in the solution at pH 7.4,

the pI of RCA120 (pI = 7.5-7.9) (*92*) is just around this pH scale, whereas the pI of PA-IL (pI =4.94)(*260*) is below 7.4. It means that in the recognition solution, the RCA120 had no electric charge, while the PA-IL carried a negative charge, which made the PA-IL more facilely to approach and bind to the glycoconjugate carrying positive charge.

Another significant finding is that the two positively charged tetra-galactosyl molecules (Molecule 4 and Molecule 7) did not have identical affinities either towards RCA120 or towards PA-IL. The fluorescence intensities of Molecule 4 were higher than Molecule 7 with a ratio of 1.3 for RCA120 and 3.5 for PA-IL. Molecule 4 has a Comb-like structure while Molecule 7 exhibits antenna architecture. The Comb-like structure thereby seems more favorable than antenna architecture for glycoconjugate binding to these two lectins.
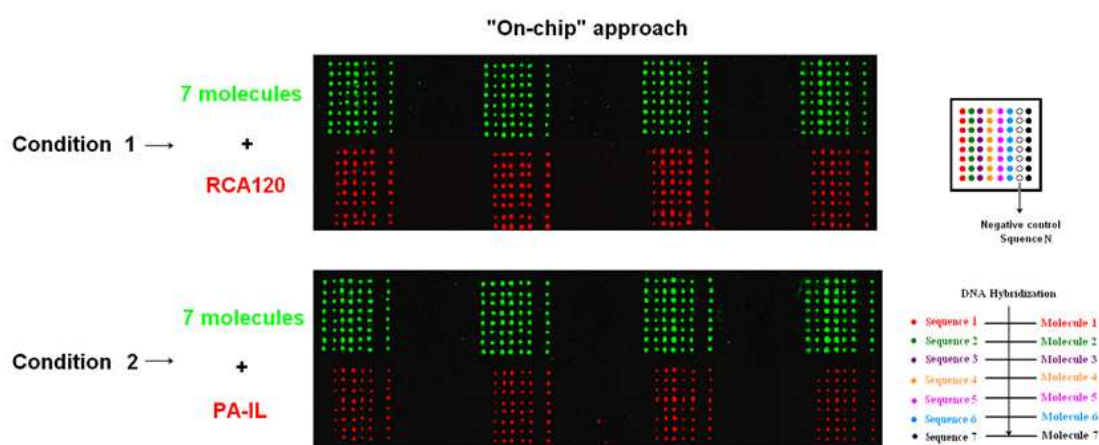
Fig5-17 Fluorescence images recorded at 532nm (a.u.) for the glycoconjugates (molecule 1-7) and at 635 nm (a.u.) for the lectin RCA120 and PA-IL, after recognition of glycoconjugate with lectins by "on-chip" approach.
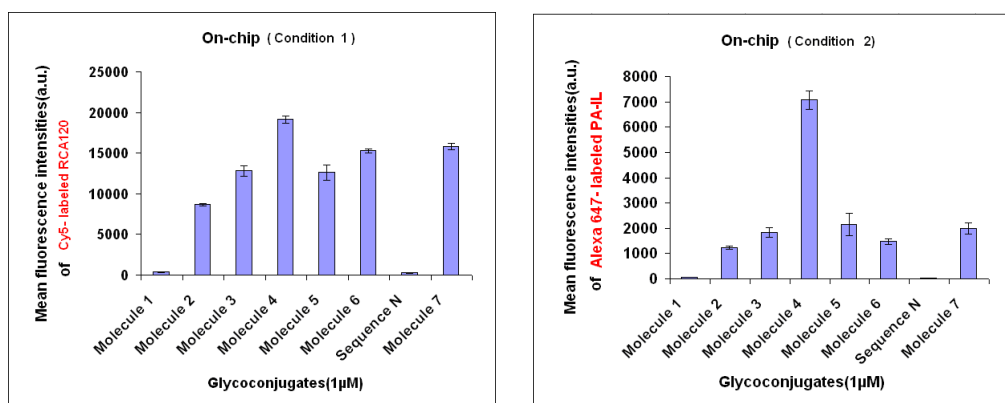
Fig5-18 Mean fluorescence intensities obtained at 635nm (a.u.) of condition 1 and condition 2 for RCA120 and PA-IL individually, after incubation with the seven molecules (Molecule 1-Molecule 7) by "on-chip" approach. No correction for the Cy5 (Alexa 647) fluorescence intensities was performed, as the Cy3 signals obtained for the seven glycomimetics at 1µM are similar (see Fig5-10).

5.3.3.2 "in-solution" approach:

For the "in-solution" approach, the solution of seven molecules (final concentration 1µM for each) were firstly incubated with the two lectins RCA120 (final concentration 0.5µM) and PA-IL (final concentration 0.5µM) respectively, and then the two incubation solutions were deposited into the corresponding microwells of Condition 1 and Condition 2 (see Fig5-16).

Some of the results shown in Fig5-19 and Fig5-20 were comparable to those obtained from "on-chip" approach. For instance, there was no non-specific glycoconjugate adsorption for Sequence N and no non-specific binding of lectin for the negative control glycoconjugate 3Man (Molecule 1). The PA-IL lectin preferred to bind to positively charged Molecule 4 (Comb-like structure with Linker 2) than negatively charged Molecule 2 and neutral Molecule 3. It also had higher affinity with Molecule 7 compare to Molecule 6. Both lectins preferred comb-like structure.

However, very surprisingly in this case, it was the Molecule 5 (Comb-like structure with Linker 1) not the Molecule 4, which showed the highest fluorescence intensity towards the two lectins (25000 a.u. for RCA120, 14000 a.u. for PA-IL). The result may be caused by the rigidness of Linker 1 (DMCH) of Molecule 5 in solution, which could keep proper spacing for the galactose residues to easily enter into the

binding sites of the lectins. In addition, under the "in-solution" recognition conditions, RCA120 displayed similar selectivity towards glycoconjugates in comparison with PA-IL.

The results indicated that the charge of the glycoconjugates was not the only factor that could influence the binding affinities, which further enhanced to the previous argument. There are many complicated essential elements that contribute to carbohydrate/lectin binding features, such as the spatial arrangement and orientation of the saccharide residue, the rigidity and optimal spacer of the linkage between the ligands (*97, 99, 211, 270*). Subtle differences in carbohydrate presentation can change the binding properties of carbohydrate binding proteins (*271-273*).
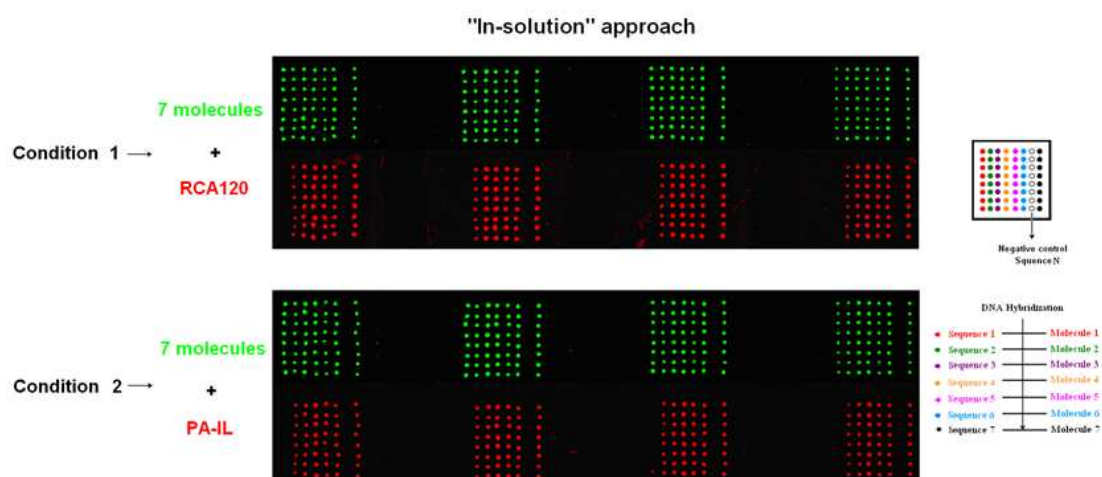
Fig5-19 Fluorescence images recorded at 532nm (a.u.) for the glycoconjugates (molecule 1-7) and at 635 nm (a.u.) for the lectin RCA120 and PA-IL, after recognition of glycoconjugate with lectins by "in-solution" approach.
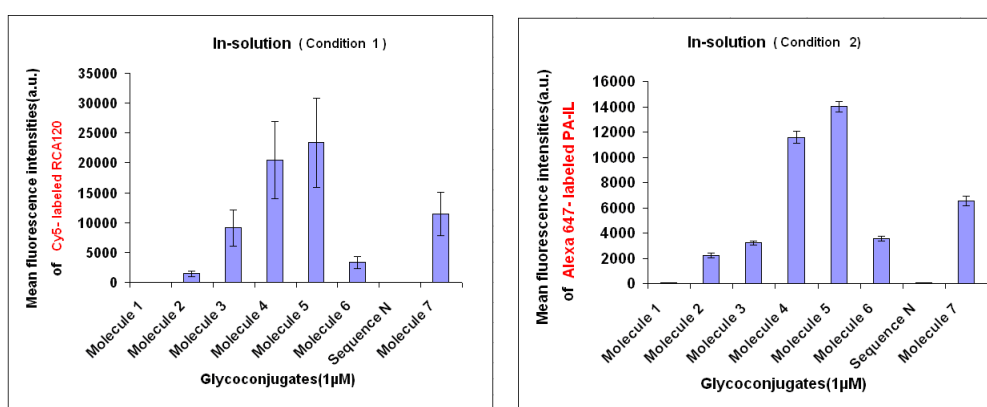
Fig5-20 Mean fluorescence intensities obtained at 635nm (a.u.) of condition 1 and condition 2 for RCA120 and PA-IL individually, after incubation with the seven molecules (Molecule 1-Molecule 7) by "in-solution" approach.

We also studied the affinities of 9 glycoconjugates (3Man, 3Gal as well as Molecule 2-8) with PA-IL on MbII by "in-solution" approach (see Annexe 3). Molecule 8 (Glycoconjugate 16, see Chapter 2, Fig2-1 or Table 2-1) was a new glycoconjugate, which has the same structure as Molecule 6 or 7 but that carries no charges. Sequence N was replaced by Sequence 8 (see Chapter 2, Table2-4) in order to offer complementary sequence for hybridization of Molecule 8. There were three goals to be addressed: 1) to do a repetition of the binding studies of Molecule1 (3Man) - Molecule7 with PA-IL on platform b using "in-solution" method; 2) to test the binding affinity of Molecule 8 towards PA-IL; 3) to make a comparison of the binding affinities of the 7 new tetra-galactosyl molecules (Molecule 2-8) with 3Gal bearing three galactose residues towards PA-IL. Detailed results are reported in Annexe 3.

All the observations above demonstrated that the multiplex assays of interactions of glycoconjugates/lectins were well performed on MbII either by "on-chip" or by "in-solution" approach. The results confirmed that PA-IL lectin could more efficiently bind to the positively charged glycoconjugates (e.g Molecule 4.) than other glycoconjugates. The highest binding signal was observed for Molecule 4 with the two lectins (RCA120 and PA-IL) in "on-chip" approach, while in "in-solution" approach, it was the Molecule 5 with the linker DMCH showed the most efficient binding. Moreover, it appeared that the two lectins preferred to bind to the glycoconjugates with Comb-like structure rather than glycoconjugates arranged in antenna architecture. Therefore in the following studies, we tried to do quantitative analysis (IC_{50}) of the glycoconjugates with Comb-like structure.

5.3.4 *Quantitative analysis (IC$_{50}$) of the affinities of glycoconjugates with PA-IL in miniaturized biosystem II (MbII)*

In Chapter 4, it was demonstrated that the semi-quantitative (IC$_{50}$ determination) assays can be performed on the slide featured with 52 round microwells by DDI "on-chip" approach. However, such a slide can be used only to determine the IC$_{50}$ value of one glycoconjugate. In order to amplify the capability of the tool and realize a high throughput semi-quantitative analysis, this time, we chose the miniaturized biosystem II (MbII) to do our study. MbII allows various glycoconjugates to be mixed and addressed to the desired spots in one single microwell allowing for parallel quantitative assays of many glycoconjugate in one slide at the same time. On the basis of this advantage, a comprehensive competition assay was designed and carried out for determination of IC$_{50}$ values of 5 glycoconjugates towards PA-IL on the MbII by "in-solution" approach (see Fig5-21).
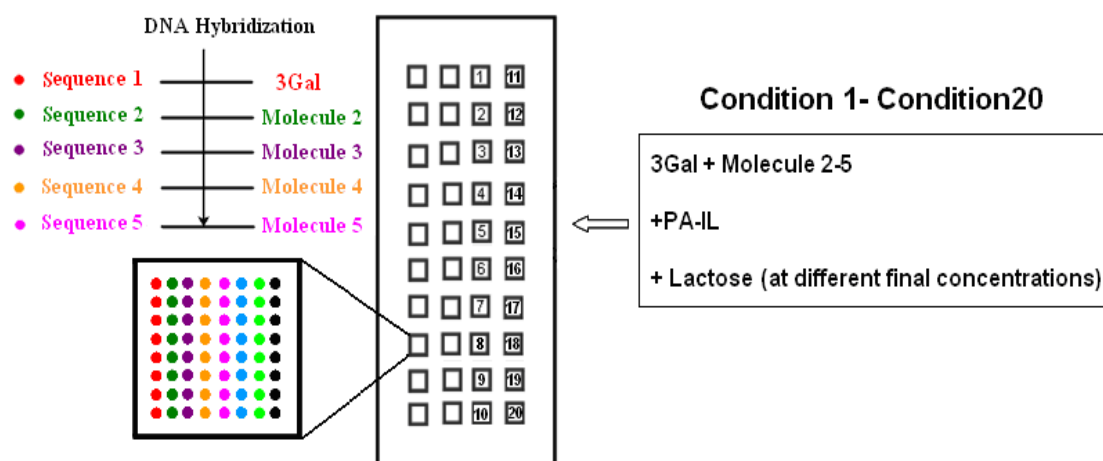
Fig5-21 Sketch map for the determination of IC$_{50}$ values of Molecule 2- Molecule 5 and 3Gal towards PA-IL on the MbII adopting "in-solution" method.

➤ **Condition 1-Condition 20: Incubation of 3Gal, Molecule 2- Molecule 5 with PA-IL, as well as lactose at different final concentrations (see Table)**

From Condition 1 to Condition 20, 3Gal (1µM), Molecule 2- Molecule 5 (1µM for each) and PA-IL (0.5µM) were incubated together with consecutively diluted concentrations of the inhibitor lactose (see Table5-5) in 20 microwells respectively. In Condition 1, where no lactose (0µM) was added, the binding results for the five glycoconjugates (Fig5-22) with PA-IL were similar compared with the results shown in Fig5-22. The fluorescence intensities of other conditions were also recorded and analyzed. The IC_{50} values for each of the five glycoconjugates were calculated by BioDataFit and summarized in Table5-6. The IC_{50} values for 3Gal towards PA-IL (9.2µM) was considerably lower than that observed towards RCA120 (*99*)(385µM). According to the potency of each galactose residue, Molecule 5 and Molecule 4 were about 64 and 45 folds higher than 3Gal respectively. It may well be that a "cluster effect" for Molecule 5 vs. 3Gal is observed. For Molecule 2 and 3, the binding affinities with PA-IL were almost at the same level. There was a nearly 150 times increase in potency of each galactose residue towards PA-IL from Molecule 2 and 3 to Molecule 4. In addition, the IC_{50} value as well as the affinity per residue for Molecule 5 was 1.4 times higher than that for Molecule 4. The results observed by IC_{50} assay and by direct reading of the fluorescence signal gave the same trend but with a higher sensitivity for the IC_{50} method.
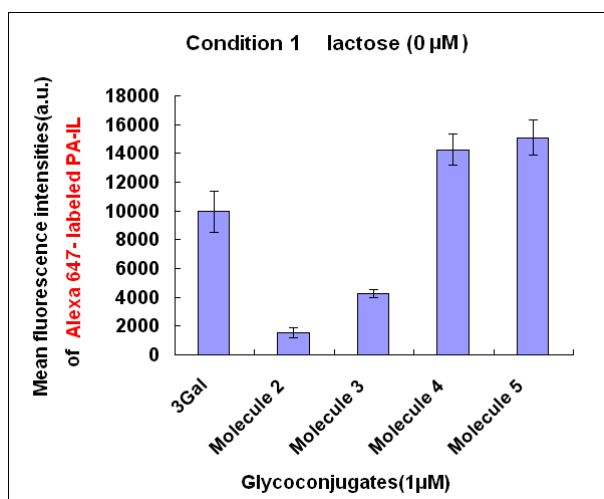
Fig5-22 Mean fluorescence intensities obtained at 635nm (a.u.) of condition 1, after incubation with five glycoconjugates (3Gal and Molecule 2-Molecule 5) with PA-IL by "in-solution" approach on the MbII.

Condition 1-20	Final Concentration of Lactose (µM)
1	0
2	0.00001
3	0.00005
4	0.0001
5	0.0005
6	0.001
7	0.005
8	0.05
9	0.1
10	1
11	5
12	10
13	50
14	100
15	500
16	1000
17	5000
18	10000
19	15000
20	30000

Table5-5 Final concentrations of inhibitor (lactose) for Condition1 to Condition 20

Glycoconjugate	Valency	Charge (Number)	IC_{50} (µM)	Relative potency[a]	Relative Potency per galactose residue[b]
3Gal	3	0	9.24	1	0.33
Molecule 2	4	-(3)	2.5	0.3	0.07
Molecule 3	4	0	3.5	0.4	0.1
Molecule 4	4	+(3)	559.5	60	15
Molecule 5	4	0	773.2	84	21

Table5-6 IC_{50} of glycoconjugates-PA-IL binding

➢ **[a] Calculated as the ratio of 3Gal to other glycoconjugates IC_{50} values.**

➢ **[b] Calculated as the ratio of relative potency to the number of galactose residues.**

5.4 Conclusions

In conclusion, two miniaturized analytical systems (MbI and MbII) were designed allowing up to 40 independent experiments to be performed with volumes as low as 0.5 µL per experiment corresponding to 2 picomoles of glycomimetic on one microscope slide. Thanks to site-specifically capture of the DDI glycoarray by nucleic acid hybridization, it was demonstrated that glycomimetics and lectins can be mixed in solution for specific recognition and subsequently be addressed at a specific location on the surface of the microwells for further detection.

Two kinds of glycoconjugate/ lectins specific recognition models were successfully performed in MbI by "in-solution" approach of DDI. The "in-solution approach" should allow circumventing any recognition problems that could occur due to the chip surface.

Based on the validation of MbI, a new microsystem MbII was fabricated. Although cross-hybridization phenomenon has observed for one glycoconjugates (Molecule 7), the developed MbII still allowed performing a parallel analysis of binding properties for eight glycoconjugates towards lectins in one single microwell, which dramatically extend the capability of high throuput detection of DDI glycoarray. The binding features of seven new synthesized glycoconjugates as well as 3Gal and 3Man towards two lectins (PA-IL and RCA120) were studied in MbII by both DDI approaches. The positively charged glycoconjugates showed greater avidity toward PA-IL lectin. The "cluster effect" was further demonstrated by affinities of the tetra-galactosyl glycomimetic (Molecule 5) vs. tri-galactosyl glycomimetic (3 Gal) with respect to PA-IL in DDI "in-solution" approach. Moreover, it seems that the glycoconjugates with Comb-like structure can be more efficiently recognized by RCA120 and PA-IL than glycoconjuates arranged in antenna architecture.

Finally, a simultaneous quantitative analysis (determination of IC_{50} values) of binding affinities of five glycoconjugates with PA-IL was satisfactorily carried out within a single experiment on MbII.

To sum up, the two miniaturized analytical systems based on DDI glycoarray not

only can reduce the material consumption, but also provide rapid and sensitive access to comprehensive binding profiles, which facilitated the carbohydrate-lectin binding detection and quantification. We thereby anticipate that the miniaturized analytical systems described herein should be useful for both the fundamental research and the application area, such as virus detection, drugs screening and discovery.

6 APPLY DDI GLYCOARRAY TO STUDY THE INTERACTIONS OF INFLUENZA VIRUSES / GLYCOCONJUGATES

6.1 Introduction and context

Influenza (flu) is an acute respiratory disease caused by influenza virus, which affects millions of people each year and results in severe morbidity and mortality throughout the world, normally occurring in temperate climates in winter. According the report of WHO, influenza virus is responsible for about 250000-500000 deaths per year and it also the second cause of infectious mortality after pneumonias (*274*).

The cyclic character of the influenza epidemics is related to the regular appearance of new antigenic or drug resistant species in the circulating influenza viruses. Therefore searching for new antiviral drugs is a great challenge in front of the emergence of new species of pandemic virus. Since the first stage of the infection of influenza virus is mediated by the interaction of hemagglutinin (antigenic protein on the surface of the virus) with the sialic-acid residues on the surface of the host cell (see 6.1.2). Molecules with high affinity for hemagglutinin would be potent candidates of new antiviral drugs to block the hemagglutinin/sialic-acid interaction and then further interdict the virus replication. Sialylated glycomimetics are potential candidates providing good spatial arrangement and physico-chemical properties. In order to obtain the high affinities glycomimetics, it is necessary to do a large number of screening tests of interaction between influenza virus and sialylated glycomimetics. Glycoarrays are ideal tools in doing such high throughput tests. As demonstrated in previous studies, DDI glycoarrays were efficient tools for study the glycoconjugates/lectins interaction. The objectives of this study were to design/develop efficient DDI glycoarrays protocols for the rapid study of recognitions

between glycoconjugates and influenza virus.

In this section, firstly the main properties of the influenza viruses will be reviewed aiming to provide basic information with regard to the essential structures and classifications of the influenza viruses; then the influenza virus replication mechanisms will be described; finally the research status of the two main antigenic protein on the surface of the virus (hemagglutinin and neuraminidase) and the main goals of this study will be introduced.

6.1.1 Characterization and classification of influenza virus

Influenza viruses are spherical wrapped (80-120nm diameter), negative-sense and single-stranded RNA viruses which belong to the family of orthomyxovirus (*275, 276*). The genome of influenza viruses consists of 8 segments which comprises about 13,500 bases and encodes for 11 proteins (*276, 277*). Based on the antigenic differences in the major internal proteins of the virus, i.e. Nucleoprotein (NP) and Matrix protein (M1) (see Fig6-1), influenza viruses can be classified into three serological groups: influenza A, B, and C viruses (*275, 278, 279*). Influenza A and C viruses were isolated from human, birds and several animals, whereas influenza B viruses circulates only among the humans (*275*). Major outbreaks are associated with influenza A or B viruses. However, the gravest infection is usually caused by influenza A.

There are two main antigenic proteins on the surface of Influenza A virus: hemagglutinin (H or HA) and neuraminidase (Sialidase, N or NA) (*277, 278*) (see Fig6-1). HA is a membrane-spanning glycoprotein (~225 kD) and is also a sialic acid specific lectin. It shaped like a cylinder of approximately 13.5 nanometres length. It is composed of three identical monomers, which are constructed into a central α-helical coiled-coil and three globular heads. The globular heads contain both the sialic acid-binding sites and the antigenic epitopes (*279, 280*). The neuraminidase (sialidase), is a mushroom-shaped enzyme, which is composed of four identical

disulfide-linked, co-planar and roughly spherical subunits anchored to the viral membrane though a thin long stem (10 nanometres) (see Fig6-1) (*281*).

According to HA and NA, influenza A virus can be further divided into 16 HA (H1-H16) and 9 NA (N1-N9) subtypes (*277, 282, 283*), of which two strains H1N1 and H3N2 have already lead to serious pandemic (*278*) and begun to circulate among the humans causing annual epidemics.
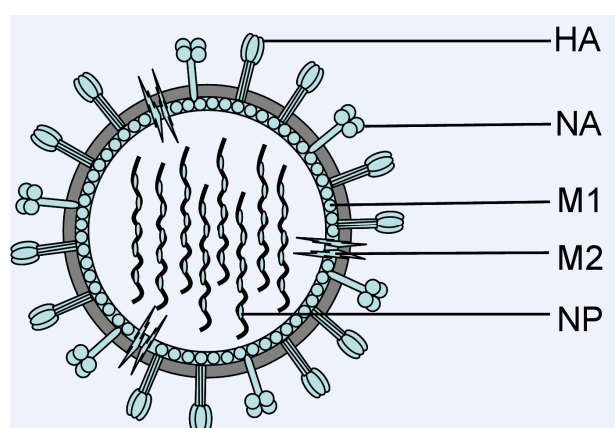
Fig6-1 Schematic diagram of an influenza A virus. The external proteins: Hemagglutinin (HA), Neuraminidase (NA) and an ion channel protein (Matrix protein 2, M2); The internal proteins: Matrix protein 1 (M1) and Nucleoprotein (NP).

6.1.2   *Mechanisms of influenza virus replication*

Since the genome of influenza virus is only composed by a single-strand RNA, it can only replicate in living host cell (*284*). The replication of influenza virus can be divided into three main steps: the first step is the adherence of the influenza virus to the host cell; the second step is the multiplication of the virus in the host cell; the last one is the release of the new particles of the influenza virus (see Fig6-2).

Adherence of the influenza virus to the host cell

The influenza virus firstly adheres to the host cell. This process is performed by the HA binding to sialic acid residues of glycoconjugates on the membrane of the host cell (*285*), which initiates the replication cycle.

The multiplication of the virus in the host cell

The virus then undergoes endocytosis and fusion in the cytoplasm of the host cell (*286*). Once the virus is fused, the genome of the virus will be delivered to the nucleus of the host cell places. After that, the virus genome will be replicated or transcribed by the enzymes and translated by ribosomes of the host cell (*287, 288*). Thus taking advantage of the abundant materials of the host cell, new proteins and genomes of the virus will be produced.

The release of the new particles of the influenza virus

The new copies of viral proteins and genome will be transported out of the nucleus of the host cell and assembled near the cell membrane. The new virus particles are formed by budding. However the new viruses are still adhere to the host cell via HA binding to sialic acid residues. NA will then cleave the sialic acid residues and liberate the new viruses (*285*). The released new viruses could therefore start a new cycle of replication.
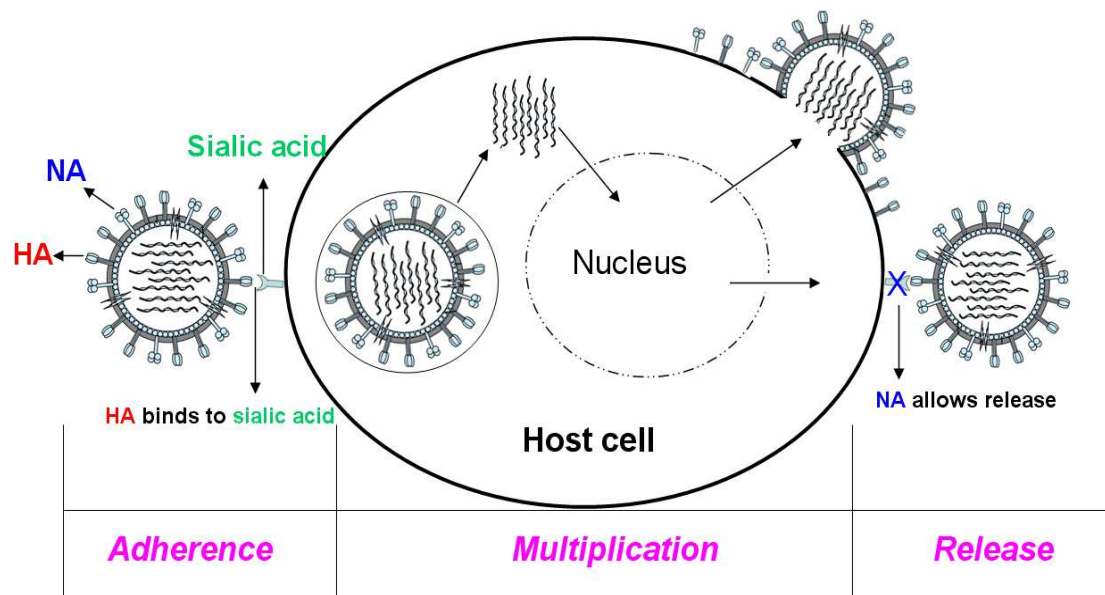
Fig6-2 Scheme of an influenza virus replication

6.1.3 Literature review on HA and NA

Understanding the infection mechanism induced by the virus and the implied biological interactions is of crucial importance in preventing the infection processes of influenza viruses. Previous efforts about influenza virus were mainly focused on the two surface antigenic proteins HA and NA (*282, 283, 289, 290*), due to the important biological roles of the two proteins. As just described in 6.1.2, HA is a natural receptor for sialic acid, in consequence the adherence of virus to the host cell is mediated via the HA binding to the terminal sialic acid residues of the glycoconjugates on the cell surface. Moreover, it has been proved that HA also played significant roles in the virus internalization and the viral envelope fusion (*279, 289, 291, 292*). Generally, the HA of human viruses bind strongly to the α 2-6 linked sialosides (especially to sialic acid α 2-6 galactose), the HA of avian viruses prefer to bind to α 2-3 linked sialosides (especially to sialic acid α 2-3 galactose) (*9, 293, 294*), whereas the HA of the porcine strains bind to both of the two α 2-6 linked and α 2-3 linked sialosides (*2*). However, only a few amino acid substitutions or mutations in the HA protein may alter the receptor binding preference (*278, 295*). NA participates in the last stages of viral infection, it can cleave the sialic acid from the host cell by hydrolyzing the ketosidic linkage in sialosides (*293*), which resulting in the escape of the neovirion after budding (*275*).

To date, vaccination is a conventional method for the prevention of influenza infection, but the process of vaccine production is usually cumbersome and costly, and always complicated by antigenic drift and shift of the viral RNA encoded HA (*290*). Therapeutic approaches as a complement of the vaccination have been developed for several years. NA is one of the drug discovery targets. Currently, two NA inhibitors drugs (zanamivir and oseltamivir) are synthesised and approved for clinical use (*296*). They mimic sialic acid and can prevent the detachment of the neovirions. Unfortunately, the great challenge of the drug resistant is still remaining.

HA is also a drug discovery target, however, very few data exists concerning molecules allowing tight binding to HA and blocking its activity. The main reasons is

probably because, as all lectins, the affinity of HA to monovalent sialosides is relatively low (K_d only in the mM range) (*290, 297*). Moreover, most of the classical rapid tests are lacking of sensitivity, and a distinct binding profile observed for each HA could not be obtained by the usual cell-based assays, such as hemagglutination assays, hemagglutination inhibition assays (*278, 295*).

In recent years, glycoarrays have been developed and shown promise in studies of influenza virus. In nature the virus takes advantage of several simultaneous HA and sialic acid interactions to perform a tight binding (*298*). Because glycoarray technologies possess intrinsic properties to mimic such natural interactions, they can be employed to profile and determine the specificities of HA (*10, 12*). Thus, Stevens *et al* have used glycoarray containing 200 carbohydrates and glycoconjugates to determine the HAs receptor preferences of human and avian virus. The obtained results have clearly shown the broad receptor specificities of α 2-6 or α 2-3 sialic acid linkages, as well as some fine receptor differences in HA specificities such as the glycan size, charge, extra sulfation and fucosylation (*299*). Blixt and co-workers employed a covalent glycan array to profile the specificity of the whole H1N1 virus A/Puerto Rico/8/34 (*194*). The obtained resultes were comparable with those observed from cell-based assays (*300*).

In previous chapters, DDI glycoarrays have been proved to be very efficient platforms for profiling the interactions of glycoconjugate/lectin. We herein expect to apply this technology to the study of influenza viruses. The interaction of glycoconjugates with the whole virus is more complex than glycoconjugate/lectin interactions. Therefore, in order to set up ideal DDI glycoarray based platforms for investigating the binding feature of the whole viruses, a lot of parameters and conditions need to be optimized. Moreover, as described in our previous studies, many glycoconjugates have been synthesized based on glycomimetics (carbohydrate/DNA conjugates) synthetic strategy and their affinities towards lectins were evaluated. Some of the glycoconjugates (e.g. G 3, see Chapter 3 and 4) displayed high binding avidity with lectins.

Therefore, eight Cy3-labeled glycoconjugates (Glycoconjugates 17-24, see

Chapter 2 Fig2-1 or Table2-1) bearing sialic acid-containing glycan residues and displaying different structures were synthesized, using the same strategy as reported in Chapter 2, 2.1 and annexe 1. The binding features of these glycoconjugates with two types of viruses (Alexa647-labeled influenza viruses H1N1/PR8 and H3N2/Moscow provided by the team Virologie-Influenza, FRE 3011- CNRS) were profiled with DDI glycoarray by "on-chip" and "in-solution" approaches.

6.2 Materials and methods

6.2.1 DDI glycoarray fabrication

The first step for DDI glycoarray fabrication is to set up a DNA anchoring platform, the procedures were the same as described in Chapter 2 2.2. In this study, we used glass slide containing 52 round microreactors (see Chapter 2, Fig2-2). In each microreactor, ssDNA Sequence 1 (see Chapter 2, Table 2-4) was printed on to the surface.

Name[a] of glycoconjugate	Saccharide residue (Number)	Linker[b]	Spatial arrangement
G 17	β-Lactose (2)	Linker 1	Antenna
G 18	Neu5Ac(α-2,6) Lactose (2)	Linker 1	Antenna
G19	α-Neu5AC (3)	Linker 2	Comb-like
G 20	α-Neu5AC (3)	Linker 2	Comb-like
G 21	α-Neu5AC (3)	Linker 3	Comb-like
G 22	α-Neu5AC (3)	Linker 3	Comb-like
G 23	β-Lactose (1)	Linker 4	linear
G 24	Neu5Ac(α-2,6) Lactose (1)	Linker 4	linear

Table6-1 Main characters of glycoconjugates (G 17-24)

[a] Name of glycoconjugate designated in Chapter 2 (see Fig2-1)

**[b] Linkage between every two phosphodiesters of the structure of the glycoconjugates(*206*).
Linker 1: Pentaerythritol; Linker 2: tetraethyleglycol Linker 3: 1, 4-cyclohexanedimethanol
(DMCH); Linker 4: Cyclohexanedimethanol (DMCH) and Trishydroxymethylethane**

Unless otherwise specified, after printing Sequence 1 the slide was blocked by 4%BSA (see Chapter 2 2.3). Then, for "on-chip" approach, the glycoconjugates (see Table6-1) at 1µM were immobilized on chip by hybridizing with Sequence 1 as presented in Chapter 2.4.2.

6.2.2 First studies on glycoconjugates/influenza virus recognition

Unlike the glycoconjugates/lectins interactions, the process of glycoconjugates/ influenza virus interaction is more complicated. Many factors will influence the binding outcomes. For example, the two DDI glycoarray strategies perhaps lead to different binding results; the blocking method (BSA and casein blocking) may have effect on the signal/noise ratio; the degree of the labeling of the virus may affect the activity of the HA on the virus surface; NA on the virus surface could destroy the sialic acid on the glycoarray (*278*); in addition, the storage method of the labeled-virus (e.g. at -20°C) might result in deactivation of the virus.

All those factors mentioned above should be taken into account for the glycoconjugates/ influenza virus recognition. As a consequence, several experiments were designed in order to evaluate the two DDI glycoarray strategies ("on-chip" and "in-solution" approach) and to optimize the recognition conditions.

a) Evaluate two DDI glycoarray strategies ("on-chip" and "in-solution" approach)

For "on-chip" approach, the two kind of viruses H1N1/PR8 (5×10^7 TCID$_{50}$/100µl, Alexa647-labeled amount 10µg) and H3N2/Moscow (5×10^7 TCID$_{50}$/100µl, Alexa647-labeled amount 10µg) were mixed with the NA inhibitor zanamivir (0.75µM, final concentration) in PBS $1 \times$ (pH 7.4)-Tween 20 (0.05%) respectively. And the two solutions were added into the corresponding microwells of the glycoarray where six glycoconjugates (G 17-G 22, see Table6-1) were immobilized. Then the slides were incubated at 37°C in a water vapour saturated chamber for 2 h.

For "in-solution" approach, H1N1/PR8 and H3N2/Moscow were mixed with the NA inhibitor zanamivir (0.75μM, final concentration) as well as the glycoconjugates (1μM, G17-G22, see Table6-1) in PBS 1× (pH 7.4)-Tween 20 (0.05%) respectively. And the two solutions were added into the corresponding microwells of the DNA anchoring platform. Then the slides were incubated at 37°C in a water vapour saturated chamber for 2 h.

After incubation, the slides were successively rinsed in PBS 1× (pH 7.4)-Tween 20 at 0.05%, PBS 1× (pH 7.4), and DI water. Then the slide was dried by Spray duster. After that, 0.5μL of 1%PFA (paraformaldehyde) was added into each microwell and incubated for 2-3min in order to fix the virus on the arrays. Finally, the slide was rinsed in DI water and dried by Spray duster.

b) *Optimize the recognition conditions*

b.1) *Test the capping step (two blocking methods: BSA and Casein blocking)*

In this experiment, two slides were prepared. After set up the DNA anchoring platforms, one slide was blocked by 4% BSA as described in Chapter 2 2.3. For the casein blocking method which was adapted from (*9*), the blocking step was performed by immersing the slide bearing DNA in 1% casein (Sigma, Steinheim) solution for 2 h at 37°C. The slide was then washed in PBS 1× (pH 7.4)-Tween 20 at 0.05% for 3×3min followed by PBS 1× (pH 7.4) 3 times, and finally rinsed with DI water and dried by centrifugation. After blocking, the glycoconjugates G 17, G 18, G 23 and G 24 (1μM, see Table6-1) were all immobilized onto the two slides. The viruses H1N1/PR8 (10^6 $TCID_{50}$/100μl, Alexa647-labeled amount 5μg) was mixed with the NA inhibitor zanamivir (0.75μM, final concentration) in PBS 1× (pH 7.4)-Tween 20 (0.05%) respectively. And the solution was added into the corresponding microwells of the two glycoarrays. Then the slides were incubated at 37°C in a water vapour saturated chamber for 2 h. The next procedures were the same as presented in section a).

b.2) Investigate the effect of the Alexa 647 –labeling degree of the virus.

The H1N1/PR8 (10^{10} TCID$_{50}$/100µl) virus labeled with two Alexa647 amounts (5µg and 20µg) were mixed with the NA inhibitor zanamivir (0.75µM, final concentration) in PBS 1× (pH 7.4)-Tween 20 (0.05%) (Roth, Karlsruhe, Germany) respectively. Zanamivir was added in order to avoid NA to cleave the sialic acid form the glycoconjugates on the glycoarray. And then the two solutions were added into the corresponding microwells of the glycoarray where G 17 and G 18 (1µM, see Table6-1) were immobilized. After that, the slides were incubated at 37°C in a water vapour saturated chamber for 2 h. The next procedures were the same as presented in section a).

b.3) Compare the affinities of fresh Alexa647-labeled virus and Alexa647-labeled virus stored at -20°C towards its receptor

100µL solutions of virus H1N1/PR8 (10^{10} TCID$_{50}$/100µl, Alexa647-labeled amount 5µg), fresh virus (4°C) and virus stored at -20°C, were mixed with the NA inhibitor zanamivir (0.75µM, final concentration) in PBS 1× (pH 7.4)-Tween 20 (0.05%) respectively. And then the two solutions were added into the corresponding microwells of the glycoarray where G 17 and G 18 (1µM, see Table6-1) were immobilized. After that, the slides were incubated at 37°C in a water vapour saturated chamber for 2 h. The next procedures were the same as described in section a).

6.3 Results and discussion

a) Evaluate two DDI glycoarray strategies ("on-chip" and "in-solution" approach)

The receptor-binding characteristics of H1N1/PR8 and H3N2/Moscow were profiled by both DDI glycoarray strategies "on-chip" and "in-solution" approaches. Six glycoconjugates (G 17-G 22, see Table6-1) were tested. G 17 (bearing two lactose residues) and G 18 (bearing two Neu5Ac (α-2, 6) lactose residues) were expected to be negative control and positive control respectively. Other four molecules (G 19-G

22) all possess three α-Neu5ACs. The H1N1/PR8 and H3N2/Moscow binding results were displayed in Fig6-3 and Fig6-4 respectively. According to the results, very surprisingly, high signals were observed from H1N1/PR8 and H3N2/Moscow for G 17, which was not expected to be recognized by the two viruses, either by "on-chip" approach or by "in-solution" approach. On the contrary, the signals obtained for positive control G 18 were relatively lower than that for G 17 (see Fig6-3 a, b and Fig 6-4 b), except that detecting from H3N2/Moscow by "on-chip" approach (see Fig6-4 a). On one hand, the signals obtained for G 17 may relate to high non-specific adsorption. On the other hand, the low signal observed for G18 may be related to weak specific interaction (interaction of HA with G18).

Non-specific binding contribute to a significant source of measurement error, as a consequence, to make the evaluation the binding affinities of these glycoconjugates was very difficult and unpredictable.

In order to understand low signal to noise ratio, the following investigations were carried:

1) The blocking method to reduce non-specific adsorption;

2) The influence of the labeling degree by Alexa647 on the activity of the virus.

3) The effect of storage conditions
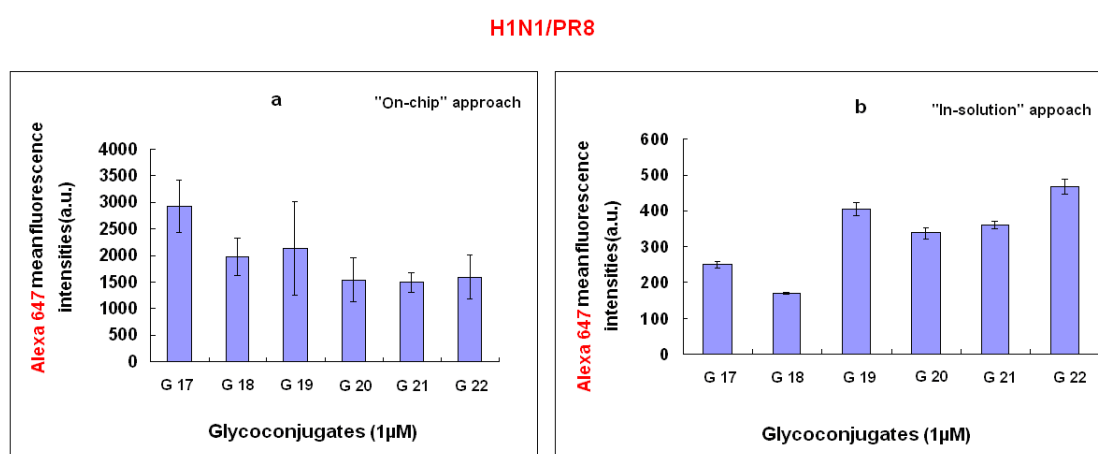
H1N1/PR8

Fig6-3 Mean fluorescence intensities at 635 nm (a.u.) of the Alexa647-labeled H1N1/PR8 after recognition with G 17-G 22 by "on-chip" approach (after correction) a) and "in-solution" approach b)
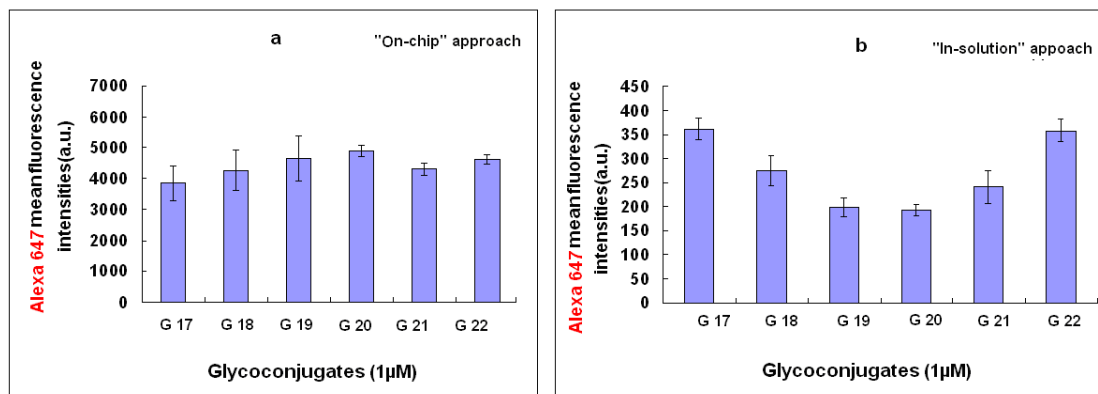
Fig6-4 Mean fluorescence intensities at 635 nm (a.u.) of the Alexa647-labeled H3N2/Moscow after recognition with G 17-G 22 by "on-chip" approach (after correction) a) and "in-solution" approach b)

b)   Optimize the recognition conditions

b.1) Test the capping step (two blocking method: BSA and Casein blocking)

As observed in previous sections, non-specific adsorptions were detected on DDI glycoarrays in the study of the influenza virus and glycoconjugates interactions. In order to optimize the DDI glycoarray platform and reduce the non-specific adsorption, herein we employed a new blocking method (casein blocking) (*9*) and made comparison with the previous BSA blocking method. Two glass slides (Slide^{BSA}, Slide^{casein}) were prepared by using BSA and casein blocking methods respectively. In each slide, the affinities of four glycoconjugates: G 17 and G 18 as well as two new glycoconjugates (G 23 and G 24) (see Table6-1) were tested towards the Alexa647-labeled H1N1. G 17 and G 18 almost have the same structure except bearing two lactose residues and two lactose-α-2,6Neu5AC moieties respectively. G 23 and G 24 also nearly have the same structures but bear one lactose residue and one lactose-α-2,6Neu5AC moiety respectively. Herein the two glycoconjugates G 17 and G 23 were expected to be negative controls; while G 18 and G 24 were expected to be positive controls. After immobilization of the glycoconjugates on the two slides, the Cy3 signals were recorded (see Fig6-5 a, b). As shown in Fig6-5 a) and b), the Cy3

fluorescence intensities for the four glycoconjugates are comparable on each slide (40000-5000 a.u. for Slide^{BSA}; 10000-13000 a.u. for Slide^{casein}). After incubation with Alexa647-labeled H1N1, the Alexa647 signals were also recorded with respect to the glycoconjugates

Fig6-5 a) Mean fluorescence intensities at 532 nm (a.u.) of the Cy3-labeled glycoconjugates G17, G 18, G 23 and G 24 immobilization on the BSA blocking DNA chip; b) Mean fluorescence intensities at 532 nm (a.u.) of the Cy3-labeled glycoconjugates G17, G 18, G 23 and G 24 immobilization on the casein blocking DNA chip; A) Mean fluorescence intensities (after correction) at 635 nm (a.u.) of the Alexa647-labeled H1N1/PR8 after recognition with glycoconjugates G17, G 18, G 23 and G 24 on the BSA blocking glycoarray; B) Mean fluorescence intensities (after correction) at 635 nm (a.u.) of the Alexa647-labeled H1N1/PR8 after recognition with glycoconjugates G17, G 18, G 23 and G 24 on the casein blocking glycoarray

. As shown in Fig6-5 A), on the Slide^{BSA}, which blocked by BSA, the Alexa647 signals observed for the two negative controls G 17 and G 23 were comparable with those obtained from the positive controls G 18 and G 24 respectively (ratio of G18 vs. G17 was1.05; ratio of G24 vs.G23 was 0.75). Similarly, on the Slide^{casein} (see Fig6-5 B), which blocked by casein, the Alexa647 signals detected for the two positive

controls G 18 and G 24 were almost the same as that observed for the negative controls G 17 and G 23 respectively (ratio of G18 vs. G17 was 1.13; ratio of G24 vs.G23 was 1.1). According to the results, it appears that the blocking method did not have great effect in reducing the non-specific adsorption.

b.2) Investigate the effect of the Alexa 647 –labeling degree of the virus.
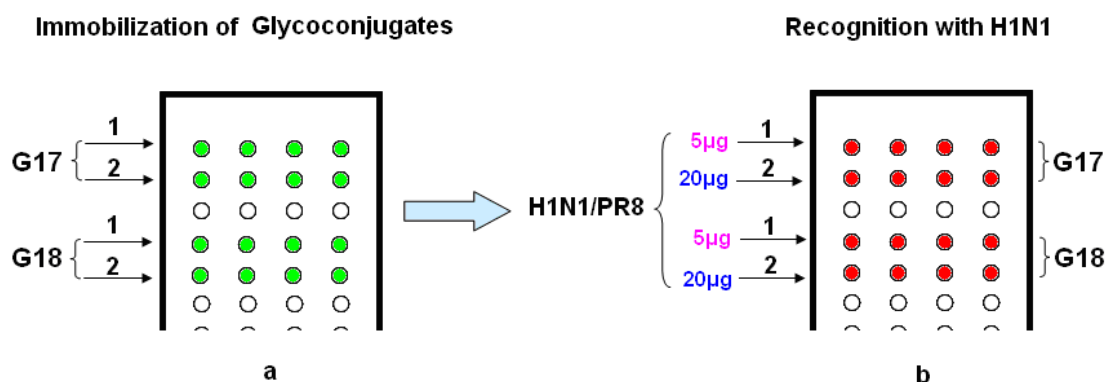
Fig6-6 Sketch map for test Alexa647-labeled amount effect. a) Fabricate glycoarray by immobilization of G17 and G18. b) Recognition of G17 and G18 with two Alexa647-labeled amounts of H1N1/PR8 (5μg and 20μg).

In this part of work, in order to study the effect of Alexa 647-labeling degree for activities of the virus on the DDI glycoarray, two glycoconjugates G17 bearing two β-lactose residues and G18 bearing two Neu5Ac (α-2, 6) Lactose moieties (see Table6-1) were tested with respect to the H1N1/PR8 with two Alexa647-labeled amounts 5μg and 20μg. G 17 and G 18 were expected to be negative and positive control respectively. The tests were performed by "on-chip approach". After immobilization of G17 and G18 (see Fig6-6 a), an immobilization control was performed by measuring the Cy3 fluorescence intensities. The Cy3 fluorescence intensities were determined as the average mean Cy3 fluorescence signal of four spots per line. The results (see Fig6-7 a) showed that the average Cy3 fluorescence intensities for G 17 and G 18 were quite similar (~27000-34000 a.u.), indicating identical glycoconjugates immobilization density. Then every two lines of microwells, where G17 or G18 were immobilized, were incubated with H1N1/PR8 virus labeled

with two different Alexa 647 amounts (5 and 20 µg in line 1 and 2 respectively) (see Fig6-6 b).

After incubated with H1N1, the Alexa647 signals were recorded (see Fig6-7 b). At 5µg Alexa647-labeled amounts, the Alexa647 signals obtained for the negative control G 17 (~ 400 a.u.) were higher than that were expected (see Fig6-4 b, G17 1), which demonstrated that there were some non-specific adsorptions of the virus; while for the positive control G18, relatively weak but significant increase of signals were observed (~ 560 a.u.), which was higher than that detected for G17. It indicated that besides the non-specific adsorption, there were weak specific interactions between G18 and virus. With the increasing of the Alexa647-labeled amounts from 5µg to 20µg (increased 4 times), the Alexa647 signals obtained for the negative control G 17 (see Fig6-7 b, G17 1, 2) were also increased by about 4 times (~ 1500 a.u.), which indicated that the increase signal may only be related to the increased degree of labeling., The Alexa647 signals obtained for the G 18 (see Fig6-7 b, G18 1, 2) were only increased about 2 times (~1100 a.u.) compared to G18 5 µg labeled virus, and were almost at the same level as that observed for G17 (see Fig6-7 b, G17 2 , G18 2),). It may well be that increased Alexa647 amounts induced the lost of specific interaction with G18 resulting to only non-specific adsorptions similarly to G17. Normally, the label target of Alexa647 is the proteins on the virus surface, the lectin HA thereby is one of the target for Alexa647. The more quantity of Alexa647 is used, the more activity of HA might be limited.   In section a) a ratio between 2×10^{-7} and 5×10^{-6} of µg of Alexa/ $TCID_{50}$ were used, and here we found that a ratio of 2×10^{-9} Alexa/ $TCID_{50}$ already impair the activities of HA present on the surface of the virus.

In summary, it appeared that compared with the higher Alexa 647 –labeling degree (20µg) of influenza virus, 5µg Alexa647-labeled amounts of the virus was more suitable to do the study of the glycoconjugates/influenza virus interactions on DDI glycoarray (5×10^{-10} Alexa/ $TCID_{50}$).
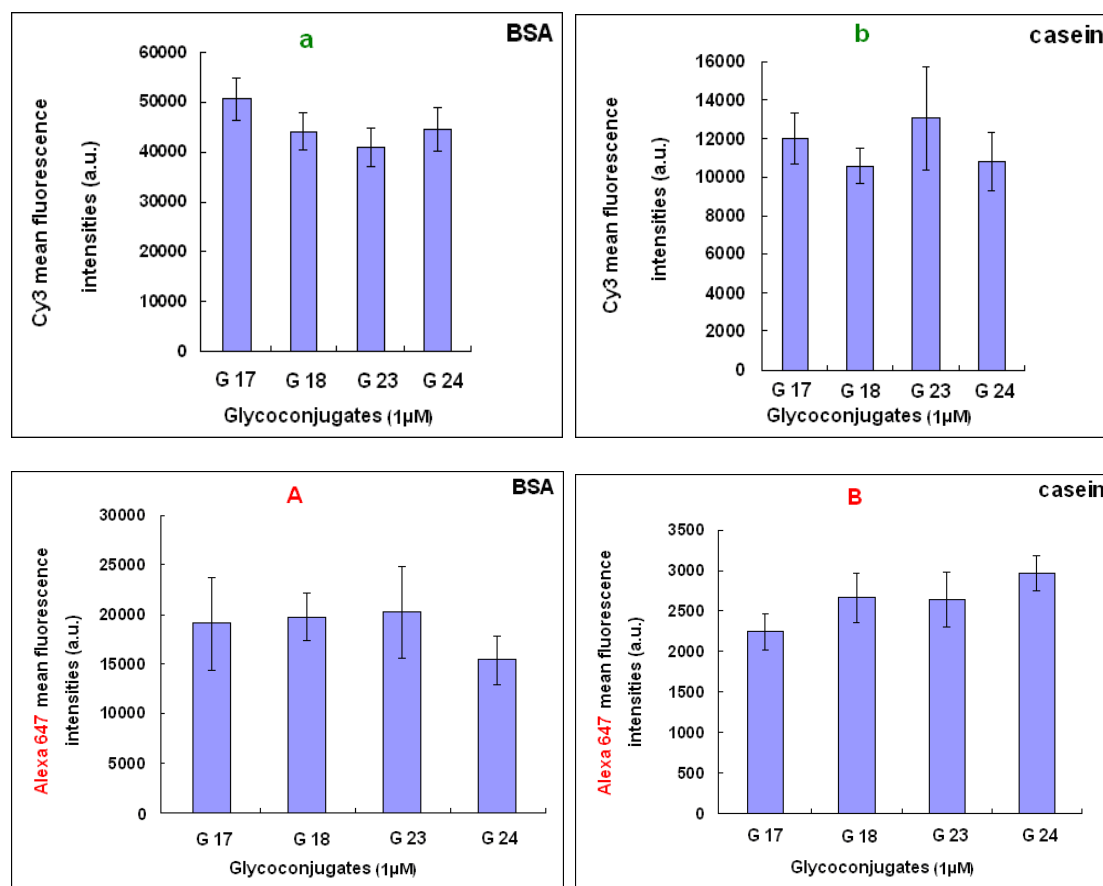
Fig6-7 a) Mean fluorescence intensities at 532 nm (a.u.) of the Cy3-labeled glycoconjugates immobilization on the DNA chip. b) Mean fluorescence intensities (after correction) at 635 nm (a.u.) of the Alexa647-labeled H1N1/PR8 of two Alexa647-labeled amounts 5μg and 20μg after recognition with Molecule 2.

b.3) Compare the affinities of fresh Alexa647-labeled virus and Alexa647-labeled virus stored at -20°C towards its receptor
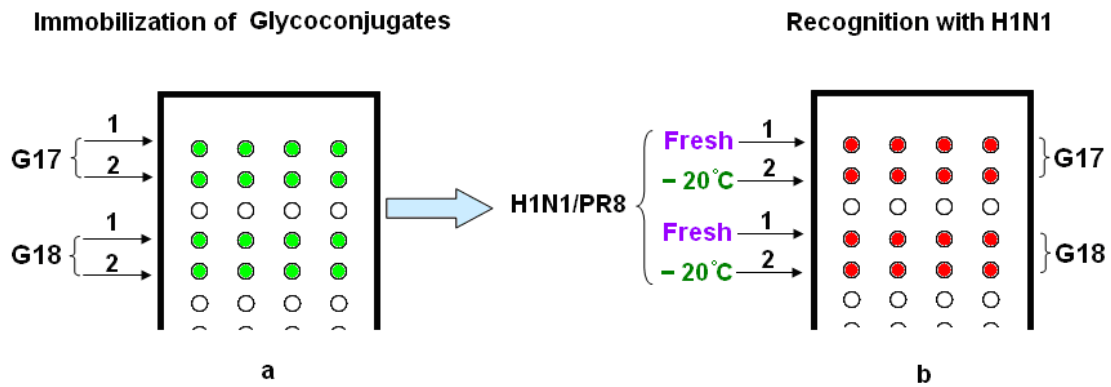
Fig6-8 Sketch map for test Alexa647-labeled amount effect. a) Fabricate glycoarray by immobilization of Molecule 2. b) Recognition of Molecule 2 with Alexa647-labeled H1N1/PR8 stored at 4°C or -20°C.

In this section, an assay was designed to test whether the Alexa647-labeled virus stored at 4°C or -20°C will affect activities of the virus and the interactions of glycoconjugates/influenza virus (see Fig6-8) on DDI glycoarray. As the section above (section c), herein the two glycoconjugates G 17 (negative control) and G 18 (positive control) were also tested by "on-chip approach". After immobilization of G17 and G18 (see Fig6-8 a), the Cy3 fluorescence intensities were recorded (see Fig6-9 a). The

results showed in Fig6-9 a) displayed a homogeneous immobilization of G 17 and G 18 (~ 20000 -25000 a.u.).

After incubation with the virus (see Fig6-8 b), the Alexa647 fluorescence intensities were recorded and shown in Fig6-9 b. When G 17 and G 18 were incubated with the fresh Alexa647-labeled virus (stored at 4°C), the Alexa647 signals obtained for the two glycoconjugates G 17 and G 18 had the same trend as that observed in section a) (See Fig 6-7 b, G 17 1 and G 18 1): relatively higher non-specific adsorptions were detected for the negative control G17 (~420 a.u., See Fig 6-9 b, G 17 1). However, the Alexa647 signals obtained for the positive control G 18 were slightly higher than that observed for G 17 (~610 a.u., See Fig 6-9 b, G 18 1). After storage of the labeled virus at -20 °C, incubation of the two glycoconjugates leads to Alexa647 signals for the two glycoconjugates were all at background level (~50-70 a.u.)

A test for the determination of the viral HA titre was also carried out by our co-workers at the same time, a sharp decline of the HA titre were observed for the freezed Alexa647-labeled virus in comparison with the fresh Alexa647-labeled virus, which indicated the activity of the virus were also greatly decreased.

These results clearly demonstrated that only the fresh Alexa647-labeled influenza virus could be used for the investigation of the glycoconjugates/virus interactions on DDI glycoarray.
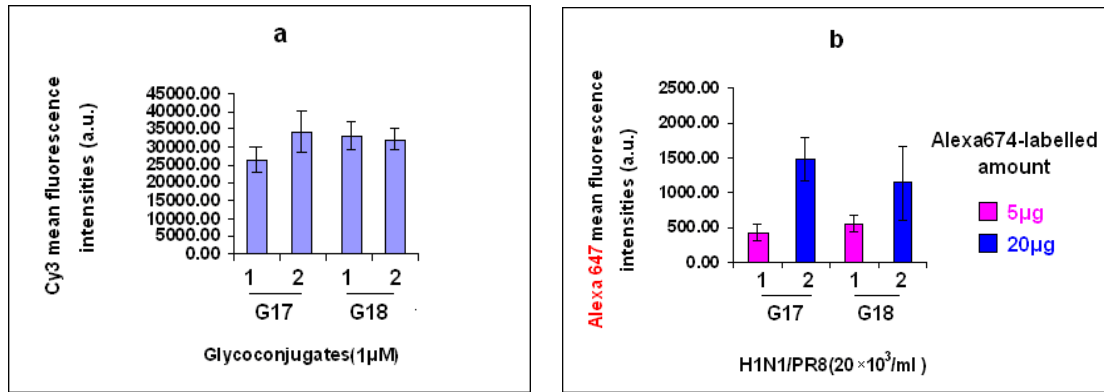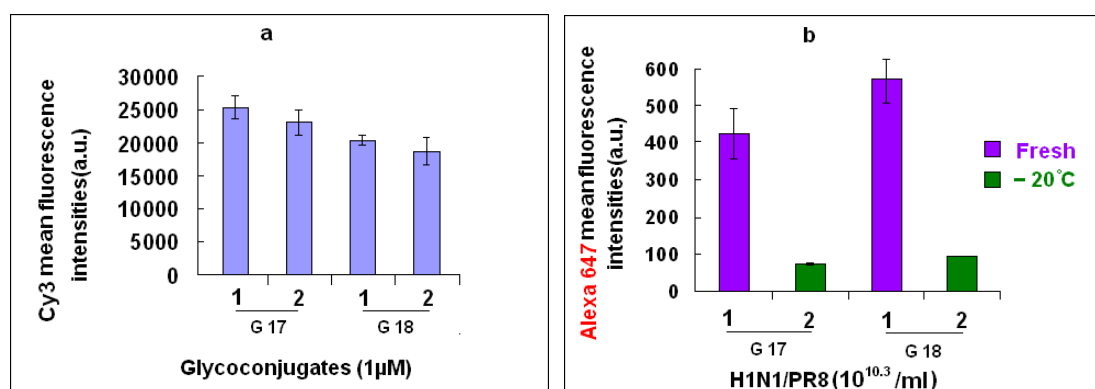

Fig6-9 a) Mean fluorescence intensities at 532 nm (a.u.) of the Cy3-labeled glycoconjugate Molecule 2 immobilization on the DNA chip. b) Mean fluorescence intensities (after correction) at 635 nm (a.u.) of the Alexa647-labeled H1N1/PR8 stored at 4°C or -20°C after recognition with Molecule 2.

6.4 Conclusions

In this chapter, we tried to apply DDI glycoarray to investigate interactions of two influenza viruses H1N1/PR8 and H3N2/Moscow with glycoconjugates. As noted before, the biological relevance of the binding processes of the whole influenza viruses with glycoconjugates are far more than understood and more complicated than lectin/glycoconjugates interactions (*278*). Although the optimal platform and protocol based on DDI glycoarrays for profiling influenza viruses/glycoconjugates interactions have not yet been established, the preliminary studies still provided some interesting results. Firstly non-specific adsorptions of influenza virus were observed on the DDI glycoarray for both of the two DDI strategies ("on-chip" approach or by "in-solution" approach). In order to find out ways to reduce the non-specific adsorption, comparison tests of two blocking methods (BSA and casein blocking method) were performed. The results demonstrated that the alteration of the blocking method was unhelpful in increasing the signal/noise ratio. We also found that with the increasing of the Alexa647-labelling degree of the virus, the activity of the HA on the surface of the virus decreased and further impacted the affinity of the virus towards the glycoconjugate on the glycoarray. Moreover, very weak binding signal was obtained from the freezed Alexa647-labeled virus in comparison with the fresh Alexa647-labeled virus on the DDI glycoarray. Although these primary results showed promising in the construction of an ideal platform of DDI glycoarray for the investigation of influenza virus/ glycoconjugates interactions, great efforts still need to be made in fully solving the non-specific adsorption problem, indeed the non-specific adsorption of influenza virus were also detected for the spots where only ssDNA or dsDNA were printed, which might be one of the reasons for the non-specific adsorption of influenza virus on DDI glycoarray.

CONCLUSION

In this thesis, the validation and development of DNA-directed immobilization (DDI) glycoarrays and miniaturized analytical biosystems for quantitative and simultaneous analysis of various synthetic glycoconjugates are described. In addition, some preliminary studies regarding the binding features of influenza viruses on DDI glycoarrays were also reported. The validation and development comprised the elaboration of miniaturized microsystems, optimization of the immobilization parameters (including glycoconjugates concentration, choice of DNA sequences …) as well as the development of a semi-quantitative test (IC_{50}) and of recognition protcols.

The carbohydrate immobilization strategies are of great importance for the efficiency of a glycoarray. Two carbohydrate immobilization methods, DDI and direct covalent grafting, were compared on the borosilicate glass slide. At 0.5µM, DDI led to a stronger fluorescence signal (by a factor of 4.5) and to a lower detection limit (20nM) than covalent immobilisation (higher than 200nM), indicating that the DDI carbohydrate immobilization is more efficient in comparison with covalent grafting methods.

Two kinds of microsystems were developed and multiplex tests were successfully performed in one single microwell. For proof of concept, the first miniaturized biosystem (Mb I, in abbr.) was fabricated to investigate two lectin/glycoconjugate specific recognition models by "in-solution" approach. Two kinds of lectin/glycoconjugate complexes were well addressed on to the right spots on the surface of Mb I thanks to the specificity of DNA/DNA hybridization. On the basis of validation of the "in-solution" approach in Mb I, a developed miniaturized biosystem (Mb II, in abbr.) was set up, which allowed the mixture of eight different glycoconjugates or glycoconjugate/lectin complexes to be sorted and captured by hybridization with the complementary DNA sequences printed on the surface of Mb II. Moreover, a quantitative assay for the determination of IC_{50} values of five

glycoconjugates was simultaneous performed on Mb II.

The affinities of galactose clusters with different multivalencies (1, 3, 4, 8 and 10), spatial arrangements (Comb-like, crown geometry and antenna), charged (negative, neutral or positive) and different linkers were tested for their binding affinities with respect to RCA120 and PA-IL lectins using direct fluorescent scanning and IC_{50} assays. The results demonstrated that the Comb-like trivalent cluster was displayed the most efficient binding to the two lectins among all the galactose clusters.

For RCA 120, a cluster effect was observed with comb-like structures bearing linker DMCH: a 23 times increase in potency per galactose residue was observed from trivalent cluster to monovalent cluster. At pH 7.4 (near the pI of RCA 120), no effect of the charge of the glycocluster was observed.

PA-IL preferred comb-like structures. The binding was enhanced by a positive charge on the glycomimetic structure. On the contrary to RCA 120, PA-IL showed no affinity for crown structures. IC_{50} assays suggested that overall the affinity of PA-IL for the different galactosyl structures tested was one or two order of magnitude lower than the one observed with RCA 120.

Surprisingly, we obtained different results between the "on-chip" and "in-solution approach". For the "in-solution" approach, the highest affinity was observed for the four galactose residues with DMCH linker in comb like structure (G10).

Initial attempts were undertaken to apply DDI glycoarray for the study of the interactions of two influenza viruses H1N1/PR8 and H3N2/Moscow with glycoconjugates. The preliminary studies showed that both the fluorescent labeled quantity of the influenza viruses and the storage methods of the labeled viruses can affect the binding affinities with the glycoconjugates. Furthermore only weak interactions were observed. More efforts still need to be done for minimizing the non-specific adsorption and increasing the affinities towards the glycoconjugates in order to increase the Signal/Noise ratios.

In summary the studies described in this thesis have demonstrated that DDI carbohydrate immobilization is more efficient than the covalent grafting for glycoarray fabrication. The DDI glycoarrays and miniaturized DDI biosystems were

very powerful, sensitive and high throughput tools for profiling glycoconjugate/lectin interactions and for quantitative analysis (determination of IC$_{50}$ values) of the affinities glycoconjugates/lectins interactions. Although an ideal platform and protocol based on DDI glycoarray for investigating the glycoconjugates/influenza viruses interactions are not yet established, the preliminary results still look promising.

In perspectives of this work, we must notice that the biosystems were validated with 8 different glycomimetics, but it is evident that these systems could be improved by increasing the number of parallel analysis. It would require a larger set of DNA sequences able to hybridize with their respective complementary sequences with an equivalent hybridization yields. During this work, we used a detection based on the fluorescent labeling. The same concept of miniaturized DDI biosystems could also be adapted with others type of transduction (optical as Surface Plasmon Resonance – SPR- or electronics as impedances, or mechanics as cantilever) for reading the interactions without labeling. Two main parameters, the Limit of Detection (LOD) and linear range, depend both on transducer and the considered biochemical interactions. These two parameters may need to be determined for each potential biosensor. For example, based on fluorescence detection (Cy5 labeling) and DDI glycoarray, a LOD in the 2-20nM range and a linear range of 0.02µM to 2µM (semi loge scale) were observed for RCA120. Integration of transducer systems in miniaturized biosystems for a sensitive, specific and direct detection will be future challenges.

REFERENCES

1.   Matthews, C. K., Van Holde, K. E., and Ahern, K. G. (1999) Biochemistry 3rd edition. Benjamin Cummings. ISBN 0-8053-3066-6.

2.   Varki, A., Cummings, R. D., Esko, J. D., Freeze, H. H., Stanley, P., Bertozzi, C. R., Hart, G. W., and Etzler, M. E. (2009) Essentials of Glycobiology, Cold Spring Harbor Laboratory Press

3.   Laine, R. A. (1994) A calculation of all possible oligosaccharide isomers both branched and linear yields 1.05 x 10(12) structures for a reducing hexasaccharide: the Isomer Barrier to development of single-method saccharide sequencing or synthesis systems, *Glycobiology 4*, 759-767.

4.   Pilobello, K. T., and Mahal, L. K. (2007) Deciphering the glycocode: the complexity and analytical challenge of glycomics, *Curr Opin Chem Biol 11*, 300-305.

5.   Varki, A. (1993) Biological roles of oligosaccharides: all of the theories are correct, *Glycobiology 3*, 97-130.

6.   Sytkowski, A. J., Feldman, L., and Zurbuch, D. J. (1991) Biological activity and structural stability of N-deglycosylated recombinant human erythropoietin, *Biochem Biophys Res Commun 176*, 698-704.

7.   Fukuda, M., Sasaki, H., and Fukuda, M. N. (1989) Structure and role of carbohydrate in human erythropoietin, *Adv Exp Med Biol 271*, 53-67.

8.   McEver, R. P. (2002) Selectins: lectins that initiate cell adhesion under flow, *Curr Opin Cell Biol 14*, 581-586.

9.   Childs, R. A., Palma, A. S., Wharton, S., Matrosovich, T., Liu, Y., Chai, W., Campanero-Rhodes, M. A., Zhang, Y., Eickmann, M., Kiso, M., Hay, A., Matrosovich, M., and Feizi, T. (2009) Receptor-binding specificity of pandemic influenza A (H1N1) 2009 virus determined by carbohydrate microarray, *Nat Biotechnol 27*, 797-799.

10.   Kumari, K., Gulati, S., Smith, D. F., Gulati, U., Cummings, R. D., and Air, G. M. (2007) Receptor binding specificity of recent human H3N2 influenza viruses, *Virol J 4*, 42.

11.   Amonsen, M., Smith, D. F., Cummings, R. D., and Air, G. M. (2007) Human parainfluenza viruses hPIV1 and hPIV3 bind oligosaccharides with alpha2-3-linked sialic acids that are distinct from those bound by H5 avian influenza virus hemagglutinin, *J Virol 81*, 8341-8345.

12.   Stevens, J., Blixt, O., Tumpey, T. M., Taubenberger, J. K., Paulson, J. C., and Wilson, I. A. (2006) Structure and Receptor Specificity of the Hemagglutinin from an H5N1 Influenza Virus *Science 312*, 404-410.

13.   Sharon, N., and Lis, H. (2004) History of lectins: from hemagglutinins to biological recognition molecules, *Glycobiology 14*, 53R-62R.

14.   Lis, H., and Sharon, N. (1998) Lectins: Carbohydrate-Specific Proteins That Mediate Cellular Recognition, *Chem Rev 98*, 637-674.

15.   Ambrosi, M., Cameron, N. R., and Davis, B. G. (2005) Lectins: tools for the molecular understanding of the glycocode, *Org Biomol Chem 3*, 1593-1608.

16.   Peumans, W. J., Van Damme, E. J., Barre, A., and Rouge, P. (2001) Classification of plant lectins in families of structurally and evolutionary related proteins, *Adv Exp Med Biol 491*, 27-54.

17.   Kilpatrick, D. C. (2002) Animal lectins: a historical introduction and overview, *Biochim Biophys Acta 1572*, 187-197.

18.   Mislovicova, D., Gemeiner, P., Kozarova, A., and Kozar, T. (2009) Lectinomics I. Relevance of exogenous plant lectins in biomedical diagnostics, *Biologia 64*, 1-19.

19.   Baenziger, J. U., and Maynard, Y. (1980) Human hepatic lectin. Physiochemical properties and specificity, *J Biol Chem 255*, 4607-4613.

20.   Goldstein, I. J., and Hayes, C. E. (1978) The lectins: carbohydrate-binding proteins of plants and animals, *Adv Carbohydr Chem Biochem 35*, 127-340.

21.   Lis, H., and Sharon, N. (1973) The biochemistry of plant lectins (phytohemagglutinins), *Annu Rev Biochem 42*, 541-574.

22. Sumner, J. B. (1919) The globulins of the jack bean, canavalia ensiformis., *J Biol Chem 37*, 137-142.

23. Edelman, G. M., Cunningham, B. A., Reeke, G. N., Jr., Becker, J. W., Waxdal, M. J., and Wang, J. L. (1972) The covalent and three-dimensional structure of concanavalin A, *Proc Natl Acad Sci U S A 69*, 2580-2584.

24. Nasi, A., Picariello, G., and Ferranti, P. (2009) Proteomic approaches to study structure, functions and toxicity of legume seeds lectins. Perspectives for the assessment of food quality and safety, *J Proteomics 72*, 527-538.

25. De Oliveira, T. M., Delatorre, P., da Rocha, B. A., de Souza, E. P., Nascimento, K. S., Bezerra, G. A., Moura, T. R., Benevides, R. G., Bezerra, E. H., Moreno, F. B., Freire, V. N., de Azevedo, W. F., Jr., and Cavada, B. S. (2008) Crystal structure of Dioclea rostrata lectin: Insights into understanding the pH-dependent dimer-tetramer equilibrium and the structural basis for carbohydrate recognition in Diocleinae lectins, *J Struct Biol*.

26. Tachibana, H., Cheng, X. J., Kobayashi, S., Okada, Y., Itoh, J., and Takeuchi, T. (2007) Primary structure, expression and localization of two intermediate subunit lectins of Entamoeba dispar that contain multiple CXXC motifs, *Parasitology 134*, 1989-1999.

27. Meyer, A., Rypniewski, W., Celewicz, L., Erdmann, V. A., Voelter, W., Singh, T. P., Genov, N., Barciszewski, J., and Betzel, C. (2007) The mistletoe lectin I--phloretamide structure reveals a new function of plant lectins, *Biochem Biophys Res Commun 364*, 195-200.

28. Gourdine, J. P., Markiv, A., and Smith-Ravin, J. (2007) The three-dimensional structure of codakine and related marine C-type lectins, *Fish Shellfish Immunol 23*, 831-839.

29. Delatorre, P., Rocha, B. A., Gadelha, C. A., Santi-Gadelha, T., Cajazeiras, J. B., Souza, E. P., Nascimento, K. S., Freire, V. N., Sampaio, A. H., Azevedo, W. F., Jr., and Cavada, B. S. (2006) Crystal structure of a lectin from Canavalia maritima (ConM) in complex with trehalose and maltose reveals relevant mutation in ConA-like lectins, *J Struct Biol 154*, 280-286.

30. Manoj, N., and Suguna, K. (2001) Signature of quaternary structure in the sequences of legume lectins, *Protein Eng 14*, 735-745.

31. Weis, W. I. (1994) Lectins on a roll: the structure of E-selectin, *Structure 2*, 147-150.

32. Barondes, S. H., Cooper, D. N., Gitt, M. A., and Leffler, H. (1994) Galectins. Structure and function of a large family of animal lectins, *J Biol Chem 269*, 20807-20810.

33. Chawla, D., Animashaun, T., Hughes, R. C., Harris, A., and Aitken, A. (1993) Bowringia mildbraedii agglutinin: polypeptide composition, primary structure and homologies with other legume lectins, *Biochim Biophys Acta 1202*, 38-46.

34. Olsen, K. W. (1983) Prediction of three-dimensional structure of plant lectins from the domains of concanavalin A, *Biochim Biophys Acta 743*, 212-218.

35. Van Driessche, E., Strosberg, A. D., and Kanarek, L. (1976) Studies on the structure of lectins: I. Pea (Pisum sativum) lectin, *Arch Int Physiol Biochim 84*, 677-679.

36. Olsnes, S., Refsnes, K., Christensen, T. B., and Pihl, A. (1975) Studies on the structure and properties of the lectins from Abrus precatorius and Ricinus communis, *Biochim Biophys Acta 405*, 1-10.

37. Gemeiner, P., Mislovicova, D., Tkac, J., Svitel, J., Patoprsty, V., Hrabarova, E., Kogan, G., and Kozar, T. (2009) Lectinomics II. A highway to biomedical/clinical diagnostics, *Biotechnol Adv 27*, 1-15.

38. Nagahora, H., Ishikawa, K., Niwa, Y., Muraki, M., and Jigami, Y. (1992) Expression and secretion of wheat germ agglutinin by Saccharomyces cerevisiae, *Eur J Biochem 210*, 989-997.

39. Nagano, C. S., Calvete, J. J., Barettino, D., Perez, A., Cavada, B. S., and Sanz, L. (2008) Insights into the structural basis of the pH-dependent dimer-tetramer equilibrium through crystallographic analysis of recombinant Diocleinae lectins, *Biochem J 409*, 417-428.

40. Hyun, S., Lee, E. H., Park, J., and Yu, J. (2008) Tentacle type peptides as artificial lectins against sulfated Lewis X and A, *Bioorg Med Chem Lett 18*,

4011-4014.

41.   Fitches, E., Wiles, D., Douglas, A. E., Hinchliffe, G., Audsley, N., and Gatehouse, J. A. (2008) The insecticidal activity of recombinant garlic lectins towards aphids, *Insect Biochem Mol Biol 38*, 905-915.

42.   Hyun, S., Kim, J., Kwon, M., and Yu, J. (2007) Selection and syntheses of tentacle type peptides as 'artificial' lectins against various cell-surface carbohydrates, *Bioorg Med Chem 15*, 511-517.

43.   Streicher, H., and Sharon, N. (2003) Recombinant plant lectins and their mutants, *Methods Enzymol 363*, 47-77.

44.   Yue, K. T., MacDonald, J. F., Pekhletski, R., and Hampson, D. R. (1995) Differential effects of lectins on recombinant glutamate receptors, *Eur J Pharmacol 291*, 229-235.

45.   Young, N. M., Watson, D. C., Yaguchi, M., Adar, R., Arango, R., Rodriguez-Arango, E., Sharon, N., Blay, P. K., and Thibault, P. (1995) C-terminal post-translational proteolysis of plant lectins and their recombinant forms expressed in Escherichia coli. Characterization of "ragged ends" by mass spectrometry, *J Biol Chem 270*, 2563-2570.

46.   Sharon, N. (2007) Lectins: carbohydrate-specific reagents and biological recognition molecules, *J Biol Chem 282*, 2753-2764.

47.   Krishnamoorthy, L., and Mahal, L. K. (2009) Glycomic analysis: an array of technologies, *ACS Chem Biol 4*, 715-732.

48.   Sharon, N. (1993) Lectin-carbohydrate complexes of plants and animals: an atomic view, *Trends Biochem Sci 18*, 221-226.

49.   Adar, R., and Sharon, N. (1996) Mutational studies of the amino acid residues in the combining site of Erythrina corallodendron lectin, *Eur J Biochem 239*, 668-674.

50.   Elgavish, h., and Shaanan, B. (1997) Lectin-carbohydrate interactions: different folds, common recognition principles, *Trends Biochem Sci 22*, 462-467.

51.   Weis, W. I., and Drickamer, K. (1996) Structural Basis of Lectin-Carbohydrate

Recognition, *Annu Rev Biochem 65*, 441-473.

52. Rini, J. M. (1995) Lectin Structure, *Annu Rev Biophys Biomol Struct 24*, 551-577.

53. Elgavisha, S., and Shaanana, B. (1998) Structures of the Erythrina corallodendron lectin and of its complexes with mono- and disaccharides, *J Mol Biol 277*, 971-932.

54. Ladmiral, V., Melia, E., and Haddleton, D. M. (2004) Synthetic glycopolymers: an overview, *Eur Polym J 40*, 431-449.

55. Morvan, F., Meyer, A., Jochum, A., Sabin, C., Chevolot, Y., Imberty, A., Praly, J. P., Vasseur, J. J., Souteyrand, E., and Vidal, S. (2007) Fucosylated pentaerythrityl phosphodiester oligomers (PePOs): automated synthesis of DNA-based glycoclusters and binding to *Pseudomonas aeruginosa* lectin (PA-IIL), *Bioconjug Chem 18*, 1637-1643.

56. Lee, R. T., and Lee, Y. C. (2000) Affinity enhancement by multivalent lectin-carbohydrate interaction, *Glycoconj J 17*, 543-551.

57. Lee, Y. C. (1992) Biochemistry of carbohydrate-protein interaction, *The FASEB Journal 6*, 3193-3200.

58. Gagneux, P., and Varki, A. (1999) Evolutionary considerations in relating oligosaccharide diversity to biological function, *Glycobiology 9*, 747-755.

59. Gabius, H. J. (1997) Animal lectins, *Eur J Biochem 243*, 543-576.

60. Gabius, H. J., and Wu, A. M. (2006) The emerging functionality of endogenous lectins: A primer to the concept and a case study on galectins including medical implications, *Chang Gung Med J 29*, 37-62.

61. Sharon, N., and Lis, H. (2004) History of lectins: from hemagglutinins to biological recognition molecules, *Glycobiology 14*, 53R-62R.

62. Ambrosi, M., Cameron, N. R., and Davis, B. G. (2005) Lectins: tools for the molecular understanding of the glycocode, *Org Biomol Chem 3*, 1593-1608.

63. Naismith, J. H., and Field, R. A. (1996) Structural Basis of Trimannoside Recognition by Concanavalin A *J Biol Chem 271*, 972-976.

64. Gunther, G. R., Wang, J. L., Yahara, I., Cunningham, B. A., and Edelman, G.

M. (1973) Concanavalin A derivatives with altered biological activities, *Proc Natl Acad Sci U S A 70*, 1012-1016.

65.   Edelman, G. M., Cunningham, B. A., Reeke, G. N., r., J., Becker, J. W., Waxdal, M. J., and Wang, J. L. (1972) The Covalent and Three-Dimensional Structure of Concanavalin A, *Proc Natl Acad Sci U S A 69*, 2580-2584.

66.   Chatterjee, A., and Mandal, D. K. (2005) Quaternary association and reactivation of dimeric concanavalin A, *International Journal of Biological Macromolecules 35*, 103-109.

67.   Loris, R., Hamelryck, T., Bouckaert, J., and Wyns, L. (1998) Legume lectin structure, *Biochimica et Biophysica Acta 1383*.

68.   Srinivas, V. R., Reddy, G. B., Ahmad, N., Swaminathan, C. P., Mitra, N., and Surolia, A. (2001) Legume lectin family, the 'natural mutants of the quaternary state', provide insights into the relationship between protein stability and oligomerization, *Biochim Biophys Acta 1527*, 102-111.

69.   Bhattacharyya, L., Koenig, S. H., Brown, R. D., and Brewer, C. (1991) Interactions of asparagine-linked carbohydrates with concanavalin A. Nuclear magnetic relaxation dispersion and circular dichroism studies, *J Biol Chem 266*, 9835-9840.

70.   Scott, J. K., Loganathan, D., Easley, R. B., Gong, X., and Goldstein, I. J. (1992) A family of concanavalin A-binding peptides from a hexapeptide epitope library, *Proc Natl Acad Sci U S A 89*, 5398-5402.

71.   Jain, D., Kaur, K. J., Goel, M., and Salunke, D. M. (2000) Structural Basis of Functional Mimicry between Carbohydrate and Peptide Ligands of Con A, *Biochem Biophys Res Commun 272*, 843-849.

72.   Pashov, A., MacLeod, S., Saha, R., Perry, M., VanCott, T. C., and Kieber-Emmons, T. (2005) Concanavalin A binding to HIV envelope protein is less sensitive to mutations in glycosylation sites than monoclonal antibody 2G12, *Glycobiology 15*, 994-1001.

73.   Yu, M., Sato, H., Seiki, M., and Thompson, E. W. (1995) Complex Regulation of Membrane-Type Matrix Metalloproteinase Expression and Matrix

Metalloproteinase-2 Activation by Concanavalin A in MDA-MB-231 Human Breast Cancer Cells1, *Ca Res 55*, 3272-3277.

74. Overall, C. M., and Sodek, J. (1990) Concanavalin A produces a matrix-degradative phenotype in human fibroblasts. Induction and endogenous activation of collagenase, 72-kDa gelatinase, and Pump-1 is accompanied by the suppression of the tissue inhibitor of matrix metalloproteinases, *J Biol Chem 265*.

75. Gilboa-Garber, N., Katcoff, D. J., and Garber, N. C. (2000) Identification and characterization of pseudomonas aeruginosa PA-IIL lectin gene and protein compared to PA-IL, *FEMS Immunol Med Microbiol 29*, 53-57.

76. Sabin, C., Mitchell, E. P., Pokorna, M., Gautier, C., Utille, J.-P., Wimmerova, M., and Imberty, A. (2006) Binding of different monosaccharides by lectin PA-IIL from Pseudomonas aeruginosa: Thermodynamics data correlated with X-ray structures, *FEBS Lett 580*, 982-987.

77. Gilboa-Garber, N. (1972) Inhibition of broad spectrum hemagglutinin from Pseudomonas aeruginosa by D-galactose and its derivatives, *FEBS Lett 20*, 242-244.

78. Gilboa-Garber, N., Mizrahia, L., and Garber, N. (1972) Purification of the galactose-binding hemagglutinin of Pseudomonas aeruginosa by affinity column chromatography using sepharose, *FEBS Lett 28*, 93-95.

79. Gilboa-Garber, N. (1982) Pseudomonas aeruginosa lectins., *Methods Enzymol 83*, 378-385.

80. Imberty, A., Wimmerová, M., Mitchell, E. P., and Gilboa-Garber, N. (2004) Structures of the lectins from Pseudomonas aeruginosa: insights into the molecular basis for host glycan recognition, *Microbes Infect 6*, 221-228.

81. Garber, N., Guempel, U., Belz, A., Gilboa-Garber, N., and Doyle, R. J. (1992) On the specificity of the D-galactose-binding lectin (PA-I) of Pseudomonas aeruginosa and its strong binding to hydrophobic derivatives of D-galactose and thiogalactose, *Biochim Biophys Acta 1116*, 331-333.

82. Bajolet-Laudinat, O., Bentzmann, S. G, Tournier, J. M., Madoulet, C.,

Plotkowski, M. C., Chippaux, C., and Puchelle, E. (1994) Cytotoxicity of Pseudomonas aeruginosa internal lectin PA-I to respiratory epithelial cells in primary culture., *Infect Immun 62*, 4481-4487.

83. Laughlin, R. S., Musch, M. W., Hollbrook, C. J., Rocha, F. M., Chang, E. B., and Alverdy, J. C. (2000) The Key Role of Pseudomonas aeruginosa PA-I Lectin on Experimental Gut-Derived Sepsis, *Ann Surg 232*, 133-142.

84. Baenziger, J. U., and Fiete, D. (1979) Structural Determinants of Ricinus communis Agglutinin and Toxin Specificity for Oligosaccharides, *J Biol Chem 254*, 9795-9799.

85. Green, E. D., JBrodbeck, R. M., and Baenziger, U. (1987) Lectin affinity high-performance liquid chromatography. Interactions of N-glycanase-released oligosaccharides with Ricinus communis agglutinin I and Ricinus communis agglutinin II, *J Biol Chem 262*, 12030-12039.

86. Solis, D., Fernandez, P., Diaz-Maurino, T., Jimenez-Barbero, J., and Martin-Lomas, M. (1993) Hydrogen-bonding pattern of methyl β-lactoside binding to the Ricinus communis lectins, *Eur J Biochem 214*, 677-683.

87. Sphyris, N., Lord, J. M., Wales, R., and Roberts, L. M. (1995) Mutational Analysis of the Ricinus Lectin B-chains, *J Biol Chem 270*, 20292-20297.

88. Brandta, N. N., Chikisheva, A. Y., Sotnikova, A. I., Savochkinab, Y. A., Agapovb, I. I., and Tonevitskyc, A. G. (2005) Ricin, ricin agglutinin, and the ricin binding subunit structural comparison by Raman spectroscopy *J Mol Struct 735-736*, 293-298.

89. Utsumi, T., Ide, A., and Funatsu, G. (1989) Ricin A-chain induces fusion of small unilamellar vesicles at neutral pH, *FEBS Lett 242*, 255-258.

90. Sweeney, E. C., Tonevitsky, A. G., Temiakov, D. E., Agapov, II, Saward, S., and Palmer, R. A. (1997) Preliminary crystallographic characterization of ricin agglutinin, *Proteins 28*, 586-589.

91. Gao, Y., Eguchi, A., Kakehi, K., and Lee, Y. C. (2005) Synthesis and molecular recognition of carbohydrate-centered multivalent glycoclusters by a plant lectin RCA120, *Bioorg Med Chem 13*, 6151-6157.

92. Karamanska, R., Mukhopadhyay, B., Russell, D. A., and Field, R. A. (2005) Thioctic acid amides: convenient tethers for achieving low nonspecific protein binding to carbohydrates presented on gold surfaces, *Chem Commun*, 3334-3336.

93. Itakura, Y., Nakamura-Tsuruta, S., Kominami, J., Sharon, N., Kasai, K., and Hirabayashi, J. (2007) Systematic Comparison of Oligosaccharide Specificity of Ricinus communis Agglutinin I and Erythrina Lectins: a Search by Frontal Affinity Chromatography, *J Biol Chem 142*, 459-469.

94. Tu, A. T., Keeler, R. F., Hardegree, M. C., and Moss, J. (1983) Handbook of natural toxins, *6*, 250.

95. D'Agata, R., Grasso, G., Iacono, G., Spoto, G., and Vecchio, G. (2006) Lectin recognition of a new SOD mimic bioconjugate studied with surface plasmon resonance imaging, *Org Biomol Chem 4*, 610-612.

96. Cartellieri, S., Helmholz, H., and Niemeyer, B. (2001) Preparation and Evaluation of Ricinus communis Agglutinin Affinity Adsorbents Using Polymeric Supports, *Anal Biochem 295*, 66-75.

97. Zhang, J., Pourceau, G., Meyer, A., Vidal, S., Praly, J. P., Souteyrand, E., Vasseur, J. J., Morvan, F., and Chevolot, Y. (2009) Specific recognition of lectins by oligonucleotide glycoconjugates and sorting on a DNA microarray, *Chem Commun*, 6795-6797.

98. Moni, L., Pourceau, G., Zhang, J., Meyer, A., Vidal, S., Souteyrand, E., Dondoni, A., Morvan, F., Chevolot, Y., Vasseur, J. J., and Marra, A. (2009) Design of triazole-tethered glycoclusters exhibiting three different spatial arrangements and comparative study of their affinities towards PA-IL and RCA 120 by using a dna-based glycoarray, *ChemBioChem 10*, 1369-1378.

99. Zhang, J., Pourceau, G., Meyer, A., Vidal, S., Praly, J. P., Souteyrand, E., Vasseur, J. J., Morvan, F., and Chevolot, Y. (2009) DNA-directed immobilisation of glycomimetics for glycoarrays application: Comparison with covalent immobilisation, and development of an on-chip IC_{50} measurement assay., *Biosens Bioelectron 24*, 2515-2521.

100. Fan, H., and Mark, A. E. (2003) Relative stability of protein structures determined by X-ray crystallography or NMR spectroscopy: a molecular dynamics simulation study, *Proteins 53*, 111-120.

101. Rejto, P. A., and Freer, S. T. (1996) Protein conformational substates from X-ray crystallography, *Prog Biophys Mol Biol 66*, 167-196.

102. Kannan, K. K. (1977) The x-ray crystallography technique in protein sequencing, *Mol Biol Biochem Biophys 25*, 75-122.

103. Pallan, P. S., and Egli, M. (2009) Pairing geometry of the hydrophobic thymine analogue 2,4-difluorotoluene in duplex DNA as analyzed by X-ray crystallography, *J Am Chem Soc 131*, 12548-12549.

104. Ohishi, H., Tukamoto, K., Odoko, M., Grzeskowiak, K., Maezaki, N., Okabe, N., Tanaka, T., and Ishida, T. (2005) The development of crystallization and X-ray crystallography method of long stem DNA, *Nucleic Acids Symp Ser (Oxf)*, 67-68.

105. Peek, M. E., and Williams, L. D. (2001) X-ray crystallography of DNA-drug complexes, *Methods Enzymol 340*, 282-290.

106. Schlichting, I. (2005) X-ray crystallography of protein-ligand interactions, *Methods Mol Biol 305*, 155-166.

107. Schwefel, D., Maierhofer, C., Beck, J. G., Seeberger, S., Diederichs, K., Moller, H. M., Welte, W., and Wittmann, V. (2010) Structural Basis of Multivalent Binding to Wheat Germ Agglutinin, *J Am Chem Soc. 132*, 8704-8719

108. Banerjee, R., Das, K., Ravishankar, R., Suguna, K., Surolia, A., and Vijayan, M. (1996) Conformation, protein-carbohydrate interactions and a novel subunit association in the refined structure of peanut lectin-lactose complex, *J Mol Biol 259*, 281-296.

109. Bush, C. A., Martin-Pastor, M., and Imberty, A. (1999) Structure and conformation of complex carbohydrates of glycoproteins, glycolipids, and bacterial polysaccharides, *Annu Rev Biophys Biomol Struct 28*, 269-293.

110. Michalski, J. C., Wieruszeski, J. M., Alonso, C., Cache, P., Montreuil, J., and Strecker, G. (1991) Characterization and 400-MHz 1H-NMR analysis of

urinary fucosyl glycoasparagines in fucosidosis, *Eur J Biochem 201*, 439-458.

111. Angulo, J., Rademacher, C., Biet, T., Benie, A. J., Blume, A., Peters, H., Palcic, M., Parra, F., and Peters, T. (2006) NMR analysis of carbohydrate-protein interactions, *Methods Enzymol 416*, 12-30.

112. Pierce, M. M., Raman, C. S., and Nall, B. T. (1999) Isothermal titration calorimetry of protein-protein interactions, *Methods 19*, 213-221.

113. Velazquez-Campoy, A., Leavitt, S. A., and Freire, E. (2004) Characterization of protein-protein interactions by isothermal titration calorimetry, *Methods Mol Biol 261*, 35-54.

114. Damian, L., Fournier, D., Winterhalter, M., and Paquereau, L. (2005) Determination of thermodynamic parameters of Xerocomus chrysenteron lectin interactions with N-acetylgalactosamine and Thomsen-Friedenreich antigen by isothermal titration calorimetry, *BMC Biochem 6*, 11.

115. Szabo, P., Dam, T. K., Smetana, K., Jr., Dvorankova, B., Kubler, D., Brewer, C. F., and Gabius, H. J. (2009) Phosphorylated human lectin galectin-3: analysis of ligand binding by histochemical monitoring of normal/malignant squamous epithelia and by isothermal titration calorimetry, *Anat Histol Embryol 38*, 68-75.

116. Dam, T. K., and Brewer, C. F. (2002) Thermodynamic studies of lectin-carbohydrate interactions by isothermal titration calorimetry, *Chem Rev 102*, 387-429.

117. Tudos, A. J., and B.M., S. R. (2008) Handbook of Surface Plasmon Resonance ISBN (online): 978-1-84755-822-0 ISBN (print): 978-0-85404-267-8

118. van der Merwe, P. A. (2001) Surface Plasmon Resonance in Protein-Ligand interactions: hydrodynamics and calorimetry ISBN : 9780199637461.

119. Duverger, E., Frison, N., Roche, A. C., and Monsigny, M. (2003) Carbohydrate-lectin interactions assessed by surface plasmon resonance, *Biochimie 85*, 167-179.

120. Beccati, D., Halkes, K. M., Batema, G. D., Guillena, G., Carvalho de Souza, A.,

van Koten, G., and Kamerling, J. P. (2005) SPR studies of carbohydrate-protein interactions: signal enhancement of low-molecular-mass analytes by organoplatinum(II)-labeling, *ChemBioChem 6*, 1196-1203.

121. Krotkiewska, B., Pasek, M., and Krotkiewski, H. (2002) Interaction of glycophorin A with lectins as measured by surface plasmon resonance (SPR), *Acta Biochimica Polonica 49*, 481-490.

122. Hutchinson, A. M. (1994) Characterization of glycoprotein oligosaccharides using surface-plasmon resonance, *Anal Biochem 220*, 303-307.

123. Bachhawat, K., Thomas, C. J., Amutha, B., Krishnasastry, M. V., Khan, M. I., and Surolia, A. (2001) On the stringent requirement of mannosyl substitution in mannooligosaccharides for the recognition by garlic (Allium sativum) lectin. A Surface Plasmon Resonance Study, *J Biol Chem 276*, 5541-5546.

124. Van Damme, E. J., Astoul, C. H., Barre, A., Rouge, P., and Peumans, W. J. (2000) Cloning and characterization of a monocot mannose-binding lectin from Crocus vernus (family Iridaceae), *Eur J Biochem 267*, 5067-5077.

125. Vornholt, W., Hartmann, M., and Keusgen, M. (2007) SPR studies of carbohydrate-lectin interactions as useful tool for screening on lectin sources, *Biosens Bioelectron 22*, 2983-2988.

126. van der Merwe, P. A., Crocker, P. R., Vinson, M., Barclay, A. N., Schauer, R., and Kelm, S. (1996) Localization of the putative sialic acid-binding site on the immunoglobulin superfamily cell-surface molecule CD22, *J Biol Chem 271*, 9273-9280.

127. van der Merwe, P. A., McNamee, P. N., Davies, E. A., Barclay, A. N., and Davis, S. J. (1995) Topology of the CD2-CD48 cell-adhesion molecule complex: implications for antigen recognition by T cells, *Curr Biol 5*, 74-84.

128. Dhayal, M., and Ratner, D. M. (2009) XPS and SPR analysis of glycoarray surface density, *Langmuir 25*, 2181-2187.

129. Campbell, C. T., and Kim, G. (2007) SPR microscopy and its applications to high-throughput analyses of biomolecular binding events and their kinetics, *Biomaterials 28*, 2380-2392.

130. Gu, C. P., Huang, J. R., Ni, N., Li, M. Q., and Liu, J. H. (2008) Detection of DNA hybridization based on SnO2 nanomaterial enhanced fluorescence, *J Phys Appl Phys 41*.

131. Li, H., Ying, L., Green, J. J., Balasubramanian, S., and Klenerman, D. (2003) Ultrasensitive coincidence fluorescence detection of single DNA molecules, *Anal Chem 75*, 1664-1670.

132. Eggertson, M. J., and Craig, D. B. (2000) Laser-induced fluorescence detector for liquid chromatography: applications to protein analysis, *Biomed Chromatogr 14*, 156-159.

133. Engvall, E., and Perlmann, P. (1971) Enzyme-linked immunosorbent assay (ELISA). Quantitative assay of immunoglobulin G, *Immunochemistry 8*, 871-874.

134. Walker, J. M., and Rapley, R. (2005) Medical Biomethods Handbook ISBN: 1588293343 419-427.

135. Gervay, J., and McReynolds, K. D. (1999) Utilization of ELISA technology to measure biological activities of carbohydrates relevant in disease status, *Curr Med Chem 6*, 129-153.

136. Alban, S., and Gastpar, R. (2001) Development of SPC-ELISA: a new assay principle for the study of sulfated polysaccharide-protein interactions, *J Biomol Screen 6*, 393-400.

137. Gull, I., Wirth, M., and Gabor, F. (2007) Development of a sensitive and reliable ELISA for quantification of wheat germ agglutinin, *J Immunol Methods 318*, 20-29.

138. Afrough, B., Dwek, M. V., and Greenwell, P. (2007) Identification and elimination of false-positives in an ELISA-based system for qualitative assessment of glycoconjugate binding using a selection of plant lectins, *Biotechniques 43*, 458, 460, 462 passim.

139. Mahmood, N., and Hay, A. J. (1992) An ELISA utilizing immobilised snowdrop lectin GNA for the detection of envelope glycoproteins of HIV and SIV, *J Immunol Methods 151*, 9-13.

140. Duk, M., Mitra, D., Lisowska, E., Kabat, E. A., Sharon, N., and Lis, H. (1992) Immunochemical studies on the combining site of the A + N blood type specific Moluccella laevis lectin, *Carbohydr Res 236*, 245-258.

141. Kratz, E., Poland, D. C., van Dijk, W., and Katnik-Prastowska, I. (2003) Alterations of branching and differential expression of sialic acid on alpha-1-acid glycoprotein in human seminal plasma, *Clin Chim Acta 331*, 87-95.

142. Duk, M., Lisowska, E., Wu, J. H., and Wu, A. M. (1994) The biotin/avidin-mediated microtiter plate lectin assay with the use of chemically modified glycoprotein ligand, *Anal Biochem 221*, 266-272.

143. Vincenzi, S., Zoccatelli, G., Perbellini, F., Rizzi, C., Chignola, R., Curioni, A., and Peruffo, A. D. (2002) Quantitative determination of dietary lectin activities by enzyme-linked immunosorbent assay using specific glycoproteins immobilized on microtiter plates, *J Agric Food Chem 50*, 6266-6270.

144. van der Schaal, I. A., Logman, T. J., Diaz, C. L., and Kijne, J. W. (1984) An enzyme-linked lectin binding assay for quantitative determination of lectin receptors, *Anal Biochem 140*, 48-55.

145. Martinod, S. R. (1985) Quantitative detection of lectin receptors on cell membranes using an enzyme linked lectin binding assay, *Prep Biochem 15*, 171-181.

146. Hendriks, H. G., Koninkx, J. F., Draaijer, M., van Dijk, J. E., Raaijmakers, J. A., and Mouwen, J. M. (1987) Quantitative determination of the lectin binding capacity of small intestinal brush-border membrane. An enzyme linked lectin sorbent assay (ELLSA), *Biochim Biophys Acta 905*, 371-375.

147. Drouin, J., Izaguirre, C. A., and Patenaude, P. (1988) Quantitation of cell membrane glycoproteins in pathological conditions using a lectin-bound enzyme-linked immunosorbent assay (ELISA). Application to human platelets in the Bernard-Soulier syndrome, *J Immunol Methods 110*, 217-223.

148. Maierhofer, C., Rohmer, K., and Wittmann, V. (2007) Probing multivalent carbohydrate-lectin interactions by an enzyme-linked lectin assay employing

covalently immobilized carbohydrates, *Bioorg Med Chem 15*, 7661-7676.

149. Kohn, M., Benito, J. M., Ortiz Mellet, C., Lindhorst, T. K., and Garcia Fernandez, J. M. (2004) Functional evaluation of carbohydrate-centred glycoclusters by enzyme-linked lectin assay: ligands for concanavalin A, *ChemBioChem 5*, 771-777.

150. Moldoveanu, Z., Wyatt, R. J., Lee, J. Y., Tomana, M., Julian, B. A., Mestecky, J., Huang, W. Q., Anreddy, S. R., Hall, S., Hastings, M. C., Lau, K. K., Cook, W. J., and Novak, J. (2007) Patients with IgA nephropathy have increased serum galactose-deficient IgA1 levels, *Kidney Int 71*, 1148-1154.

151. Pan, T., Li, R., Wong, B. S., Kang, S. C., Ironside, J., and Sy, M. S. (2005) Novel antibody-lectin enzyme-linked immunosorbent assay that distinguishes prion proteins in sporadic and variant cases of Creutzfeldt-Jakob disease, *J Clin Microbiol 43*, 1118-1126.

152. Flogel, M., Lauc, G., Gornik, I., and Macek, B. (1998) Fucosylation and galactosylation of IgG heavy chains differ between acute and remission phases of juvenile chronic arthritis, *Clin Chem Lab Med 36*, 99-102.

153. Wang, D., Liu, S., Trummer, B. J., Deng, C., and Wang, A. (2002) Carbohydrate microarrays for the recognition of cross-reactive molecular markers of microbes and host cells, *Nat Biotechnol 20*, 275-281.

154. Houseman, B. T., and Mrksich, M. (2002) Carbohydrate arrays for the evaluation of protein binding and enzymatic modification, *Chem Biol 9*, 443-454.

155. Fukui, S., Feizi, T., Galustian, C., Lawson, A. M., and Chai, W. (2002) Oligosaccharide microarrays for high-throughput detection and specificity assignments of carbohydrate-protein interactions, *Nat Biotechnol 20*, 1011-1017.

156. Drickamer, K., and Taylor, M. E. (2002) Glycan arrays for functional glycomics, *Genome Biol 3*, REVIEWS1034.

157. Seeberger, P. H., and Werz, D. B. (2007) Synthesis and medical applications of oligosaccharides, *Nature 446*, 1046-1051.

158. Feizi, T., Fazio, F., Chai, W., and Wong, C. H. (2003) Carbohydrate microarrays - a new set of technologies at the frontiers of glycomics, *Curr Opin Struct Biol 13*, 637-645.

159. de Paz, J. L., and Seeberger, P. H. (2006) Recent advances in carbohydrate microarrays, *QSAR Comb Sci 25*, 1027-1032.

160. Shin, I., Park, S., and Lee, M. R. (2005) Carbohydrate microarrays: an advanced technology for functional studies of glycans, *Chemistry 11*, 2894-2901.

161. Park, S., and Shin, I. (2007) Carbohydrate microarrays for assaying galactosyltransferase activity, *Org Lett 9*, 1675-1678.

162. Kawahashi, Y., Doi, N., Takashima, H., Tsuda, C., Oishi, Y., Oyama, R., Yonezawa, M., Miyamoto-Sato, E., and Yanagawa, H. (2003) In vitro protein microarrays for detecting protein-protein interactions: application of a new method for fluorescence labeling of proteins, *Proteomics 3*, 1236-1243.

163. Murthy, B. N., Voelcker, N. H., and Jayaraman, N. (2006) Evaluation of alpha-D-mannopyranoside glycolipid micelles-lectin interactions by surface plasmon resonance method, *Glycobiology 16*, 822-832.

164. Suda, Y., Arano, A., Fukui, Y., Koshida, S., Wakao, M., Nishimura, T., Kusumoto, S., and Sobel, M. (2006) Immobilization and clustering of structurally defined oligosaccharides for sugar chips: an improved method for surface plasmon resonance analysis of protein-carbohydrate interactions, *Bioconjug Chem 17*, 1125-1135.

165. Yonzon, C. R., Jeoung, E., Zou, S., Schatz, G. C., Mrksich, M., and Van Duyne, R. P. (2004) A comparative analysis of localized and propagating surface plasmon resonance sensors: the binding of concanavalin a to a monosaccharide functionalized self-assembled monolayer, *J Am Chem Soc 126*, 12669-12676.

166. Culf, A. S., Cuperlovic-Culf, M., and Ouellette, R. J. (2006) Carbohydrate microarrays: survey of fabrication techniques, *OMICS 10*, 289-310.

167. Karamanska, R., Clarke, J., Blixt, O., Macrae, J. I., Zhang, J. Q., Crocker, P.

R., Laurent, N., Wright, A., Flitsch, S. L., Russell, D. A., and Field, R. A. (2008) Surface plasmon resonance imaging for real-time, label-free analysis of protein interactions with carbohydrate microarrays, *Glycoconj J 25*, 69-74.

168. Smith, E. A., Thomas, W. D., Kiessling, L. L., and Corn, R. M. (2003) Surface plasmon resonance imaging studies of protein-carbohydrate interactions, *J Am Chem Soc 125*, 6140-6148.

169. Disney, M. D., and Seeberger, P. H. (2004) Carbohydrate arrays as tools for the glycomics revolution *DDT: TARGETS   3*, 151-158.

170. Mercey, E., Sadir, R., Maillart, E., Roget, A., Baleux, F., Lortat-Jacob, H., and Livache, T. (2008) Polypyrrole oligosaccharide array and surface plasmon resonance imaging for the measurement of glycosaminoglycan binding interactions, *Anal Chem 80*, 3476-3482.

171. Gondran, C., Dubois, M. P., Fort, S., Cosnier, S., and Szunerits, S. (2008) Detection of carbohydrate-binding proteins by oligosaccharide-modified polypyrrole interfaces using electrochemical surface plasmon resonance, *Analyst 133*, 206-212.

172. Dubois, M. P., Gondran, C., Renaudet, O., Dumy, P., Driguez, H., Fort, S., and Cosnier, S. (2005) Electrochemical detection of Arachis hypogaea (peanut) agglutinin binding to monovalent and clustered lactosyl motifs immobilized on a polypyrrole film, *Chem Commun (Camb)*, 4318-4320.

173. Morelle, W., Faid, V., and Michalski, J. C. (2004) Structural analysis of permethylated oligosaccharides using electrospray ionization quadrupole time-of-flight tandem mass spectrometry and deutero-reduction, *Rapid Commun Mass Spectrom 18*, 2451-2464.

174. Morelle, W., and Michalski, J. C. (2004) Sequencing of oligosaccharides derivatized with benzylamine using electrospray ionization-quadrupole time of flight-tandem mass spectrometry, *Electrophoresis 25*, 2144-2155.

175. Morelle, W., Donadio, S., Ronin, C., and Michalski, J. C. (2006) Characterization of N-glycans of recombinant human thyrotropin using mass spectrometry, *Rapid Commun Mass Spectrom 20*, 331-345.

176. Morelle, W., and Michalski, J. C. (2005) The mass spectrometric analysis of glycoproteins and their glycan structures, *Curr Anal Chem 1*, 29-57.

177. Bryan, M. C., Fazio, F., Lee, H. K., Huang, C. Y., Chang, A., Best, M. D., Calarese, D. A., Blixt, O., Paulson, J. C., Burton, D., Wilson, I. A., and Wong, C. H. (2004) Covalent display of oligosaccharide arrays in microtiter plates, *J Am Chem Soc 126*, 8640-8641.

178. Gurard-Levin, Z. A., and Mrksich, M. (2008) Combining Self-Assembled Monolayers and Mass Spectrometry for Applications in Biochips, *Annu Rev Anal Chem 1*, 767-800.

179. Song, E. H., and Pohl, N. L. (2009) Carbohydrate arrays: recent developments in fabrication and detection methods with applications, *Curr Opin Chem Biol 13*, 626-632.

180. Wang, D. (2003) Carbohydrate microarrays, *Proteomics 3*, 2167-2175.

181. Hirabayashi, J. (2003) Oligosaccharide microarrays for glycomics, *Trends Biotechnol 21*, 141-143; discussion 143.

182. Fazio, F., Bryan, M. C., Blixt, O., Paulson, J. C., and Wong, C. H. (2002) Synthesis of sugar arrays in microtiter plate, *J Am Chem Soc 124*, 14397-14402.

183. Zhi, Z.-L., Laurent, N., Powell, A. K., Karamanska, R., Fais, M., Voglmeir, J., Wright, A., Blackburn, J. M., Crocker, P. R., Russell, D. A., Flitsch, S., Field, R. A., and Turnbull, J. E. (2008) A Versatile Gold Surface Approach for Fabrication and Interrogation of Glycoarrays, *ChemBioChem 9*, 1568 - 1575.

184. Adams, E. W., Ueberfeld, J., Ratner, D. M., O'Keefe, B. R., Walt, D. R., and Seeberger, P. H. (2003) Encoded fiber-optic microsphere arrays for probing protein-carbohydrate interactions, *Angew Chem Int Ed Engl 42*, 5317-5320.

185. Park, S., Lee, M. R., and Shin, I. (2009) Construction of carbohydrate microarrays by using one-step, direct immobilizations of diverse unmodified glycans on solid surfaces, *Bioconjug Chem 20*, 155-162.

186. Larsen, K., Thygesen, M. B., Guillaumie, F., Willats, W. G., and Jensen, K. J. (2006) Solid-phase chemical tools for glycobiology, *Carbohydr Res 341*,

1209-1234.

187.   Seo, J. H., Adachi, K., Lee, B. K., Kang, D. G., Kim, Y. K., Kim, K. R., Lee, H. Y., Kawai, T., and Cha, H. J. (2007) Facile and rapid direct gold surface immobilization with controlled orientation for carbohydrates, *Bioconjug Chem 18*, 2197-2201.

188.   Miura, Y., Sasao, Y., Dohi, H., Nishida, Y., and Kobayashi, K. (2002) Self-assembled monolayers of globotriaosylceramide (Gb3) mimics: surface-specific affinity with shiga toxins, *Anal Biochem 310*, 27-35.

189.   Angeloni, S., Ridet, J. L., Kusy, N., Gao, H., Crevoisier, F., Guinchard, S., Kochhar, S., Sigrist, H., and Sprenger, N. (2005) Glycoprofiling with micro-arrays of glycoconjugates and lectins, *Glycobiology 15*, 31-41.

190.   Chevolot, Y., Martins, J., Milosevic, N., Leonard, D., Zeng, S., Malissard, M., Berger, E. G., Maier, P., Mathieu, H. J., Crout, D. H., and Sigrist, H. (2001) Immobilisation on polystyrene of diazirine derivatives of mono- and disaccharides: biological activities of modified surfaces, *Bioorg Med Chem 9*, 2943-2953.

191.   Chevolot, Y., Bucher, O., Leonard, D., Mathieu, H. J., and Sigrist, H. (1999) Synthesis and characterization of a photoactivatable glycoaryldiazirine for surface glycoengineering, *Bioconjug Chem 10*, 169-175.

192.   Leonard, D., Chevolot, Y., Heger, F., Martins, J., Crout, D. H. G., Sigrist, H., and Mathieu, H. J. (2001) ToF-SIMS and XPS study of photoactivatable reagents designed for surface glycoengineering part III. 5-carboxamidopentyl-N-[m-[3-(trifluoromethyl)diazirin-3-yl]phenyl-beta-D -galactopyranosyl]-(1-> 4)-1-thio-beta-D-glucopyranoside (lactose aryl diazirine) on diamond, *Surf Interface Anal 31*, 457-464.

193.   Leonard, D., Chevolot, Y., Bucher, O., Sigrist, H., and Mathieu, H. J. (1998) ToF-SIMS and XPS study of photoactivatable reagents designed for surface glycoengineering - Part I. N-(m-(3-(trifluoromethyl)diazirine-3-yl)phenyl)-4-maleimido-butyramide (MAD) on silicon, silicon nitride and diamond, *Surf Interface Anal 26*,

783-792.

194. Blixt, O., Head, S., Mondala, T., Scanlan, C., Huflejt, M. E., Alvarez, R., Bryan, M. C., Fazio, F., Calarese, D., Stevens, J., Razi, N., Stevens, D. J., Skehel, J. J., van Die, I., Burton, D. R., Wilson, I. A., Cummings, R., Bovin, N., Wong, C. H., and Paulson, J. C. (2004) Printed covalent glycan array for ligand profiling of diverse glycan binding proteins, *Proc Natl Acad Sci U S A 101*, 17033-17038.

195. Biskup, M. B., Muller, J. U., Weingart, R., and Schmidt, R. R. (2005) New methods for the generation of carbohydrate arrays on glass slides and their evaluation, *ChemBioChem 6*, 1007-1015.

196. Lee, M. R., and Shin, I. (2005) Fabrication of chemical microarrays by efficient immobilization of hydrazide-linked substances on epoxide-coated glass surfaces, *Angew Chem Int Ed Engl 44*, 2881-2884.

197. Schwarz, M., Spector, L., Gargir, A., Shtevi, A., Gortler, M., Altstock, R. T., Dukler, A. A., and Dotan, N. (2003) A new kind of carbohydrate array, its use for profiling antiglycan antibodies, and the discovery of a novel human cellulose-binding antibody, *Glycobiology 13*, 749-754.

198. Brun, M. A., Disney, M. D., and Seeberger, P. H. (2006) Miniaturization of microwave-assisted carbohydrate functionalization to create oligosaccharide microarrays, *ChemBioChem 7*, 421-424.

199. Park, S., Lee, M. R., Pyo, S. J., and Shin, I. (2004) Carbohydrate chips for studying high-throughput carbohydrate-protein interactions, *J Am Chem Soc 126*, 4812-4819.

200. Houseman, B. T., Gawalt, E. S., and Mrksich, M. (2003) Maleimide-functionalized self-assembled monolayers for the preparation of peptide and carbohydrate biochips, *Langmuir 19*, 1522-1531.

201. Shin, I. (2007) In: Bewley, C.A. (Ed.), Protein-Carbohydrate Interactions in Infectious Diseases. , *RCS, Cambridge*, pp. 221–247.

202. Bryan, M. C., Lee, L. V., and Wong, C. H. (2004) High-throughput identification of fucosyltransferase inhibitors using carbohydrate microarrays,

Bioorg Med Chem Lett 14, 3185-3188.

203. Kohn, M., Wacker, R., Peters, C., Schroder, H., Soulere, L., Breinbauer, R., Niemeyer, C. M., and Waldmann, H. (2003) Staudinger ligation: a new immobilization strategy for the preparation of small-molecule arrays, *Angew Chem Int Ed Engl 42*, 5830-5834.

204. Bochner, B. S., Alvarez, R. A., Mehta, P., Bovin, N. V., Blixt, O., White, J. R., and Schnaar, R. L. (2005) Glycan array screening reveals a candidate ligand for Siglec-8, *J Biol Chem 280*, 4307-4312.

205. Linman, M. J., Taylor, J. D., Yu, H., Chen, X., and Cheng, Q. (2008) Surface plasmon resonance study of protein-carbohydrate interactions using biotinylated sialosides, *Anal Chem 80*, 4007-4013.

206. Chevolot, Y., Bouillon, C., Vidal, S., Morvan, F., Meyer, A., Cloarec, J. P., Jochum, A., Praly, J. P., Vasseur, J. J., and Souteyrand, E. (2007) DNA-based carbohydrate biochips: a platform for surface glyco-engineering, *Angew Chem Int Ed Engl 46*, 2398-2402.

207. Schallus, T., Jaeckh, C., Feher, K., Palma, A. S., Liu, Y., Simpson, J. C., Mackeen, M., Stier, G., Gibson, T. J., Feizi, T., Pieler, T., and Muhle-Goll, C. (2008) Malectin: a novel carbohydrate-binding protein of the endoplasmic reticulum and a candidate player in the early steps of protein N-glycosylation, *Mol Biol Cell 19*, 3404-3414.

208. Disney, M. D., and Seeberger, P. H. (2004) The use of carbohydrate microarrays to study carbohydrate-cell interactions and to detect pathogens, *Chem Biol 11*, 1701-1707.

209. Nimrichter, L., Gargir, A., Gortler, M., Altstock, R. T., Shtevi, A., Weisshaus, O., Fire, E., Dotan, N., and Schnaar, R. L. (2004) Intact cell adhesion to glycan microarrays, *Glycobiology 14*, 197-203.

210. Parthasarathy, N., Saksena, R., Kovac, P., Deshazer, D., Peacock, S. J., Wuthiekanun, V., Heine, H. S., Friedlander, A. M., Cote, C. K., Welkos, S. L., Adamovicz, J. J., Bavari, S., and Waag, D. M. (2008) Application of carbohydrate microarray technology for the detection of Burkholderia

pseudomallei, Bacillus anthracis and Francisella tularensis antibodies, *Carbohydr Res*.

211. Oyelaran, O., and Gildersleeve, J. C. (2009) Glycan arrays: recent advances and future challenges, *Curr Opin Chem Biol 13*, 406-413.

212. Barkley, A., and Arya, P. (2001) Combinatorial chemistry toward understanding the function(s) of carbohydrates and carbohydrate conjugates, *Chemistry 7*, 555-563.

213. Simanek, E. E., McGarvey, G. J., Jablonowski, J. A., and Wong, C. H. (1998) Selectinminus signCarbohydrate Interactions: From Natural Ligands to Designed Mimics, *Chem Rev 98*, 833-862.

214. Bouillon, C., Meyer, A., Vidal, S., Jochum, A., Chevolot, Y., Cloarec, J. P., Praly, J. P., Vasseur, J. J., and Morvan, F. (2006) Microwave assisted "click" chemistry for the synthesis of multiple labeled-carbohydrate oligonucleotides on solid support, *J Org Chem 71*, 4700-4702.

215. Aguilar-Moncayo, M., Mellet, C. O., Garcia Fernandez, J. M., and Garcia-Moreno, M. I. (2009) Synthesis of thiohydantoin-castanospermine glycomimetics as glycosidase inhibitors, *J Org Chem 74*, 3595-3598.

216. Uhrig, M. L., Szilagyi, L., Kover, K. E., and Varela, O. (2007) Synthesis of non-glycosidic 4,6'-thioether-linked disaccharides as hydrolytically stable glycomimetics, *Carbohydr Res 342*, 1841-1849.

217. Patel, A., and Lindhorst, T. K. (2006) Multivalent glycomimetics: synthesis of nonavalent mannoside clusters with variation of spacer properties, *Carbohydr Res 341*, 1657-1668.

218. Andriuzzi, O., Gravier-Pelletier, C., Bertho, G., Prange, T., and Le Merrer, Y. (2005) Synthesis and glycosidase inhibitory activity of new hexa-substituted C8-glycomimetics, *Beilstein J Org Chem 1*, 12.

219. Garcia-Moreno, M. I., Diaz-Perez, P., Ortiz Mellet, C., and Garcia Fernandez, J. M. (2003) Synthesis and evaluation of isourea-type glycomimetics related to the indolizidine and trehazolin glycosidase inhibitor families, *J Org Chem 68*, 8890-8901.

220. Angyalosi, G., Grandjean, C., Lamirand, M., Auriault, C., Gras-Masse, H., and Melnyk, O. (2002) Synthesis and mannose receptor-mediated uptake of clustered glycomimetics by human dendritic cells: effect of charge, *Bioorg Med Chem Lett 12*, 2723-2727.

221. Bernardi, A., Arosio, D., Manzoni, L., Micheli, F., Pasquarello, A., and Seneci, P. (2001) Stereoselective synthesis of conformationally constrained cyclohexanediols: a set of molecular scaffolds for the synthesis of glycomimetics, *J Org Chem 66*, 6209-6216.

222. Witczak, Z. J., Lorchak, D., and Nguyen, N. (2007) A click chemistry approach to glycomimetics: Michael addition of 2,3,4,6-tetra-O-acetyl-1-thio-beta-D-glucopyranose to 4-deoxy-1,2-O-isopropylidene-L-glycero-pent-4-enopyranos-3-ulose--a convenient route to novel 4-deoxy-(1-->5)-5-C-thiodisaccharides, *Carbohydr Res 342*, 1929-1933.

223. Vidal, P., Vauzeilles, B., Bleriot, Y., Sollogoub, M., Sinay, P., Jimenez-Barbero, J., and Espinosa, J. F. (2007) Conformational behaviour of glycomimetics: NMR and molecular modelling studies of the C-glycoside analogue of the disaccharide methyl beta-D-galactopyranosyl-(1-->3)-beta-D-glucopyranoside, *Carbohydr Res 342*, 1910-1917.

224. Paquette, L. A., and Zhang, Y. (2006) From common carbohydrates to enantiopure cyclooctane polyols and glycomimetics via deoxygenative zirconocene ring contraction, *J Org Chem 71*, 4353-4363.

225. Ogata, M., Hidari, K. I., Murata, T., Shimada, S., Kozaki, W., Park, E. Y., Suzuki, T., and Usui, T. (2009) Chemoenzymatic Synthesis of Sialoglycopolypeptides As Glycomimetics to Block Infection by Avian and Human Influenza Viruses, *Bioconjug Chem*.

226. Nishimura, Y. (2009) Gem-diamine 1-N-iminosugars as versatile glycomimetics: synthesis, biological activity and therapeutic potential, *J Antibiot (Tokyo) 62*, 407-423.

227. Magnani, J. L., and Ernst, B. (2009) Glycomimetic drugs - A new source of

therapeutic opportunities, *Discov Med 8*, 247-252.

228. Ernst, B., and Magnani, J. L. (2009) From carbohydrate leads to glycomimetic drugs, *Nat Rev Drug Discov 8*, 661-677.

229. Barchi, J. J., Jr. (2000) Emerging roles of carbohydrates and glycomimetics in anticancer drug design, *Curr Pharm Des 6*, 485-501.

230. Welch, K. T., Turner, T. A., and Preast, C. E. (2008) Rational design of novel glycomimetics: inhibitors of concanavalin A, *Bioorg Med Chem Lett 18*, 6573-6575.

231. Bernardi, A., Arosio, D., Potenza, D., Sanchez-Medina, I., Mari, S., Canada, F. J., and Jimenez-Barbero, J. (2004) Intramolecular carbohydrate-aromatic interactions and intermolecular van der Waals interactions enhance the molecular recognition ability of GM1 glycomimetics for cholera toxin, *Chemistry 10*, 4395.

232. Garcia-Herrero, A., Montero, E., Munoz, J. L., Espinosa, J. F., Vian, A., Garcia, J. L., Asensio, J. L., Canada, F. J., and Jimenez-Barbero, J. (2002) Conformational selection of glycomimetics at enzyme catalytic sites: experimental demonstration of the binding of distinct high-energy distorted conformations of C-, S-, and O-glycosides by E. Coli beta-galactosidases, *J Am Chem Soc 124*, 4804-4810.

233. Grandjean, C., Angyalosi, G., Loing, E., Adriaenssens, E., Melnyk, O., Pancre, V., Auriault, C., and Gras-Masse, H. (2001) Novel hyperbranched glycomimetics recognized by the human mannose receptor: quinic or shikimic acid derivatives as mannose bioisosteres, *ChemBioChem 2*, 747-757.

234. Diaz Perez, V. M., Garcia Moreno, M. I., Ortiz Mellet, C., Fuentes, J., Diaz Arribas, J. C., Canada, F. J., and Garcia Fernandez, J. M. (2000) Generalized anomeric effect in action: synthesis and evaluation of stable reducing indolizidine glycomimetics as glycosidase inhibitors, *J Org Chem 65*, 136-143.

235. Kim, M. K., Brandley, B. K., Anderson, M. B., and Bochner, B. S. (1998) Antagonism of selectin-dependent adhesion of human eosinophils and

neutrophils by glycomimetics and oligosaccharide compounds, *Am J Respir Cell Mol Biol 19*, 836-841.

236. Nuti, F., Paolini, I., Cardona, F., Chelli, M., Lolli, F., Brandi, A., Goti, A., Rovero, P., and Papini, A. M. (2007) Fmoc-protected iminosugar modified asparagine derivatives as building blocks for glycomimetics-containing peptides, *Bioorg Med Chem 15*, 3965-3973.

237. Murphy, P. V. (2007) Peptidomimetics, glycomimetics and scaffolds from carbohydrate building blocks, *Eur J Org Chem*, 4177-4187.

238. D'Onofrio, J., de Champdore, M., De Napoli, L., Montesarchio, D., and Di Fabio, G. (2005) Glycomimetics as decorating motifs for oligonucleotides: solid-phase synthesis, stability, and hybridization properties of carbopeptoid-oligonucleotide conjugates, *Bioconjug Chem 16*, 1299-1309.

239. Arya, P., Kutterer, K. M., and Barkley, A. (2000) Glycomimetics: a programmed approach toward neoglycopeptide libraries, *J Comb Chem 2*, 120-126.

240. Lee, Y. C., and Lee, R. T. (1995) Carbohydrate-Protein Interactions: Basis of Glycobiology, *Acc Chem Res 28*, 321-327.

241. Wacker, R., Schroder, H., and Niemeyer, C. M. (2004) Performance of antibody microarrays fabricated by either DNA-directed immobilization, direct spotting, or streptavidin-biotin attachment: a comparative study, *Anal Biochem 330*, 281-287.

242. Niemeyer, C. M. Semisynthetic DNA-protein conjugates for biosensing and nanofabrication, *Angew Chem Int Ed Engl 49*, 1200-1216.

243. Niemeyer, C. M. (2001) Bioorganic applications of semisynthetic DNA-protein conjugates, *Chemistry 7*, 3188-3195.

244. Niemeyer, C. M. (2002) The developments of semisynthetic DNA-protein conjugates, *Trends Biotechnol 20*, 395-401.

245. Schroeder, H., Ellinger, B., Becker, C. F. W., Waldmann, H., and Niemeyer, C. M. (2007) Generation of live-cell microarrays by means of DNA-directed immobilization of specific cell-surface ligands, *Angew Chem Int Ed Engl 46*,

4180-4183.

246.   Chevolot, Y., Bouillon, C., Vidal, S., Morvan, F., Meyer, A., Cloarec, J.-P.,
        Jochum, A., Praly, J.-P., Vasseur, J.-J., and Souteyrand, E. (2007) DNA-Based
        Carbohydrate Biochips: A Platform for Surface Glyco-Engineering., *Angew
        Chem Int Ed Engl. 46*, 2398 -2402.

247.   Mazurczyk, R., El Khoury, G., Dugas, V., Hannes, B., Laurenceau, E., Cabrera,
        M., Krawczyk, S., Souteyrand, E., Cloarec, J. P., and Chevolot, Y. (2008)
        Low-cost, fast prototyping method of fabrication of the microreactor devices
        in soda-lime glass, *Sens Actuators B-Chem 128*, 552-559.

248.   Berlier, J. E., Rothe, A., Buller, G., Bradford, J., Gray, D. R., Filanoski, B. J.,
        Telford, W. G., Yue, S., Liu, J., Cheung, C. Y., Chang, W., Hirsch, J. D.,
        Beechem, J. M., and Haugland, R. P. (2003) Quantitative comparison of
        long-wavelength Alexa Fluor dyes to Cy dyes: fluorescence of the dyes and
        their bioconjugates, *J Histochem Cytochem 51*, 1699-1712.

249.   Iqbal, A., Arslan, S., Okumus, B., Wilson, T. J., Giraud, G., Norman, D. G., Ha,
        T., and Lilley, D. M. (2008) Orientation dependence in fluorescent energy
        transfer between Cy3 and Cy5 terminally attached to double-stranded nucleic
        acids, *Proc Natl Acad Sci U S A 105*, 11176-11181.

250.   Ishii, Y., Yoshida, T., Funatsu, T., Wazawa, T., and Yanagida, T. (1999)
        Fluorescence resonance energy transfer between single fluorophores attached
        to a coiled-coil protein in aqueous solution, *Chem Phys 247*, 163-173.

251.   Dugas, V., Depret, G., Chevalier, B., Nesme, X., and Souteyrand, E. (2004)
        Immobilization of single-stranded DNA fragments to solid surfaces and their
        repeatable specific hybridization: covalent binding or adsorption?, *Sens
        Actuator B-Chem 101*, 112-121.

252.   Lallemand, D., Rouillat, M. H., Dugas, V., Chevolot, Y., Souteyrand, E., and
        Phaner-Goutorbe, M. (2007) AFM characterization of ss-DNA probes
        immobilization: a sequence effect on surface organization, *JPCS 61*, 658-662.

253.   Herne, T. M., and Tarlov, M. J. (1997) Characterization of DNA probes
        immobilized on gold surfaces, *J Am Chem Soc 119*, 8916-8920.

254. Niemeyer, C. M., Boldt, L., Ceyhan, B., and Blohm, D. (1999) DNA-Directed immobilization: efficient, reversible, and site-selective surface binding of proteins by means of covalent DNA-streptavidin conjugates, *Anal Biochem 268*, 54-63.

255. Firon, N., Ashkenazi, S., Mirelman, D., Ofek, I., and Sharon, N. (1987) Aromatic alpha-glycosides of mannose are powerful inhibitors of the adherence of type 1 fimbriated Escherichia coli to yeast and intestinal epithelial cells, *Infect Immun 55*, 472-476.

256. Imberty, A., Chabre, Y. M., and Roy, R. (2008) Glycomimetics and glycodendrimers as high affinity microbial anti-adhesins, *Chemistry 14*, 7490-7499.

257. Lundquist, J. J., and Toone, E. J. (2002) The cluster glycoside effect, *Chem Rev 102*, 555-578.

258. Mammen, M., Choi, S. K., and Whitesides, G. M. (1998) Polyvalent interactions in biological systems: Implications for design and use of multivalent ligands and inhibitors, *Angew Chem Int Ed Engl. 37*, 2755-2794.

259. Andre, S., Sansone, F., Kaltner, H., Casnati, A., Kopitz, J., Gabius, H. J., and Ungaro, R. (2008) Calix[n]arene-based glycoclusters: bioactivity of thiourea-linked galactose/lactose moieties as inhibitors of binding of medically relevant lectins to a glycoprotein and cell-surface glycoconjugates and selectivity among human adhesion/growth-regulatory galectins, *ChemBioChem 9*, 1649-1661.

260. Imberty, A., wimmerova, M., Mitchell, E. P., and Gilboa-Garber, N. (2004) Structures of the lectins from Pseudomonas aeruginosa: insight into the molecular basis for host glycan recognition, *Microbes Infect 6*, 221-228.

261. Zhi, Z. L., Laurent, N., Powell, A. K., Karamanska, R., Fais, M., Voglmeir, J., Wright, A., Blackburn, J. M., Crocker, P. R., Russell, D. A., Flitsch, S., Field, R. A., and Turnbull, J. E. (2008) A versatile gold surface approach for fabrication and interrogation of glycoarrays, *ChemBioChem 9*, 1568-1575.

262. Branderhorst, H. M., Ruijtenbeek, R., Liskamp, R. M., and Pieters, R. J. (2008)

Multivalent carbohydrate recognition on a glycodendrimer-functionalized flow-through chip, *ChemBioChem 9*, 1836-1844.

263. Cecioni, S., Lalor, R., Blanchard, B., Praly, J. P., Imberty, A., Matthews, S. E., and Vidal, S. (2009) Achieving High Affinity towards a Bacterial Lectin through Multivalent Topological Isomers of Calix[4]arene Glycoconjugates, *Chem-Eur J 15*, 13232-13240.

264. Kuno, A., Uchiyama, N., Koseki-Kuno, S., Ebe, Y., Takashima, S., Yamada, M., and Hirabayashi, J. (2005) Evanescent-field fluorescence-assisted lectin microarray: a new strategy for glycan profiling, *Nat Methods 2*, 851-856.

265. Biessen, E. A., Beuting, D. M., Roelen, H. C., van de Marel, G. A., van Boom, J. H., and van Berkel, T. J. (1995) Synthesis of cluster galactosides with high affinity for the hepatic asialoglycoprotein receptor, *J Med Chem 38*, 1538-1546.

266. Lee, Y. C., Townsend, R. R., Hardy, M. R., Lonngren, J., Arnarp, J., Haraldsson, M., and Lonn, H. (1983) Binding of synthetic oligosaccharides to the hepatic Gal/GalNAc lectin. Dependence on fine structural features, *J Biol Chem 258*, 199-202.

267. Balboni, I., Limb, C., Tenenbaum, J. D., and Utz, P. J. (2008) Evaluation of microarray surfaces and arraying parameters for autoantibody profiling, *Proteomics 8*, 3443-3449.

268. Gordus, A., and MacBeath, G. (2006) Circumventing the problems caused by protein diversity in microarrays: implications for protein interaction networks, *J Am Chem Soc 128*, 13668-13669.

269. Vieillard, J., Mazurczyk, R., Morin, C., Hannes, B., Chevolot, Y., Desbene, P. L., and Krawczyk, S. (2007) Application of microfluidic chip with integrated optics for electrophoretic separations of proteins, *J Chromatogr B Analyt Technol Biomed Life Sci 845*, 218-225.

270. Collins, B. E., and Paulson, J. C. (2004) Cell surface biology mediated by low affinity multivalent protein-glycan interactions, *Curr Opin Chem Biol 8*, 617-625.

271. Wolfenden, M. L., and Cloninger, M. J. (2005) Mannose/glucose-functionalized dendrimers to investigate the predictable tunability of multivalent interactions, *J Am Chem Soc 127*, 12168-12169.

272. Gestwicki, J. E., Cairo, C. W., Strong, L. E., Oetjen, K. A., and Kiessling, L. L. (2002) Influencing receptor-ligand binding mechanisms with multivalent ligand architecture, *J Am Chem Soc 124*, 14922-14933.

273. Horan, N., Yan, L., Isobe, H., Whitesides, G. M., and Kahne, D. (1999) Nonstatistical binding of a protein to clustered carbohydrates, *Proc Natl Acad Sci U S A 96*, 11782-11786.

274. Ng, A. K., Wang, J. H., and Shaw, P. C. (2009) Structure and sequence analysis of influenza A virus nucleoprotein, *Sci China C Life Sci 52*, 439-449.

275. Zambon, M. C. (1999) Epidemiology and pathogenesis of influenza, *J Antimicrob Chemother 44 Suppl B*, 3-9.

276. Lederberg, J. (2001) H1N1-influenza as Lazarus: genomic resurrection from the tomb of an unknown, *Proc Natl Acad Sci U S A 98*, 2115-2116.

277. Subbarao, K., and Joseph, T. (2007) Scientific barriers to developing vaccines against avian influenza viruses, *Nat Rev Immunol 7*, 267-278.

278. Stevens, J., Blixt, O., Paulson, J. C., and Wilson, I. A. (2006) Glycan microarray technologies: tools to survey host specificity of influenza viruses, *Nat Rev Microbiol 4*, 857-864.

279. Islam, T., and von Itzstein, M. (2007) Anti-influenza drug discovery: are we ready for the next pandemic?, *Adv Carbohydr Chem Biochem 61*, 293-352.

280. Amorij, J. P., Huckriede, A., Wilschut, J., Frijlink, H. W., and Hinrichs, W. L. (2008) Development of stable influenza vaccine powder formulations: challenges and possibilities, *Pharm Res 25*, 1256-1273.

281. Colman, P. M. (1994) Influenza virus neuraminidase: structure, antibodies, and inhibitors, *Protein Sci 3*, 1687-1696.

282. Plotkin, J. B., Dushoff, J., and Levin, S. A. (2002) Hemagglutinin sequence clusters and the antigenic evolution of influenza A virus, *Proc Natl Acad Sci U S A 99*, 6263-6268.

283. Claas, E. C., Osterhaus, A. D., van Beek, R., De Jong, J. C., Rimmelzwaan, G. F., Senne, D. A., Krauss, S., Shortridge, K. F., and Webster, R. G. (1998) Human influenza A H5N1 virus related to a highly pathogenic avian influenza virus, *Lancet 351*, 472-477.

284. Smith, A. E., and Helenius, A. (2004) How viruses enter animal cells, *Science 304*, 237-242.

285. Wagner, R., Matrosovich, M., and Klenk, H. D. (2002) Functional balance between haemagglutinin and neuraminidase in influenza virus infections, *Rev Med Virol 12*, 159-166.

286. Steinhauer, D. A. (1999) Role of hemagglutinin cleavage for the pathogenicity of influenza virus, *Virology 258*, 1-20.

287. Cros, J. F., and Palese, P. (2003) Trafficking of viral genomic RNA into and out of the nucleus: influenza, Thogoto and Borna disease viruses, *Virus Res95*, 3-12.

288. Kash, J. C., Goodman, A. G., Korth, M. J., and Katze, M. G. (2006) Hijacking of the host-cell response and translational control during influenza virus infection, *Virus Res 119*, 111-120.

289. Skehel, J. J., and Wiley, D. C. (2000) Receptor binding and membrane fusion in virus entry: the influenza hemagglutinin, *Annu Rev Biochem 69*, 531-569.

290. Glick, G. D., Toogood, P. L., Wiley, D. C., Skehel, J. J., and Knowles, J. R. (1991) Ligand recognition by influenza virus. The binding of bivalent sialosides, *J Biol Chem 266*, 23660-23669.

291. Couceiro, J. N., Paulson, J. C., and Baum, L. G. (1993) Influenza virus strains selectively recognize sialyloligosaccharides on human respiratory epithelium; the role of the host cell in selection of hemagglutinin receptor specificity, *Virus Res 29*, 155-165.

292. Borrego-Diaz, E., Peeples, M. E., Markosyan, R. M., Melikyan, G. B., and Cohen, F. S. (2003) Completion of trimeric hairpin formation of influenza virus hemagglutinin promotes fusion pore opening and enlargement, *Virology 316*, 234-244.

293. Carbain, B., Martin, S. R., Collins, P. J., Hitchcock, P. B., and Streicher, H. (2009) Galactose-conjugates of the oseltamivir pharmacophore--new tools for the characterization of influenza virus neuraminidases, *Org Biomol Chem 7*, 2570-2575.

294. Kuchipudi, S. V., Nelli, R., White, G. A., Bain, M., Chang, K. C., and Dunham, S. (2009) Differences in influenza virus receptors in chickens and ducks: Implications for interspecies transmission, *J Mol Genet Med 3*, 143-151.

295. Glaser, L., Stevens, J., Zamarin, D., Wilson, I. A., Garcia-Sastre, A., Tumpey, T. M., Basler, C. F., Taubenberger, J. K., and Palese, P. (2005) A single amino acid substitution in 1918 influenza virus hemagglutinin changes receptor binding specificity, *J Virol 79*, 11533-11536.

296. De Clercq, E. (2006) Antiviral agents active against influenza A viruses, *Nat Rev Drug Discov 5*, 1015-1025.

297. Sigal, G. B., Mammen, M., Dahmann, G., and Whitesides, G. M. (1996) Polyacrylamides bearing pendant alpha-sialoside groups strongly inhibit agglutination of erythrocytes by influenza virus: The strong inhibition reflects enhanced binding through cooperative polyvalent interactions, *J Am Chem Soc 118*, 3789-3800.

298. Fazekasdest, G., and Gottschalk, A. (1963) Studies on Glycoproteins. X. Equilibrium Measurements on Influenza Virus-Glycoprotein Systems, *Biochim Biophys Acta 78*, 248-257.

299. Stevens, J., Blixt, O., Glaser, L., Taubenberger, J. K., Palese, P., Paulson, J. C., and Wilson, I. A. (2006) Glycan microarray analysis of the hemagglutinins from modern and pandemic influenza viruses reveals different receptor specificities, *J Mol Biol 355*, 1143-1155.

300. Rogers, G. N., and D'Souza, B. L. (1989) Receptor binding properties of human and animal H1 influenza virus isolates, *Virology 173*, 317-322.

ANNEXE 1

Glycoconjugate 1 （G1）

Glycoconjugate 2 （G2）

Glycoconjugate 3（G3）

Glycoconjugate 4（G4）
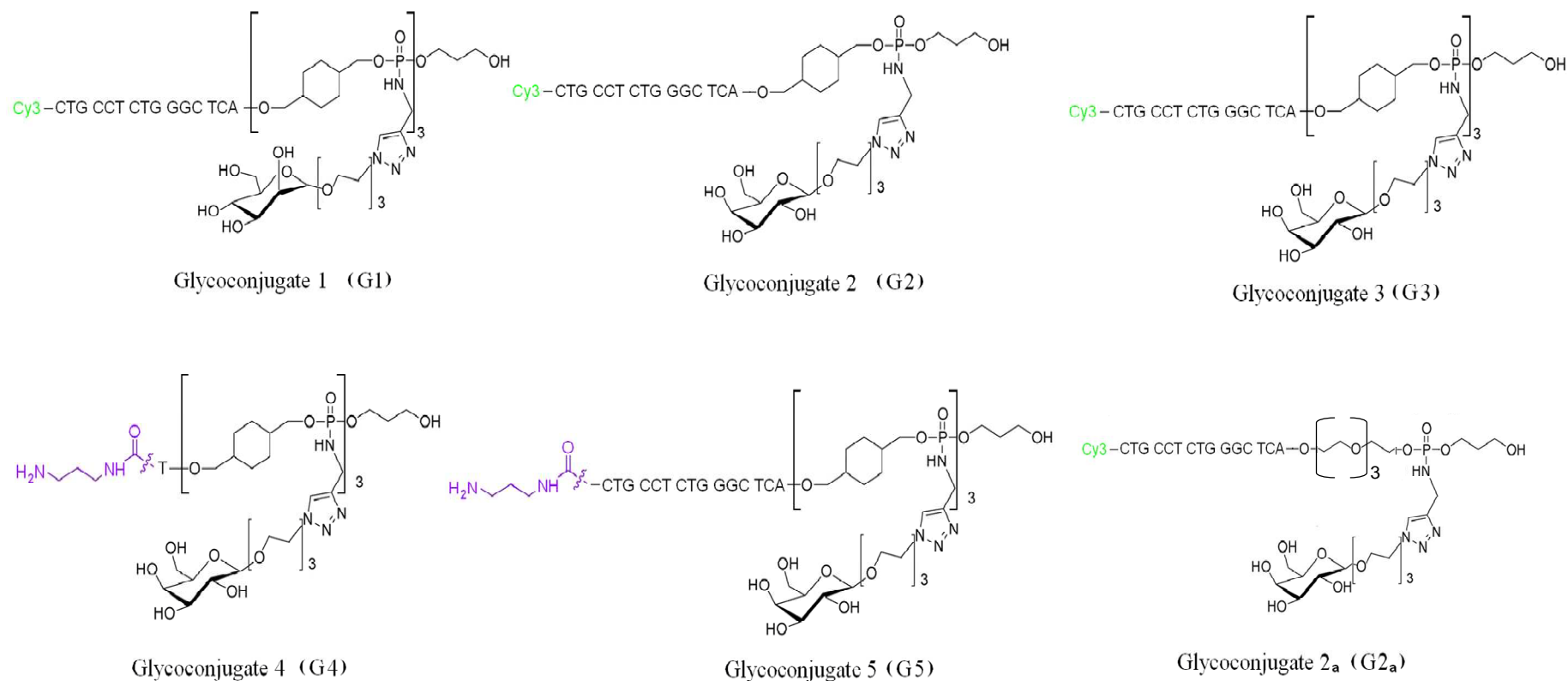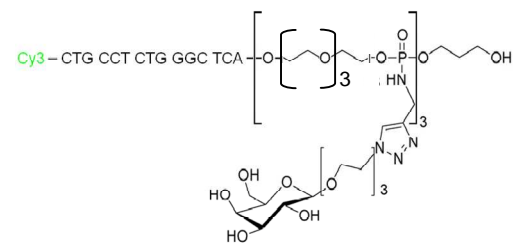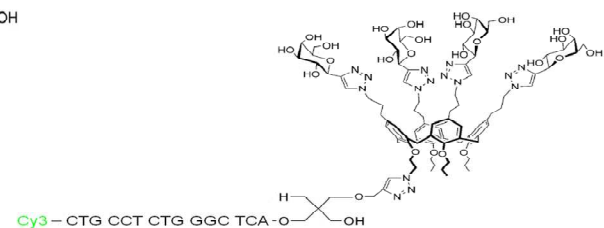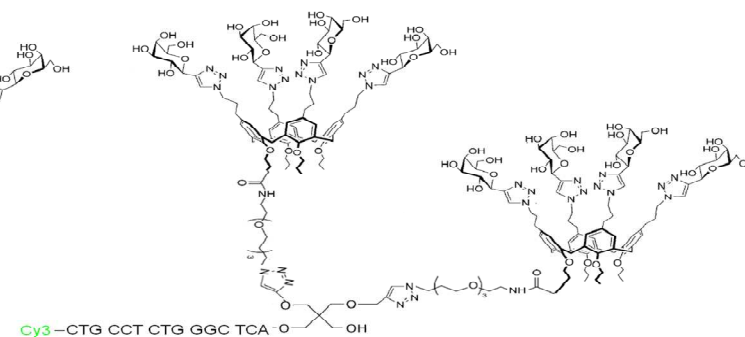
Glycoconjugate 5（G5）

Glycoconjugate 2_a （G2_a）

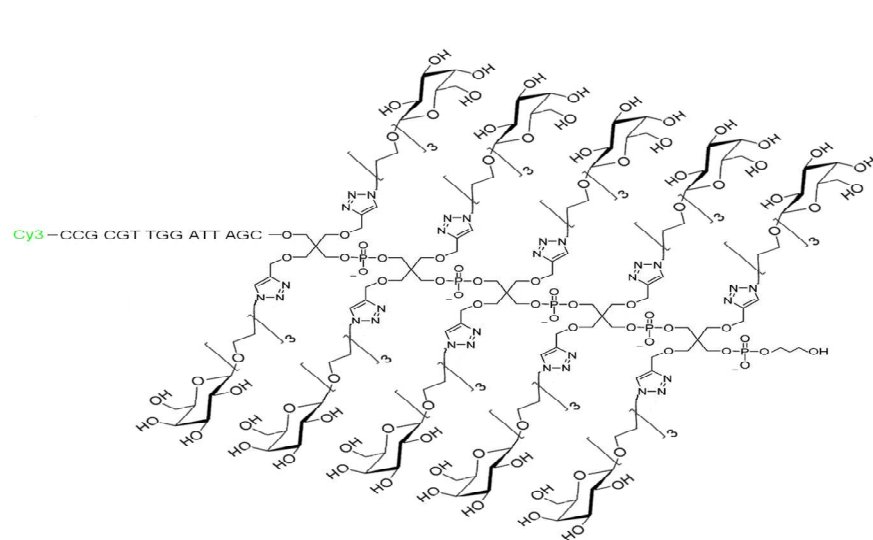*Fig1 Structures of 5'-Cy3-DNA tag- glycomimetics (glycoconjugates)*

Glycoconjugate 3ₐ（G3ₐ）

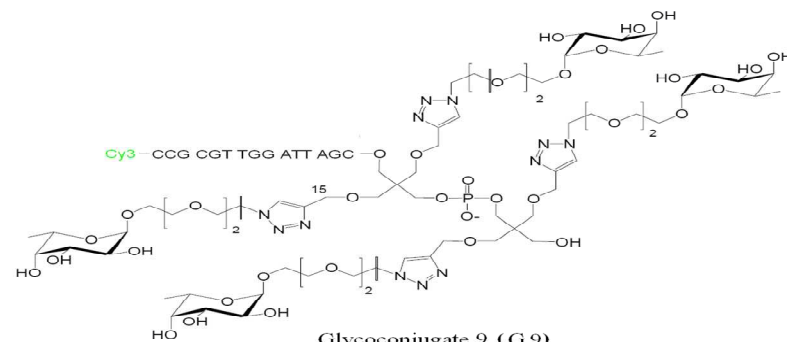Glycoconjugate 6 （G6）

Glycoconjugate 7 （G7）

Glycoconjugate 8 （G8）

Glycoconjugate 9 （G9）

Glycoconjugate 10 （G10）

Fig1 (Continued).

Glycoconjugate 11 (G11)

Glycoconjugate 12 (G12)

Glycoconjugate 13 (G13)

Glycoconjugate 14 (G14)

Glycoconjugate 15 (G15)

Glycoconjugate 16 (G16)
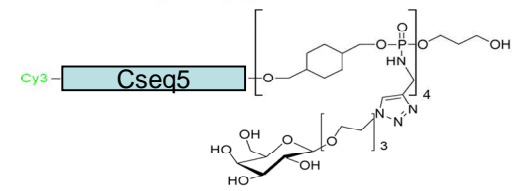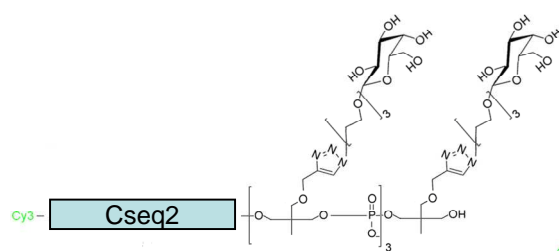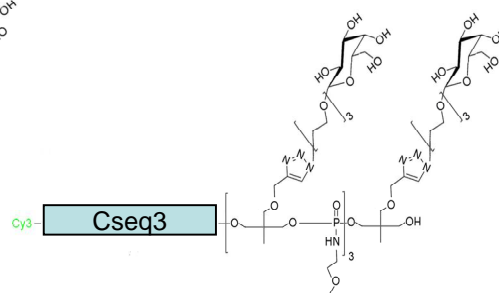
Fig1 (continued)
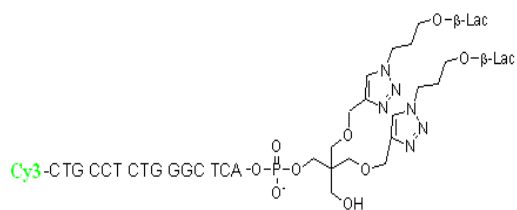
Glycoconjugate 17 (G 17)
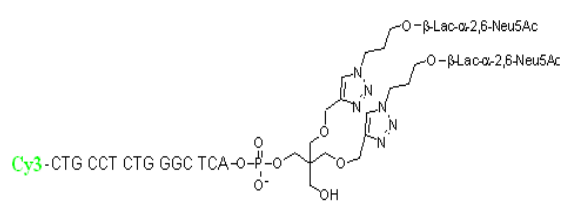
Glycoconjugate 18 (G 18)
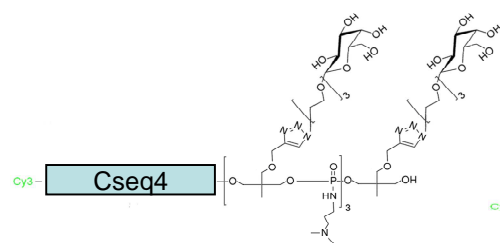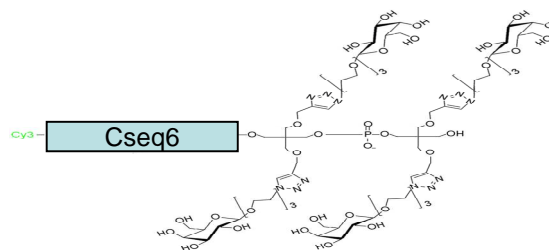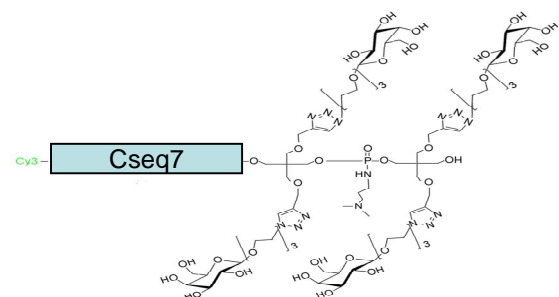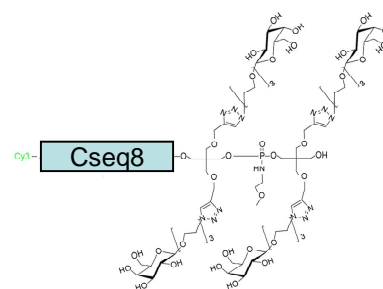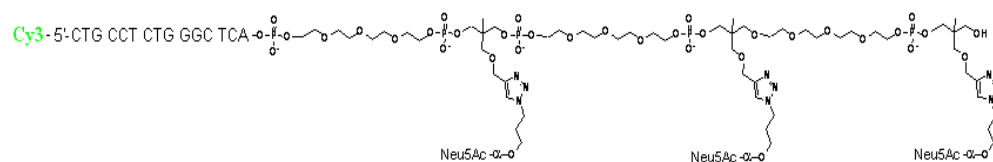
Glycoconjugate 19 (G 19)
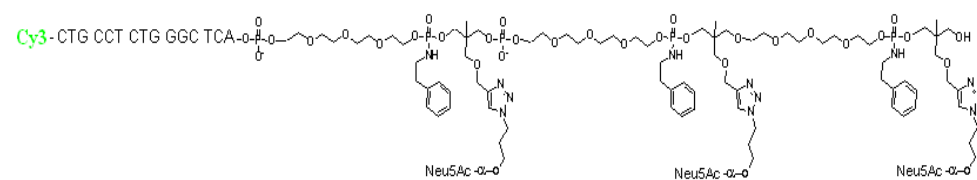
Glycoconjugate 20 (G 20)
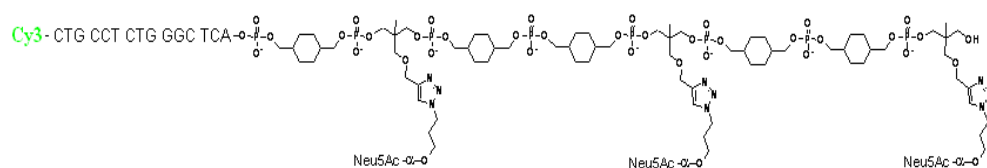
Glycoconjugate 21 (G 21)
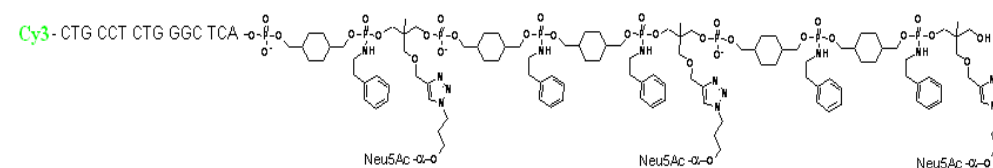
Glycoconjugate 22 (G 22)
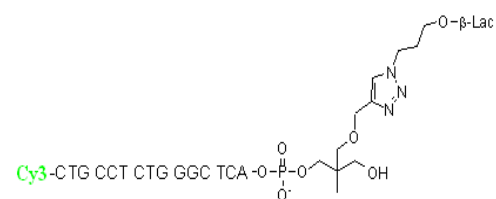
Glycoconjugate 23 (G 23)
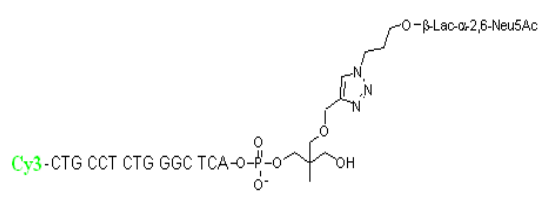
Glycoconjugate 24 (G 24)

Fig1 (continued)

182

ANNEXE 2

1 Synthesis of glycoconjugates 1, 2 and 3
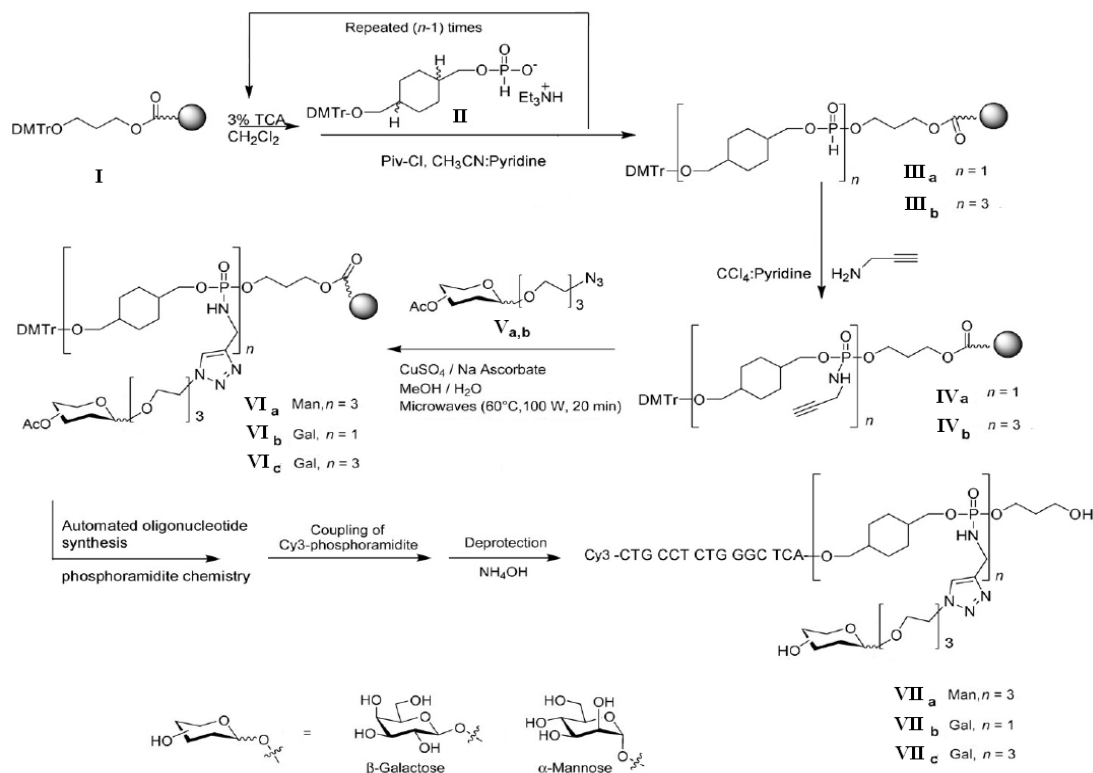
Scheme1. General synthetic scheme for the preparation of glycoconjugates 1-3; TCA=trichloroacetic acid, Piv=pivaloyl, adapted from (1)

The synthesis processes of glycoconjugates 1, 2 and 3 (see Chapter 2, Fig2-1) were reported by Chevolot et al. (1). Glycoconjugates 1, 2 and 3 were synthesized according to Scheme 1. In brief, starting from the solid support I, The dimethoxytrityl (DMTr) group was removed and then either one or three H-phosphonate monoester building blocks II were introduced, to afford diesters III_a and III_b. Amidative oxidation of the H-phosphonate by carbon tetrachloride in the presence of propargylamine led to mono- and triynes IV_a and IV_b, which were then conjugated with the galactose azide derivative V_b by means of microwave-assisted 1, 3-dipolar cycloaddition, affording solid-supported conjugates VI_b and VI_c (2). The

corresponding trimannoside derivative VI$_a$ was synthesized from V$_a$. The oligonucleotide was then synthesized and labeled with the fluorescent residue Cy3. Chimeric 5'-Cy3–3'-oligosaccharide oligonucleotides VII$_a$, VII$_b$ and VII$_c$ (corresponding to Glycoconjugate 1, 2 and 3) were obtained after deprotection by treatment with aqueous ammonia. Each conjugate was purified by preparative HPLC and characterized by MALDI-TOF mass spectrometry.

2 Synthesis of glycoconjugates 4 and 5

Glycoconjugate 4 n = 1 B = T
Glycoconjugate 5 n =15 Sequence: 5'-CTG CCT CTG GGC TCA-3'
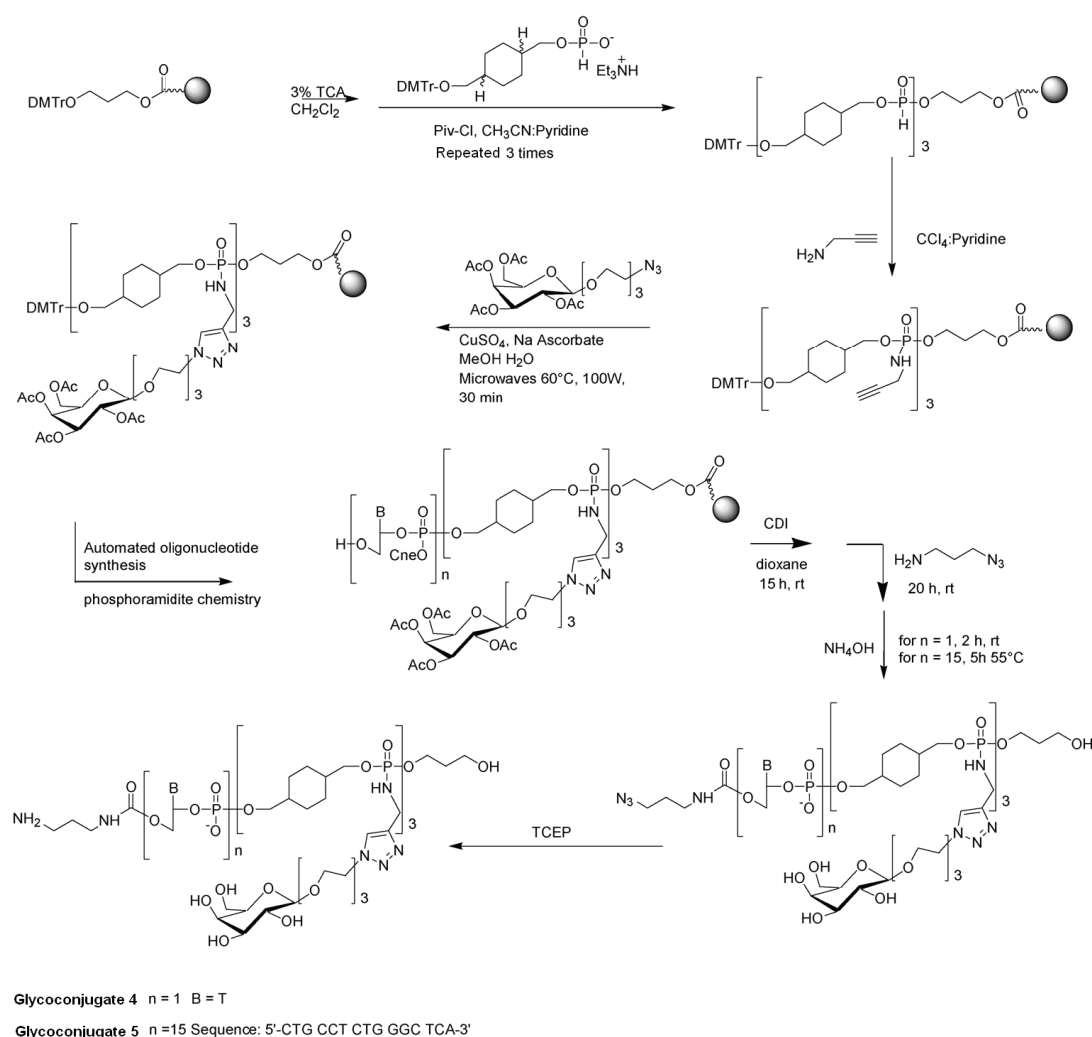
Scheme2. Synthesis of 5'-amino glycoconjugates 4 and 5; TCA= trichloroacetic acid, Piv = pivaloyl, CDI = carbonyl diimidazole, adapted from (3).

The synthesis procedures of Amino-functionalised Glycoconjugates 4 and 5 (see

Chapter 2, Fig2-1) were referred to (*3*). Glycoconjugates 4 and 5 were synthesized according to Scheme 2. Starting from 1, 3-propanediol on solid support, according to standard H-phosphonate chemistry, three H-phosphonate monoesters of 1, 4-dimethanolcyclohexane were introduced. Amidative oxidation by carbon tetrachloride in the presence of propargylamine led to the scaffold with three alkyne functions. Cu (I)-catalyzed alkyne-azide 1, 3-dipolar cycloaddition was performed between 1-azido-3, 6-dioxaoct-8-yl 2, 3, 4, 6-tetra-O-acetyl-ß-D-galactopyranoside (*1*) and solid-supported tris-alkyne constructs using CuSO4 and sodium ascorbate under microwave assistance (*2*). The resulting trisgalactosylated compound was then elongated with a thymidine as a UV tag or with 15 nucleotides using phosphoramidite chemistry on a DNA synthesizer. After elongation, treatment with carbonyldiimidazole for 15 h at room temperature and then with 3-azido-propylamine for 20 h at room temperature followed by deprotection with concentrated ammonia afforded the 5'-azido-functionalised tris-galactosylated glycomimetics in solution. A final treatment with tris (2-carboxyethyl) phosphine (TCEP) yielded the corresponding 5'-amino glycoconjugates 4 and 5.

3 Synthesis of glycoconjugates 6 and 7

3.1 Synthesis of C-galactosyl calix[4]arene clusters

The synthesis processes of two kinds of calix[4]arene-based glycoclusters was reported by Moni et al.(*4*), briefly (see Scheme3), the starting known compound (*5*) tetraallyl- calix[4]arene 1 was monoglycosylated by treatment with commercially available a-d-mannofuranose diacetonide (2, 1.1 equiv) under Mitsunobu conditions (*6*), and the three residual hydroxyl groups were then protected as O-propyl ethers to give compound 3 , then the multiple hydroboration-oxidation of the four allyl groups at the upper rim of 3 was readily carried out to give the tetrol 4. Subsequent transformation by azidation with diphenylphosphoryl azide and sodium azide, followed by removal of the mannofuranose fragment by acidic hydrolysis, afforded the tetraazide 5. The tetraazidated calixarene 5 is a key intermediate, as the two new

calix[4]arene-based glycoclusters were all synthesized from the compound 5 but in different synthesis processes.   For the glycocluster 10, the free hydroxy group of 5 was alkylated with the short N-Boc ethylamino chain to give 6, Click chemistry(*7-9*) was then carried out on the tetraazide 6 by introducing the known (*10*) ethynyl tetra-O-acetyl-b-d-C-galactopyranoside 7, the N-Boc group of resulting compound 8 was removed under acidic conditions, followed by a diazotransfer reaction (*11*) to convert the amino function into the azido group, afforded 9. Finally, after treatment with ammonia in methanol, the compound 9 was converted
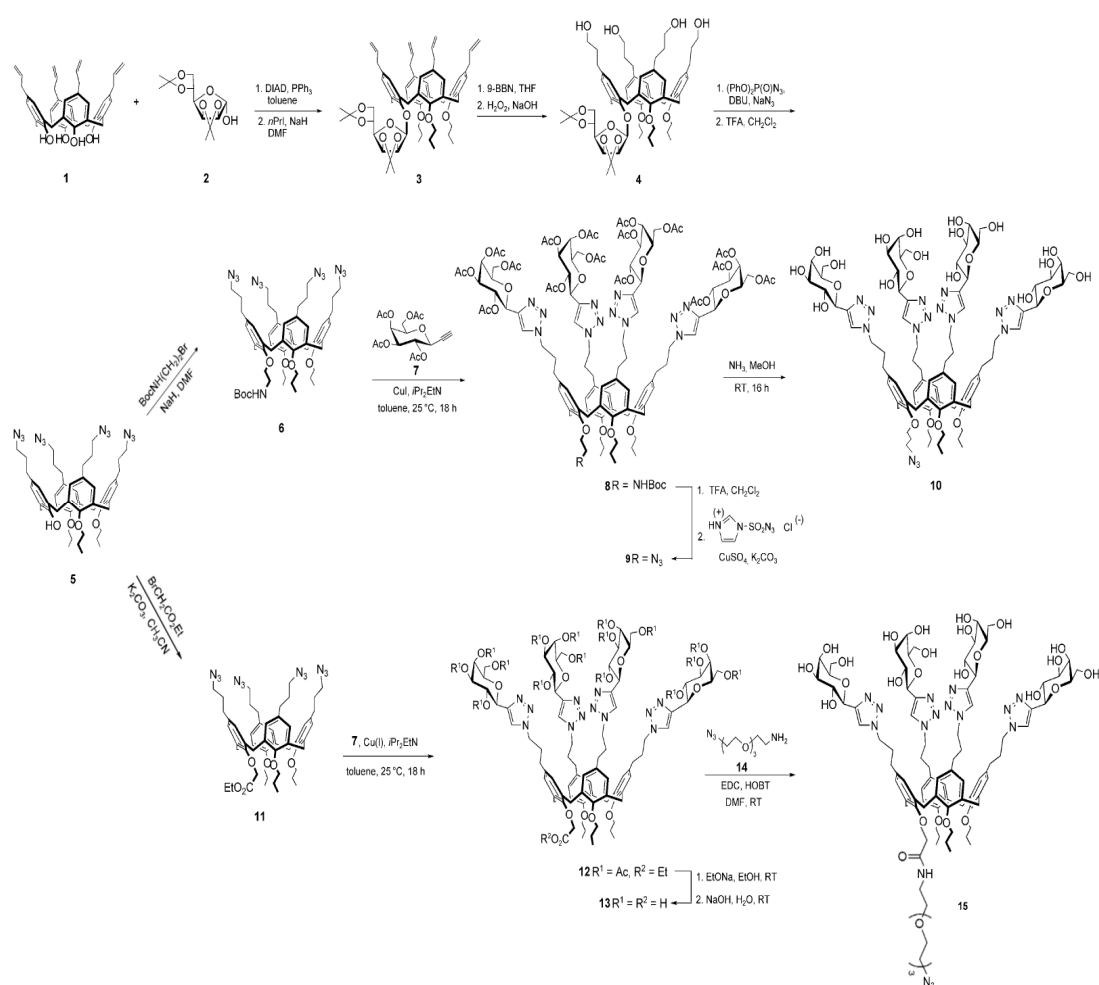
Scheme3. Synthesis of calix[4]arene-based glycoclusters 10 and 15, adapted from (4)

into the target calix[4]arene 1, which features a single azido group at its lower rim and carbohydrate residues at its upper rim. For the glycocluster 15, bearing a long tether holding the azido group at the lower rim, the tetraazide 5 was derivatized as the ethyl ester 11, Click chemistry (*7-9*) was then performed to get glycocluster 12.

Transesterification of 12, followed by basic hydrolysis, afforded compound 13. Finally, 14 was converted into the glycocluster 15 by N-(3-dimethylaminopropyl)-N'-ethyl-carbodiimide-activated (EDC-activated) amidic coupling (*12*) of the free carboxylic group with the commercially available 11-azido-3, 6, 9-trioxaundecan-1-amine 14.

3.2 Synthesis of calixarene glycocluster-ssDNA conjugates 6 and 7

Oligonucleotides were prepared with a DNA synthesizer by standard phosphoramidite chemistry (*13*) on CPG (controlled pore glass) solid support, a porous borosilicate material frequently used for DNA synthesis. Two different solid-supported materials, 16 (*14*) and 17(*15*) (see Scheme4.), featuring one and two alkyne residues, respectively, were used for the synthesis of oligonucleotides 18 and 19; each displayed the same sequence (CTG CCT CTG GGT TCA)(1) and was labelled on the 5' end with the fluorescent dye Cy3. Treatment of 18 and 19 with concentrated aqueous ammonia released the oligonucleotides from the solid support and removed the protecting groups (that is, b-cyanoethyl, benzoyl, and isobutyryl). The oligonucleotides 20 and 21 were isolated, their purities were established by analytical HPLC, and they were characterized by MALDI-TOF mass spectrometry. Because the alkyne-functionalized oligonucleotides 20 and 21 were water-soluble compounds, we set out to carry out their coupling with the azide-functionalized glycoclusters 10 and 15, respectively, in water using CuSO4 and sodium ascorbate as the source of copper(I). Both reactions were performed under microwave irradiation (2) conditions in order to achieve high reaction rates and therefore to avoid some phosphodiester hydrolysis due to the presence of copper(I) ion.(*16*) The crude products from the click reactions were purified by preparative HPLC and characterized by MALDI-TOF mass spectrometry to give the final glycoconjugates 6 and 7 (see Chapter 2, Fig2-1).

Scheme4. Synthesis of calixarene glycocluster-ssDNA conjugates Glycoconjugate 6 and glycoconjugate 7 , adapted from (4).

4 Synthesis of glycoconjugate 8

Glycoconjugate 8 (see Chapter 2, Fig2-1) was synthesized as described for the synthesis of Glycoconjugates 1-3, but in this case the alkyne functions were introduced by using a dialkyne phosphoramidite derivative (*14, 17*). Thus, starting from universal solid supported propane-1, 3-diol, five dialkyne phosphoramidite derivatives were incorporated by phosphoramidite chemistry. The introduction of the ten galactose residues was performed by microwave-assisted click chemistry, and then the oligonucleotide was synthesized and labeled with a Cy3 phosphoramidite. The desired glycoconjugate 8 was obtained after ammonia treatment and HPLC purification.

5 Synthesis of glycoconjugate 9

Scheme5. Synthesis of glycoconjugate 9, adapted from(18)

Glycoconjugates 9 (see Chapter 2, Fig2-1) were synthesized according to Scheme 5. Starting from the bis-propargyl solid support I, bis-propargyl phosphoramidite II and commercially-available cytidine phosphoramidite were added to afford the

solid-supported tetra-propargyl scaffold III. And then the solid-supported tetra-propargyl scaffold III were added protected O-2, 3, 4- tri acetyl fucosyl azide IV , CuSO4, freshly prepared sodium ascorbate, and water. The resulting preparation was treated in a sealed tube with microwave synthesizer Initiator from Biotage, set at 60°C and 100 W for 30 min with a 30 s premixing time to afford 5. After oligonucleotide elongation, deprotection and purification, 5'-Cy3-Oligonucleotide 3'-tetrafucose VII was finally obtained.

REFERENCES

1. Chevolot, Y., Bouillon, C., Vidal, S., Morvan, F., Meyer, A., Cloarec, J. P., Jochum, A., Praly, J. P., Vasseur, J. J., and Souteyrand, E. (2007) DNA-based carbohydrate biochips: a platform for surface glyco-engineering, *Angew Chem Int Ed Engl. 46*, 2398-2402.

2. Bouillon, C., Meyer, A., Vidal, S., Jochum, A., Chevolot, Y., Cloarec, J. P., Praly, J. P., Vasseur, J. J., and Morvan, F. (2006) Microwave assisted "click" chemistry for the synthesis of multiple labeled-carbohydrate oligonucleotides on solid support, *J Org Chem 71*, 4700-4702.

3. Zhang, J., Pourceau, G., Meyer, A., Vidal, S., Praly, J. P., Souteyrand, E., Vasseur, J. J., Morvan, F., and Y., C. (2009) DNA-directed immobilisation of glycomimetics for glycoarrays application: Comparison with covalent immobilisation, and development of an on-chip IC_{50} measurement assay., *Biosens Bioelectron*.

4. Moni, L., Pourceau, G., Zhang, J., Meyer, A., Vidal, S., Souteyrand, E., Dondoni, A., Morvan, F., Chevolot, Y., Vasseur, J. J., and Marra, A. (2009) Design of triazole-tethered glycoclusters exhibiting three different spatial arrangements and comparative study of their affinities towards PA-IL and RCA 120 by using a dna-based glycoarray, *ChemBioChem 10*, 1369-1378.

5. Gutsche, C. D., Levine, J. A., and Sujeeth, P. K. (1985) Calixarenes .17.

Functionalized Calixarenes - the Claisen Rearrangement Route, *J Org Chem 50*, 5802-5806.

6. Dondoni, A., Marra, A., Scherrmann, M. C., Casnati, A., Sansone, F., and Ungaro, R. (1997) Synthesis and properties of O-glycosyl calix[4]arenes (calixsugars), *Chem Eur J 3*, 1774-1782.

7. Dondoni, A., and Marra, A. (2006) C-glycoside clustering on calix[4]arene, adamantane, and benzene scaffolds through 1,2,3-triazole linkers, *J Org Chem 71*, 7546-7557.

8. Marra, A., Moni, L., Pazzi, D., Corallini, A., Bridi, D., and Dondoni, A. (2008) Synthesis of sialoclusters appended to calix[4]arene platforms via multiple azide-alkyne cycloaddition. New inhibitors of hemagglutination and cytopathic effect mediated by BK and influenza A viruses, *Org Biomol Chem 6*, 1396-1409.

9. Vecchi, A., Melai, B., Marra, A., Chiappe, C., and Dondoni, A. (2008) Microwave-enhanced ionothermal CuAAC for the synthesis of glycoclusters on a calix[4]arene platform, *J Org Chem 73*, 6437-6440.

10. Lowary, T., Meldal, M., Helmboldt, A., Vasella, A., and K., B. (1998) Novel Type of Rigid C-Linked Glycosylacetylene–Phenylalanine Building Blocks for Combinatorial Synthesis of C-linked Glycopeptides, *J Org Chem 63*, 9657-9668.

11. Goddard-Borger, E. D., and Stick, R. V. (2007) An efficient, inexpensive, and shelf-stable diazotransfer reagent: imidazole-1-sulfonyl azide hydrochloride, *Org Lett 9*, 3797-3800.

12. Castellano, R. K., Rudkevich, D. M., and Rebek, J., Jr. (1997) Polycaps: reversibly formed polymeric capsules, *Proc Natl Acad Sci U S A 94*, 7132-7137.

13. Beaucage, S. L., and Caruthers, M. H. (1981) Deoxynucleoside phosphoramidites—A new class of key intermediates for deoxypolynucleotide synthesis, *Tetrahedron Lett 22*, 1859-1862.

14. Pourceau, G., Meyer, A., Vasseur, J. J., and Morvan, F. (2008) Combinatorial

and automated synthesis of phosphodiester galactosyl cluster on solid support by click chemistry assisted by microwaves, *J Org Chem 73*, 6014-6017.

15. Lietard, J., Meyer, A., Vasseur, J. J., and Morvan, F. (2008) New strategies for cyclization and bicyclization of oligonucleotides by click chemistry assisted by microwaves, *J Org Chem 73*, 191-200.

16. Kumar, R., El-Sagheer, A., Tumpane, J., Lincoln, P., Wilhelmsson, L. M., and Brown, T. (2007) Template-directed oligonucleotide strand ligation, covalent intramolecular DNA circularization and catenation using click chemistry, *J Am Chem Soc 129*, 6859-6864.

17. Morvan, F., Meyer, A., Jochum, A., Sabin, C., Chevolot, Y., Imberty, A., Praly, J. P., Vasseur, J. J., Souteyrand, E., and Vidal, S. (2007) Fucosylated pentaerythrityl phosphodiester oligomers (PePOs): automated synthesis of DNA-based glycoclusters and binding to Pseudomonas aeruginosa lectin (PA-IIL), *Bioconjug Chem 18*, 1637-1643.

18. Zhang, J., Pourceau, G., Meyer, A., Vidal, S., Praly, J. P., Souteyrand, E., Vasseur, J. J., Morvan, F., and Chevolot, Y. (2009) Specific recognition of lectins by oligonucleotide glycoconjugates and sorting on a DNA microarray, *Chem Commun*, 6795-6797.

ANNEXE 3

1. Cross-hybridization tests molecule 1-7 as well as molecule 8 under "on-chip" condition (see Fig1)

After the Cross-hybridization tests of the seven molecules (molecule 1-7) on the DNA anchoring platform of MbII described in chapter 5, a cross-hybridization assay of molecule 1-7 plus molecule 8 were performed on a new DNA anchoring platform of MbII of which Sequence 8 instead of Sequence N was deposited into each microwell (see Fig1). Molecule 8 is corresponding to Glycoconjugate 16 (see Chapter2 Fig2-1). The objectives are to confirm 1) whether cross-hybridization will occur or not after Molecule 8 added into the MbII and 2) whether Molecule 1-7 will cross-hybridize with the Sequence 8 printed on the new DNA anchoring platform of MbII.
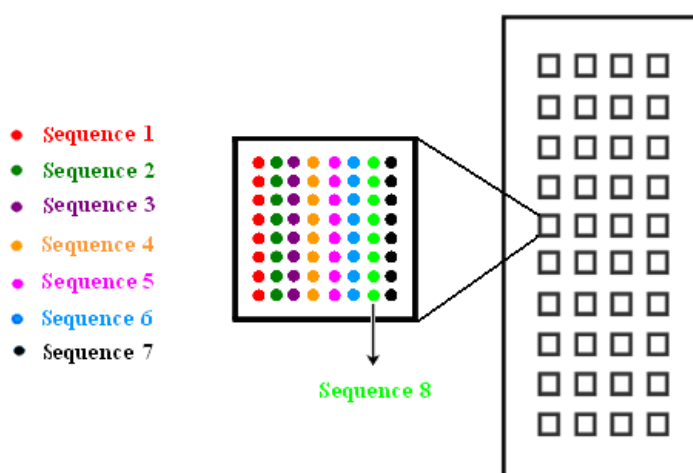

Fig1 Sketch map of new DNA anchoring platform of Mb II: Sequence 1-8 were printed on the bottom of each microwell resulting in one column and eight spots for each sequence, 64 spots in all.

We adopted the same strategies as mentioned in chapter 5, under Condition 1-8 (see Fig2) only one of the eight molecules (1µM, final concentration) was added into

the corresponding microwell, accompanied by seven complementary sequences. For Condition I, all eight molecules (Molecule 1-8) (1µM per glycoconjugate, final concentration) were mixed together and added into each microwell. After incubation, the slide was scanned and analyzed.

According to the mean fluorescence intensities acquired from the eight conditions (Condition 1-8), the ratios of fluorescence intensity of specific vs. non-specific hybridization of the eight molecules were calculated and summarized in Table1. As discussed above, there were no cross-hybridizations detected for six molecules (molecule 1-6) with the seven sequences (Sequence 1-7) at DNA anchoring platform a). In this section, the ratios for molecule 1- 6 were about 10^2 (see Table1), demonstrating that the six molecules had no cross- hybridizations not only with Sequence 1-7, but also with Sequence 8. In addition, cross-hybridization was also found for Molecule 7 which cross-hybridized with Sequence 6 in a ratio of 1.9. For Molecule 8, no cross-hybridization was observed (with a ratio of 84).

Fig2 Sketch map of cross-hybridization assay of eight molecules (molecule 1-8) under "on-chip" glycoconjugate hybridization condition on the DNA anchoring platform b) at 1µM.

➢ **Condition 1-8: At 1µM, in each microwell, incubation of one of the eight molecules (molecule 1-8) with other seven Cseq (complementary sequences) except its corresponding complementary sequences. e.g.: for condition 1, incubation molecule 1 with Cseq2-Cseq8 except Cseq1; for condition2, incubation molecule 2 with Cseq1, and Cseq3-Cseq8 except**

Cseq2.

➢ **Condition I: At 1μM, in each microwell, incubation of all eight molecules (molecule 1-8).**

	Ratio of fluorescence intensity of specific vs. non-specific hybridization for Condition 1-8 at 1μM
Molecule 1	274
Molecule 2	230
Molecule 3	114
Molecule 4	127
Molecule 5	301
Molecule 6	269
Molecule 7	1.9
Molecule 8	84

Table1 Ratio of fluorescence intensity of specific vs. non-specific hybridization of eight molecules for Condition1 to Condition 8, after cross-hybridization test under "on-chip" glycoconjugate hybridization condition on MbII.

2. Cross-hybridization tests of molecule 1-7 as well as Molecule 8 under "in-solution" condition

Based on the same strategies, cross-hybridization tests were also preceded on DNA platform b) for all eight molecules (see Fig3). The results (see Table 2) indicated that there were no cross-hybridizations for most of the eight molecules with ratios around 10, except Molecule 7 for which the fluorescence intensities of specific hybridization only 1.2 times higher than non-specific hybridization.

"In-solution" approach

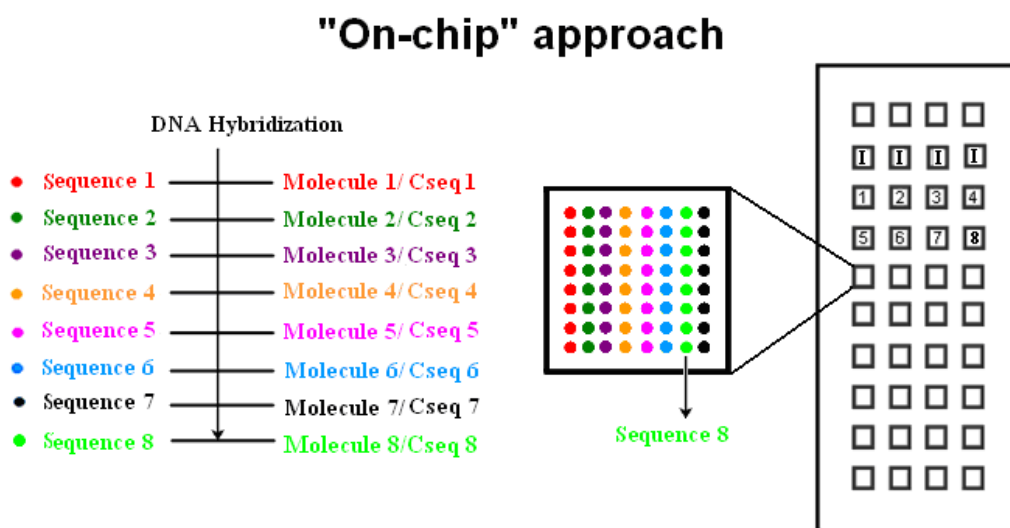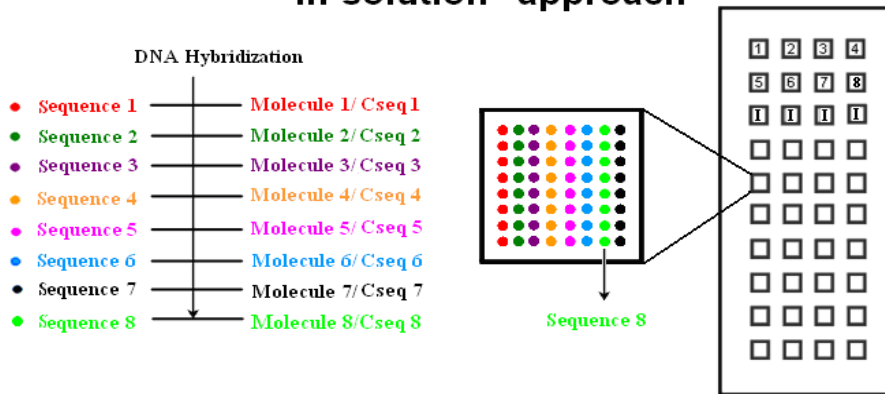*Fig3 Sketch map of cross-hybridization assay of eight molecules (molecule 1-8) under "in-solution" glycoconjugate hybridization condition on the MbII. Each of the eight sequences (sequence1-8) was expected to only hybridize with its corresponding molecule (molecule1-8) or complementary sequences (Cseq1-Cseq8).*

➤ **Condition 1-8: At 1µM, in each microwell, incubation of one of the eight molecules (molecule 1-8) with other seven Cseq (complementary sequences) except its corresponding complementary sequences. e.g.: for condition 1, incubation molecule 1 with Cseq2-Cseq8 except Cseq1; for condition2, incubation molecule 2 with Cseq1, and Cseq3-Cseq8 except Cseq2.**

➤ **Condition I: At 1µM, in each microwell, incubation of all eight molecules (molecule 1-8).**

	Ratio of fluorescence intensity of specific vs. non-specific hybridization for "in-solution" Condition 1-8 at 1µM
Molecule 1	9
Molecule 2	9,4
Molecule 3	26
Molecule 4	18
Molecule 5	45
Molecule 6	32
Molecule 7	1.2
Molecule 8	23

Table2 Ratio of fluorescence intensity of specific vs. non-specific hybridization of seven

3. Study of binding affinities of glycoconjugates towards PA-IL

We then studied the affinities of all the 9 glycoconjugates (3Man, 3Gal as well as Molecule 2-8, see Table3) with PA-IL on DNA anchoring platform b) of MbII by "in-solution" approach. As shown in the sketch map of the experiment (see Fig4), 3Man or 3Gal was mixed with Molecule 2-8 and incubated with PA-IL in Condition 1 and Condition 2 respectively. The goal of this part of work was 1) to do a repetition of the binding studies of Molecule1 (3Man) - Molecule7 with PA-IL on platform b using "in-solution" method; 2) to test the binding affinity of Molecule 8 towards PA-IL; 3) to make a comparison of the binding affinities of the 7 new tetra-galactosyl molecules (Molecule 2-8) with 3Gal bearing three galactose residues towards PA-IL.

The results observed in Fig5 exhibited a good repetition for Molecule1-7 in comparison with the results shown in chapter 5 Fig5-20. The results also shown that the signals obtained for Molecule 8 were very low, demonstrating no significant binding affinity with PA-IL. In addition, as far as the 3Gal was concerned, although the 7 new molecules (Molecule 2-8) all contain one more galactose residue compare to 3Gal, they did not show enhanced affinities towards PA-IL, except Molecule 4 and Molecule 5. In other words, the multivalency and "cluster effect" were only represented by Molecule 4 and Molecule 5 vs. 3Gal. these results provide further evidence to previous judgments that the spatial arrangement is a more important binding infector than the number of the saccharide residue.

Name[a] of glycoconjugate	Alias[b]	Saccharide residue (Number)	Charge (Number)	Linker[c]	Spatial arrangement
G 1	3Man /Molecule 1	Mannose (3)	0	Linker 1	Comb-like
G 3	3Gal	Galactose (3)	0	Linker 1	Comb-like
G 11	Molecule 2	Galactose (4)	- (3)	Linker 2	Comb-like
G 12	Molecule 3	Galactose (4)	0	Linker 2	Comb-like
G 13	Molecule4	Galactose (4)	+ (3)	Linker 2	Comb-like
G 10	Molecule 5	Galactose (4)	0	Linker 1	Comb-like
G 14	Molecule 6	Galactose (4)	- (1)	Linker 3	Antenna
G 15	Molecule 7	Galactose (4)	+ (1)	Linker 3	Antenna
G 16	Molecule 8	Galactose (4)	0	Linker 3	Antenna

Table3 Main characters of glycoconjugates (3Gal and Molecule 1-7)

[a] Name of glycoconjugate designated in Chapter 2 (see Fig2-1 and Table2-1)

[b] Name of glycoconjugate designated in this Chapter

[c] Linkage between every two phosphodiesters of the structure of the glycoconjugates(206).

Linker 1, Linker 2 and Linker 3 correspond to 1, 4-cyclohexanedimethanol (DMCH); Trishydroxymethylethane and Pentaerythritol.
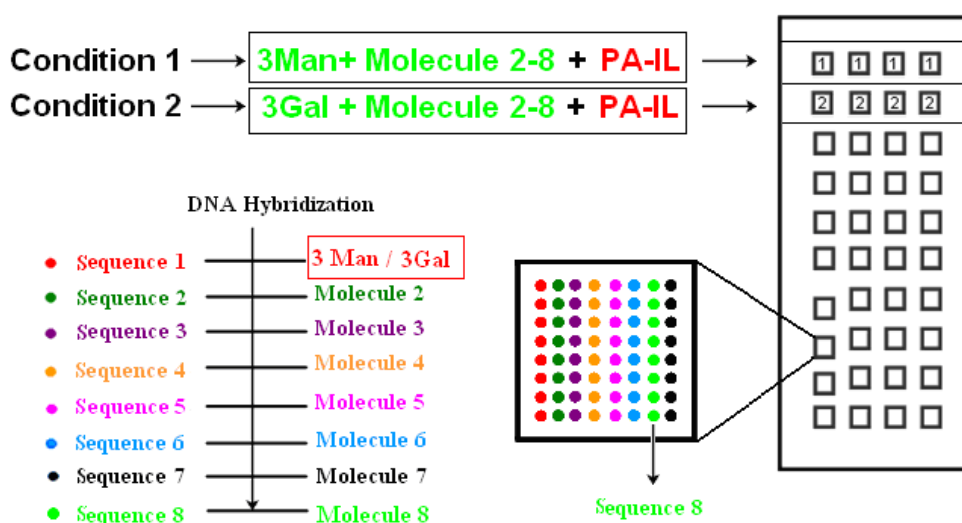
Fig4 Sketch map of the determination of binding affinities of Molecule 2- Molecule 8 with

3Man (Molecule 1) or 3Gal towards PA-IL on MbII by "in-solution" method

➢ **Condition 1: Incubation of 3Man, Molecule 2- Molecule 8 with PA-IL**

➢ **Condition 2: Incubation of 3Gal, Molecule 2- Molecule 8 with PA-IL**

Fig5 Mean fluorescence intensities obtained at 635nm (a.u.) of condition 1 and condition 2 for PA-IL, after incubation with the molecules by "in-solution" approach on MbII.

ABBREVIATIONS

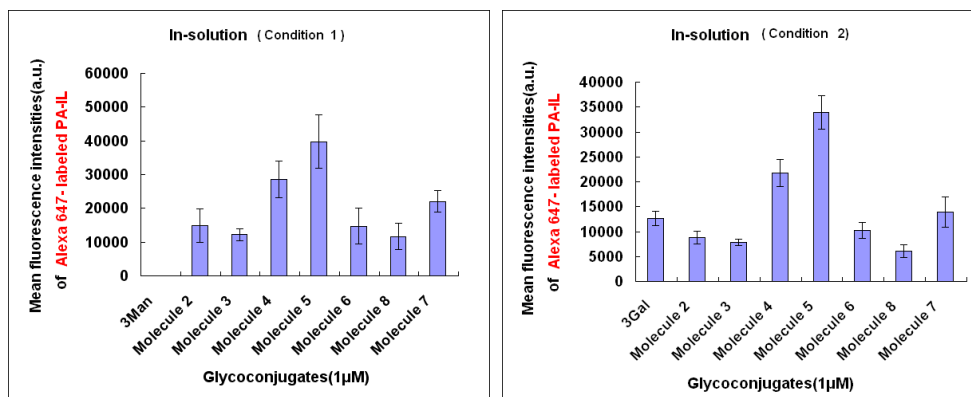|	
AFM	Atomic Force Microscopy
BOE	Buffered Oxide Etchant
BSA	Bovine serum albumin
Cy3	Cyanine 3
Cy5	Cyanine 5
ConA	Concanavalin A
DDI	DNA-directed immobilization
DI water	Deionized water
DMCH	1, 4-cyclohexanedimethanol
ELISA	Enzyme-Linked Immunosorbent Assay
Flu	Influenza
FRET	Fluorescent Resonance Energy Transfer
GBP(s)	glycan-binding protein(s)
HSQC	Heteronuclear Single-Quantum Correlation
H or HA	Hemagglutinin
HIV	Human Immunodeficiency Virus
ITC	Isothermal Titration Calorimetry
M1	Matrix protein
MS	Mass spectrometry
MALDI-TOF-MS	Matrix assisted laser desorption ionisation time-of-flight mass
N or NA	Neuraminidase or Sialidase
Neu5AC	N-Acetylneuraminic acid
NHS	N-hydroxysuccinimide
NMR	Nuclear Magnetic Resonance
NOE/STD	Nuclear Overhauser Effect/ Saturation Transfer Difference
NOESY	Nuclear Overhauser Effect Spectroscopy
NP	Nucleoprotein

PA-IIL	*Pseudomonas aeruginosa* lectin II
PA-IL	*Pseudomonas aeruginosa* lectin I
PBS	Phosphate-buffered saline
PFA	Paraformaldehyde
pI	Isoelectric point
RCA120	Ricinus communis agglutinin I
RF power	Radio Frequency power
RUs	Response or Resonance units
SDS	Sodium Dodecyl Sulfate
SIV	Simian Immunodeficiency Virus
SPC-ELISA	Sulfated polysaccharide-coating enzyme-linked immunosorbent assay
SPR	Surface Plasmon Resonance
SSC	Sodium Saline Citrate
$TCID_{50}$	Tissue culture infective dose 50
trNOESY	Transferred rotating-frame Overhauser effect spectroscopy
WGA	Wheat germ agglutinin

CURRICULUM VITAE

Educations

1. Sep.2007-Nov.2010: Ecole Lyons Centrale de Lyon (France)

    PhD of chemistry and nanotechnology (carbohydrate glycoarray)

2. Sep.2004 - Mar.2007: Shanghai Jiao Tong University (Shanghai, China)

    Master of Biological Technology

3. Sep.1998 - Jul.2002: Hebei University of Science & Technology (Shijiazhuang, China)

    Bachelor of Biological Engineering

List of publications

1-"DNA-directed immobilisation of glycomimetics for glycoarrays application: Comparison with covalent immobilisation, and development of an on-chip IC_{50} measurement assay"

J. Zhang, G. Pourceau, A. Meyer, S. Vidal, J-P. Praly, E. Souteyrand, J-J. Vasseur, F. Morvan, Y. Chevolot, *Biosensors and Bioelectronics* 2009, 24, 2515-2521.

2-"Design of Triazole-Tethered Glycoclusters Exhibiting Three Different Spatial Arrangements and Comparative Study of Their Affinity for PAIL and RCA 120 Using a DNA-Based Glycoarray"

L.Moni, G. Pourceau, J. Zhang, A. Meyer, S. Vidal, E. Souteyrand, A. Dondoni, F. Morvan, Y. Chevolot, J-J. Vasseur, and A. Marra, ChemBioChem 2009, 10, 1369 – 1378

3-"Specific recognition of lectins by oligonucleotide glycoconjugates and sorting on a

DNA microarray"

J. Zhang, G. Pourceau, A.Meyer, S. Vidal, J.-P. Praly, E. Souteyrand, J.-J. Vasseur, F. Morvan and Y. Chevolot, ChemComm, 2009, 6795-6797

Scientific communications

1-Probing glycomimetic/lectin interaction by means of DNA directed carbohydrate arrays

J. Zhang, G. Pourceau, S. Vidal, F. Morvan, A. Meyer, J.-P. Praly, J.-J, Vasseur, E. Souteyrand and Y. Chevolot

Poster presentation

1st TransAlpine Conference on Nanoscience and Nanotechnologies

Nanotransalpl 2008, Lyon, 27-29 octobre 2008

2-New DNA based glycoarrays for sensitive biosensing carbohydrate-protein interactions.

J. Zhang, Y. Chevolot, E.Souteyrand, F.Morvan, J.-J.Vasseur, and S. Vidal

Orale presentation

2nd Sine French Workshop, Paris, 19 mai 2008.

3-New DNA based glycoarrays for sensitive biosensing carbohydrate-protein interactions

Orale presentation

J. Zhang, S. Vidal, F. Morvan, A. Meyer, J.-P. Praly, J.-J. Vasseur, E. Souteyrand and Y. Chevolot

Colloque de Recherche Intergroupe Ecoles Centrales (CRIEC) 2008, Nantes, 9-10 Juin 2008.

4-New DNA based glycoarrays for sensitive biosensing carbohydrate-protein

interactions.

Orale presentation

J. Zhang, S. Vidal, F. Morvan, A. Meyer, J.-P. Praly, J.-J. Vasseur, E. Souteyrand and Y. Chevolot

Journée des Doctorants INL, Lyons, 9 juillet 2008.

5-Synthesis of glycoclusters by click chemistry assisted by microwaves.

Orale presentation

G. Pourceau, J. Zhang, L.Moni, A.Meyer, S.Vidal, Y.Chevolot, A.Dondoni, A.Marra, E.Souteyrand, J. J.Vasseur, F.Morvan.

Microwave-assisted organic and peptide synthesis.

La Grande Motte, France, 2009

6-Criblage de Glycomimétiques par utilisation de puces ADN comme plateforme d'analyse

Orale presentation

J. Zhang, G. Pourceau, L. Moni, A.Meyer, S. Vidal, A. Dondoni, J.-P. Praly, A. Marra, F. Morvan, J.-J, Vasseur, E. Souteyrand and Y. Chevolot

Première journée Lyonnaise des Biomolécules JLB 2009, Lyon, France, 4 juin 2009

7-Synthesis of calix[4]arene-based glycoclusters and study of their affinity of PA-IL and RCA120 using a DNA-based glycoarray

Orale presentation

L. Moni, G. Pourceau, J. Zhang, A.Meyer, Vidal, E. Souteyrand, A.Dondoni, F. Morvan, Y. Chevolot, J.-J, Vasseur, A. Marra.

Organic chemistry and biotechnology: Challenges and opportunities, Forte dei Marmi, Italy, 20-23 mai 2009

8-Développement d'un système de multianalyse pour l'étude des interactions sucres/protéines (Glycoarrays)

Poster presentation

Zhang J., Pourceau G., Morvan F., Meyer A., Vidal S., Moulés V., Terrier O., Praly J-P., Bruno Lina, Vasseur J-J., Souteyrand E., Chevolot Y.

Journées Nationales du Réseau Doctoral de Microélectronique (JNRDM) - 12ème édition, Lyon, France,18-20 mai 2009

9-DNA Directed Immobilisation of glycomimetics for Biosensing applications

Poster and orale presentation

Zhang J., Pourceau G., Meyer A., Vidal S., Praly J-P., Souteyrand E. , Morvan F., Vasseur and Chevolot Y.

Gordon Conference on Carbohydrate, Tilton, USA, 14-19 juin 2009

10-Biosensing carbohydrate-protein interactions by introducing a platform of DNA-Directed Immobilisation (DDI) glycoarrays

Orale presentation

Zhang J., Pourceau G., Moni, L., Meyer A., Vidal S. , Dondoni A., Praly J-P., Marra A., Souteyrand E., Vasseur J-J., Morvan F., Chevolot Y.

3ẽmes Entretiens pour la Recherche Centrales – Beihang, Pékin, China, 10-12 juin 2009

11-Développement d'un microsystème d'analyse pour l'étude des interactions saccharides/ Virus Influenza

Orale presentation

J. Zhang, G. Pourceau, L. Moni, V. Moulés, A. Meyer, S. Vidal, A. Dondoni, B. Lina, J-P. Praly, A. Marra, E. Souteyrand, J-J. Vasseur, F. Morvan et Y. Chevolot.

Colloque évènement du programme INTERFACE PHYSIQUE CHIMIE BIOLOGIE : SOUTIEN A LA PRISE DE RISQUE : "Physics, Chemistry and Biology meet together under the pine trees **»,** FREJUS, 30 september -3 octobre 2009

12-Criblage de glycomimétiques par utilisation de puces à ADN comme plateforme d'analyse

Orale presentation

J. Zhang, G. Pourceau, L. Moni, A. Meyer, S. Vidal, A. Dondoni, J-P. Praly, A. Marra, E. Souteyrand, J-J. Vasseur, F. Morvan et Y. Chevolot

Journée du Club Nano Micro Technologies, Ecully, 25-26 mars 2010

13-DNA Chips used as an universal platform for glycoarray devices

Orale presentation

J. Zhang, Y. Chevolot, E. Souteyrand, S. Vidal, J-P. Praly, G. Pourceau, F. Morvan, A. Meyer, J.J. Vasseur, L. Moni, A. Dondoni, A. Marra.

Biosensor 2010, Glasgow Scotland, 26-28 Juin 2010

14-Etude des interactions glycomimétiques/lectines grâce à l'utilisation des puces à ADN comme plateforme universelle d'ancrage

Orale presentation

J. Zhang, G. Pourceau, L. Moni, A. Meyer, S. Vidal, A. Dondoni, J-P. Praly, A. Marra, E. Souteyrand, J-J. Vasseur, F. Morvan et Y. Chevolot

Première Journée Scientifique du GIS IMIS, Besançon, 3 juin 2010

15-Glycobiologie : Etudes des intéractions lectines/glycomimétiques grâce à l'utilisation de puces à ADN comme plateforme d'ancrage universelle

Poster presentation

J. Zhang, G. Pourceau, A. Goudot, A. Meyer, S. Vidal, J-P. Praly, E. Souteyrand, J-J. Vasseur, F. Morvan and Y. Chevolot

Troisième colloque du LIA-LN2, Saint-Alexis-des-Monts (Ca), 12-16 juillet 2010

Résumé

La glycomique est la science qui s'intéresse à l'étude structurelle et fonctionnelle des saccharides, également appelés hydrates de carbone (ou carbohydrates). Les saccharides (aussi appelés glycanes dans ce cas) sont impliqués dans un très grand nombre d'évènements biologiques « normaux » et/ou pathologiques. Les relations entre la structure du saccharide et ses fonctions biologiques sont étudiées à l'aide de techniques conventionnelles telles que la cristallographie, la RMN, l'ITC, la plasmonique de surface. Ces études sont longues et couteuses et restent souvent limitées du fait de la très grande diversité des structures saccharidiques et de la difficulté à obtenir des saccharides pures en quantité importante. Pour pallier ces difficultés, nous proposons d'adapter la technologie biopuce qui permet d'effectuer un nombre très élevé d'études en parallèle (High Throughput Screening) avec des quantités réduites de matériels biologiques ou biochimiques.

Cette thèse vise donc le développement de puces à sucres (ou glycoarray, carbohydrate array) avec deux principales innovations : 1) l'utilisation comme sondes de glycomimétiques qui miment les hydrates de carbone naturels mais dont la synthèse est plus aisée ; 2) l'immobilisation des sondes glycomimétiques sur la puce via l'hybridation d'ADN.

La synthèse à façon des glycomimétiques permet d'obtenir des sondes de structures et de nature chimique diverses et offre la possibilité d'ajouter pour chaque type de sondes une étiquette ADN pour d'une part immobiliser les glycomimétiques de manière orientée sur la puce par DDI (DNA Directed Immobilisation) et d'autre part localiser et identifier les glycomimétiques sur la puce. Ces glycomimétiques ont été synthétisés par l'Institut des Biomolécules Max Mousseron de Montpellier en collaboration avec l'Institut de Chimie et Biochimie Moléculaire et Supramoléculaire de Lyon.

Une première partie de ce travail a été de valider l'élaboration des puces à sucre puis d'augmenter les capacités d'analyses des glycoarrays basés sur la DDI. Pour cela l'efficacité de l'immobilisation par DDI a été comparée à une immobilisation covalente. Nos résultats ont montré une reconnaissance supérieure par la lectine RCA 120 de glycomimétiques immobilisés par DDI aux faibles concentrations en glycomimétiques. La miniaturisation de la puce a consisté à graver 40 microréacteurs sur un format lame de microscope. Chaque microréacteur formant une puce de 64 plots différents, on peut ainsi réaliser 40 expériences indépendantes. Grâce à ce type de glycoarrays, des tests d'IC$_{50}$ ont permis d'obtenir des données quantitatives de l'affinité des glycomimétiques/lectines en utilisant d'infimes quantités de matériels biologiques. D'autre part, nous avons démontré la possibilité d'accélérer les études d'interactions sucres/lectines en poolant simultanément 8 glycomimétiques et 2 lectines.

La deuxième partie de la thèse a été d'utiliser les glycoarrays pour étudier les paramètres structuraux (distribution spatiale, nature chimique de la molécule, charge…) permettant d'exacerber l'affinité lectines/glycomimétiques. Trois lectines ont été étudiées : RCA120 (lectine modèle d'origine végétale) et deux lectines PA-IL et PA-IIL facteurs de virulence de la bactérie *Pseudomonas aeruginosa*. Trois types d'architectures de glycomimétiques (en peigne, en antenne et en couronne) ainsi que l'effet de la charge portée (+, -, neutre) ont été étudiés. L'architecture en peigne a clairement montré une affinité supérieure vis-à-vis des 2 lectines (PA-IL et PA-IIL) et PA-IL marque une préférence pour les structures chargées positivement. Soulignons que les interactions monovalentes sucres/lectines sont souvent faibles (mM). L'utilisation de ligands multivalents avec une disposition spatiale des résidus saccharidiques optimale, peut induire une affinité supérieure à la somme des affinités individuelles de chacun des résidus (« effet cluster »). Dans cette étude, les effets « cluster » ont été mis en évidence. Enfin, les interactions virus influenza/ glycomimétiques ont été abordées.

Mots clés

Glycobiologie, Microarray, puce ADN, chimie de surface, interaction sucre/lectine, carbohydrate, DNA immobilisation